ISSN 0021-9673

VOL. 635 NO. 1 APRIL 9, 1993

JOURNAL OF CHROMATOGRAPHY

INCLUDING ELECTROPHORESIS AND OTHER SEPARATION METHODS

JOURNAL OF CHROMATOGRAPHY

INCLUDING ELECTROPHORESIS AND OTHER SEPARATION METHODS

Scope. The *Journal of Chromatography* publishes papers on all aspects of **chromatography, electrophoresis** and related methods. Contributions consist mainly of research papers dealing with chromatographic theory, instrumental developments and their applications. The section *Biomedical Applications*, which is under separate editorship, deals with the following aspects: developments in and applications of chromatographic and electrophoretic techniques related to clinical diagnosis or alterations during medical treatment; screening and profiling of body fluids or tissues related to the analysis of active substances and to metabolic disorders; drug level monitoring and pharmacokinetic studies; clinical toxicology; forensic medicine; veterinary medicine; occupational medicine; results from basic medical research with direct consequences in clinical practice. In *Symposium volumes*, which are under separate editorship, proceedings of symposia on chromatography, electrophoresis and related methods are published.

Submission of Papers. The preferred medium of submission is on disk with accompanying manuscript (see *Electronic manuscripts* in the Instructions to Authors, which can be obtained from the publisher, Elsevier Science Publishers B.V., P.O. Box 330, 1000 AH Amsterdam, Netherlands). Manuscripts (in English; *four* copies are required) should be submitted to: Editorial Office of *Journal of Chromatography*, P.O. Box 681, 1000 AR Amsterdam, Netherlands, Telefax (+31-20) 5862 304, or to: The Editor of *Journal of Chromatography, Biomedical Applications*, P.O. Box 681, 1000 AR Amsterdam, Netherlands. Review articles are invited or proposed in writing to the Editors who welcome suggestions for subjects. An outline of the proposed review should first be forwarded to the Editors for preliminary discussion prior to preparation. Submission of an article is understood to imply that the article is original and unpublished and is not being considered for publication elsewhere. For copyright regulations, see below.

Publication. The *Journal of Chromatography* (incl. *Biomedical Applications*) has 40 volumes in 1993. The subscription prices for 1993 are:

J. Chromatogr. (incl. *Cum. Indexes*, *Vols. 601–650*) + *Biomed. Appl.* (Vols. 612–651):
Dfl. 8520.00 plus Dfl. 1320.00 (p.p.h.) (total *ca.* US$ 5622.75)

J. Chromatogr. (incl. *Cum Indexes*, *Vols. 601–650*) only (Vols. 623–651):
Dfl. 7047.00 plus Dfl. 957.00 (p.p.h.) (total *ca.* US$ 4573.75)

Biomed. Appl. only (Vols. 612–622):
Dfl. 2783.00 plus Dfl. 363.00 (p.p.h.) (total *ca.* US$ 1797.75).

Subscription Orders. The Dutch guilder price is definitive. The US$ price is subject to exchange-rate fluctuations and is given as a guide. Subscriptions are accepted on a prepaid basis only, unless different terms have been previously agreed upon. Subscriptions orders can be entered only by calender year (Jan.–Dec.) and should be sent to Elsevier Science Publishers, Journal Department, P.O. Box 211, 1000 AE Amsterdam, Netherlands, Tel. (+31-20) 5803 642, Telefax (+31-20) 5803 598, or to your usual subscription agent. Postage and handling charges include surface delivery except to the following countries where air delivery via SAL (Surface Air Lift) mail is ensured: Argentina, Australia, Brazil, Canada, China, Hong Kong, India, Israel, Japan*, Malaysia, Mexico, New Zealand, Pakistan, Singapore, South Africa, South Korea, Taiwan, Thailand, USA. *For Japan air delivery (SAL) requires 25% additional charge of the normal postage and handling charge. For all other countries airmail rates are available upon request. Claims for missing issues must be made within six months of our publication (mailing) date, otherwise such claims cannot be honoured free of charge. Back volumes of the *Journal of Chromatography* (Vols. 1–611) are available at Dfl. 230.00 (plus postage). Customers in the USA and Canada wishing information on this and other Elsevier journals, please contact Journal Information Center, Elsevier Science Publishing Co. Inc., 655 Avenue of the Americas, New York, NY 10010, USA, Tel. (+1-212) 633 3750, Telefax (+1-212) 633 3764.

Abstracts/Contents Lists published in Analytical Abstracts, Biochemical Abstracts, Biological Abstracts, Chemical Abstracts, Chemical Titles, Chromatography Abstracts, Current Awareness in Biological Sciences (CABS), Current Contents/Life Sciences, Current Contents/Physical, Chemical & Earth Sciences, Deep-Sea Research/Part B: Oceanographic Literature Review, Excerpta Medica, Index Medicus, Mass Spectrometry Bulletin, PASCAL-CNRS, Referativnyi Zhurnal, Research Alert and Science Citation Index.

US Mailing Notice. *Journal of Chromatography* (ISSN 0021-9673) is published weekly (total 52 issues) by Elsevier Science Publishers (Sara Burgerhartstraat 25, P.O. Box 211, 1000 AE Amsterdam, Netherlands). Annual subscription price in the USA US$ 4573.75 (subject to change), including air speed delivery. Second class postage paid at Jamaica, NY 11431. **USA POSTMASTERS**: Send address changes to *Journal of Chromatography*, Publications Expediting, Inc., 200 Meacham Avenue, Elmont, NY 11003. Airfreight and mailing in the USA by Publications Expediting.

See inside back cover for Publication Schedule, Information for Authors and information on Advertisements.

0021-9673/93/$06.00

This issue is printed on acid-free paper.

Printed in the Netherlands

VOL. 635, NO. 1 JOURNAL OF CHROMATOGRAPHY APRIL 9, 1993

CONTENTS

(Abstracts/Contents Lists published in Analytical Abstracts, Biochemical Abstracts, Biological Abstracts, Chemical Abstracts, Chemical Titles, Chromatography Abstracts, Current Awareness in Biological Sciences (CABS), Current Contents/Life Sciences, Current Contents/Physical, Chemical & Earth Sciences, Deep-Sea Research/Part B: Oceanographic Literature Review, Excerpta Medica, Index Medicus, Mass Spectrometry Bulletin, PASCAL-CNRS, Referativnyi Zhurnal, Research Alert and Science Citation Index)

REGULAR PAPERS

Column Liquid Chromatography

Theoretical study of the ion-exchange preparative chromatography of a two-protein mixture
by J.C. Bellot and J.S. Condoret (Toulouse, France) (Received December 23rd, 1992) 1

Normal-phase high-performance liquid chromatography with highly purified porous silica microspheres
by J.J. Kirkland, C.H. Dilks, Jr. and J.J. DeStefano (Newport, DE, USA) (Received December 17th, 1992) . . . 19

Influence of polymer morphology on the ability of imprinted network polymers to resolve enantiomers
by B. Sellergren and K.J. Shea (Irvine, CA, USA) (Received December 24th, 1992) 31

Quantitation of non-ideal behavior in protein size-exclusion chromatography
by P.L. Dubin, S.L. Edwards and M.S. Mehta (Indianapolis, IN, USA) and D. Tomalia (Midland, MI, USA) (Received November 6th, 1992) 51

Retention indices of phenols for internal standards in reversed-phase high-performance liquid chromatography. Application to retention prediction and selectivities of mobile phases and packing materials
by S. Yamauchi (Tokushima, Japan) (Received December 1st, 1992) 61

Chromatographic analysis of the reaction between thiosalicylic acid and selenious acid in methanol
by Y. Saito and M. Chikuma (Matsubara, Japan) (Received December 22nd, 1992) 71

Salting-out solvent extraction for pre-concentration of benzalkonium chloride prior to high-performance liquid chromatography
by J.E. Parkin (Perth, Australia) (Received December 15th, 1992) 75

High-performance liquid chromatographic determination of PZ-peptidase activity
by T. Chikuma, W. Tanaka, K. Yamada, Y. Ishii and A. Tanaka (Tokyo, Japan) and T. Kato (Yokohama, Japan) (Received December 24th, 1992) 81

Chromatographic investigations of oligomeric α,ω-dihydroxy polyethers by reversed-phase high-performance liquid chromatography and evaporative light scattering and UV detection
by K. Rissler, H.-P. Künzi and H.-J. Grether (Marly, Switzerland) (Received December 17th, 1992) 89

Gas Chromatography

Comparison of different methods for the prediction of retention times in programmed-temperature gas chromatography
by G. Castello, P. Moretti and S. Vezzani (Genova, Italy) (Received December 21st, 1992) 103

Electrophoresis

Theoretical aspects of chiral separation in capillary electrophoresis. III. Application to β-blockers
by S.A.C. Wren and R.C. Rowe (Macclesfield, UK) (Received November 6th, 1992) 113

Chiral separations by complexation with proteins in capillary zone electrophoresis
by S. Busch, J.C. Kraak and H. Poppe (Amsterdam, Netherlands) (Received December 22nd, 1992) 119

Determination of gold(I) and silver(I) cyanide in ores by capillary zone electrophoresis
by M. Aguilar, A. Farran and M. Martínez (Barcelona, Spain) (Received December 22nd, 1992) 127

SHORT COMMUNICATIONS

Column Liquid Chromatography

Estimation of inter-detector lag in multi-detection gel permeation chromatography
by A.D. Sagar, S.J. Sofia and E.W. Merrill (Cambridge, MA, USA) (Received January 13th, 1993) 132

(Continued overleaf)

Contents (continued)

Multichannel coulometric detection coupled with liquid chromatography for determination of phenolic esters in honey
by E. Joerg and G. Sontag (Vienna, Austria) (Received January 12th, 1993) 137

Analysis of phenolic and flavonoid compounds in juice beverages using high-performance liquid chromatography with coulometric array detection
by P. Gamache, E. Ryan and I.N. Acworth (Bedford, MA, USA) (Received January 25th, 1993) 143

Stability of furosine during ion-exchange chromatography in comparison with reversed-phase high-performance liquid chromatography
by J. Hartkopf and H.F. Erbersdobler (Kiel, Germany) (Received January 19th, 1993) 151

High-performance liquid chromatographic determination of mexiletine in film-coated tablets using a new polymeric stationary phase
by E. Lamparter (Ingelheim am Rhein, Germany) (Received December 11th, 1992) 155

Chemical reduction of FD&C Yellow No. 5 to determine combined benzidine
by V.M. Davis and J.E. Bailey, Jr. (Washington, DC, USA) (Received January 7th, 1993) 160

Planar Chromatography

Mapping of derivatised biogenic amines by two-dimensional thin-layer chromatography. A comparative study
by N.P.J. Price and D.O. Gray (London, UK) (Received January 8th, 1993) 165

Electrophoresis

Electrophoretic determination of stability constants of Zn(II)- and Cd(II)–nitrilotriacetate–penicillamine mixed complexes
by S.K. Srivastava, V.K. Gupta, B.B. Tiwari and I. Ali (Roorkee, India) (Received December 24th, 1992) 171

BOOK REVIEW

Thin-layer chromatography; reagents and detection methods; physical and chemical detection methods: fundamentals, reagents I, Vol. 1a (by H. Jork, W. Funk, W. Fischer and H. Wimmer), reviewed by E. Heftmann (Orinda, CA, USA) 176

JOURNAL OF CHROMATOGRAPHY

VOL. 635 (1993)

JOURNAL of CHROMATOGRAPHY

INCLUDING ELECTROPHORESIS AND OTHER SEPARATION METHODS

ELSEVIER

AMSTERDAM — LONDON — NEW YORK — TOKYO

0021-9673/93/$06.00

Printed in the Netherlands

Journal of Chromatography, 635 (1993) 1–17
Elsevier Science Publishers B.V., Amsterdam

CHROM. 24 827

Theoretical study of the ion-exchange preparative chromatography of a two-protein mixture

J.C. Bellot and J.S. Condoret*

Département de Génie Biochimique et Alimentaire, UA–CNRS 544, Institut National des Sciences Appliquées, Avenue de Rangueil, F-31077 Toulouse (France)

(First received October 13th, 1992; revised manuscript received December 23rd, 1992).

ABSTRACT

Preparative ion-exchange chromatography of a two-protein mixture is theoretically considered by the use of numerical simulations. The mathematical model is a combination of the semi-ideal model for the chromatographic process, with the stoichiometric displacement model for the basic interactions between proteins and the stationary phase. A study of the selectivity of the adsorption, which appears to be dependent on the loading of the column, makes possible a better understanding of the chromatograms obtained with either isocratic or gradient elution. Special stress is been laid on the effect of overloading the column by pointing out displacement effects between proteins. The influence of important adsorption parameters, such as the characteristic charge or maximum loading capacity, was investigated by considering criteria of production rate, recovery yield and enrichment of products.

INTRODUCTION

The preparative purification of biomolecules from complex mixtures is now emerging as an important challenge for the pharmaceutical and biotechnology industries and, among all the techniques at their disposal, ion-exchange chromatography is one of the most effective. This technique is nowadays widely used for the analysis and purification of peptides, proteins or polynucleotides [1]. However, despite its numerous applications, this useful technique really suffers from a lack of the theoretical bases necessary for a good understanding of the retention of polymeric ions, such as proteins.

A great amount of work has already been carried out in order to understand the phenomena encountered with small organic or inorganic ions [2–4]. Considering amino acids, Saunders *et al.* [5] and Dye *et al.* [6] have contributed to the understanding of their retention behaviour on ion-exchange resins. All these models were satisfactory but their extension to larger molecules such as proteins, usually characterized by a complex three-dimensional structure, is not straightforward. In addition, the number and spatial distribution of the molecule charges interacting with the support are not easy to evaluate.

Nevertheless, a simple model has been developed during the last decade to describe the retention of proteins in ion-exchange chromatography. This model, the stoichiometric displacement model (S.D.M.), was sucessfully used to predict and simulate the chromatographic behaviour of proteins under analytical conditions. Nevertheless, numerical problems arising from the non-linearity of adsorption isotherms in the high concentration range, combined with the mathematical complexity of their expression, have limited the use of the S.D.M. to analytical chromatography.

Recently, the development of a numerical method using the S.D.M., and simulating the

* Corresponding author.

0021-9673/93/$06.00

isocratic or gradient elution of a single protein in ion-exchange chromatography for mass overload conditions, was reported by Cysewski *et al.* [7]. This original work, applied to the study of the chromatographic behaviour of concentrated proteins, is a milestone in the research on the optimum operating conditions in the preparative ion-exchange chromatography of proteins. Their paper also contributes to a better understanding of the chromatographic peak shapes.

In this work, we extended the study of Cysewski *et al.* [7] to the theoretical study of the separation of a two-protein mixture. Our aim was not to describe accurately all the physical phenomena that occur in ion-exchange chromatography, which is not possible when considering the simplifying hypotheses of the S.D.M. combined with the shortcomings of the numerical modelling, but to study and compare as a whole the respective behaviour of isocratic and gradient preparative elution in order to draw some general conclusions. This was done first through a study of the evolution of the selectivity with the loading factor, and then through the calculation of parameters specific to preparative separations such as the recovery yield, the enrichment factor and the production rate.

MODELLING THE ADSORPTION OF PROTEINS

Introduction

The ion-exchange chromatography of proteins is often operated with pH or counter-ion concentration variations, especially when gradient elution is used. These variations may affect the tertiary structure of the protein and therefore the charge distribution which notably influences, but in a little known and unpredictable way, the affinity of the protein for the support [8]. In addition, the characteristics of the stationary phase, such as its charge density and its physical structure, take on real importance. A model taking into account all these effects and parameters would be of extreme complexity and would need too much information about the proteins and the stationary phase concerned. It has been found more appropriate to develop a model requiring less information and which, even though restricted by its initial hypotheses, could give correct predictions for a limited range of operating conditions. This has been the basic idea for the S.D.M.

Historical background

The basic principles of ion-exchange chromatography, *i.e.*, electrostatic interaction chromatography, were established by Walton [9]. However, they were restricted to small molecules, either organic or otherwise. In order to describe adsorption of polymeric ions with mono-, di- or trivalent counter ions, a simple model derived from the work of Boardman and Partridge [10] was developed by Regnier and co-workers [1,11]. Its major features were restated precisely by Velayudhan and Horváth [12] who, 2 years later, presented a detailed analysis of the formalism of the model [13]. An interesting study was also reported by Whitley *et al.* [8].

Basic hypotheses

This is a non-mechanistic model based on the mass action law, whose main principle is that the displacement of an adsorbed solute is followed by the stoichiometric adsorption of the displacing agent, in such a way as to maintain the electroneutrality of the stationary phase [10,14]. Therefore, the adsorbed salt concentration must be considered to account for the competition for the adsorption sites between this salt and the mobile phase solutes.

In the equations of the model presented below, the proteins in solution will be assumed to behave ideally, *i.e.*, their liquid phase concentration will be considered to be a correct measurement of their activity. Their activity coefficient will be then taken as equal to 1 over the whole concentration range. This hypothesis, unrealistic even in the preparative mode characterized by mass overload conditions, is nevertheless commonly accepted by most workers for the sake of simplicity [13].

For well defined experimental conditions, the S.D.M. considers two distinct co-ion categories: co-ions of the first type, which are liberated from the protein when it binds to the support, and co-ions of the second type, which remain attached during this adsorption process. From this point of view, the protein may therefore be

considered as a neutral salt which is totally dissociated in solution into a poly-ion , *i.e.*, the protein is bound to co-ions of the second type, and first-type co-ions are free in solution [13]. These latter therefore remain thermodynamically unchanged during the adsorption process, and simply maintain the solution electroneutrality. In fact, they are not considered in the final equations of the model.

The properties of a biopolymer, *e.g.*, its charge, valency, tertiary structure and size, are assumed not to vary during the separation process operated at constant pH.

The stationary phase must be homogeneous and must have pores of constant shape and size with a sufficiently large diameter to prevent any parallel separation by exclusion.

This model does not take into account hydrophobic interactions [7,15].

Description of the model

The adsorption–desorption equilibrium of a protein in ion exchange may be represented by the following equation:

$$m_A P_i + m_i A^s = m_A P_i^s + m_i A \quad (1)$$

where P_i and P_i^s represent the protein in the flowing mobile phase and adsorbed on the stationary phase, respectively. A is the counter ion (or displacing ion) in the mobile phase and A^s is the counter ion adsorbed; the valency of the counter ion is m_A and the protein is m_i-valent with respect to the chromatographic support. Let us specify that when a mixture of proteins is considered, an equilibrium equation such as that in eqn. 1 is written for each protein.

In a first approach, m_i, called the characteristic charge [16], may be defined as the number of monovalent counter ions displaced when the protein adsorbs or, in other words, the number of charged residues of the protein in direct contact with the fixed charges of the support [13]. Also, m_i has another significance which seems more complex to handle. In fact, it accounts for several possible associations between the protein and the support. Indeed, for given operating conditions, such as pH and salt concentration, several preferential orientations may co-exist, as shown Whitley *et al.* [8], who pointed out at least two kinds of different binding forms for each protein they studied. These preferential orientations may depend on the adsorbed protein concentration [13]. In conclusion, we can say that m_i represents an average for competing binding forms and therefore its experimental value may not be an integer. Further, if all the previous hypotheses oversimplify a specific system, it will lead to an experimental value of m_i accounting for all the deviations from the ideal situation, and then m_i, initially a simple value derived from a stoichiometric equation, will be transformed into an empirical parameter. However, this does not affect the formalism of the model, as emphasized by Velayudhan and Horváth [13].

K_i, the equilibrium constant of eqn. 1, is as follows:

$$K_i = \frac{q_i^{m_A} C_A^{m_i}}{C_i^{m_A} q_A^{m_i}} \quad (2)$$

where q_i and q_A are the adsorbed protein and counter-ion concentration, respectively, calculated per unit volume of particle skeleton. The other concentrations (C_i and C_A) refer to the product in the mobile phase.

The maximum loading capacity of the exchanger, Q_x, may be defined as the sum of the sites occupied by all the proteins of the mixture and the counter ion:

$$Q_x = \sum_{i=1}^{N_c} m_i q_i + m_A q_A \quad (3)$$

where N_c is the total number of proteins. We can see that this last equation represents the stationary phase electroneutrality condition.

Substituting eqn. 3 in eqn. 2, we obtain the following isotherm equation:

$$C_i = \frac{q_i}{K_i^{1/m_A}} \left(\frac{m_A C_A}{Q_x - \sum_{i=1}^{N_c} m_i q_i} \right)^z \quad (4)$$

where Z ($= m_i/m_A$) is the stoichiometric charge ratio of the protein and the counter ion.

As already stated in a previous paper [17], in reversed-phase chromatography it is not straightforward to extrapolate from individual adsorption isotherms to competitive isotherms. It is

surprising that, when considering the ion-exchange process, this derivation does not need any other parameters and requires only a modification of the mass balance for the stationary phase, as it already appears in eqn. 3 through the summation term. We can also emphasize the ability of the S.D.M. to take into account the counter-ion concentration, which offers among other advantages the possibility of accounting for gradient elution chromatography.

It must be stressed that eqn. 4 has the disadvantage of being an implicit form of the adsorbed product concentration as a function of the liquid phase product concentration. This unusual feature is of great importance and may introduce some complications during the numerical handling of the equations of the model. Indeed, when several proteins are considered it is necessary to use a numerical method (the Newton–Raphson algorithm) for solving non-linear systems of eqns. 4 (one equation for each protein).

For very dilute solutions, the total adsorbed protein concentration becomes negligible compared with Q_x, and then eqn. 4 becomes a very easy to handle explicit equation:

$$q_i = C_i\left(\frac{Q_x}{m_A C_A}\right)^z K_i^{1/m_A} \tag{5}$$

NUMERICAL MODEL

Hypotheses and preliminary remarks

In order to have a good description of the various physical phenomena encountered in the separation process of biomolecules in preparative liquid chromatography, several models have been proposed. They may be classified into three main categories: the theory of interferences, the plate theory and the continuity equations. The last category offers the greatest number of developments for both analytical and numerical descriptions [18]. This kind of modelling was therefore chosen here and, in particular, we have used the semi-ideal model, whose numerical resolution has been undertaken using the R.G.S. method (from Rouchon and Golshan-Shirazi, its authors [29]), which is a particular algorithm based on finite differences. The simulation program was performed in FORTRAN.

The simulations will be based on an isothermal porous fixed bed, uniformly packed with one-sized spherical particles, where concentration profiles are assumed to be one-dimensional. Diffusion coefficients of solutes in the mobile and stationary phases are considered to be independent of concentration. Moreover, adsorption equilibrium is assumed to be instantaneous.

The semi-ideal model

In the general case, the continuity equation in the flowing mobile phase for each component is written as

$$\frac{\partial}{\partial t}(Fq_i + C_i) + u \cdot \frac{\partial C_i}{\partial z} = D_{i,ax} \cdot \frac{\partial^2 C_i}{\partial z^2} \tag{6}$$

z and t being spatial and time coordinates, respectively, F the phase ratio, u the interstitial fluid velocity and $D_{i,ax}$ the axial dispersion coefficient for component i. This description of the phenomena occurring during the separation should be completed by the continuity equation for the stationary phase, accounting for internal mass transfer resistances, and an expression accounting for the mass transfer rate from the mobile phase towards the stationary phase (external mass transfer resistance).

The semi-ideal model assumes that all mass transfer phenomena are very fast. The axial dispersion coefficient in eqn. 6, which accounts for molecular diffusion and dispersion due to the irregular flow through the porous medium, is therefore replaced with an apparent dispersion coefficient $D_{i,ap}$ that accounts also for external and internal mass transfer kinetics that are always considered fast but not infinitely fast [19]. Guiochon *et al.* [20] specified once again that the molecular diffusion coefficient remains constant during the separation, which is true for the range of concentrations used in preparative chromatography. Therefore, the apparent dispersion coefficient, related to this molecular coefficient, is constant.

It must be noted that, for proteins, mass transfer kinetics are usually slow [21,22]. However, as the efficiency of columns is commonly over several hundred theoretical plates, we shall assume that these limitations are correctly taken

into account by the lumped coefficient used by Guiochon *et al.* [20], *i.e.*, the apparent dispersion coefficient. Considering this coefficient, Giddings [23] has established the following expression:

$$D_{i,ap} = \frac{HL}{2t_0} = \frac{Hu}{2} \tag{7}$$

where t_0 is the retention time of an unretained molecule, L the length of the column and H the height equivalent to a theoretical plate.

The accurate numerical resolution of the semi-ideal model is not straightforward, owing to intrinsic errors of the numerical method. One solution, proposed by Guiochon *et al.* [20], is to consider an infinite efficiency of the column, *i.e.*, an infinite number of theoretical plates, and therefore a zero axial dispersion coefficient. This leads to the consideration of the ideal model, written as follows:

$$\frac{\partial}{\partial t}(Fq_i + C_i) + u \cdot \frac{\partial C_i}{\partial z} = 0 \tag{8}$$

The finite difference method has proved to be a suitable way of solving the ideal model equation, but it results in chromatographic profiles affected by a so-called "numerical diffusion", due to the finite value of the time and space increments of the discretization. Nevertheless, it does correlate well with some experimental curves. This artificial diffusion may be known, mastered and tuned to stick to the physical phenomena and the band broadening well accounted for by the semi-ideal model. Therefore, while trying to solve numerically the ideal model, a systematic error is made, resulting in the solution of the semi-ideal model. This method proved to be very effective in the work of Guiochon *et al.* [20].

NUMERICAL METHOD

Finite difference method

In this method, the movement of products, from their injection to their exit from the column, is represented by a discrete distribution of mass on a grid of spatial and temporal coordinates. Time and spatial derivatives may be transformed into finite differences using various algorithms [24]. In this work, we chose a simple numerical scheme developed by Rouchon *et al.* [25] and successfully used in numerous studies [20,26–28].

Presentation of the numerical scheme

To evaluate spatial and time derivatives we have used the following expressions:

$$\frac{\partial C_i}{\partial z} = \frac{C^j_{i,n} - C^j_{i,n-1}}{\sigma} \tag{9a}$$

$$\frac{\partial C_i}{\partial t} = \frac{C^j_{i,n-1} - C^{j-1}_{i,n-1}}{\tau} \tag{9b}$$

and finally for the stationary phase:

$$\frac{\partial q_i}{\partial t} = \frac{q^j_{i,n-1} - q^{j-1}_{i,n-1}}{\tau} \tag{9c}$$

where σ and z are the space and time increments, respectively, n refers to the space location and j to time. By defining T_i as the ratio of stationary and mobile phase concentrations ($= q_i/C_i$) and by inserting eqns. 9a–c in eqn. 8, the following scheme is obtained [24]:

$$C^j_{i,n} = C^j_{i,n-1} - \frac{\sigma}{u\tau}[(1 + FT^j_{i,n-1})C^j_{i,n-1} - (1 + FT^{j-1}_{i,n-1})C^{j-1}_{i,n-1}] = 0 \tag{10}$$

Eqn. 10 is easy to solve as it expresses explicitly the concentration of component i in the mobile phase for the cell $\binom{j}{n}$ as a function of previously calculated concentrations.

A numerical analysis of this scheme from Guiochon and co-workers [24,29,30] has shown that this algorithm leads to a numerical dispersion, and therefore to an artificial H given by

$$H = \sigma\left[\frac{u\tau}{(1 + Fk_0)\sigma} - 1\right] = \sigma(P - 1) \tag{11}$$

where k_0 is the average value of all the initial slopes of the components isotherm and P the Courant number, written as follows [24,30]:

$$P = \frac{u\tau}{(1 + Fk_0)\sigma} \tag{12}$$

As we have already stated, the replacement of actual derivatives of the ideal model by finite differences generates a numerical error at each calculation step. If time and space increments

are not carefully chosen, it will be very difficult to control their evolution, and oscillations or divergence phenomena may appear. A stability condition is therefore necessary, and the most commonly used method to check this stability is the Von Neuman analysis [30]. In our case, the deduced condition is [24]:

$$P \geqslant 1 \tag{13}$$

Eqn. 13 imposes a Courant number greater than 1. Czok and Guiochon [24] proposed a value of 2 for P. This choice, satisfying the stability condition, also has the advantage of fixing the space increment value equal to the H leading to (from eqn. 11)

$$\sigma = H \tag{14}$$

The time increment is then written as

$$\tau = \frac{2H(1 + Fk_0)}{u} \tag{15}$$

Using eqns. 14 and 15, this finite difference method is termed R.G.S., from its authors' names, Rouchon and Golshan-Shirazi [29].

From these considerations, it is now possible, from the actual value of the height equivalent to a theoretical plate of the column, to simulate, with the ideal model, actual separations affected by an apparent physical dispersion, by generating the corresponding numerical diffusion in the numerical resolution.

DESCRIPTION OF THE PROBLEM

Protein characterization

We chose two proteins, P_1 and P_2, with relatively close molecular masses ($M \approx 20\,000$ g mol^{-1}) and with a molecular diffusion coefficient equal to 10^{-6} cm^2 s^{-1} [31].

Column characteristics

The ion-exchange column chosen for the computations is 5 cm × 4.6 mm I.D. It is filled with 13-μm spherical porous particles. The total porosity (ε) is 0.85. The pore size is assumed to be large enough (1000 Å) to avoid any diffusional limitations. The phase ratio [$F = (1 - \varepsilon)/\varepsilon$] is therefore equal to 0.176. The maximum loading capacity of the exchanger (Q_x) is 11 mM, which means that 11 mM of a monovalent ion are necessary to saturate all the adsorption sites ($Q_x = 11$ mequiv. l^{-1}). The column efficiency is calculated using the Knox equation [32]:

$$h = \frac{2}{\nu} + \nu^{1/3} + \frac{\nu}{10} \tag{16}$$

where h is the reduced plate height ($h = H/d_p$), ν the reduced mobile phase velocity ($\nu = ud_p/D_m$), d_p the average particle diameter, u the interstitial fluid velocity and D_m the molecular diffusion coefficient of the protein; u will be taken as equal to 0.01 cm/s for the whole study.

The reduced mobile phase velocity is then 13, and is nearly five times larger than the mathematical value of the optimum reduced velocity ($\nu_{opt} = 2.71$, from eqn. 16) that gives the smallest H value for our operating conditions. For all the production rate calculations done below, we specify that no optimization of the mobile phase velocity has been achieved. Therefore, this velocity remains low, but we must stress that it is not very important, as our aim is to illustrate the value of the S.D.M. on a few examples. A strategy for optimization of the experimental conditions is not our purpose.

When using these numerical values, we may calculate an H value of 50 μm for both proteins, which means a number of theoretical plates of 1000 for the whole column and which corresponds to 20 000 theoretical plates per metre. The efficiency of this column is therefore excellent owing to the small particle diameter chosen and the large porosity of the column that is operated with an adequate mobile phase velocity. Further, the molecular diffusion coefficient is relatively high compared with the usual values encountered for most proteins, as this coefficient characterizes rather small proteins.

The gradient

For our study, the gradient profile we used is always linear. This linear variation of the counter-ion concentration is started directly after the feed injection. The counter ion is a small molecule that is assumed not to be affected by the axial dispersion [33]. Further, we shall assume that this displacing ion will migrate at the same velocity as the mobile phase, and therefore that

the gradient profile does not undergo any deformation [7]. No deformation of the gradient profile assumes that the protein solid-phase concentration does not affect the velocity of the counter-ion concentration to a large extent.

Definitions

Loading factor [34]. This is the ratio of the amount of injected component to the saturation capacity of the column for this considered component. It is therefore directly related to the concentration of the injected component:

$$Lf_i = \frac{C_{i,0} V_{inj} m_i}{Q_x (1-\varepsilon) SL} \quad (17)$$

where $C_{i,0}$ is the initial concentration of the injected component, V_{inj} the injection volume and S the column cross-sectional area of the column. The other parameters (m_i, Q_x, ε and L) have been defined previously.

Recovery yield. This is the ratio of the recovered amount of the desired component to the amount of this component injected at the column entrance:

$$Y_i = \frac{\int_{t_1}^{t_2} C_i \, dt}{C_{i,0} t_{inj}} \quad (18)$$

where t_{inj} is the injection time and t_1 and t_2 the time limits of the recovery of the considered component for a given degree of purity that has been fixed, in the whole study, at a value of 0.98.

Production rate. This is the amount of recovered component, at a given purity, per unit time and per unit column cross-sectional area:

$$Pr_i = \frac{\varepsilon u \int_{t_1}^{t_2} C_i \, dt}{t_c} = \frac{\varepsilon u C_{i,0} t_{inj} Y_i}{t_c} \quad (19)$$

where t_c is the cycle time. The total cycle time usually takes into account the time of feed introduction, the duration of elution and the duration of a regeneration or washing step if necessary. To simplify, we shall consider here that this regeneration duration is small enough to be neglected. The cycle time will therefore be defined as the time between the injection of the products and the time when traces of the most retained component have left the column. This simplified definition will provide us with a very convenient tool.

Enrichment factor. This is the ratio between the average of the recovered concentrations of the desired component and the initial concentration of this component:

$$E_i = \frac{\int_{t_1}^{t_2} C_i \, dt}{(t_2 - t_1) C_{i,0}} \quad (20)$$

Selectivity. The selectivity characterizes, for a binary mixture of known composition, the ability of the stationary phase to induce different migration velocities for each component, and therefore its ability to separate this mixture:

$$\alpha = (q_{P_2}/C_{P_2})/(q_{P_1}/C_{P_1}) \quad (21)$$

RESULTS AND DISCUSSION

Selectivity

We shall concentrate here on a very interesting feature of the S.D.M. that departs from the well known competitive Langmuir model generally used in reversed-phase chromatography and very occasionally in ion-exchange adsorption of proteins.

The competitive Langmuir model predicts a constant selectivity for two components, and does not account for their concentration influence or the influence of other components. This is not the case for the S.D.M., which makes it possible to obtain a much more realistic value of the selectivity in the case of ion-exchange chromatography. Regnier and Mazsaroff [35] stressed the opportunity of applying to a certain extent the S.D.M. in reversed-phase chromatography, an opportunity less rigorously examined, but which perhaps in the future will lead to an actual improvement of the modelling of liquid chromatography equilibria.

From the basic equation of the model (see eqn. 4), the selectivity is formulated as follows:

$$\alpha = \frac{(q_{P_2}/C_{P_2})}{(q_{P_1}/C_{P_1})} = \left(\frac{K_{P_2}}{K_{P_1}}\right)^{1/m_A} \times \left(\frac{Q_x - m_{P_1} q_{P_1} - m_{P_2} q_{P_2}}{m_A C_A}\right)^{(m_{P_2} - m_{P_1})/m_A} \quad (22)$$

Eqn. 22 shows that selectivity depends on, among other things, the concentration of the adsorbed components P_1 and P_2 and on the counter-ion concentration in the mobile phase. The theoretical study of such a selectivity, which includes also the influence of the respective valency of all the components in the system, will be very useful in the understanding of the performances of isocratic or gradient ion-exchange chromatography. It should be noted that Golshan-Shirazi and Guiochon [36] emphasized that the LeVan–Vermeulen model [37] can also lead to a very effective selectivity, but this work was restricted to reversed-phase chromatography. First, we shall investigate the influence of the counter-ion concentration through a particular situation.

We shall consider two proteins, P_1 and P_2, having $m_{P_1} = 6$ and $m_{P_2} = 4$ as characteristic charges, and $K_{P_1} = 3200$ and $K_{P_2} = 640$ as equilibrium constant values. These values were chosen with regard to the experimental work presented by Whitley *et al.* [8], where parameters characterizing the S.D.M. were determined. Fig. 1a shows the competitive adsorption isotherms of the two proteins, with constant relative concentrations chosen as 1:1, and also the evolution of the selectivity α. These curves are plotted as a function of the loading factor of the protein P_1. The maximum loading capacity of the stationary phase (Q_x) is 11 mM (11 mequiv. l^{-1}), the counter ion is monovalent and its concentration is 20 mM.

It can be seen in Fig. 1a that protein P_1 saturates the adsorption sites of the support ($Q_{x_{P_1}} = 11/6 = 1.83$ mM) faster than does protein P_2 ($Q_{x_{P_2}} = 2.75$ mM), this latter being, in concentrated solution, more retained than P_1. Nevertheless, in very dilute solution, the initial slope of the P_1 isotherm (88.57, from eqn. 5) is greater than that of P_2 (58.56). Therefore, in linear ion-exchange chromatography, protein P_1 is more strongly retained than P_2, but this latter, owing to its smaller size, will have a higher saturation limit. The selectivity, below 1 for dilute solutions, exceeds this value as it increases with increasing protein concentration. This evolution therefore gives evidence of a selectivity

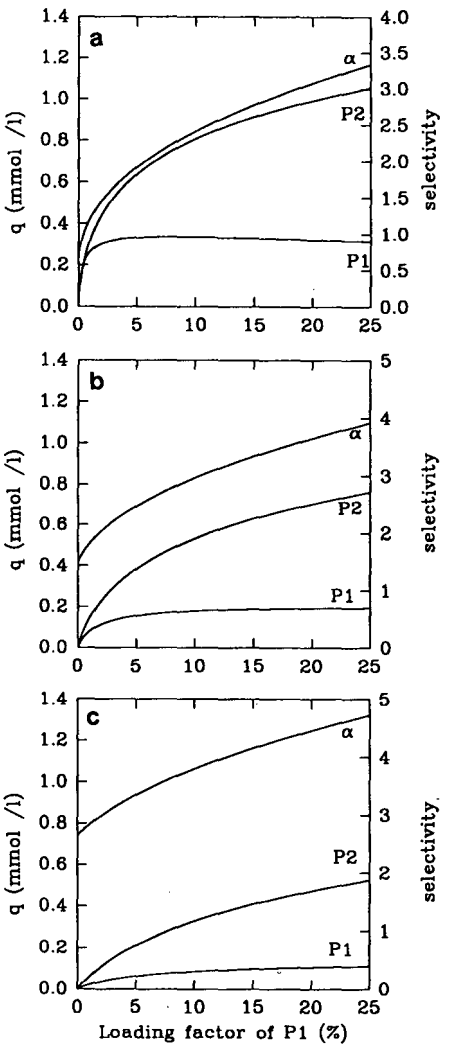

Fig. 1. Selectivity and competitive adsorption isotherms for a 1:1 binary mixture of proteins. $Q_x = 11$ mM; $m_{P_1} = 6$; $m_{P_2} = 4$; $m_A = 1$; $K_{P_1} = 3200$; $K_{P_2} = 640$. (a) $C_A = 20$ mM; (b) $C_A = 30$ mM; (c) $C_A = 40$ mM.

inversion as a function of concentrations, when the parameters are carefully chosen.

Still considering Fig. 1a, it is seen that the non-linearity of the isotherms is strongly marked, especially for protein P_1 which quickly reaches its maximum concentration on the stationary phase. However, this concentration is not the saturation limit for this protein ($Q_{x_{P_1}} = 1.83$ mM), which cannot be reached because of strong competition for the adsorption sites. The adsorbed P_1 concentration reaches its maximum

value of 0.4 m*M* for a 10% value of its loading factor, and then decreases slowly, owing to the displacement of P_1 by more strongly linked P_2 molecules. The latter will reach their saturation limit only for very high concentrations, because they will first have to displace all P_1 and counter-ion molecules. Consequently, the selectivity can only increase, and this fact is of great interest in revealing that two very close-lying products under analytical conditions may, under certain conditions, be separated more easily in the preparative mode. We shall present further a specific example of this situation.

Fig. 1b and c show the same curves as in Fig. 1a, but with different counter-ion concentrations (30 and 40 m*M*, respectively). These figures show a similar evolution of the selectivity as in Fig. 1a, but the selectivity inversion phenomenon previously mentioned is not present here. In addition, it is worth noting that, at the same loading factor, selectivity is increased with increasing counter-ion concentration.

Concerning the adsorption isotherms, it is noticeable that, for a given P_1 loading factor, the adsorbed concentration diminishes with increasing counter-ion concentration, which is directly related to eqn. 1, and gives evidence of the displacement effects of the counter ion, which is a basic feature of the S.D.M. In Fig. 1b and c, protein P_2 will saturate the stationary phase less and less easily, and therefore will displace P_1 at much higher concentrations than in Fig. 1a.

Fig. 2 presents the same parameters as in Fig. 1a, but using a divalent counter ion at 20 m*M* concentration. We note that the competitive isotherms have lost their strong non-linear character previously observed for a monovalent counter ion. These isotherms are much more oblique, illustrating the increased displacing effect of the counter ion and the difficulty, for the protein, to saturate the stationary phase. Considering isocratic elution, Cysewski *et al.* [7] demonstrated the benefit of using displacing ions with a high valency in order to limit the tails of peaks in mass overload conditions.

Fig. 3a and b show the influence of the equilibrium constants on the selectivity and the effect, on this parameter, of a large difference between the saturation capacities of the two

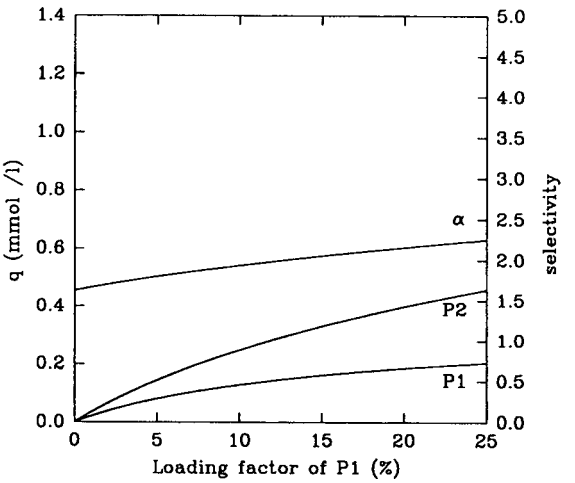

Fig. 2. Selectivity and competitive adsorption isotherms for a 1:1 binary mixture of proteins. Conditions as in Fig. 1, except the valency of the counter ion is 2.

proteins. The monovalent counter-ion concentration is 30 m*M* and the maximum loading capacity of the stationary phase is still 11 m*M* (11 mequiv. l^{-1}). Proteins P_1 and P_2 considered in Fig. 3a now have $m_{P_1} = 6$ and $m_{P_2} = 2$ as characteristic charge. The maximum adsorption capacity for P_1 is therefore 1.83 m*M* and for P_2 5.5 m*M*. In this instance the isotherms for the two proteins have similar initial slopes. Here, selectivity is increasing with the loading factor, but this evolution is markedly faster than that observed in Fig. 1a. These two proteins, whose selectivity is around 1 in dilute solution, *i.e.*, with a very close affinity for the stationary phase, exhibit a selectivity of around 7 for a 10% value of the loading factor of P_1. Above 5% for this loading factor, protein P_2, which adsorbs only on two sites ($m_{P_2} = 2$), displaces readily the over-large protein P_1, and this occurs despite the fact that the adsorption constant of P_1 ($K_{P_1} = 8200$) is much greater than that of P_2 ($K_{P_2} = 148$). In Fig. 3b, for the same previously defined characteristics, except that the P_2 valency is now taken as 3, we observe very different results. Indeed, one can see here the major influence of the equilibrium constants. These, in this instance, predominate over the differences in saturation values of the stationary phase for each protein, so that displacement of P_1 by P_2, observed in Fig. 3a, is not seen here and will appear only for very high

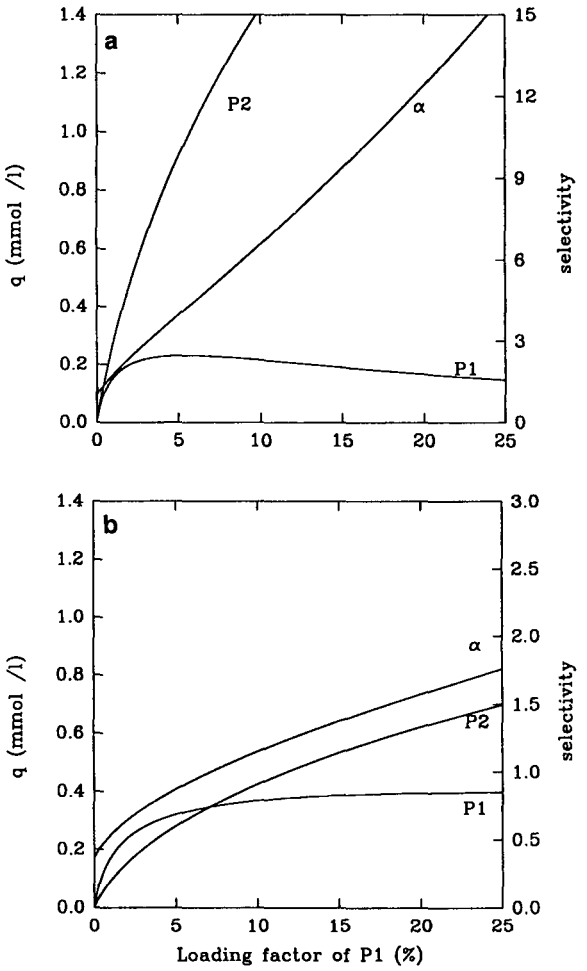

Fig. 3. Selectivity and competitive adsorption isotherms for a 1:1 binary mixture of proteins. $Q_x = 11$ mM; $K_{P_1} = 8200$; $K_{P_2} = 148$; $m_A = 1$; $C_A = 30$ mM. (a) $m_{P_1} = 6$; $m_{P_2} = 2$; (b) $m_{P_1} = 6$; $m_{P_2} = 3$.

loading factors. In other words, the great affinity of P_1 for the stationary phase compensates in a better way for the influence of its high characteristic charge.

In conclusion, we would stress the value of an accurate study of competitive isotherms in order to determine the evolution of the selectivity as a function of the protein load. This will make possible a better understanding of the results of a binary separation and may possibly provide an effective framework to the choice of good operating conditions.

As these few comments about the presented curves have demonstrated numerous parameters are linked to influence the selectivity and this is one of the main advantages of the S.D.M. in accounting, even imperfectly, for their interactions. This also emphasizes the difficulty in establishing general rules about their respective influence.

Isocratic elution and gradient elution

For ion-exchange chromatography, elution is termed isocratic when product separation occurs at a constant counter-ion concentration. When this counter-ion concentration increases during the separation, linearly or not, it is termed gradient elution. Isocratic elution (IE) and gradient elution (GE) are widely used in analytical chromatography, where numerous theoretical studies have contributed to a closer understanding of their characteristics. On the other hand, concerning the preparative mode, very few

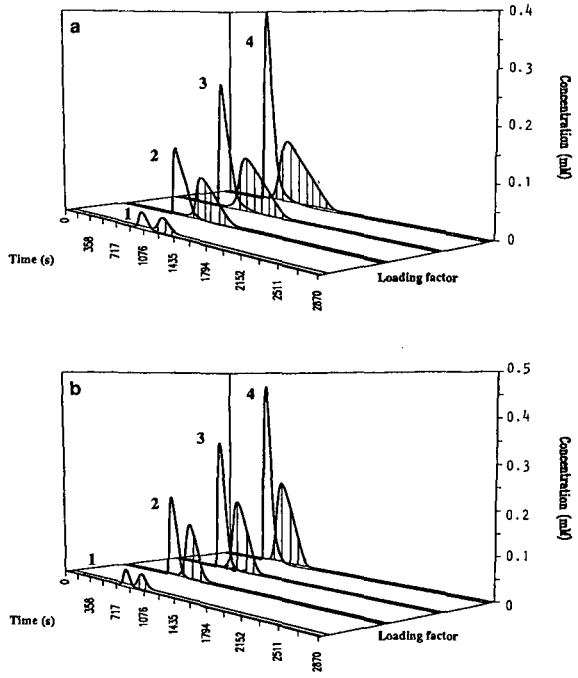

Fig. 4. Gradient elution of a 1:1 binary mixture of proteins in ion-exchange chromatography. Influence of the loading factor and the gradient steepness. (a) $\beta = 0.025$ mM s^{-1}; (b) $\beta = 0.055$ mM s^{-1}. $Q_x = 11$ mM; $L = 5$ cm; $u = 0.01$ cm s^{-1}; $\varepsilon = 0.85$; HETP = 50 μm; $m_{P_1} = 6$; $m_{P_2} = 4$; $m_A = 1$; $C_{A,i} = 20$ mM; $K_{P_1} = 3200$; $K_{P_2} = 640$. (1) $Lf_{P_1} = 2.61$; $Lf_{P_2} = 1.44$; (2) $Lf_{P_1} = 12.96$; $Lf_{P_2} = 8.64$; (3) $Lf_{P_1} = 21.6$; $Lf_{P_2} = 14.4$; (4) $Lf_{P_1} = 30.24$; $Lf_{P_2} = 20.16$.

studies have been devoted to the comparison of these two techniques. For instance, we may quote the work of Antia and Horváth [33], but restricted to reversed-phase chromatography. Our work, in ion-exchange chromatography, was inspired by their study, and some conclusions will prove identical, but specific features of the S.D.M. will be pointed out.

In preparative chromatography, the last steps of the purification usually concern a small number of components. We therefore chose here to study the separation of a mixture of two proteins, P_1 and P_2, with constant relative concentrations (1:1), with $m_{P_1} = 6$ and $m_{P_2} = 4$ as characteristic charges, and with equilibrium constants $K_{P_1} = 3200$ and $K_{P_2} = 640$. The counter ion is monovalent and the ion-exchange column has been described in a previous section. In every case considered, protein P_2 will be the most retained component, and therefore the last eluted.

Fig. 4 shows, for two different values of the gradient steepness, the evolution of chromatograms with increasing values of the loading factor. On a qualitative basis, Fig. 4 is very interesting, as one can observe the global evolution of mixing zones, and these curves will serve as an illustration for our conclusions concerning the comparison of IE and GE.

Fig. 5 presents for each protein P_1 and P_2 the evolution for 98% purity, in GE, of the recovery yield, the enrichment factor and the production rate, as a function of the loading factor of the protein under consideration. As a first general remark, we observe, whatever the gradient steepness, values of the recovery yield, the enrichment factor and the production rate that are always greater for protein P_1 than for P_2. The competition for adsorption sites and the greater affinity of P_2 for the stationary phase explain these results, which are, in fact, the consequence of the displacement of P_1 by P_2. This will be of great interest when the product to be purified is the one that is "pushed", like P_1, and therefore concentrated.

The study of the yield *versus* the loading factor provides very useful information concerning the mixing zones between products. For a fixed gradient steepness, we notice in Fig. 5a and b,

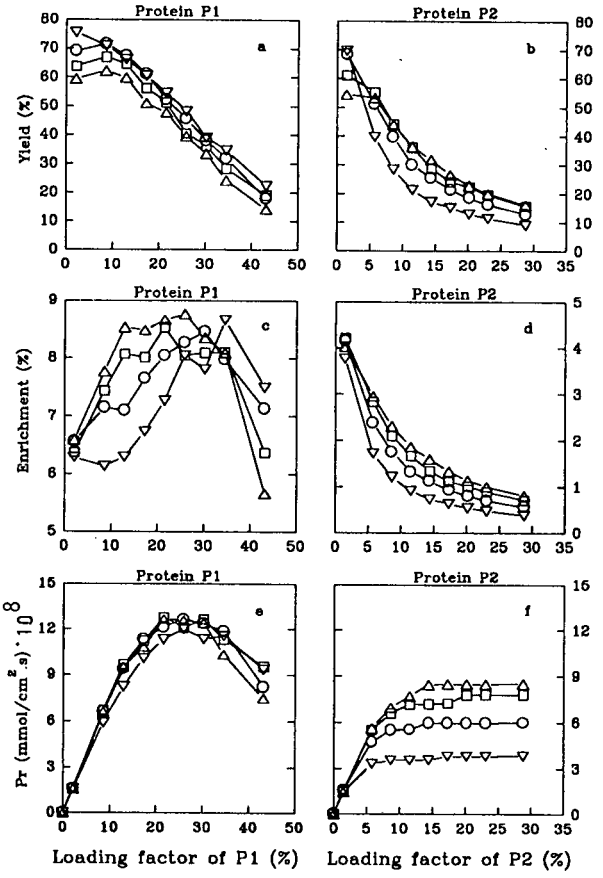

Fig. 5. Gradient elution of a 1:1 binary mixture of proteins in ion-exchange chromatography. Yield, enrichment and production rate as a function of the loading factor, for 98% purity. $L = 5$ cm; HETP = 50 μm; $\varepsilon = 0.85$; $Q_x = 11$ mM; $C_{A,i} = 20$ mM; $u = 0.01$ cm s^{-1}; $m_{P_1} = 6$; $m_{P_2} = 4$; $m_A = 1$; $K_{P_1} = 3200$; $K_{P_2} = 640$. $\nabla = \beta = 0.025$ mM s^{-1}; $\bigcirc = \beta = 0.035$ mM s^{-1}; $\square = \beta = 0.045$ mM s^{-1}; $\triangle = \beta = 0.055$ mM s^{-1}.

for both proteins, a slow decay in the yield when the loading factor increases, leading to a degradation of the separation that could have been qualitatively seen in Fig. 4. For a fixed loading factor, the recovery yield for the P_1 is inversely proportional to the gradient steepness, and this tendency is reversed for P_2, except for low loading factors. As we have seen previously (see Fig. 1), although the selectivity increases with increasing counter-ion concentration, the isotherms become simultaneously more and more oblique, leading to a weaker affinity of the protein for the stationary phase. Therefore, the more the gradient steepness increases, the less

the products are retained and have time to organize themselves in separated bands. This explains the evolution of the recovery yield for P_1 but not for P_2. For the latter, we must consider the tails of P_1 peaks that degrade the P_2 yield. Indeed, these tailings-off shorten as the gradient steepness increases, showing by the way higher displacing effects of the counter ion (Fig. 4).

Finally, there is an increase in selectivity with increasing loading factor (Fig. 1), which explains why the yield of P_1 shows a maximum for a 10% loading factor, except for the lowest gradient steepness (Fig. 5a). Above this value, the selectivity does not increase fast enough to compensate for mixing effects.

The enrichment factor is an important parameter for evaluating the performance of a separation technique and indicates the evolution of the average recovered concentration of a component with respect to the input concentration. The curves in Fig. 5c and d illustrate the displacing power of the counter ion, as one can observe, for both proteins (except for P_1 at loading factors greater than 45%), an enrichment factor in direct proportion to the gradient steepness. In addition, enrichment of P_1 increases with the loading factor, exhibits a maximum at about a 30% loading factor and then drops sharply, because of the predominance of mixing zones. We can say, therefore, that the more the column is loaded, the larger is the added displacing effect of P_2 towards P_1, so much so that the mixing zones remain negligible. P_2 enrichment decreases continuously with increasing loading factor because the tails of P_1, although displaced by P_2 and the counter ion, degrade the P_2 zone in proportion to the load, affecting zones where P_2 is the most concentrated. Respecting a fixed high degree of purity for P_2 leads to the recovery of more and more dilute fractions of P_2, explaining the small values of the enrichment.

The production rate is a useful parameter for an economic evaluation of the process. In Fig. 5e and f, the production rate of P_1 increases to a maximum for a 25–30% value of the loading factor. For P_2, it increases and then stabilizes. Hence, to a certain extent, the injection of concentrated products increases the production rate and compensates, for a while, the appearance of growing mixing zones. A weak effect, for P_1 production rate, of the gradient steepness is also seen in Fig. 5e, up to the attainment of a maximum value. In contrast, the P_2 production rate is greatly dependent on the gradient steepness and increases with increasing linear rate of change of counter-ion concentration at the inlet.

Fig. 6 gives a qualitative illustration of the influence of the loading factor and the counter-ion concentration on chromatograms in IE, and is as relevant as Fig. 4. Fig. 7 shows the same study as Fig. 5, with the same proteins, but undergoing IE. As a first overall comment, one can observe that all the parameters' values in this instance are, whatever the protein, clearly below those obtained in GE. This is an effect of the displacing power of the counter-ion gradient,

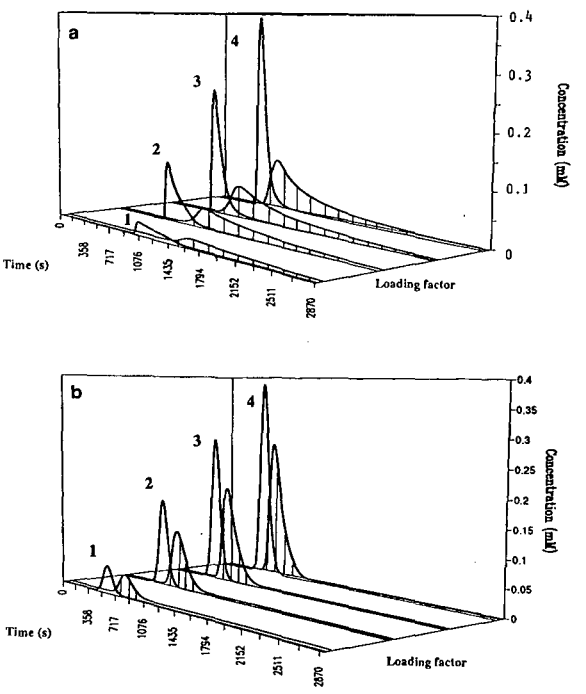

Fig. 6. Isocratic elution of a 1:1 binary mixture of proteins in ion-exchange chromatography. Influence of the loading factor and the counter-ion concentration. (a) $C_A = 25$ mM; (b) $C_A = 40$ mM. $Q_x = 11$ mM; $L = 5$ cm; $u = 0.01$ cm s^{-1}; $\varepsilon = 0.85$; HETP = 50 μm; $m_{P_1} = 6$; $m_{P_2} = 4$; $m_A = 1$; $K_{P_1} = 3200$; $K_{P_2} = 640$. (1) $Lf_{P_1} = 2.16$; $Lf_{P_2} = 1.44$; (2) $Lf_{P_1} = 12.96$; $Lf_{P_2} = 8.64$; (3) $Lf_{P_1} = 21.6$; $Lf_{P_2} = 14.4$; (4) $Lf_{P_1} = 30.24$; $Lf_{P_2} = 20.16$.

which "squeezes" the peaks, concentrates the products and favours the competition for adsorption sites. In addition, we can say that GE reduces the cycle time by limiting appreciably the tail of the last peak [33].

The recovery yield of the two proteins as a function of the loading factor (Fig. 7a and b) shows the same evolution as in GE, *i.e.*, a decrease with increasing loading factor. For a 25 m*M* counter-ion concentration, one can notice (Fig. 7a) that the P_1 recovery yield shows a maximum, accounting for the fact that the selectivity increases with the loading factor and that this augmentation predominates first over the mixing zone increase, whereas for higher counter-ion concentrations substantial mixing occurs rapidly. For a loading factor of P_1 larger than 10%, and as already observed in GE, large counter-ion concentrations lead to too fast an elution for competition phenomena to organize the components in separated zones, and therefore to improve the yield of the separation (see Fig. 7a). Lastly, very weak counter-ion concentration variations result in noticeable differences in yields (they were smaller in the GE case).

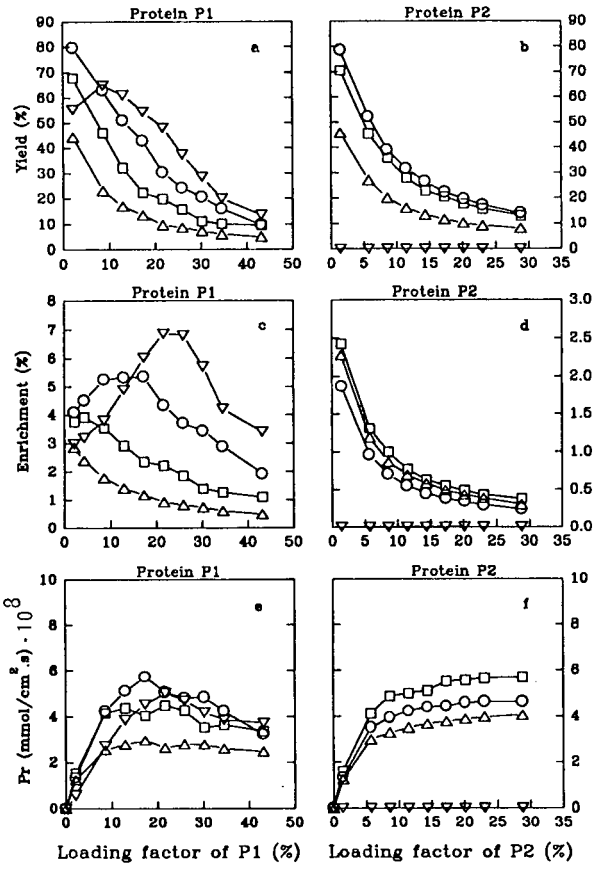

Fig. 7. Isocratic elution of a 1:1 binary mixture of proteins in ion-exchange chromatography. Yield, enrichment and production rate as a function of the loading factor, for 98% purity. $L = 5$ cm; HETP = 50 μm; $\varepsilon = 0.85$; $Q_x = 11$ m*M*; $u = 0.01$ cm s^{-1}; $m_{P_1} = 6$; $m_{P_2} = 4$; $m_A = 1$; $K_{P_1} = 3200$; $K_{P_2} = 640$. $\nabla = C_A = 25$ m*M*; $\circ = C_A = 30$ m*M*; $\square = C_A = 35$ m*M*; $\triangle = C_A = 40$ m*M*.

Concerning the P_2 yield (see Fig. 7b), the same tendencies as for protein P_1 are observed, except for a 25 m*M* counter-ion concentration, where the yield tends to a zero value, whatever the loading factor. These very small values mainly derive from the long tails of the P_1 peaks that "contaminate" P_2 peaks, and because the required purity is high this phenomenon artificially decreases the recovery yield of P_2. Other calculations (not shown here) have revealed that, for a 0.97 purity, the P_2 yield increases sharply, thus confirming this explanation.

It can also be seen that, for a given loading factor and a counter-ion concentration different from 25 m*M*, the influence of the displacing ion concentration on the P_2 yield is not the same as was observed for P_2 in GE. To explain this fact, we must consider that the tails of protein P_2, a direct consequence of a marked non-linearity of the isotherm, are much more spread in IE than in GE, and therefore the yield loss, induced by the tails of protein P_1, affects the results much less as the overlapping of the two peaks is smaller.

The evolution in IE of the enrichment for protein P_2 as a function of the loading factor (see Fig. 7d) is similar to that observed in GE, except for the particular case of a 25 m*M* counter-ion concentration. The enrichment factor for the isocratic case is anyway inferior to the gradient case, demonstrating once again the reduced displacing power of a constant counter-ion concentration.

Concerning protein P_1, we note that enrichment curves (see Fig. 7c) present a maximum. The lower the counter-ion concentration, the higher is this maximum value, the latter being obtained for higher loading factor values. For a

high counter-ion concentration (40 mM), the enrichment factor decays slowly without exhibiting a maximum. These results may be explained if we consider again the influence of the selectivity that depends on protein and counter-ion concentrations. For a low counter-ion concentration and dilute concentrations of injected products, the retention characteristics of the two proteins are more or less similar (see Fig. 1a for a 20 mM counter-ion concentration and analytical conditions), therefore leading to a poor separation. As the loading factor increases, the selectivity increases and protein P_1 is more and more displaced by protein P_2, which results in much more concentrated recovered fractions with respect to P_1. The enrichment reaches a maximum, then drops when mixing zones become too large. The more the counter-ion concentration increases, the more rapidly is the effect of the mixing zones noticed, explaining the movement of the maxima.

The evolution of the production rate of protein P_2 as a function of the loading factor (see Fig. 7f) is similar to that observed in GE, but with lower values. However, there is an optimum 35 mM counter-ion concentration, beyond which the production rate drops sharply. Concerning protein P_1 (Fig. 7e), we would also point out that a counter-ion concentration greater than 30–35 mM results in a noticeable drop in the production rate. Therefore, it is not worthwhile in IE to use high counter-ion concentrations, either for the production rate or for enrichment.

In conclusion in this section, we would stress once again the value of the S.D.M. in investigating optimum operating conditions for a separation, but we must add, as did Ghodbane and Guiochon [38] in their study on reversed-phase chromatography, that it is very difficult, at a quantitative level, to extrapolate these results to other protein mixtures. On the other hand, it seems that the overall evolution of the parameters under study may be observed in other situations, provided that the latter remain conventional. However, considering non-standard configurations, very surprising results may arise, as will be seen in the next section.

Particular case of a separation markedly favoured by a selectivity inversion

In this section, we shall show that a rapidly varying selectivity (with respect to the loading factor) and corresponding to the case in Fig. 3a, may result in increasing yields and production rates when operating at a preparative level. Antia and Horváth [33] have also shown, in reversed-phase chromatography, that the more

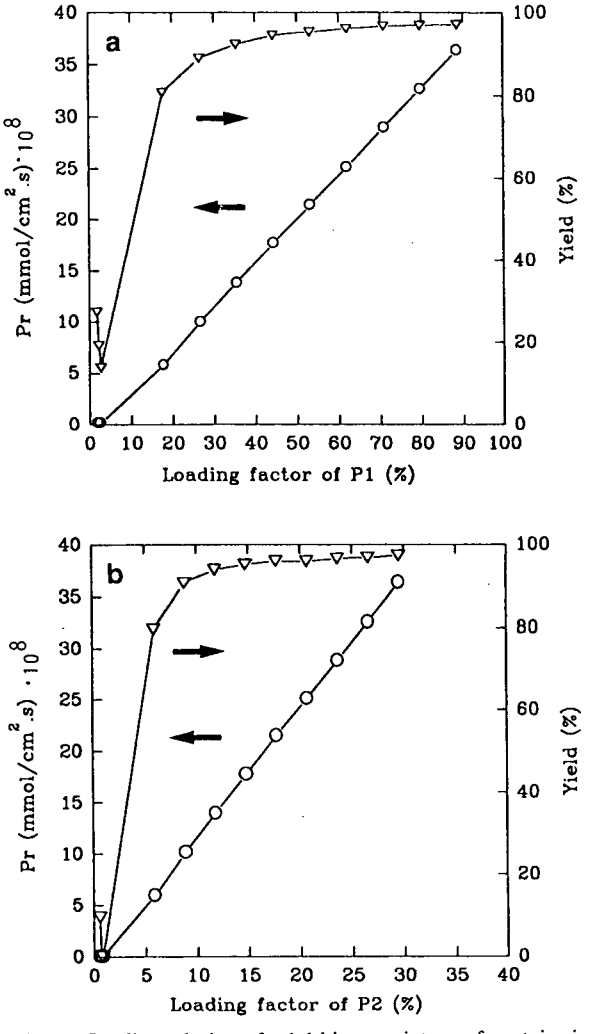

Fig. 8. Gradient elution of a 1:1 binary mixture of proteins in preparative ion-exchange chromatography. Yield and production rate for 98% purity, as a function of load. $L = 5$ cm; HETP = 50 μm; $\varepsilon = 0.85$; $\beta = 0.005$ mM s^{-1}; $Q_x = 11$ mM; $u = 0.01$ cm s^{-1}; $m_{P_1} = 6$; $m_{P_2} = 2$; $m_A = 1$; $K_{P_1} = 8200$; $K_{P_2} = 148$. (a) Protein P_1; (b) protein P_2. ○ = Production rate; ▽ = yield.

saturated the stationary phase is in the products they considered, the greater is the tendency for them to separate.

The two proteins P_1 and P_2 considered here were the same as above (see Fig. 3). Their characteristic charges are $m_{P_1} = 6$ and $m_{P_2} = 2$ and their equilibrium constants $K_{P_1} = 8200$ and $K_{P_2} = 148$. As we already specified in the comments on Fig. 3, these two proteins have very dissimilar maxima adsorption capacities, which explains the rapid evolution of the selectivity with respect to the loading factor. Proteins are injected in equimolar concentration on to the column previously equilibrated at a 20 m*M* counter-ion concentration, the latter being monovalent. The separation is performed in GE with a very low gradient steepness ($\beta = 0.005$ m*M* s^{-1}) in order to eluate the products slowly enough. Fig. 8a and b show the evolution of the yield and the production rate *versus* the loading factor of each protein and Fig. 9 shows, for different loading factors, the shape of the chromatograms for this separation.

It is noted first that the loading factor of protein P_1, whose characteristic charge is the larger, reaches high values, greater than 80%. Protein P_2, with a lower characteristic charge, although injected at the same concentration as P_1, saturates the stationary phase very slowly and does not pass beyond a 30% loading factor

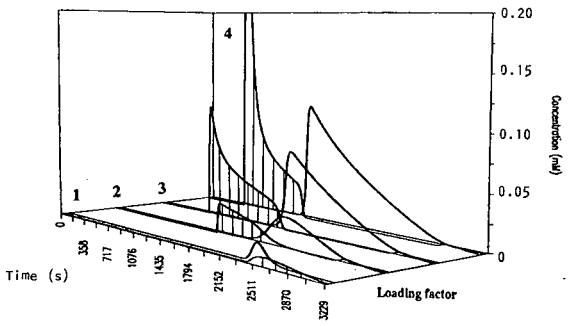

Fig. 9. Gradient elution of a 1:1 binary mixture of proteins in preparative ion-exchange chromatography. Influence of the load. $\beta = 0.005$ m*M* s^{-1}; $Q_x = 11$ m*M*; $L = 5$ cm; $u = 0.01$ cm s^{-1}; $\varepsilon = 0.85$; HETP = 50 μm; $m_{P_1} = 6$; $m_{P_2} = 2$; $m_A = 1$; $C_{A,i} = 20$ m*M*; $K_{P_1} = 8200$; $K_{P_2} = 148$. (1) $Lf_{P_1} = 1.72$; $Lf_{P_2} = 0.576$; (2) $Lf_{P_1} = 8.6$; $Lf_{P_2} = 2.88$; (3) $Lf_{P_1} = 25.8$; $Lf_{P_2} = 8.64$; (4) $Lf_{P_1} = 43$; $Lf_{P_2} = 14.4$.

value, leading to different scales for the two graphs in Fig. 8a and b.

In highly dilute solutions, at a 20 m*M* counter-ion concentration, proteins P_1 and P_2 can easily be separated in IE ($\alpha = k'_2/k'_1 = 0.19$, where k'_1 and k'_2 are the respective capacity factors). Let us specify that, under these conditions, protein P_1 is the most retained component (see the definition of the selectivity, eqn. 21). Indeed, its equilibrium constant ($K_{P_1} = 8200$) is much higher than that of P_2, and at the analytical level its poor saturation capacity ($Q_{X_{P_1}} = 1.83$) does not exert a great influence. Using GE, under the same analytical conditions as above, the separation is also good and protein P_1 is still eluted last.

At low loading factor values, the quality of the separation diminishes with increasing loading factor, as the selectivity quickly reaches a value of 1, indicating a similar affinity for both proteins (see Fig. 3a, for a 30 m*M* counter-ion concentration). The observed yield therefore drops and the production rate remains negligible. Under these conditions, we may note, on curve 1 in Fig. 9, the poor quality of the separation. As the selectivity increases continuously with increasing the loading factor, one can see an improvement in the separation through a rapid increase in the yield, up to nearly 100%, and through the linear increase of the production rate in proportion to the loading factor. Protein P_2 is now the most retained component.

Finally, two proteins, separable at an analytical level, may surprisingly show, after an inversion of the elution order, high yields and considerable production rates at a preparative level, provided that their selectivity increases very sharply with the loading factor. This result is noteworthy, but we must keep in mind that the S.D.M., which has made such calculations possible, has its limitations and its validity decreases at too high protein concentrations [7]. It is still a very useful tool that has brought to light such unconventional situations that appear probable but still deserve experimental validation.

As a conclusion to this section, it has been shown that an advantage of the S.D.M. lies in its multi-parameter character. Indeed, when experimenting in the zone where the selectivity was

near to 1, and considering that the retention time was the essential parameter, one is tempted to believe that proteins showing similar chromatographic behaviour also have similar ion-exchange interactions with the stationary phase. One might therefore have directed efforts toward modifying this interaction. In fact, as has been demonstrated here, this situation resulted from a coincidence as regards the retention time governed by two separate parameters, *i.e.*, the characteristic charge of the protein and its equilibrium constant, and this does not invalidate the ion-exchange process, merely the operating conditions chosen. Although this situation has been artificially constructed here, it serves as a clear example of the new insight given by this approach.

CONCLUSION

The stoichiometric displacement model is a first step in the understanding of protein adsorption mechanisms occurring during an ion-exchange process, and it provides a simple tool for investigating the behaviour of these polymeric ions. Although it is still restricted by oversimplified hypotheses, it remains an interesting research topic that in the future will undergo, more or less important modifications of its theoretical bases.

The work presented here has illustrated the competitive adsorption of two proteins and has considered the influence of various relevant parameters such as the counter-ion concentration, the loading factor and the saturation value of the stationary phase concentration for the protein. The preliminary study of the selectivity from competitive isotherms has proved to be a good data source in understanding isocratic or gradient elution and we have stressed the value of using gradient elution in the preparative mode. All these computations were done with a computer program, written in FORTRAN, and there is no major problem in extending its use to mixtures with more than two proteins.

Work is in progress to check experimentally the validity of the S.D.M., and to provide actual values of the parameters in our computations.

SYMBOLS

$C_{A,i}$	Initial counter-ion concentration (kmol m^{-3})
$C_{i,0}$	Concentration of component i at the column entrance (kmol m^{-3})
C_i	Concentration of component i in the flowing mobile phase (kmol m^{-3})
$D_{i,ap}$	Apparent diffusion coefficient of component i (m^2 s^{-1})
$D_{i,ax}$	Axial dispersion coefficient of component i (m^2 s^{-1})
$D_{i,m}$	Molecular diffusion coefficient of component i in the flowing mobile phase (m^2 s^{-1})
d_p	Particle diameter (m)
E_i	Enrichment factor of component i
F	Phase ratio of the column packing $[=(1-\varepsilon)/\varepsilon]$
h	Reduced plate height $(=H/d_p)$
H	Height equivalent to a theoretical plate (HETP) (m)
K_i	Equilibrium constant of component i
k_0	Average value of all the initial slopes of the components' individual isotherms
k'_i	Capacity factor for component i
L	Column length (m)
Lf_i	Load factor of component i
m_A	Valency of the counter ion
m_i	Characteristic charge of the protein i
M	Molecular mass (g mol^{-1})
N	Number of theoretical plates $(=L/$ HETP)
N_c	Number of components
P	Courant number
Pr_i	Production rate of component i (kmol m^{-2} s^{-1})
Q_x	Maximum loading capacity of the exchanger (kmol m^{-3})
Q_{x_i}	Saturation value of stationary phase concentration for component i $(=Q_x/m_i)$
q_i	Concentration of component i adsorbed on the stationary phase (calculated per unit volume of particle skeleton) (kmol m^{-3})
S	Column cross-sectional area (m^2)
t	Time coordinate (s)
t_1, t_2	Integration limits for eqns. 18–20 (s)
t_c	Cycle time (s)

t_{inj} Time of feed introduction (s)
t_0 Residence time of an unretained compound (s)
T_i Mass distribution coefficient; ratio between the amount of component i in the stationary and the mobile phases ($= q_i/C_i$)
u Interstitial fluid velocity (m s^{-1})
V_{inj} Volume of feed injection (m^3)
Z Stoichiometric charge ratio of the protein and the counter ion
z Axial coordinate (m)
Y_i Recovery yield of component i

Greek letters

α Selectivity [$= (q_i/C_i)/(q_j/C_j)$]
β Linear rate of change of counter-ion concentration at the inlet (kmol m^{-3} s^{-1})
ε Total porosity of the column packing
ν Reduced mobile phase velocity ($= ud_p/D_m$)
ν_{opt} Optimum reduced mobile phase velocity
σ Space increment of the grid for the finite difference method (m)
τ Time increment of the grid for the finite difference method (s)

REFERENCES

1 R.R. Drager and R.E. Regnier, *J. Chromatogr.*, 359 (1986) 147.
2 D.R. Jenke, *Anal. Chem.*, 56 (1984) 2674.
3 F. Murakami, *J. Chromatogr.*, 198 (1980) 241.
4 P. Jandera, M. Janderová and J. Churácek, *J. Chromatogr.*, 148 (1978) 79.
5 M.S. Saunders, J.B. Vierow and G. Carta, *AIChE. J.*, 35 (1989) 53.
6 S.R. Dye, J.P. DeCarli, II and G. Carta, *Ind. Eng. Chem. Res.*, 29 (1990) 849.
7 P. Cysewski, A. Jaulmes, R. Lemque, B. Sébille, C. Vidal-Madjar and G. Jilde, *J. Chromatogr.*, 548 (1991) 61.
8 R.D. Whitley, R. Wachter, F. Liu and N.-H.D. Wang, *J. Chromatogr.*, 465 (1989) 137.
9 H.F. Walton, in E. Heftmann (Editor), *Chromatography*, Van Nostrand Reinhold, New York, 1975, p. 312.
10 N.K. Boardman and S.M. Partridge, *Biochem. J.*, 59 (1955) 543.
11 W. Kopaciewicz, M.A. Rounds, J. Fausnaugh and F.E. Regnier, *J. Chromatogr.*, 266 (1983) 3.
12 A. Velayudhan and Cs. Horváth, *J. Chromatogr.*, 367 (1986) 160.
13 A. Velayudhan and Cs. Horváth, *J. Chromatogr.*, 443 (1988) 13.
14 F. Helfferich, *Ion Exchange*, McGraw-Hill, New York, 1970.
15 W.R. Melander, Z. El Rassi and Cs. Horváth, *J. Chromatogr.*, 469 (1989) 3.
16 Cs. Horváth, W.R. Melander and Z. El Rassi, *9th International Symposium on Column Liquid Chromatography, Edinburgh, July 1–5, 1985*, Lecture PL 3.3.
17 J.C. Bellot and J.S. Condoret, *Process Biochem.*, in press.
18 J.C. Bellot and J.S. Condoret, *Process Biochem.*, 26 (1991) 363.
19 P.C. Haarhof and H.J. Van der Linde, *Anal. Chem.*, 38 (1966) 573.
20 G. Guiochon, S. Golshan-Shirazi and A. Jaulmes, *Anal. Chem.*, 60 (1988) 1856.
21 S. Golshan-Shirazi, B. Lin and G. Guiochon, *Anal. Chem.*, 61 (1989) 1960.
22 A.M. Katti, J.-X. Huang and G. Guiochon, *Biotechnol. Bioeng.*, 36 (1990) 288.
23 J.C. Giddings, *Dynamics of Chromatography. Part 1, Principles and Theory*, Marcel Dekker, New York, 1966.
24 M. Czok and G. Guiochon, *Anal. Chem.*, 62 (1990) 189.
25 P. Rouchon, M. Schonauer, P. Valentin and G. Guiochon, *Sep. Sci.*, 22 (1987) 1793.
26 G. Guiochon and S. Ghodbane, *J. Phys. Chem.*, 92 (1988) 3682.
27 S. Golshan-Shirazi and G. Guiochon, *Anal. Chem.*, 60 (1988) 2364.
28 B.-C. Lin, S. Golshan-Shirazi, Z. Ma and G. Guiochon, *Anal. Chem.*, 60 (1988) 2647.
29 M. Czok and G. Guiochon, *Comput. Chem. Eng.*, 14 (1990) 1435.
30 B.-C. Lin, Z. Ma and G. Guiochon, *J. Chromatogr.*, 484 (1989) 83.
31 M.T. Tyn and T.W. Gusek, *Biotechnol. Bioeng.*, 35 (1990) 327.
32 J.H. Knox, *J. Chromatogr. Sci.*, 15 (1977) 352.
33 F.D. Antia and Cs. Horváth, *J. Chromatogr.*, 484 (1989) 1.
34 A.M. Katti and G. Guiochon, *Anal. Chem.*, 61 (1989) 982.
35 F.E. Regnier and I. Mazsaroff, *Biotechnol. Prog.*, 3 (1987) 22.
36 S. Golshan-Shirazi and G. Guiochon, *J. Chromatogr.*, 545 (1991) 1.
37 M.D. LeVan and T. Vermeulen, *J. Phys. Chem.*, 85 (1981) 3247.
38 S. Ghodbane and G. Guiochon, *J. Chromatogr.*, 444 (1988) 275.

Journal of Chromatography, 635 (1993) 19–30
Elsevier Science Publishers B.V., Amsterdam

CHROM. 24 845

Normal-phase high-performance liquid chromatography with highly purified porous silica microspheres☆

J.J. Kirkland*, C.H. Dilks, Jr. and J.J. DeStefano

Rockland Technologies, Inc., 538 First State Boulevard, Newport, DE 19804 (USA)

(First received October 28th, 1992; revised manuscript received December 17th, 1992)

ABSTRACT

Column reproducibility and peak shapes are improved for polar and basic solutes in normal-phase chromatography using new highly purified, low-acidity unmodified porous silica microspheres. The chromatographic characteristics of this new type B silica are compared with a conventional type A silica to determine the type and level of mobile phase modifiers needed for good results. The effect of sample type and sample loading on retention, column efficiency and peak shape also was measured. Critical normal-phase tests compared this new silica with several commercial silicas. The new silica shows special promise for developing rugged separation methods to analyze polar and basic compounds that traditionally are handled by reversed-phase chromatography. Normal-phase chromatography is well-suited for highly organic-soluble compounds and certain structures such as positional isomers.

INTRODUCTION

Normal-phase (NP) chromatography is a powerful complement to the more popular RP-HPLC method for separating non-ionic compounds. Recent surveys show that about one fifth of all HPLC separations now are performed by NP-HPLC [1]. Advantages for this method include the ability to operate with totally organic mobile phases of high solute solubility, which is especially important in preparative applications. NP-HPLC also shows extensive capability for selectivity changes by varying mobile phase constituents [2,3]. The ability to make band spacing changes with NP-HPLC usually exceeds that of the widely used reversed-phase method. NP-HPLC methods are especially useful for separating difficult mixtures containing positional isomers [3,4].

Current NP-HPLC applications commonly use columns containing polar bonded phases (*e.g.*, cyano- diol-, etc.) [5]. Columns containing unmodified silica are less popular, because of problems in maintaining a constant surface activity for repeatable separations. Conversely, retention with bonded-phase NP-HPLC columns generally is more consistent, because of the insensitivity to small concentrations of water in the sample or the mobile phase [6]. Also, there are problems in obtaining unmodified chromatographic silica with reproducible separation characteristics, as seen in the present study. Therefore, the chromatographic reproducibility of bonded-phase columns for NP-HPLC generally is viewed as superior to columns of unmodified silica [7]. Finally, polar bonded-phase columns are less retentive in NP-HPLC than those with unmodified silica, often permitting the elution of highly

* Corresponding author.

☆ This material was presented in part at the *16th International Symposium on Column Liquid Chromatography, Baltimore, MD, June 1992*. The majority of the papers presented at this symposium were published in *J. Chromatogr.*, Vols. 631 + 632 (1993).

polar compounds that are eluted with difficulty from the more retentive unmodified silica [6,8].

A common problem with unmodified silica columns with totally organic solvents is that polar compounds often show broad, tailing peaks, especially for basic components. This condition can exist even when the mobile phase contains basic additives designed to minimize this effect. Such undesirable characteristics complicate the design of rugged and reproducible quantitative methods. As a result, unmodified silica columns are not widely accepted for quantitative analyses.

On the other hand, basic compounds have been separated on unmodified silica with good band shapes using reversed-phase conditions where water was a major constituent of the mobile phase [9]. Biddlingmeyer *et al.* [10] reported that some basic drugs produced satisfactory peak shapes on silica gel using reversed-phase eluents. These and other studies (*e.g.*, ref. 11) suggest that unmodified silica, when properly deactivated with water or other strongly sorbing polar compounds, can be successfully used for separating basic and other polar solutes with good peak shape and desirable properties for quantitation.

Unmodified silica columns present a special problem that must be solved for reproducible separations: the activity of the adsorbent surface must be maintained constant [12]. The most effective procedure to stabilize this surface activity is to control the level of water adsorbed to the silica surface. This often is accomplished by fixing the concentration (humidity) of water in the mobile phase [12], a procedure viewed as awkward by many users. So, polar, usually protic, mobile phase modifiers such as methanol or propanol typically are used instead of water to control surface activity. Use of protic organic modifiers generally is successful in NP-HPLC. But, misshapen or tailing peaks can occur as a result of highly non-linear and unusual adsorption isotherms that result from such systems [11,13]. The fundamental problem remains, however, that commercial unmodified chromatographic silica often exhibits an inhomogeneous adsorbing surface. This situation can result in broad, poorly shaped peaks when used for separating many polar solutes, and especially compounds such as basic drugs.

All silica particles for HPLC are not alike. Different chromatographic silicas can vary greatly in their separation characteristics, primarily because of variations in the type and structure of silanol groups on the surface, as illustrated in Fig. 1. Silicas with a high population of unbonded silanol groups generally are more acidic and "less friendly" in the separation of many polar and basic solutes. Geminal silanols are less acidic, and less of a problem for such solutes. Silicas with a high population of internally bonded or associated silanols also are less acidic, and "more friendly" for separating polar and basic compounds [14,15]. Contamination of the silica with certain metals such as iron and nickel can cause tailing peaks with compounds that form complexes with these contaminants. Finally, inclusion of other contaminants such as aluminum in the silica lattice activates and intensifies the acidity of silanol groups [16].

Previous studies have shown that chromatographic silicas can be arbitrarily classified into types to define their potential utility as supports in reversed-phase chromatography [14,15]. So-called type A silicas generally are more acidic and less purified. These materials apparently have less energy-homogeneous surfaces, and are more likely to exhibit tailing, misshapen peaks with more polar or basic solutes. Type B silicas are more highly purified and less acidic, and often are preferred for many RP-HPLC applications [17]. Some silicas, however, exhibit intermediate properties, as verified by data presented below, and by other sources [7,17].

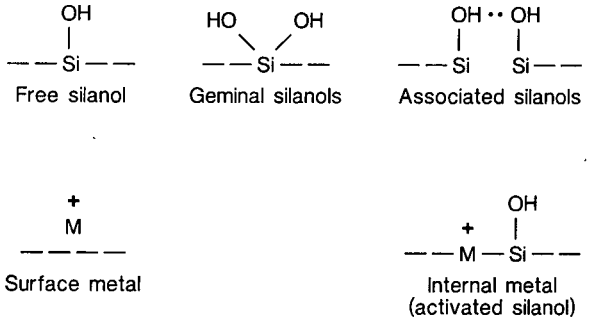

Fig. 1. The surface of silica supports for HPLC.

The present study was designed to determine the characteristics of a new porous silica microsphere, Zorbax Rx-SIL, for use in NP-HPLC (sometimes called adsorption chromatography). We postulated that the high purity (>99.995%) and low surface acidity of this type B silica could minimize or eliminate some of the problems normally associated with conventional unmodified silicas for NP-HPLC. To define utility, we studied the type and level of mobile phase modifiers required for best operation. The effect of sample type on column efficiency and peak shape also was determined. The chromatographic properties of Zorbax Rx-SIL were compared to conventional chromatographic silicas, to define the best areas of potential utility for this new silica.

EXPERIMENTAL

Separations were performed with a Model 870 pump (DuPont, Wilmington, DE, USA) with the columns at ambient temperature. Detection was with a DuPont Model 860 UV detector at 254 nm. Sample injection was with a Model 7125 sample valve (Rheodyne, Cotati, CA, USA) with a 10-μl sample loop, unless otherwise noted. HPLC-grade solvents were obtained from Baker Chemicals (Phillipsburg, NJ, USA) and EM Science (Gibbstown, NJ, USA).

Dichloromethane was used as the principal organic mobile phase constituent in this study. Various water levels in dichloromethane mobile phases were established by appropriately blending dry solvent (v/v) with water-saturated solvent in the manner previously described [11]. "Dry" dichloromethane was prepared by treating with molecular sieve type 4A pellets (EM Science, Gibbstown, NJ, USA) overnight. "Wet" dichloromethane was prepared by equilibrating overnight with EM Science Grade 12 silica gel (29–200 mesh) containing 20% (w/w) of deionized water, as described in ref. 12. Mobile phases modified with protic solvents were prepared on a mass percent basis.

Highly purified dichloromethane is needed to obtain reproducible separations with unmodified silica. Some as-received HPLC-grade dichloromethane contains impurities that deleteriously change the surface of the silica. The same experience was found with dichloromethane that was allowed to stand in previously opened bottles for several days. Measurements with deionized water equilibrated with suspect dichloromethane showed a lower pH compared to satisfactory solvent. This result suggests the breakdown of dichloromethane to yield acidic impurities in the presence of light, air and water vapor. If contaminated with impurities from off-grade dichloromethane, columns usually can be regenerated by extensive purging with HPLC-grade methanol containing 10% deionized water.

All columns were equilibrated with at least thirty column volumes of a new mobile phase before taking data. (Because of the low viscosity of totally organic solvents, this equilibration can be performed rapidly at high flow-rates.) Duplicate measurements were made to ensure complete column equilibration.

Benzyl alcohol, benzanilide, acetoacetanilide, catechol and 4-acetamidophenol were from Sigma (St. Louis, MO, USA). Caffeine was from Fisher Scientific (Fairlawn, NJ, USA). Quinoxaline and 3-pyridyl-acetonitrile were obtained from Aldrich (Milwaukee, WI, USA). Sulfanilamide was from U.S.P.C. (Rockville, MD, USA). PolyScience (Niles, IL, USA) supplied the herbicide mixture, and the plant growth hormones were from ICN Biochemicals (Cleveland, OH, USA). All test solutes were used as received.

Zorbax-SIL and Zorbax Rx-SIL columns were prepared internally. Similar columns are available from Mac-Mod Analytical (Chadds Ford, PA, USA). Zorbax-SIL columns contain a silica with a nominal surface area of 330 m^2/g. This silica arbitrarily was used as a model for type A silica during this study. As documented below, this silica is similar in characteristics to several of the type A silicas studied during this work. Zorbax Rx-SIL is a type B silica with a nominal surface area of 180 m^2/g. Typical analysis of impurities for this silica by inductively coupled plasma atomic-emission spectroscopy is: Na: 10 ppm (w/w); Ca: 4 ppm; K: <3 ppm; Al: <10 ppm; Mg: 4 ppm; Zn: 1 ppm; total: <35 ppm (no other impurities detected; 99.995% silica). All other silica columns were obtained either from Alltech, or directly from the manufacturer. All

columns tested were 15 × 0.46 cm I.D. unless otherwise noted. Particle sizes of the packings in all columns were nominally 5 μm. Chromatographic results were monitored with a Chrom-Perfect data station (Justice Innovations, Palo Alto, CA, USA).

RESULTS AND DISCUSSION

Water-deactivation of silica

Previous studies have shown that deactivation of the unmodified silica surface is required for reproducible separations with good column efficiency and sample loadability [2,11,12]. Highly polar modifiers in the organic mobile phase bind to ("hot") sites of very high energy on the silica surface. The purpose of these modifiers is to compete for these "hot" sites more effectively than the solute molecules that are to be separated. The result is that the surface of the modified silica then is more energy-homogeneous —a more linear isotherm results. This condition provides for improved column efficiency, better peak asymmetry, and higher sample loadability.

Water previously has been found to be the best deactivating agent, even though maintaining the proper water level in immiscible mobile phase solvents often is deemed as inconvenient [2,4,5]. The level of water in the mobile phase needed to optimize performance depends on the type of silica used for the packing. Therefore, a study was made on the influence of water level modifier in the organic mobile phase on solute retention, column efficiency, peak asymmetry and sample loadability.

The effect of water content in dichloromethane mobile phase on the retention of benzanilide for a typical type A silica and the new type B silica is compared in Fig. 2. This plot shows that as the amount of water increases (measured as percent of water saturation for the organic solvent), retention (k') decreases as the silica surface is deactivated. The k' *versus* percent mobile phase water-saturation plot for the type A silica shows a steeper curvature at lower water concentrations. Conversely, the type B silica shows a flatter plot as the water concentration is decreased. These effects suggest better surface homogeneity for the type B silica. Similar effects were found for phenol and benzyl alcohol as solutes. Absolute differences in retention for the two silicas is a function of differences in surface area. These and previous [11] results suggest that a 50% water-saturated mobile phase (1:1 v/v blend of "wet" and "dry" solvents) is a desirable compromise for water-deactivated systems with both silicas; retention is maintained and is less sensitive to small changes in water content.

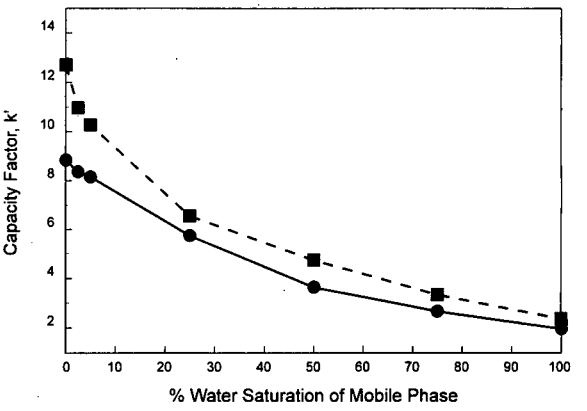

Fig. 2. Effect of mobile phase water content on retention for different silica types. Columns: 15 × 0.46 cm I.D.; mobile phase: dichloromethane; flow-rate: 1.0 ml/min; solute: 0.5 μg of benzanilide; temperature: ambient. ■ = Zorbax-SIL (type A); ● = Zorbax Rx-SIL (type B).

The effect of mobile phase water content on column efficiency is more striking for the two silica types, as shown in Fig. 3. The new type B

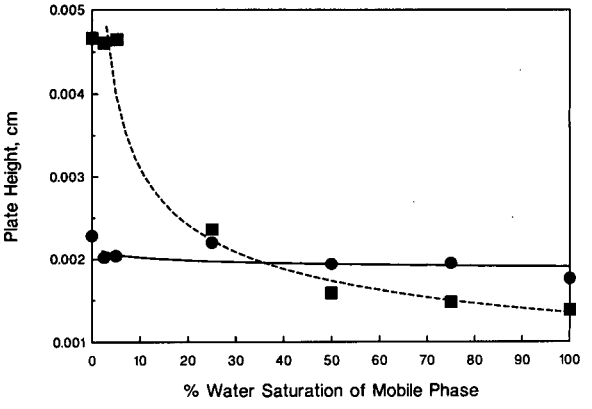

Fig. 3. Effect of mobile phase water content on column efficiency for different silica types. Conditions and symbols as in Fig. 1, except 38 μg of benzyl alcohol as solute.

silica shows little variation in the plate height of benzyl alcohol with varying water content in the mobile phase. On the other hand, the type A silica shows much poorer column efficiency (larger plate heights) at low water concentration. For dry dichloromethane the column plate height for the type A silica is more than twice that for the type B silica. Similar effects were found with benzanilide as the solute. These results suggest a non-linear adsorption isotherm for the type A silica at low water concentrations in the mobile phase. The new type B silica can be used with a wider range of water modifier concentration with little effect on separation resolution.

Peak asymmetries for benzanilide were strikingly different with varying amounts of water in the mobile phase for the two silicas, as illustrated in Fig. 4. The type A silica shows peak asymmetry values [11] in the 1.5–2.0 range with up to about 25% water saturation of the dichloromethane. As more water is added to dichloromethane, peak symmetry continuously improved. At 100% saturation, a nearly symmetrical peak was found. Conversely, with the type B silica, benzanilide showed a peak asymmetry value of *ca.* 1.4 with "dry" solvent, and an essentially symmetrical peak with all mobile phases with >10% water saturation. These data again suggest the superior surface homogeneity of the new type B silica.

The above conclusions are based on the premise that a heterogeneous silica surface leads to isotherm non-linearity and the related phenomena of large plate heights and asymmetric, tailing peaks. These effects are discussed in detail in ref. 2, and the data of this study appear to support this concept. Since peak broadening and peak tailing also are influenced by sample size, small samples were used in this study to minimize this effect, as described below. It also should be noted that kinetic effects involving slow solute adsorption/desorption can affect plate heights and peak asymmetries. Additional studies with the two silica types are needed to measure possible differences in kinetic effects.

Sample loading effects on solute retention are similar for the two silica types with 50% water-saturated dichloromethane mobile phase, as shown in Fig. 5. Depending on the solute, up to 0.01–0.1 mg of sample/g of packing is allowed before a 10% change in k' occurs. Sample loadability is surface-area dependent, so the absolute solute loadability of Zorbax SIL is higher than that of Zorbax Rx-SIL. Similar results were found for phenol as the solute. It should be noted that 50% water-saturated dichloromethane mobile phase was arbitrarily selected because of the practicality of this system. Had mobile phase with less water been used, the differences between the two silicas probably would have been more striking, as suggested by the results in Fig. 2.

The effect of sample loading on column ef-

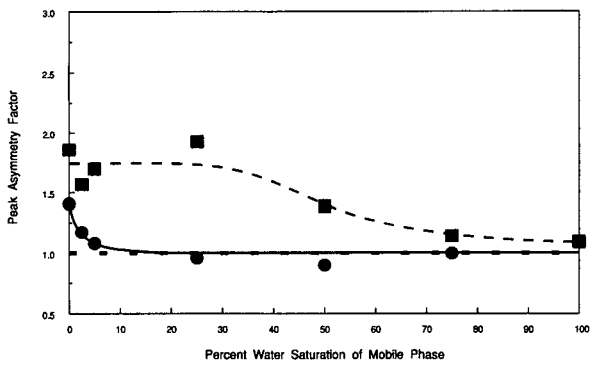

Fig. 4. Effect of mobile phase water content on peak asymmetry for different silica types. Conditions and symbols as in Fig. 1. -- (Peak asymmetry factor = 1) = symmetrical peak.

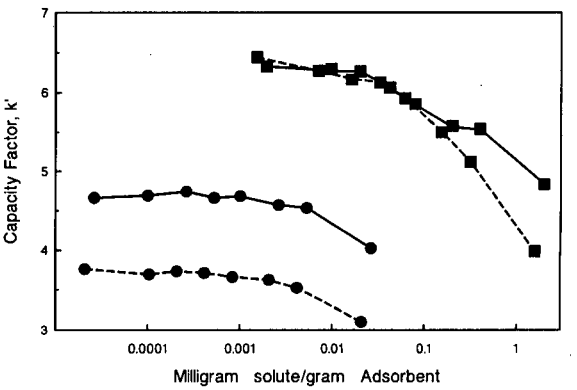

Fig. 5. Effect of solute loading on retention for different water-deactivated silica types. Conditions as in Fig. 1, except 50% (v/v) water-saturated dichloromethane; varying amounts of (■) benzyl alcohol and (●) benzanilide solutes. Solid lines: Zorbax-SIL (type A); dashed lines: Zorbax Rx-SIL (type B).

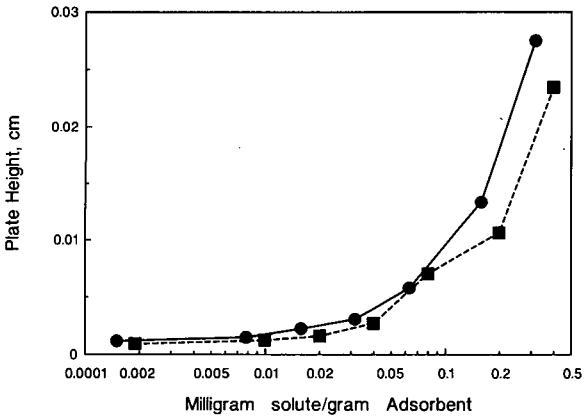

Fig. 6. Effect of solute loading on column efficiency for different water-deactivated silica types. Conditions as in Fig. 5, except benzyl alcohol as solute. ■ = Zorbax-SIL (type A); ● = Zorbax Rx-SIL (type B).

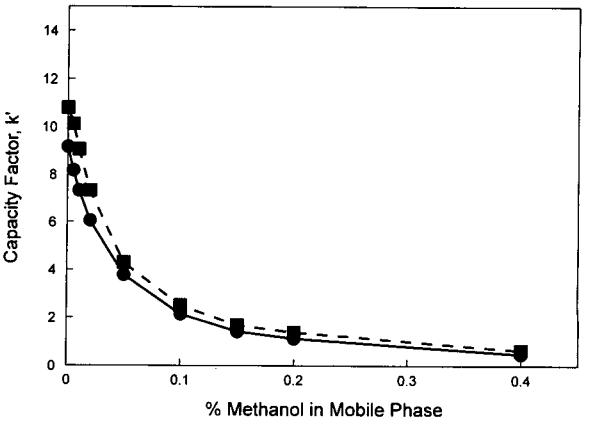

Fig. 7. Effect of methanol as modifier on retention for different silica types. Conditions and symbols as in Fig. 1, except methanol modifier; solute, 0.5 μg of benzanilide.

ficiency also is similar for the two silica types with water-saturated dichloromethane as the mobile phase, as shown in Fig. 6. Sample loadability is essentially equivalent for the two silicas, with small variations dependent on differences in packing surface area. In this system, 0.02–0.05 mg of sample was allowed before a significant change occurred in column efficiency. Again, differences between the two silicas were moderated by using 50% water-saturated mobile phase; lower concentrations of water would have accentuated differences, as indicated by the results in Fig. 3.

Deactivation of silica with protic modifiers

As mentioned above, many users consider the necessity to maintain a constant amount of water modifier in the organic mobile phase as experimentally awkward. Because of convenience, other highly-polar, organic-miscible modifiers such as methanol and propanol often are used in normal-phase separations to control and maintain the activity of the silica adsorbent. These polar organic compounds strongly bind to the silica surface, although they do not hold as tightly as water [2,18]. Because of the convenience of protic-solvent modifiers, a study was made with methanol and propanol to determine their effect on type A and B silicas.

Fig. 7 shows the effect of methanol concentration in dichloromethane phase on the capacity factor, k', of benzanilide. Similar results were found for the two silica types; both show sharply increasing k' *versus* percent methanol characteristics at low methanol concentrations. Small absolute k' differences are due to different packing surface areas. These results suggest that methanol-modified silica surfaces are less homogeneous than the water-modified silica of Fig. 2. Stated otherwise, water is a more effective deactivating agent than methanol, as previously noted [11,18]. The smaller change in k' for >0.1% methanol-modified dichloromethane suggests that at least 0.1% methanol should be used to ensure retention reproducibility for normal-phase separations.

But, the type A silica shows large changes in the plate height of benzanilide with different methanol-modifier concentrations, as illustrated in Fig. 8. Optimum plate height for the type A silica only is reached when 0.4% methanol modifier is used. In contrast, The new type B silica showed a constant plate height throughout the entire 0–0.4% methanol concentration range studied. These results again suggest the superior surface-energy homogeneity of the new type B silica.

Peak symmetries for benzanilide with 0.05% methanol modifier paralleled plate height results for the two silicas, as given in Fig. 9. Tailing peaks for the type A silica were eliminated only

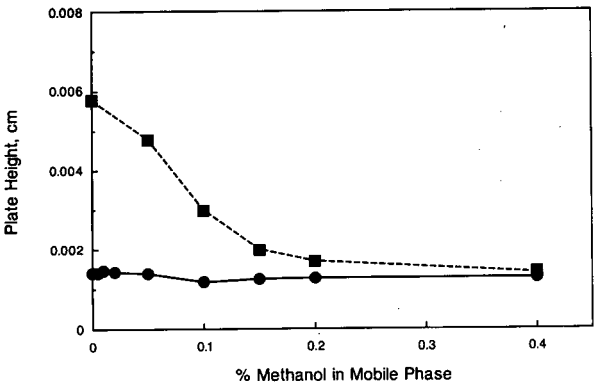

Fig. 8. Effect of methanol as modifier on column efficiency for different silica types. Conditions and symbols as in Fig. 7.

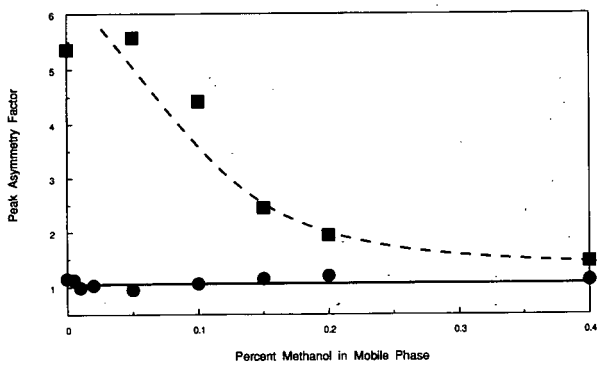

Fig. 9. Effect of methanol modifier on peak asymmetry for different silica types. Conditions and symbols as in Fig. 7.

when the methanol modifier content approached 0.4%. Similar results were found for benzyl alcohol as the solute. Phenol also showed larger asymmetry values for the type A silica, but less dramatic than for the other two solutes tested.

The effect of sample loading on retention when using methanol as the mobile phase modifier for the two silicas is shown in Fig. 10. In this study, 0.05% methanol modifier was used in an attempt to accentuate possible differences between the two silica types. The data indicate similarities for the two silicas. In both systems, 0.01–0.1 mg of solute/g of packing is allowed before a 10% change in k' occurred. The somewhat higher loading capacity of the type A silica is attributed to the higher surface area.

Similar effects of sample loading on column plate heights were found for the two silicas, as

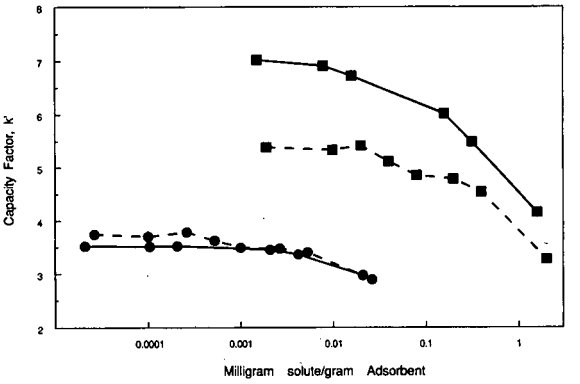

Fig. 10. Effect of solute loading on retention for different methanol-deactivated silica types. Columns as in Fig. 1; mobile phase: 0.05% methanol in dichloromethane; flow-rate: 1.0 ml/min; solutes as shown. ■ = Benzyl alcohol; ● = benzanilide; dashed lines: Zorbax-SIL (type A); solid lines: Zorbax Rx-SIL (type B).

illustrated in Fig. 11. The new type B silica shows significantly smaller plate heights, as would be expected by the data in Fig. 8 with the 0.05% methanol modifier used. The results in Fig. 11 suggest that new type B silica is somewhat more sensitive to sample load than the type A silica. However, this difference could be due to the variation in the surface areas between the two silicas. Alternatively, the apparent higher sensitivity of the new type B silica to sample mass could be a result of the smaller peak volumes generated with this column, resulting in a

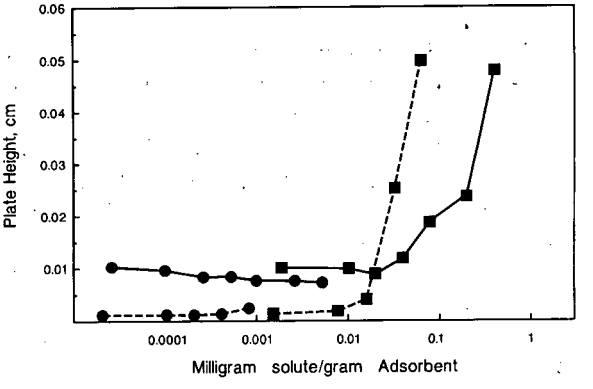

Fig. 11. Effect of solute loading on column efficiency for different methanol-deactivated silica types. Conditions as in Figure 10. ■ = Benzyl alcohol; ● = benzanilide; solid lines: Zorbax-SIL (type A); dashed lines: Zorbax Rx-SIL (type B).

higher level of overloading at the localized peak site on the packing.

Propanol also has been used as a mobile phase modifier in NP-HPLC with unmodified silicas. The effect of the amount of 2-propanol modifier in dichloromethane on the k' of solutes for the two silicas was closely similar to that found for methanol. Both silicas showed k' *versus* percent modifier plots that were essentially the same shape as for methanol. However, large plate height differences were exhibited for the two silica types with 2-propanol modifier, just as in the case for methanol in Fig. 8. The type A silica showed much larger plate heights, and more random variation in plate height as the concentration of 2-propanol was changed.

Note, however, that use of modifying protic organic solvents with some unmodified silicas can result in misshapen peaks for certain solutes. Fig. 12 compares peaks shapes from three silicas, using 0.05% methanol as the mobile phase modifier. This low level of modifier concentration was used to accentuate the effect of unfavorable modifier composition. Note the unusual peak shapes for two type A-like silicas. Benzanilide produced a broad, tailing peak with Zorbax-SIL under these conditions. With the Spherisorb column, the elution order was reversed for benzanilide and phenol, and the latter peak was broad and tailing (when chromatographed separately). Similar results were found with 2-propanol as the modifier at low concentrations. Previous studies also have shown misshapen peaks for some solutes with an unmodified silica when methanol and propanol was used as mobile phase modifiers [5]. This condition apparently is the result of complex adsorption isotherms that occur with such systems at low protic solvent modifier concentrations [6]. These and other studies suggest that protic mobile phase modifiers should be used cautiously in NP-HPLC systems with unmodified silicas. For dichloromethane the level of protic modifiers probably should exceed 0.2% (v/v) for most silicas.

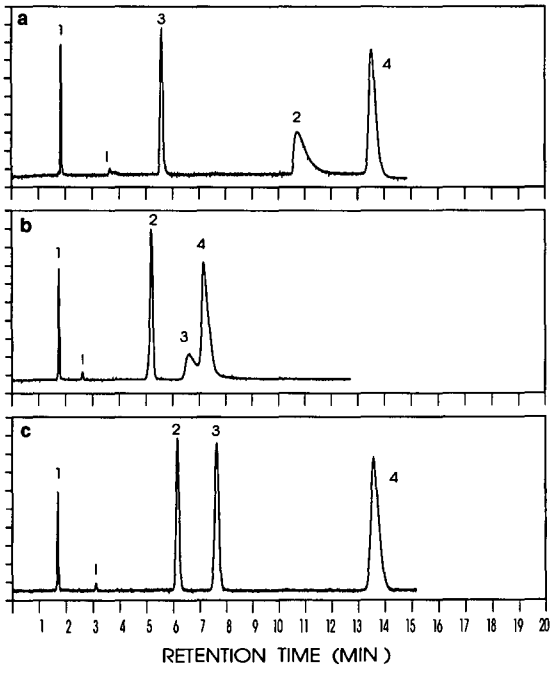

Fig. 12. Potential for misshapen peaks with protic modifiers for different silicas. Columns: 15 × 0.46 cm I.D.; mobile phase: 0.05% methanol in dichloromethane; flow-rate: 1.0 ml/min; solutes: 1 = 4 μg toluene, 2 = 0.5 μg benzanilide, 3 = 5 μg phenol, 4 = 38 μg benzyl alcohol. I = impurity. a = Zorbax-SIL, b = Spherisorb, c = Zorbax Rx-SIL.

Comparison of commercial silicas

Eight commercial unmodified silicas were compared in terms of retention, selectivity, column efficiency and peak shape, using a mixture of polar and basic compounds as model solutes. Fig. 13 shows chromatograms of this test mixture for various columns. For this study, a favorable organic modifier concentration (2% methanol) was used in the dichloromethane mobile phase, to minimize potential misshapen-peak problems such as that discussed for Fig. 12. The chromatograms in Fig. 13 show large differences in the selectivity of the various silicas. Several peak inversions are noted for the same operating conditions. Peak shapes for the various test solutes sometimes were different, and for one column, sulfanilamide was very strongly retained with a very broad peak. Fig. 14 compares the retention (as capacity factor, k') of the various test solutes for these eight columns under the same operating conditions. Strong differences in the level of retention were found, suggesting different surface areas and/or different surface activities. Retention generally seems higher for the silicas that have type A qualities.

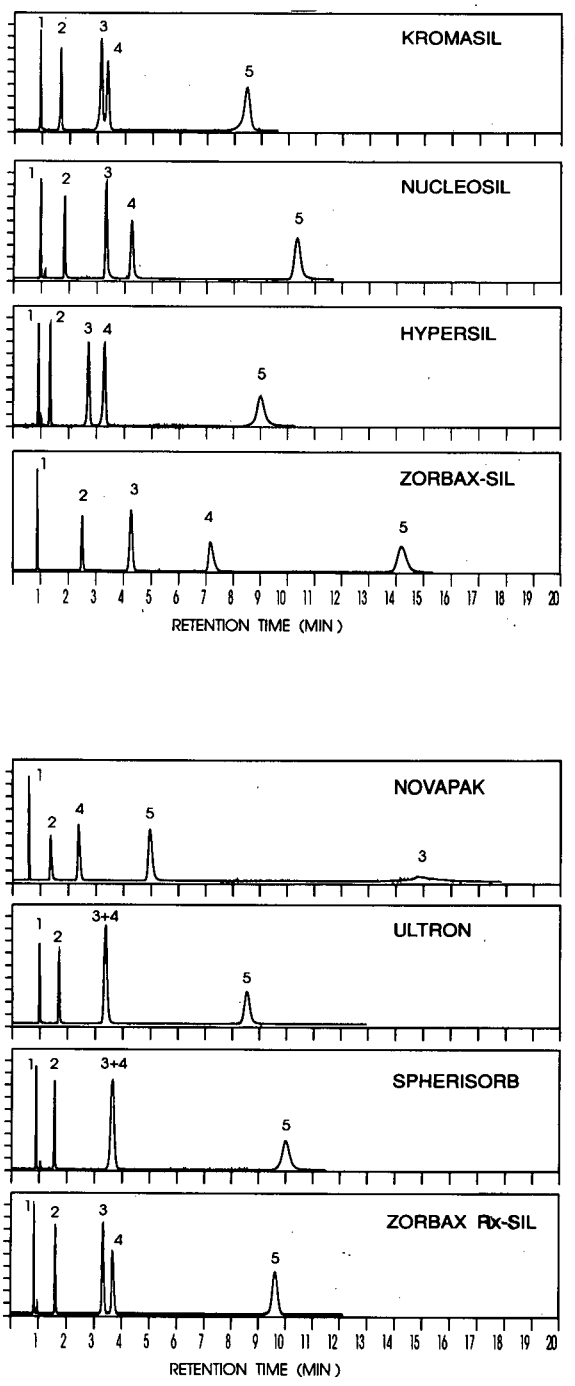

Fig. 13. Comparison of some commercial silicas: chromatograms. Columns as given in Experimental; mobile phase: 2.0% methanol in dichloromethane; flow-rate: 2.0 ml/min; solutes: 1 = 3 μg toluene, 2 = 1 μg quinoxaline, 3 = 0.25 μg sulfanilamide, 4 = 1 μg, caffeine, 5 = 0.5 μg 4-acetamidophenol.

Plate heights for various commercial unmodified silica columns are compared in Fig. 15. Efficiency generally appears highest for the silicas that resemble type B materials. Fig. 16 compares the peak asymmetry factors for each column. In this case, the difference in peak asymmetry values (positive or negative) from the theoretical Gaussian value of 1.0 is given for each silica column. Again, best peak shape is favored for type B-like silicas. Note, however, that column plate height and peak asymmetry comparisons are dependent on true packing particle sizes, and on column packing efficiency. Therefore, the comparisons in Figs. 15 and 16 should be viewed with care.

While the comparisons in Figs. 13–16 are informative, we believe that the test mixture used is not sufficiently critical to probe some of the important features of chromatographic silica. Accordingly, another test mixture was devised that shows more striking differences in the various silicas studied. Again, 2% methanol in dichloromethane was used as the mobile phase; no other modifier were used. In this test mixture, toluene is a neutral solute used to estimate t_0, and to define the effectiveness of the column packing method. Acetoacetanilide and catechol interact with heavy metals by different mechanisms to form complexes that can result in tailing or missing peaks. 3-Pyridyl-acetonitrile strongly sorbs to acidic sites, so this highly basic compound is a useful probe for the acidic nature of the silica.

Fig. 17 shows chromatograms of this definitive test mixture that were obtained on eight commercial silica columns. Kromasil and Nucleosil gave similar results in this test; all four compounds eluted, with catechol tailing badly for both silicas and with reduced peak areas. Kromasil exhibited peak fronting for 3-pyridyl-acetonitrile; there also is the hint of an unresolved impurity in the beginning of the acetoacetanilide peak. Acetoacetanilide tailed somewhat with Nucleosil. Catechol was totally missing from the Hypersil chromatogram, with the other test solutes eluting normally. Zorbax-SIL failed to elute 3-pyridyl-acetonitrile, but the other solutes eluted normally, with overlapping of two compounds. Novapak gave results similar to

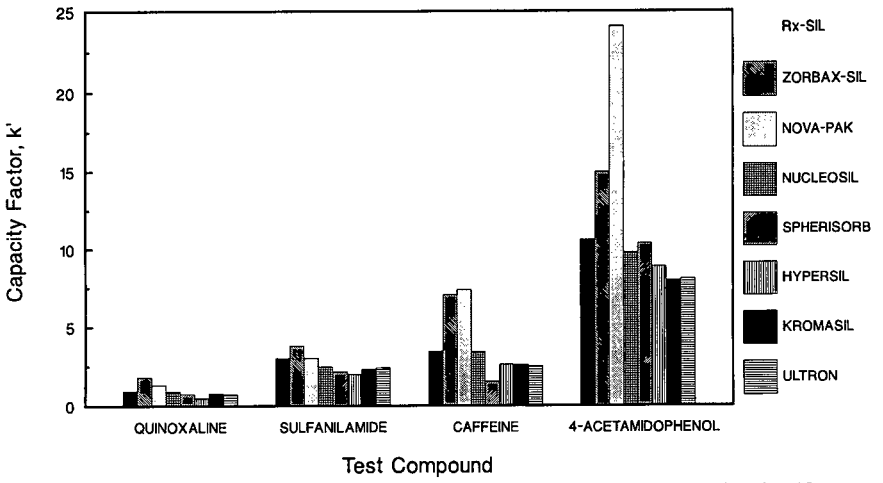

Fig. 14. Comparison of some commercial silicas: retention. Conditions as in Fig. 13.

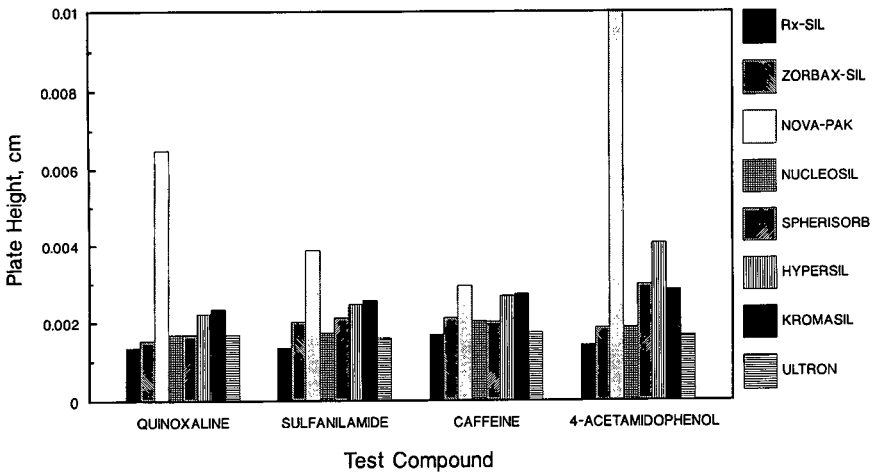

Fig. 15. Comparison of some commercial silicas: column efficiency. Conditions as in Fig. 1

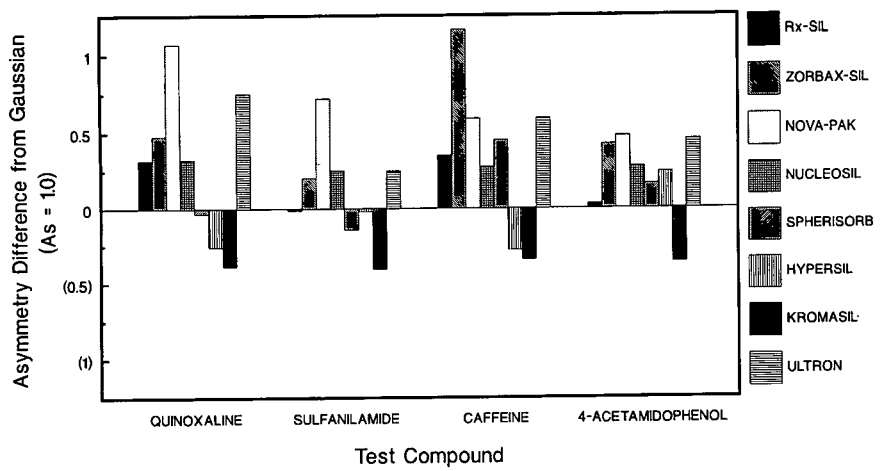

Fig. 16. Comparison of some commercial silicas: peak asymmetry. Conditions as in Fig. 1

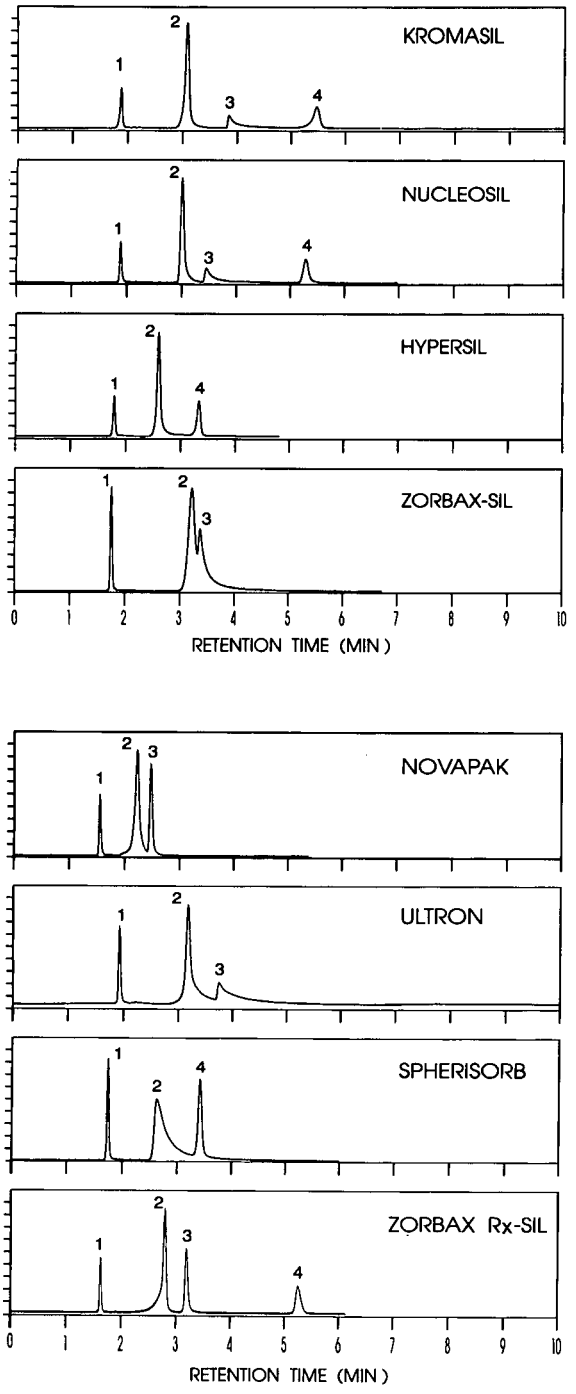

Fig. 17. Comparison of some commercial silicas: chromatograms. Columns as given in Experimental; mobile phase: 2.0% methanol in dichloromethane; flow-rate: 1.0 ml/min; sample volume: 1.0 μl; solutes: 1 = 1 μg toluene; 2 = 0.04 μg acetoacetanilide; 3 = 1 μg catechol; 4 = 0.1 μg 3-pyridyl-acetonitrile.

Zorbax-SIL; the basic probe did not elute, but the other solutes eluted normally. Ultron also did not elute the basic probe, and catechol was reduced in size with tailing. Spherisorb completely captured catechol, with tailing of acetoacetanilide. Zorbax Rx-SIL eluted all test solutes normally, again with evidence of a small impurity at the beginning of the acetoacetanilide peak.

The results of the studies summarized in Figs. 13–17 generally agree with the listing given in ref. 11 regarding silica supports best suited for the reversed-phase chromatography of basic compounds. Highly polar and basic compounds are most favorably chromatographed with less-acidic, highly purified type B silicas. In the present study of the characteristics of some unmodified silicas for NP-HPLC, results suggest that the order of desirable type B qualities are: Zorbax Rx-SIL > Nucleosil > Kromasil ≈ Hypersil > Spherisorb > Zorbax-SIL > Ultron > Novapak. Differences between successive listings may not be significant in all applications, since the chromatographic effects may be compound dependent.

Chromatographic reproducibility

A prime consideration in the use of unmodified silicas for NP-HPLC is separation reproducibility with various lots of materials over long time periods. Constant characteristics of the silica is required for repeatable separations and rugged analytical methods. Fig. 18 shows the variation found in manufactured lots of Zorbax

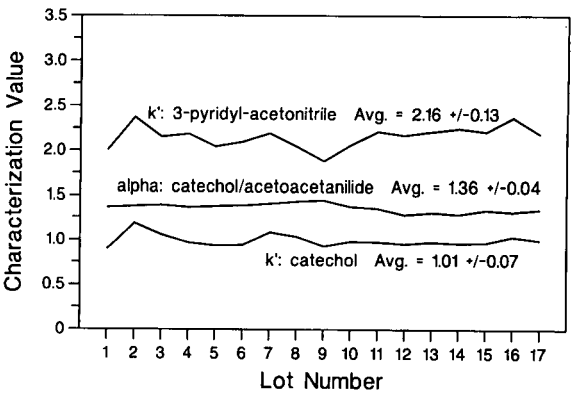

Fig. 18. Chromatographic reproducibility of Zorbax Rx-SIL silica. Conditions as for Fig. 17.

Rx-SIL over a two-year period. Small standard deviations were found in k' values for the highly sensitive compounds used in the test system described for Fig. 17. Slight k' variations are due to small changes in the surface areas of the various lots. More importantly, the α values for the sensitive catechol/acetoacetanilide pair show small variations over this two-year span, suggesting the potential for reproducible separations and rugged analytical methods with this silica.

CONCLUSIONS

In this study, large differences in retention and band spacing in normal-phase chromatography were found for eight different commercial unmodified silicas. The silicas studied show gross variations in separation resolution and analytical reproducibility. Highly purified, less-acidic type B silicas (*e.g.*, Zorbax Rx-SIL) generally give superior results and better reproducibility in NP-HPLC. Still, good performance in some applications is available from some more acidic, less-pure silicas.

These studies reaffirm that deactivation with water usually gives the best chromatographic results with all silica types. The surfaces of water-deactivated silicas appear most homogeneous, producing more efficient columns and superior peak shapes. Still, methanol and 2-propanol are effective and more convenient deactivating agents when used at appropriate levels (*e.g.*, >0.2% in dichloromethane). In some systems, however, these modifiers may cause misshapen peaks for some solutes, particularly when used at low concentrations.

REFERENCES

1 R.E. Majors, *LC–GC*, 9 (1991) 686.
2 L.R. Snyder, *Principles of Adsorption Chromatography*, Marcel Dekker, New York, 1968, Ch. 4.
3 L.-A. Trueddson and B. E. F. Smith, *J. Chromatogr.*, 214 (1981) 291.
4 B. Stancher and F. Zonta, *J. Chromatogr.*, 234 (1982) 244.
5 L.R. Snyder, J.L. Glajch and J.J. Kirkland, *Practical HPLC Method Development*, Wiley, New York, 1988, Ch. 4.
6 E.L. Weiser, A.W. Salotta, A.M. Flach and L.R. Snyder, *J. Chromatogr.*, 303 (1984) 840.
7 L.R. Snyder, J.L. Glajch and J.J. Kirkland, *Practical HPLC Method Development*, Wiley, New York, 1988, Ch. 3.
8 A.W. Salloto, E.I. Weiser, K.P. Caffey, R.L. Corty, S.C. Racine and L.R. Snyder, *J. Chromatogr.*, 498 (1990) 55.
9 R.J. Flanagan and I. Jane, *J. Chromatogr.*, 323 (1985) 173.
10 B.A. Bidlingmeyer, J. Korpi and J. Little, *Chromatographia*, 2 (1982) 83.
11 J.J. Kirkland, *J. Chromatogr.*, 83 (1973) 149.
12 L.R. Snyder and J.J. Kirkland, *Introduction to Modern Liquid Chromatography*, Wiley, New York, 1979, Ch. 9.
13 S. Golshan-Shirazi and G. Guiochon, *J. Chromatogr.*, 461 (1989) 19.
14 J. Köhler, D.B. Chase, R.D. Farlee, A.J. Vega and J.J. Kirkland, *J. Chromatogr.*, 352 (1986) 275.
15 J. Köhler and J.J. Kirkland, *J. Chromatogr.*, 385 (1987) 125.
16 R.K. Iler, *The Chemistry of Silica*, Wiley, New York, 1979, p. 711.
17 M.A. Stadalius, J.S. Berus and L.R. Snyder, *LC–GC*, 5 (1987) 495.
18 L.R. Snyder, in J.J. Kirkland (Editor), *Modern Practice of Liquid Chromatography*, Wiley-Interscience, New York, 1971, Ch. 4.

Journal of Chromatography, 635 (1993) 31–49
Elsevier Science Publishers B.V., Amsterdam

CHROM. 24 831

Influence of polymer morphology on the ability of imprinted network polymers to resolve enantiomers

Börje Sellergren[☆] and Kenneth J. Shea*

Department of Chemistry, University of California, Irvine CA 92717 (USA)

(First received July 28th, 1992; revised manuscript received December 24th, 1992)

ABSTRACT

Network copolymers imprinted with L-phenylalanine anilide (L-PheNHPh) exhibit an affinity for the print molecule. The binding of L-PheNHPh to the polymer can be quantitatively evaluated by employing the material as a stationary phase in a HPLC experiment. The degree of separation of the D and L enantiomers of PheNHPh (α value) is used to establish the influence of polymer morphology on polymer performance. Factors that promote stabilization of the template-polymerizable monomer complex prior to polymerization results in polymers with stronger and more selective binding of the substrate. Interestingly, a gel-like non-porous polymer performed similarly to a mesoporous polymer. Performance is also improved upon heat treatment of the polymers and various ways to inhibit the molecular recognition effect are demonstrated.

INTRODUCTION

During the last years, molecular imprinting or template polymerization has attracted considerable attention as a means of producing polymers exhibiting molecular recognition properties [1–21]. In this approach, a template is bound reversibly to functionalized monomers and copolymerized in solution with a cross-linking monomer. The resulting polymer can be freed from template by hydrolysis or extraction. In a subsequent rebinding step the polymers bind with preference for the original template molecule in competition with structurally related molecules.

An approach based on the ability of the template and functional monomer to interact by non-covalent interactions with each other was employed in the imprinting of enantiomers of amino acid derivatives [7–9]. Highly cross-linked copolymers of MAA (methacrylic acid) and EDMA (ethyleneglycoldimethacrylate) proved to be the most efficient matrix in the molecular recognition process. In the liquid chromatographic mode the polymers showed a pronounced selectivity for their original template molecule and in several cases base line separations of the corresponding enantiomers were achieved [10–12]. The polymers also were able to recognize subtle structural differences in the template. For instance enantiomer as well as substrate discrimination between phenylalanine anilide (PheNHPh) and phenylalanine N-methylanilide [13], carbobenzyloxyaspartic acid and carbobenzyloxyglutamic acid [12], and recently between phenylalanine ethyl ester (PheOEt) and diethyl-2-amino-3-phenylethylphosphonate [Phe(P)$(OEt)_2$] [14] has been demonstrated.

For a systematic use of the template-imprinted polymers as chromatographic stationary phases it is of interest to understand the factors that affect the rebinding strength and selectivity as well as

* Corresponding author.
☆ Present address: Department of Analytical Chemistry, University of Lund, P.O. Box 124, S-22100 Lund, Sweden.

0021-9673/93/$06.00

the factors underlying the extensive peak broadening that has so far been observed. The nature of the print molecule clearly affected these observations. For instance, print molecules containing two or three strong interaction sites (proton accepting or hydrogen bonding groups) towards methacrylic acid gave polymers exhibiting higher selectivity, stronger binding and broader peaks compared to polymers prepared using print molecules with fewer or weaker interaction sites (*cf.* L-PheNHPh *versus* L-*p*-amino-PheNHPh, L-PheOEt *versus* L-*p*-amino-PheOEt and L-PheOEt *versus* L-PheNHEt) [11]. It was therefore suggested that these results were due to the strength and molecularity of the association between the template and MAA prior to polymerization. This was supported by a ^{1}H NMR and chromatographic study of a titration of the template L-PheNHPh with MAA [10]. The results showed that multimolecular assemblies between MAA and the print molecule existed in solution prior to polymerization. A complementarity between the functional groups at the binding sites and the template thus appears to play a major role in the molecular recognition process. Moreover the shape and rigidity of the template assemblies have been suggested to affect selectivity [10,12]. By carefully designed template imprinting systems based on reversible covalent interactions, the importance of the shape [15] and rigidity [16] of the template as well as the distance between the functional groups at the sites [17,18] have been assessed independently. Thus it was concluded that all factors affected the template rebinding selectivity.

Assuming the interactions between MAA and the print molecule to be electrostatic and hydrogen bonding in nature, the properties of the solvent (porogen) used in the imprinting step in terms of hydrogen bond capacity and polarity is likely to influence the strength of the interactions. Since these properties also are important in the solvation of the growing polymer chains and thus in the mechanism of pore structure formation, different porogens may lead to polymers with different morphologies. Likewise, other ways to promote the formation of template assemblies such as decreasing the polymerization temperature [20] or increasing the concentration of MAA in the monomer mixture [21] may also result in polymers with widely different morphologies.

Due to these complications an understanding of the individual role of the above-mentioned factors requires a study including a large number of polymers prepared under different conditions. Unambiguous relations between chromatographic performance (selectivity, retention and resolution) and polymer morphology on the one hand, and solubility parameters (hydrogen bonding, polar and dispersive) and polymerization temperature on the other is expected to give valuable information about the molecular recognition mechanism. In this study we have made a complete characterization of a number of imprinted polymers prepared in presence of L-PheNHPh as print molecule using various solvents as porogens. Moreover, thermally initiated and low-temperature photoinitiated polymers have been compared. The influence of functional and structural changes of the polymers were assessed by introducing variable length amide-based cross-linking monomers [22]. Finally, methods of inhibiting the specific rebinding were attempted as a way to gain insight into the molecular recognition mechanism.

EXPERIMENTAL

General procedures

D- and L-PheNHPh [10] and the bismethacrylamide monomers [22] were synthesized as described elsewhere. The methacrylate monomers were obtained from Aldrich. EDMA was purified by extraction with 10% sodium hydroxide brine and drying over anhydrous magnesium sulfate followed by distillation. MAA was purified by drying over anhydrous magnesium sulfate followed by distillation. The porogens were all distilled under a positive nitrogen atmosphere prior to use and all other reagents were purified according to standard procedures. The UV lamp used in the photopolymerizations was a medium-pressure mercury vapour lamp (Conrad-Hanovia) of 550 W with 33 W in the 320–400 nm interval. Scanning electron micrographs were obtained at the UCI Electron Microscope

Facility. The FT-IR spectrum was recorded on an Analect RFX 40 instrument, the differential scanning calorimetry (DSC) was performed on a DuPont 910 DSC instrument and thermogravimetric analysis (TGA) on a DuPont 951 TGA instrument. The cross-polarization magic angle spinning (CP-MAS) ^{13}C NMR spectra were kindly run by Prof. David Sherrington (University of Strathclyde, UK) on a Bruker 25-147MHz instrument. All chromatographic evaluations were done using a Waters 484 UV detector, Waters 501 pump equipped with a U6K injector and a Hewlett-Packard integrating recorder.

Polymerizations

The polymers were prepared as shown in Scheme 1. To 3.8 ml (20 mmol) EDMA, 0.34 ml (4 mmol) MAA and 240 mg (1 mol) L-PheNHPh in 5.6 ml porogen (resulting in Fm = volume porogen/total volume of porogen + monomers = 0.57) were added 40 mg (0.25 mmol) azo-bis-isobutyronitrile (AIBN) as initiator. The mixture was transferred to a 50-ml thick-walled glass tube. This was freeze thaw degassed three times and sealed under vacuum. The thermally initiated polymerization was done at 60°C in an oil bath (T-polymers) and the photochemically initiated polymerization (P-polymers) at 15°C in a thermostatted water bath (see also Table I for definition of polymer abbreviations). The tubes were symmetrically placed at *ca.* 10 cm distance from a UV light source and turned at regular intervals for a symmetric exposure. After 24 h the tubes were crushed and the polymers ground

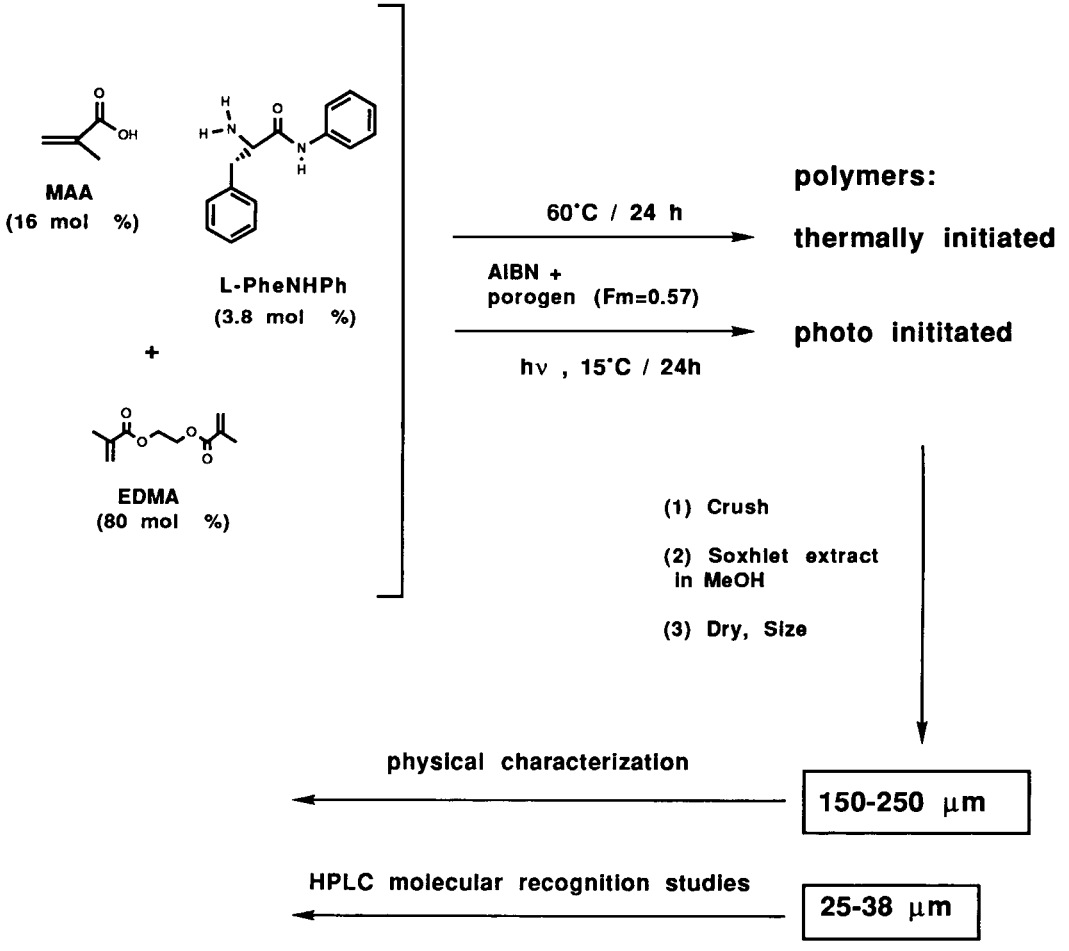

Scheme 1.

in a mortar, followed by soxhlet extraction in methanol for 12 h. The polymers were then dried overnight under vacuum at 50°C and sieved to a 150–250 μm and a 25–38 μm particle size fraction. The preparation of the polymers using the bismethacrylamide monomers is described in Table X. IR (KBr) of P1: 3458 (br), 2991, 2960, 1730, 1639, 1633, 1481, 1462, 1454, 1390, 1369, 1323, 1298, 1261, 1161, 1051, 957, 880, 816, 754 and 528 cm^{-1}. CP-MAS ^{13}C NMR of P2 and T2: δ 177, 168, 137, 127, 63 (br), 57 (br), 46, 24 (br), 19 ppm. The level of unsaturation was estimated by a comparison of the integrals at 177 and 168 ppm corresponding to non-conjugated and conjugated carbonylcarbons as described elsewhere [23].

Polymer density and solvent swelling studies

Dry polymer (1 ml, 150–250 μm) was placed in a 5-ml calibrated graduated cylinder and weighed. This gave the apparent dry density of the polymer. Excess solvent was then added and the polymer was stirred in order to remove air bubbles. The cylinder was then tapped until no further settling was observed. The swelling given as volume swollen polymer per volume dry polymer was read after 12 h. In another experiment swelling as a function of pH was studied. The polymer (0.5 ml, 150–250 μm) was placed in a volume-calibrated NMR tube and 2 ml MeCN–0.1 *M* NaCl (7:3) was added. Sodium hydroxide (1 *M*) was added in 40-μl increments with 3 h interval. Before each addition swelling and pH were measured.

Solvent uptake studies

Dry polymer (1.00 g, 150–250 μm) was placed in a scintillation vial and cyclohexane was added dropwise while the polymer was regularly agitated. Addition was stopped when the particles lost their ability to flow freely. The solvent was then allowed to evaporate until the particles just became free flowing. From the weight of the vial and the cyclohexane density, the solvent uptake, given as volume of solvent absorbed per weight of dry polymer, could be calculated.

Pore analysis

Pore and surface area analysis were performed by N_2 adsorption and Hg penetration on Micromeritics ASAP 2000 and PS3200, respectively. In the N_2 adsorption a sample of polymer (150–250 μm) corresponding to *ca.* 20 m^2 (0.1–0.5 g) was degassed at 170°C overnight under vacuum. The adsorption and desorption isotherms were then recorded using a 200-point pressure table and 15 s equilibration time. This gave a pore size distribution of pores between 17 and 2000 Å. In the Hg-penetration experiments a pore size distribution of pores between 1000 and 50 000 Å was instead obtained. The surface area was determined using the BET model, the *t*-plot using Harkins–Jura average thickness equation and the pore distribution using the BJH model [24].

Splitting of template

The recovery of template after soxhlet extraction in methanol was determined by HPLC on a reversed-phase C_{18} column using *p*-aminophenylacetate as internal standard and MeOH–3% HOAc (1:1) as eluent. All polymers except the one polymerized at 120°C [P1(120°C)] showed a recovery of 60–70%. Additional recovery is believed to occur upon acid wash since a high recovery (*ca.* 90%) has been observed by other techniques [8,10]. The polymer prepared at 120°C showed extensive breakdown of the template. The high accessibility of the carboxylic acid groups as indicated by the potentiometric titrations also indicates that the splitting yield is actually higher.

Chromatographic evaluation

The polymers with the 25–38 μm grain size fraction were slurry packed into 100-mm stainless steel columns [5 mm I.D. containing *ca.* 0.5 g (dry weight) of polymer after packing] using mobile phase A as solvent [MeCN–H_2O–HOAc (92.5:2.5:5, v/v/v)]. After having passed *ca.* 50 ml at a flow-rate of 10 ml/min the column was equilibrated at 1 ml/min until a stable base line was reached. The flow-rate was 1 ml/min, the volume of injected solute 10 μl and the detection wavelength 260 nm, unless otherwise stated. The capacity factor was calculated as $(t - t_0)/t_0$, where t is the retention time of the solute and t_0 the retention time of a non-retained void marker ($NaNO_3$). The separation factor (α) measures the relative retention between the enantiomers

($\alpha = k'_L/k'_D$) and h the reduced plate height from the number of theoretical plates (n) as $h = L/(d_p n)$, where L = column length (10 cm), d_p = average particle diameter (31.5 μm) and $n = 5.55(t/t_{1/2})^2$ ($t_{1/2}$ is the peak width at half height). The resolution factor R_s [25] and the asymmetry factor A_s [26] were obtained graphically as described elsewhere.

Polymer esterification

Dry polymer, 0.52 g of P1 and 0.41 g of P1BL of the 25–38-μm grain size fraction, was agitated in 10 ml dry tetrahydrofuran (THF) in 50-ml erlenmeyer flasks. Diazomethane, generated from 11.5 mmol of diazald (Aldrich), was added as an etheral solution giving a yellow color of the polymer slurry. The flasks were agitated gently and after addition they were closed with septa and opened to atmosphere with a small needle. After 12 h the color had faded and the addition was repeated. The yellow color now persisted and the excess diazomethane was quenched after 12 h with acetic acid. The polymers were then washed with excess THF and dried under vacuum at 50°C.

RESULTS AND DISCUSSION

Following the procedure shown in Scheme 1, a number of polymers were prepared by either photochemical or thermal initiation using L-PheNHPh as print molecule with solvents of various polarity and hydrogen bonding capacity as porogens (Table I). Polymers were also prepared excluding the print molecule (BL) or using benzylamine (BA) as print molecule. The polymers were then processed as indicated and subjected to physical characterization or to chromatographic evaluation.

Physical appearance, swelling and solvent uptake

Depending on which porogen was used either transparent, translucent or opaque polymers

TABLE I

SWELLING AND SOLVENT UPTAKE OF L-PheNHPh IMPRINTED POLYMERS

Polymer[a]	Porogen	Density[b] (g/ml)	Swelling[c] (ml/ml)	Solvent uptake[d] (ml/g)	Specific swelling[e] (ml/g)
T1	MeCN	0.35	1.19	1.12	3.4
T1BL	MeCN	0.31	1.19	1.11	3.8
T1BA	MeCN	0.38	1.31	1.10	3.4
T2	THF	0.38	1.27	1.11	3.3
P1	MeCN	0.38	1.36	1.00	3.6
P1BL	MeCN	0.34	1.31	1.07	3.9
P1BA	MeCN	0.36	1.31	1.12	3.6
P1(120°C)	MeCN	0.36	1.35	1.03	3.8
P2[f]	THF	0.52	1.84	0.53	3.5
P3[f]	$CHCl_3$	0.58	2.11	0.10	3.6
P4[f]	C_6H_6	0.40	1.55	0.91	3.9
P5[f]	DMF	0.51	1.97	0.38	3.9
P6[f]	CH_2Cl_2	0.58	2.01	0.14	3.5
P7	Isopropanol	0.29	1.10	1.14	3.8
P8	HOAc (glacial)	0.40	1.45	0.86	3.6

[a] The polymers were prepared as described in the experimental section and in Scheme 1 where T represents thermal initiation and polymerization at 60°C and P photochemical initiation and polymerization at 15°C. P1(120°C) was prepared by treating a polymer prepared as P1 at 120°C for 24 h before work up. BL indicates a blank polymer prepared in absence of template and BA a polymer prepared using benzylamine as template.

[b] Apparent density of 150–250-μm particles.

[c] Swelling in acetonitrile given as an average of two measurements with a spread of less than 3%.

[d] Volume of cyclohexane taken up per gram of polymer given as average of two measurements with a spread of less than 6%.

[e] Swelling divided by apparent density.

[f] These polymers appeared transparent.

were obtained. The transparent polymers cracked upon opening of the polymerization tubes and slowly turned opaque, probably due to shrinkage upon porogen evaporation. The shrinkage is reflected in the apparent dry density of the polymers (Table I). Indeed the polymers showing transparency had the highest density and thus shrunk the most upon drying. The gravimetric yields of polymerization was high (92–108%). It is interesting to note that the transparent polymers were prepared using porogens with a refractive index (n_D) (see Table V) higher than 1.4. Thus the transparency may be due to a refractive index match rather than to a certain pore structure.

In Table I swelling and solvent uptake data is seen for all the polymers in acetonitrile. Some general observations can be made. The photoinitiated polymers showed higher swelling than the thermally initiated ones. The same was true for the transparent polymers *versus* the opaque materials. If the swelling is expressed as the volume of swollen polymer per gram of dry polymer (specific swelling) it is seen that all polymers take up the same amount of acetonitrile indicating a fully reversible swelling–shrinking process as was seen in the polymerization of trimethylolpropanetrimethacrylate (TRIM) [27]. The uptake of cyclohexane is also given in Table I. Since little swelling was observed in this solvent the uptake data should reflect the permanent pore volume of these polymers. The photopolymers in general showed lower solvent uptakes than the corresponding thermally initiated polymers. The same relationship was observed for the transparent *versus* the opaque polymers. Interestingly a linear inverse relationship was found between the swelling and solvent uptake for these polymers, again indicating a reversible swelling–shrinking process. Polymer P6 was subjected to heat treatment in the dry state under vacuum. This resulted in a decrease in the swelling and solvent uptake in agreement with a recent study of TRIM polymers [27]. The decreased swelling was in the TRIM study explained by a heat-induced packing of the microspheres which could be reversed by heating the polymer in presence of solvent. The swelling was also studied in a series of solvents of different polarity (Table II). The swelling was highest in the polar solvents (except for water) and lower in toluene and cyclohexane. According to the solubility parameters in Tables V and VI toluene and cyclohexane are poor solvents for linear co-polymers of MMA–EA–MAA (EA = ethylacrylate). No difference in swelling was observed when the experiment was performed in the presence of 10 or 100 m*M* template (L-PheNHPh) excluding any stabilizing cross-linking effect from the template. Swelling also tended to be lower for the blank polymers compared to the corresponding templated polymers (Table II). It is possible that the carboxylic acid dimers, which are more abundant in the blank polymer, serve as a non-covalent cross-linking agent.

TABLE II

SWELLING IN VARIOUS SOLVENTS

Swelling in ml/ml was determined in the various solvents as described in the experimental section. These values are averages of two measurements with a spread of less than 3%. The polymers were dried under vacuum at 60°C between measurements. MP = mobile phase used in the chromatographic evaluation: MeCN–H_2O–HOAc (96.25:1.25:2.5, v/v/v). L-10 represents addition of 10 m*M* of L-PheNHPh (template) to the swelling solvent.

Solvent	Polymers					
	T1	T1BL	T2	P1	P1BL	P2
MeCN	1.19	1.19	1.31	1.36	1.31	1.84
MP	1.17	1.14	1.29	1.36	1.30	1.80
MeOH	1.17	1.19	1.30	1.37	1.29	1.83
Toluene	1.13	1.12	1.30	1.30	1.25	1.71
THF	1.19	1.17	1.30	1.35	1.31	1.79
H_2O	1.19	1.13	1.28	1.30	1.28	1.77
Cyclohexane	0.98	1.06	1.05	1.10	1.09	1.40
MeCN + L-10						1.87
MeCN + L-100						1.88
MeCN + D-10						1.93

Spectroscopic and thermal analysis

A typical FT-IR spectrum of a templated polymer is given in Fig. 1a. The resonances of interest from the vinyl and the carboxyl groups are indicated. The former may allow an estimate of the extent of unreacted double bonds and the latter give information of the hydrogen bonding state of the carboxyl groups. A well resolved

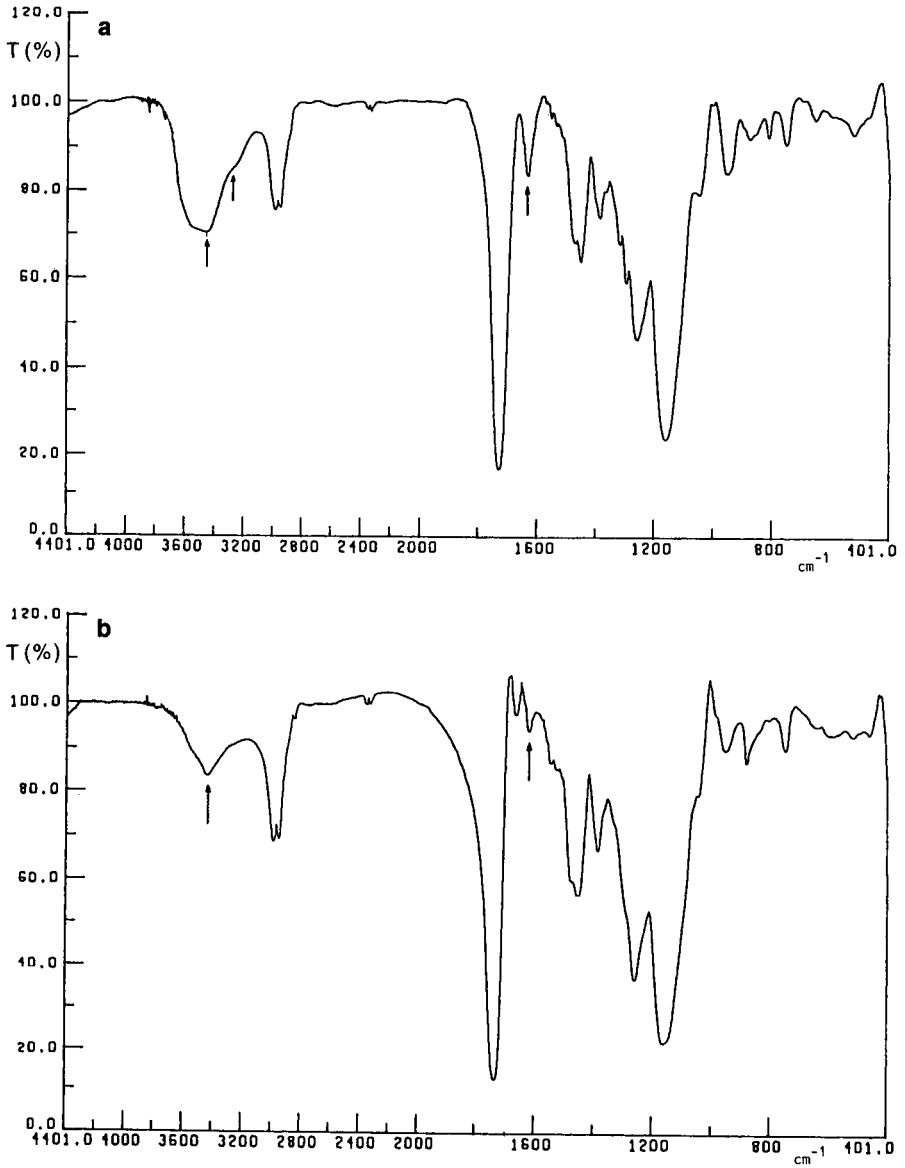

Fig. 1. FT-IR spectrum of (a) polymer P1(120°C) and (b) diazomethane-treated P1. The arrows at 3440 and 3300 cm^{-1} indicate the carboxylic acid OH stretch for the monomers and the hydrogen-bonded dimers, respectively and the arrow at 1639 cm^{-1} indicates the band arising from the vinyl–proton bonding.

band at 1639 cm^{-1} is attributed to =C–H bending and the broad band at 3300–3700 cm^{-1} to the carboxyl OH stretch. The FT-IR spectra of all polymers were indistinguishable indicating that they all contained approximately the same amount of unreacted double bonds and that no detectable difference in hydrogen bonding in the polymers is present. In IR studies on MMA–MAA copolymers [28] a band at 3300 cm^{-1} was attributed to carboxylic acid dimers while one at 3440 cm^{-1} was attributed to monomers. Interestingly a maximum was observed at 3440 cm^{-1} and an inflection at 3300 cm^{-1}. However strong absorbance was also observed at a higher wavenumber indicating a population of isolated carboxylic acid groups.

Thermal analysis was performed by TGA and DSC. All of the polymers studied showed a high thermostability with no mass loss under 200°C. Between 220 and 480°C all mass was lost and in this interval the polymers showed variations in the onset of mass loss, the steepness of the mass loss curve and in the endotherms of decomposition (Table III). The thermally initiated polymers appeared slightly less stable than the photochemically initiated materials although they contain a lower amount of unreacted double bonds. Based on CP-MAS ^{13}C-NMR experiments on T2 and P2 a level of unsaturation of *ca.* 6 and 9%, respectively, was found. Moreover, polymer P6, which belongs to the gel-like non-porous materials, showed a higher stability than P1 which is mesoporous. These variations may be related to the polymer morphology.

Pore analysis

Nitrogen adsorption–desorption and mercury porosimetry are techniques for the determination of polymer pore structures in the dry state [24]. Nitrogen sorption commonly revealed Type IV isotherms which indicate mesoporosity (Fig. 2a). Most of the polymers showed a hysteresis loop where the desorption branch did not close but leveled off either below or above the adsorption branch. This was pronounced for the polymers exhibiting the highest swelling and the lowest solvent uptake (Table I). Such behavior has been explained by shrinking of the polymer when subjected to increasing pressure at the liquid N_2 temperature and thus entrapment of N_2 molecules inside the polymer matrix [29]. During gas release from the pores of a certain size a lower relative pressure is thus required than one that can be calculated from the Kelvin equation [24]. Possibly the shrinking effect can be reduced by using a gas with lower saturation pressure P_0 (CO_2) which would allow measurements at a higher temperature [29]. It should be noted that some of the polymers, in particular those which previously showed the lowest solvent uptake and the highest swelling (Table I), strongly retained the helium used in the free volume measurements. As a result, manual degassing had to be applied at elevated temperatures (170°C) after the cold free space measurement.

Since the adsorption average pore diameter was in closer agreement than the desorption diameter with values obtained from the BET calculation the former is reported in Table IV. In general a narrow size distribution in the desorption plot (Fig. 2b) and a lower average pore diameter compared to the adsorption plot (Fig. 2c) indicates the existence of "bottle shape" pores [24]. The results of the study is summarized in Table IV. The polymers showed a wide distribution of surface areas and pore volumes. P3 and P6 were non-porous with essentially no surface area or internal pore volume. P7 on the other hand showed a macroporous character requiring Hg porosimetry (>1000 Å) to include all pores. The remaining polymers were mesoporous in character.

TABLE III

THERMOSTABILITY OF IMPRINTED POLYMERS

The temperatures for 0 and 100% mass loss were determined from the point where the trace departed from or reached the base line.

Polymer	Temperature (°C) at x% mass loss				
	0	25	50	75	100
T1	235	340	375	415	468
T1BL	250	330	360	400	460
T1BA	250	365	395	425	467
T2	246	315	357	405	458
P1	229	377	404	430	465
P1BL	225	372	409	436	485
P1BA	240	363	395	421	465
P1(120°C)	227	362	400	425	460
P2	252	365	397	424	463
P6	234	392	419	435	474

Particle texture

Scanning electron micrographs reveal the difference in morphology between the polymers (Fig. 3). Polymer P6, which belongs to the non-porous materials, shows a smooth featureless image with no observable pores. Fractures were observed probably arising from stress created during shrinking. P7 on the other hand showed a rough surface with clearly visible pores. A trend towards rougher surfaces and larger pores was

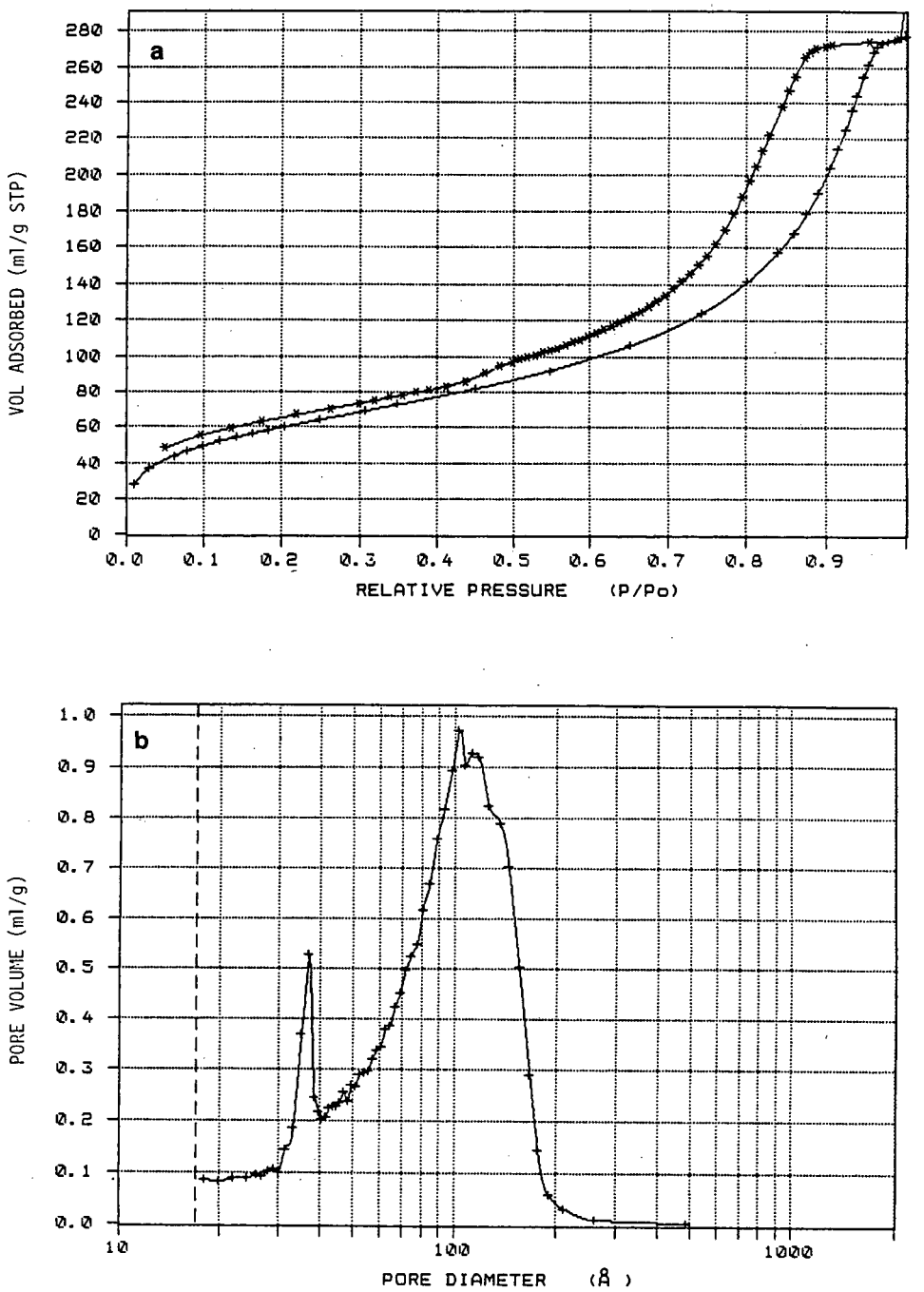

Fig. 2.

(Continued on p. 40)

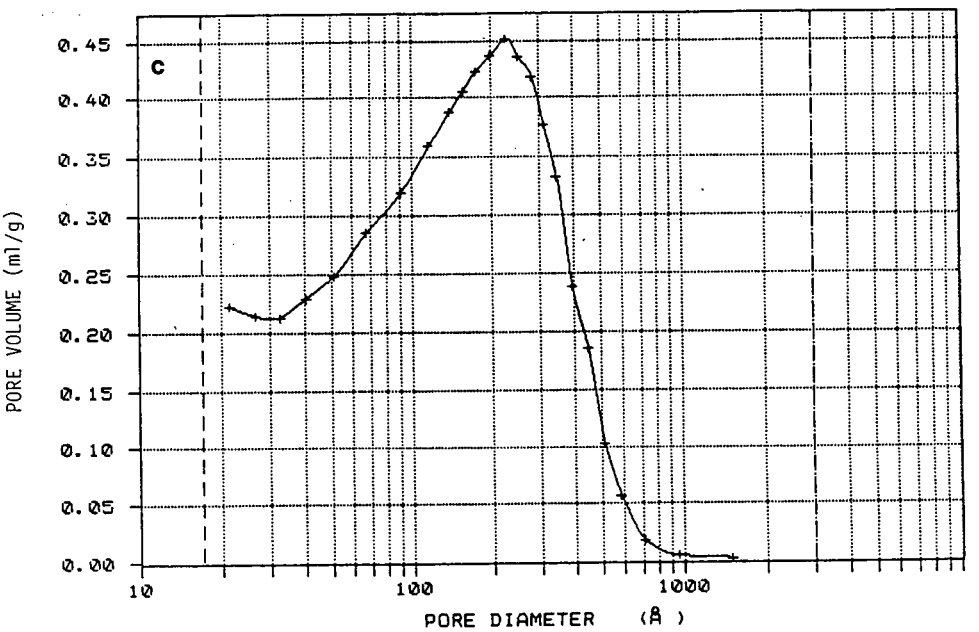

Fig. 2. (a) Nitrogen adsorption–desorption isotherm of polymer P1 after helium outgassing at 150°C. + = adsorption; * = desorption. (b) Pore size distribution calculated using the BJH model on the desorption isotherm. (c) As in b on the adsorption isotherm. P_0 = nitrogen saturation pressure, STP = standard temperature and pressure.

seen in the order: P6 < P1 < T1 < P7 which is in agreement with the pore analysis (Table IV).

Aspects of polymer pore structure formation

In the imprinting process low-temperature polymerization is preferable for several reasons. When the template interacts by non-covalent interactions with the monomers a negative ΔS for complex formation will favor complexation at low temperature. Side reactions may be minimized in particular for labile templates. Lower temperatures will lower the number of stable conformers which in turn may lead to sites of a more defined geometry. In spite of these advantages free radical polymerization of network polymers at low temperature can result in undesired changes in polymer morphology. Often a large portion of unreacted double bonds remains in the polymer leading to high swelling, low pore volume and low surface areas [27]. These changes may adversely affect the rebinding selectivity. In this study a complete polymer characterization is therefore necessary.

Knowledge about the solubility parameters (δ) for the porogen and the polymer allow an estimate of the heat of mixing per unit volume according to:

$$\Delta H_m/V = (\delta_1 - \delta_2)^2 \Phi_1 \Phi_2 \quad (1)$$

where δ_1 is related to the energy of vaporization of species 1 and Φ_1 its volume fraction in the mixture (species 1 and 2 are assumed to be non-interacting) [30]. A minimum ΔG is obtained when $\delta_1 = \delta_2$ implying a maximum solvation of the growing polymer chains (good solvent). In Table V the porogens have been classified according to their solubility parameter divided into a dispersive, a dipole–dipole and a hydrogen bond term [30]. Depending on the size of the hydrogen bond term the porogens have been further classified as either poorly, moderately or strongly hydrogen bonding. A correct estimate of δ of the polymers is difficult due to their cross-linked nature which gives rather small swelling factors. Often however the solubility parameter is close to the one of the predominat-

TABLE IV

SURFACE AREA AND PORE ANALYSIS ON THE IMPRINTED POLYMERS

Polymer	N_2 adsorption					Hg porosimetry		
	Surf. area (BET)[a] (m^2/g)	Pore volume[b] (ml/g)	Pore diameter[c] (Å)	Micropore volume[d] (ml/g)	Micropore surf. area[d] (m^2/g)	Pore volume[e] (ml/g)	Surf. area[e] (m^2/g)	Pore diameter[f] (Å)
T1	317	0.89	118	0.036	85	0.04	1	1500
T1BL	326	0.89	119	0.051	109			
T1BA	276	0.82	123	0.030	67			
T2	382	0.73	89	0.054	116			
P1	256	0.60	94	0.012	30	0.06	1.5	1500
P1BL	267	0.72	91	0.009	31			
P1BA	253	0.66	104	0.011	34			
P1(120°C)	266	0.65	96	0.010	33			
P2	194	0.24	52	0.006	16			
P3	3.5	0.007	91	0.0004	0.9			
P4	216	0.43	78	0.005	15			
P5	127	0.17	52	0.002	9.7			
P6	3.8	0.007	71	0.0003	0.9	0.02	02	1500
P7	49	0.20	121	0.003	9.0	0.74	11	1800
P8	267	0.52	77	0.008	29			

[a] Determined using the BET model on a seven-point linear plot.
[b] BJH cumulative adsorption pore volume of pores between 17 and 3000 Å.
[c] BJH adsorption average pore diameter (4 · pore volume/surface area) of pores between 17 and 3000 Å.
[d] Based on a *t*-plot using Harkins–Jura average thickness.
[e] Cumulative pore volume and surface area of pores between 1000 Å and 10 μm.
[f] Average pore diameter of pores between 1000 Å and 10 μm calculated as 4 · pore volume/surface area.

ing monomer. As seen in Table VI all porogens have δ values in the range of either *p*-MAA, *p*-MMA or *p*-MMA–MAA–EA.

The mechanism of pore structure formation in network polymers has been thoroughly reviewed [31,32]. A detailed analysis of polymer pore structure formation in the preparation of highly cross-linked TRIM was recently reported [27]. It is particularly interesting to note the influence of the solvating ability of the porogen on the pore structure formation. Performing the polymerization in a good solvent (toluene) favors intermolecular cross-links giving a relatively homogeneous network. The phase separation is controlled by the formation of solvent swollen gel particles which coagulate to form grains. These in turn coagulate to build up the pore system of the polymer. The links between the grains appear to be flexible since this type of polymer shrinks upon drying and swells to the original volume upon reimmersion in solvent. A poor solvent (isooctane) will promote agglomeration leading to the formation of dense highly cross-linked microspheres. The phase separation under these conditions is controlled by precipitation of the microspheres giving a relatively open pore structure where the strong links between the microspheres produce less shrinking and swelling. It should be noted that the number of residual double bonds in the polymers was about the same. Therefore, the authors did not attribute the different swellings to variable levels of cross-linking.

As seen in Table IV and from the structural data (Table I) no obvious correlation exists between $(\delta_1 - \delta_2)^2$ (Tables V, VI) and the polymer morphology in the present study. However in analogy with the TRIM system [27], the specific swelling (volume of polymer plus acetonitrile per gram of dry polymer) of the polymers was constant regardless of the dry state morphology and volume swelling. In addition, the

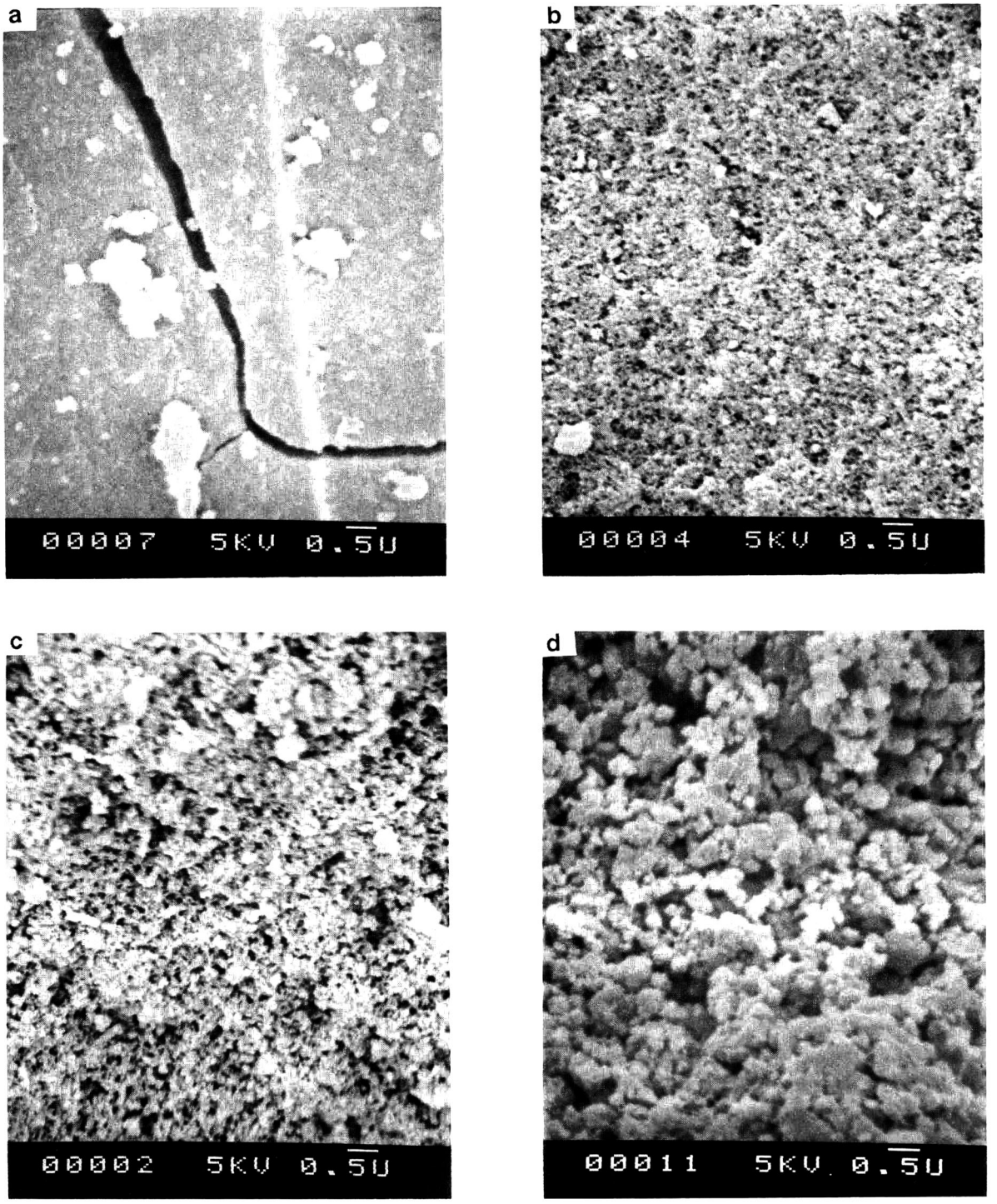

Fig. 3. Scanning electron micrographs of (a) P6, (b) P1, (c) T1 and (d) P7 photographed at 8000× magnification.

TABLE V

SOLUBILITY PARAMETERS, HYDROGEN BOND CAPACITY AND REFRACTIVE INDICES OF THE SOLVENTS [30]

The solubility parameter δ has been divided into a dispersive term δ_d, a polar term δ_p and a hydrogen bond term δ_h. H bond is a measure of the hydrogen bond capacity of the solvent in terms of both donor and acceptor ability, P = poor, M = moderate and S = strong. n_D = Refractive index.

Solvent	δ_d	δ_p	δ_h	δ ($MPa^{0.5}$)	H bond	n_D
MeCN	15.3	18.0	6.1	24.6	P	1.34
THF	16.8	5.7	8.0	19.4	M	1.41
$CHCl_3$	17.8	3.1	5.7	19.0	P	1.45
C_6H_6	18.4	0	2.0	18.6	P	1.50
DMF	17.4	13.7	11.3	24.8	M	1.43
CH_2Cl_2	18.2	6.3	6.1	20.3	P	1.42
Isopropanol	15.8	6.1	16.4	23.5	S	1.38
HOAc	14.5	8.0	13.5	21.3	S	1.37
MeOH	15.1	12.3	29.3	29.7	S	
Toluene	18.0	1.4	2.0	18.6	P	
H_2O	15.5	16.0	42.4	47.9	S	
Cyclohexane	16.8	0	0.2	16.8	P	

TABLE VI

SOLUBILITY PARAMETERS OF POLYMERS IN SOLVENTS OF DIFFERENT HYDROGEN BOND CAPACITY [30]

The solubility parameter ranges were obtained for commercial polymers given in the Polymer Handbook [30].

Polymer	δ ($MPa^{0.5}$) Solvent hydrogen bonding capacity		
	Poor	Moderate	Strong
MMA	18.2–26	17.4–27.2	0
MAA	0	20.3	26.0–29.7
MMA–EA–MAA (40:40:20 mol%)	0	18.2–22.1	19.4–29.7

number of residual double bonds appeared to be about the same for all polymers (see under spectroscopic analysis). It is therefore possible that a similar mechanism as proposed for the TRIM polymerization is operating in the template polymerizations in this study. This implies that the swollen state morphology of the polymers may be quite similar.

Polymer selectivity

All the polymers were initially evaluated in the liquid chromatographic mode for their ability to separate D- and L-PheNHPh using the standard criteria for chromatographic characterization [26]. These include the polymer selectivity reflected in the separation factor (α), the binding reflected in the retention or the capacity factor (k'), the column efficiency or dispersion reflected in the reduced plate height (h), band spreading due to slow adsorption–desorption kinetics or a non-linear binding isotherm reflected in the peak asymmetry (A_s) and finally the efficiency of a separation reflected in the resolution (R_s). Due to peak asymmetry (mainly for the mostly retained enantiomer) the assumptions that the peak retention time is equal to the peak maximum retention time and that the peak width is proportional to the peak standard deviation are now only approximations. However since the L peak exhibits tailing the true retention time should be longer. The given α values are therefore low estimates of the true values. The eluting strength of the mobile phase was chosen in order to balance the interactions between the solute and the stationary phase. In this regard the existence of mobile phase complexes has earlier been shown and in addition a quantitative analysis of their stability has been presented [10]. The mobile phases were: A = 92.5:2.5:5 and B = 96.25:1.25:2.5 (v/v/v) MeCN–H_2O–HOAc. This gave in all cases a k' of the least retained

solute between one and two allowing a more accurate determination of the separation factor α, *i.e.* a determination that is less dependent on an accurate determination of the void elution. The latter was determined using acetone as void marker which in the mobile phase coeluted with acetonitrile and sodium nitrate.

In Table VII the α values obtained at two sample loads for all polymers are shown. In addition results from the swelling and pore analysis as well as the hydrogen bonding capacity of the porogen has been included. As mentioned above, the polymer morphology in the dry state range from gel-like non-porous with a high swellability (P3, P6) to macroporous with a lower swellability (P7). Since the mass-specific swelling is similar for all polymers (Table I) the polymers may show a more similar morphology in the swollen state. *Nevertheless, no obvious correlation appears to exist between selectivity and polymer morphology. Instead, a correlation between the hydrogen bonding capacity of the porogen and the polymer selectivity can be seen.* Thus a trend towards lower α values upon increase in the hydrogen bonding capacity of the porogen is observed. This is in line with the previously proposed recognition model based on ion-pairing and hydrogen-bonding interactions [10]. A similar trend is seen for the thermally initiated polymers which as expected showed lower selectivity than the photoinitiated polymers. It should be noted that neither the dipole nor the dispersion term show any correlation with the polymer selectivity (*cf.* Tables V, VII).

Polymer saturation capacity

Using the mobile phase A unusual chromatographic behavior was seen in the low concentration regime (<100 nmole applied), leading to peak splitting and local minima and maxima in the plots of k' and α *versus* sample load. The origin of these effects are mainly mobile phase related and probably involve slow mobile phase equilibria with acetic acid [14]. By using buffered mobile phases these problems were eliminated. By increasing the sample load of D,L-PheNHPh

TABLE VII

CHROMATOGRAPHIC ENANTIOMER SELECTIVITY AND RESULTS FROM THE SWELLING AND PORE ANALYSIS IN RELATION TO HYDROGEN BOND CAPACITY OF POROGEN

The chromatographic separations were carried out as described in the experimental section using a mobile phase: MeCN–H_2O–HOAc, 92.5:2.5:5 %, v/v and applying two different sample loads of D,L-PheNHPh. NR = non-resolved peak maxima.

Polymer	Porogen	H bond type	Swelling (ml/ml)	Pore volume (ml/g)	Surface area (m^2/g)	Separation factor α ($= k'_L/k'_D$) Sample load of D,L-PheNHPh	
						12.5 nmol	100 nmol
P1	MeCN	P	1.36	0.60	256	5.8	2.6
P3	$CHCl_3$	P	2.11	0.007	3.5	4.5	2.6
P4	C_6H_6	P	1.55	0.43	216	6.8	2.4
P6	CH_2Cl_2	P	2.01	0.007	3.8	8.2	2.4
P5[a]	DMF	M	1.97	0.17	127	2.0	NR
P2	THF	M	1.84	0.24	194	4.1	1.5
P7[a]	Isopropanol	S	1.10	0.86	49	3.5	2.4
P8[a]	HOAc	S	1.45	0.52	267	1.9	NR
T1	MeCN	P	1.19	0.89	317	3.1	NR
T2	THF	M	1.27	0.73	382	1.6	NR
P1(120°C)	MeCN	P	1.35	0.65	266	3.7	2.4
P6(120°C)[b]	CH_2Cl_2	P	1.90	–	–	NR	2.3

[a] Mobile phase MeCN–H_2O–HOAc, 96.3:1.2:2.5 %, v/v.
[b] Treated under vacuum in the dry state at 120°C for 24 h. Solvent uptake: 0.09 ml/g.

the separation factor typically decreased rapidly, leveling off at a sample load of *ca.* 100 nmol (Fig. 4a). The steepness of the slope depended on porogen, polymerization temperature as well as on eventual heat treatment of the polymer. This is in qualitative agreement with our earlier published binding study on thermally initiated polymers at elevated column temperature although a higher saturation capacity was in that case observed [11]. By finishing the polymerization for 24 h at 120°C [P1(120°C)] a polymer that showed higher saturation capacity and improved chromatographic performance was obtained (Fig. 4), reflected in the higher resolution factors (R_s) observed for this polymer. *It is clear from earlier reported saturation capacities of imprinted polymers that polymers prepared by thermal initiation [10] are superior to those prepared by photoinitiation [20] allowing in the former case sample loads of ca. 2.4 mg/g (column temperature: 80°C) and in the latter case 0.5 mg/g polymer, respectively with resolved peak maxima.* It should be noted that the saturation capacity (number of available binding sites) of the polymers in this study is low in relation to the amount of template added to the monomer

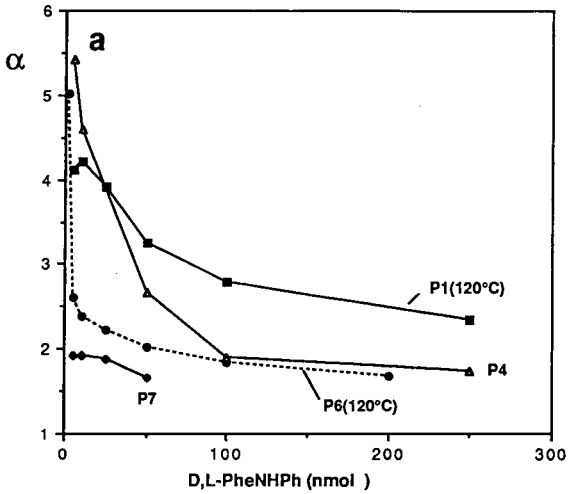

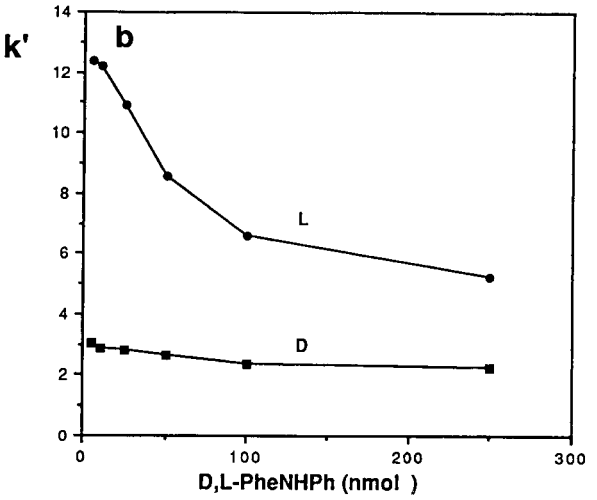

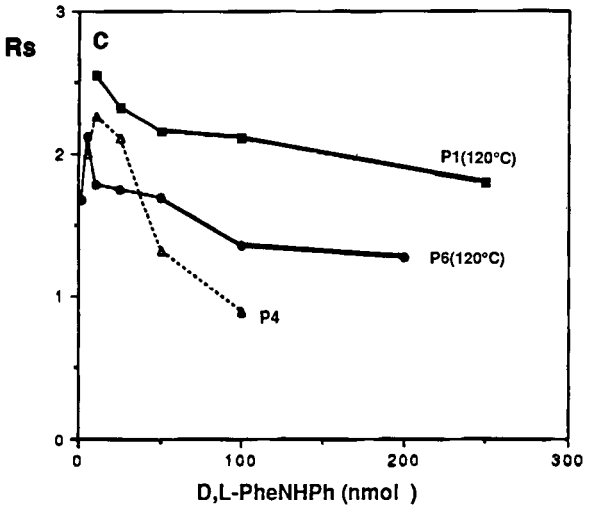

Fig. 4. (a) Separation factor (α), (b) capacity factor (k') of P1(120°C) and (c) resolution (R_s) *versus* sample load on various polymers in the study using MeCN–0.05 *M* potassium phosphate (KP) buffer pH 7 (7:3) as mobile phase.

mixture (theoretical maximum number of sites). This number can be estimated from the loading factor giving column overloading [34]. Severe overloading normally occurs at loading factors well below the saturation capacity of the column (5–10%). This corresponds to a saturation capacity of *ca.* 20 μmol/g for polymer P1(120°C) which implies that only 10% of the theoretical maximum number of sites are active. Similar low saturation capacities were observed in independent batch and frontal chromatographic binding studies [21,35]. In these studies a monosite Langmuir isotherm was assumed. In view of the site heterogeneity as indicated by Fig. 4 a Langmuir binary site model as proposed by Dickey [36] several years ago may better describe the observed binding isotherm. Alternatively a multisite model as described by Wulff *et al.* [37] may be used where an association constant for each newly covered site is calculated.

In studies employing reversible covalent binding between the functional monomer and the print molecule clearly higher saturation capacities are observed allowing a 2–3 fold excess of substrate to sites to be applied in the rebinding studies [15–19]. This typically results in *ca.* 90% rebinding based on the splitting yield. In non-covalent imprinting higher saturation capacities can be expected by using lower polymerization temperatures, a larger amount of functional monomer or by matching functional groups that are known to interact strongly in solution.

Effect of heat treatment on chromatographic performance

In view of the previously reported swelling effects upon heat treatment of TRIM polymers [27], the effect of such treatment upon the chromatographic performance was investigated. Two photoinitiated polymers showing different dry state morphologies were subjected to heat treatment in the dry state (Table VIII). For the gel-like polymer (P6) this resulted in a lower swelling (see Table VII) and lower α values at low sample loads (mobile phase A). The decrease in selectivity appeared to be reversible since, after a prolonged run in buffered mobile phases, a repeated run using mobile phase A resulted in high α values at low sample loads. In the buffered mobile phase at pH 7 the polymer exhibited high efficiency with low h and high R_s comparable to P1(120°C) (Fig. 5). At pH 7 the polymer was then subjected to additional heat treatment. This had only little effect on the selectivity and performance.

These results contrasted with results obtained

TABLE VIII

EFFECT OF HEAT TREATMENT ON CHROMATOGRAPHIC PERFORMANCE OF POLYMER P4 AND P6

The chromatographic experiments were performed using as mobile phase MeCN–0.05 *M* KP buffer, pH 7 (7:3) at a flow-rate of 1 ml/min and injecting 10 nmol of D,L-PheNHPh as described in the experimental section. NR = no enantiomeric resolution. VB = very broad.

Treatment	Stationary phase	k'_L	α	h_D	h_L	h_0	R_s
None	P4	8.3	4.1	32	138	7	2.2
	P6[c]	6.9	8.2	77	264	26	1.5
Heat 120°C, 17 h dry[a]	P4	4.6	2.1	30	99	8	1.5[d]
	P6[c]	0.8	NR	113		6	NR
	P6	4.4	2.0	23	35	6	1.9
Heat 130°C, 4 h in mobile phase[b]	P4	1.9	1.6	158		14	<1[d]
	P6[c]	16	6.4	106	VB	8	1.8
	P6	5.7	2.3	33	91	10	1.7

[a] The polymer was heated under vacuum followed by column repacking.
[b] The column was immersed in an oil bath and heated keeping the flow-rate at 1 ml/min.
[c] Mobile phase: MeCN–HOAc–H_2O (92.5:5:2.5, v/v/v).
[d] Column length: 5 cm.

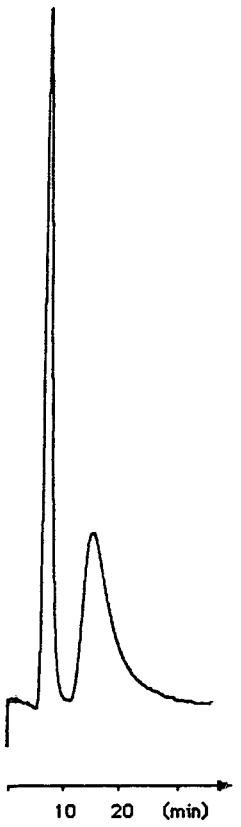

Fig. 5. Elution profile of 10 nmol D,L-PheNHPh applied on an L selective heat treated polymer (P6) using as mobile phase: MeCN–0.05 *M* KP buffer, pH 7 (7:3) at a flow-rate of 1 ml/min.

using the more porous polymer (P4). After initial dry heat treatment lower k' and α were observed as well as a poorer performance (higher h). This trend continued upon the subsequent wet heat treatment. The seemingly higher thermostability of the gel-like polymer (P6) was also indicated by the thermal analysis (see Table III). Variable temperature runs on this polymer may therefore allow an estimate of the energetics of the binding.

Chemical modifications affecting binding and selectivity

The photoinitiated template and plank polymers prepared using acetonitrile as porogen (P1 and P1BL) were treated with a large excess of diazomethane for 48 h. This was followed by a reinvestigation of swelling, solvent uptake, FT-IR, DSC, TGA and chromatographic performance (Table IX). A somewhat lower swelling and solvent uptake was observed. Interestingly a clear loss of selectivity is seen in the large decrease in the separation factor showing the importance of the ion pair and hydrogen bonding interactions for recognition. In the IR spectrum (Fig. 1b) only part of the OH band disappeared, mostly the absorbances at higher wavenumbers. This is to be expected since the free carboxylic acid groups should be more reactive than the hydrogen bonded groups. Also a large decrease in the vinyl band at 1639 cm^{-1} was seen probably due to a 1,3 addition of diazomethane to unreacted double bonds. Thus a large proportion of unreacted double bonds seems to be accessible. The DSC and TGA traces for both polymers were almost identical. An endotherm at low temperature was observed corresponding to a mass loss which could be attributed to the weight of a methylester group. This was not observed in

TABLE IX

INHIBITION OF SUBSTRATE RECOGNITION

The diazomethane and base treatment was performed on polymer P1 and P4, respectively, as described in the Experimental section. The mobile phase was MeCN–H_2O–HOAc (92.5:2.5:5 %, v/v) and the sample load was 10 nmol of D,L-PheNHPh.

Treatment	State	Swelling (ml/ml)	Solvent uptake (ml/g)	k'_L	α ($= k'_L/k'_D$)
CH_2N_2	–COOH	1.36	0.78	7.5	5.8
	–COOMe	1.20	0.68	1.7	1.4
MeOH–10% NaOH	Unhydrolyzed	1.55		2.0	5.6
(4:1 %, v/v)	Hydrolyzed	1.70		1.2	2.3

the untreated polymer. In another experiment the polymers were stirred at room temperature in MeOH–10% NaOH (4:1) overnight. This gave rise to a substantial release of methacrylic acid and a higher swelling. The treatment resulted in a partial loss of selectivity and binding (Table IX). The increase in swelling has been attributed to hydrolysis of cross-links in the polymer [33] which may explain the partial loss of selectivity due to the larger degree of flexibility in the polymer backbone.

Use of bismethacrylamides in non-covalent imprinting

The use of bismethacrylamides as functional monomers in non-covalent imprinting was evaluated by preparing a series of polymers as indicated in Table X. The chromatographic evaluation was then performed as indicated (Table X). The amide monomers containing an aliphatic spacer gave reduced retention and selectivity compared to the ester monomers (EDMA). When increasing the length of the spacer the separation factor and retention decreased. However upon introduction of an aromatic spacer, stronger binding was observed, while the selectivity was in the same order as that observed using the standard EDMA-based polymer. Since selectivity remained unchanged it is likely that the increase in binding is due to a stabilizing interaction in the site affecting both enantiomers equally [38].

TABLE X

EVALUATION OF BISAMIDE CROSS-LINKERS IN THE IMPRINTING OF L-PHENYLALANINE ANILIDE

Cross-linker R =	k'_D	α $(=k'_L/k'_D)^a$
$-O-CH_2CH_2-O-$[c]	8.4	6.4(a)
$-NH-C_6H_6-NH-(m)$[b]	11.8	6.3(b)
$-NH-CH_2CH_2-NH-$	5.5	2.4(a)
$-NH-(CH_2)_4-NH-$	1.1	1.6(c)
$-NH-(CH_2)_6-NH-$	1.7	1.6(c)

[a] The polymers were prepared using a monomer composition of EDMA (38 mol%), MAA (38 mol%) and the amide (or ester) cross-linker (19 mol%) in the presence of L-PheNHPh as template (4 mol%). The polymerization was carried out at 75°C under nitrogen for 48 h using AIBN (1 mol%) as initiator and MeCN as porogen ($F_m = 0.57$). They were then crushed and washed in MeCN–HOAc (3:1) for two days whereby 30–60% of the template was recovered [as determined by HPLC (RP-18)]. The polymers were then sieved to 25–38 μm and packed into columns. In the chromatographic evaluation the retention of the D enantiomer was determined using as mobile phase: MeCN–H_2O–HOAc (97.5:1.25:1.25 %, v/v). Since the separation factor does not vary with the mobile phase composition the separation factors were determined at a mobile phase composition where the L enantiomer was eluted within a reasonable time. This corresponded to a composition of MeCN–H_2O–HOAc of (a) 95:2.5:2.5, (b) 92.5:2.5:5 and (c) 97.5:1.25:1.25 %, v/v.

[b] Prepared using EDMA (34 mol%) and cross-linker (23 mol%).

[c] Prepared using EDMA (57 mol%).

CONCLUSIONS

A complete characterization of a series of photo and thermally initiated polymers imprinted with L-PheNHPh was performed. The materials varied widely in dry state morphology from gel-like non-porous to macroporous. The swollen state morphology however appears to be more homogeneous since a certain mass of polymer swelled to the same volume in acetonitrile. The largest influence on the selectivity and strength of the substrate rebinding was due to the polymerization temperature and the hydrogen bonding capacity of the porogen while the polymer morphology appeared to be less important. Photochemically initiated polymerization at low temperature and the use of a porogen with poor hydrogen bonding capacity promoted high selectivity and strong binding.

The polymers showed a high thermostability with only small variations between the polymers as judged from thermal analysis but larger variations as judged from the effect of heat treatment upon chromatographic performance (change in α, R_s and h). This appeared to be related to the polymer dry state morphology where the gel-like polymers were more stable than the corresponding porous polymers (polymers prepared using different porogens). Polymers subjected to heat-treatment after polymerization showed a higher column efficiency and saturation capacity compared to the untreated polymers. This resulted in a performance comparable to some of

today's commercially available chiral stationary phases.

The selective rebinding of the substrate to the polymer could be inhibited by either esterification of the carboxylic acid groups of the polymer or by subjecting the polymers to aqueous base treatment. Finally, amide-based cross-linkers were evaluated as a possible way of introducing additional sites of interaction for the substrate. Only the aromatic-based cross-linker gave comparable selectivity to the EDMA polymers. This also resulted in a stronger substrate binding suggesting an additional interaction at the sites.

The data as a whole support the suggested recognition model that invoke electrostatic and hydrogen bonding interactions between the polymer and the substrate. Finally and perhaps more importantly, a porous polymer structure is not a requirement in order to achieve an efficient chromatographic matrix in molecular imprinting. Similar separations were thus seen using a non-porous swellable material and a porous material of lower swellability. This result may be informative about the domains in the polymer structure in which the recognition sites are located.

ACKNOWLEDGEMENTS

We are grateful to the National Science Foundation (Division of Materials Research) and to a research grant from Swedish Natural Science Research Council. We also wish to thank Dr. David Sherrington (University of Strathclyde, UK) for the solid-state ^{13}C NMR results.

REFERENCES

1 G. Wulff, in W.T. Ford (Editor), *Polymeric Reagents and Catalysts* (*ACS Symposium Series*, No. 308), American Chemical Society, Washington, DC, 1986, pp. 186–230.
2 F.H. Dickey, *Proc. Natl. Acad. Sci.*, 35 (1949) 227.
3 R. Curti and U. Colombo, *J. Am. Chem. Soc.*, 74 (1952) 3961.
4 G. Wulff, W. Vesper, R. Grobe-Einsler and A. Sarhan, *Makromol. Chem.*, 178 (1977) 2799.
5 K.J. Shea and E.A. Thompson, *J. Org. Chem.*, 43 (1978) 4253.
6 J. Damen and D.C. Neckers, *Tetrahedron Lett.*, (1980) 1913.
7 L. Andersson, B. Sellergren and K. Mosbach, *Tetrahedron Lett.*, 25 (1984) 5211.
8 B. Sellergren, B. Ekberg and K. Mosbach, *J. Chromatogr.*, 347 (1985) 1.
9 B. Sellergren, in R. Epton (Editor), *Innovations and Perspectives in Solid Phase Synthesis. Peptides, Polypeptides and Oligonucleotides. Macroorganic Reagents and Catalysts*, SPCC (UK), Birmingham, 1990, pp. 293–307.
10 B. Sellergren, M. Lepistö and K. Mosbach, *J. Am. Chem. Soc.*, 110 (1988) 5853.
11 B. Sellergren, *Chirality*, 1 (1989) 63.
12 L.I. Andersson and K. Mosbach, *J. Chromatogr.*, 516 (1990) 313.
13 M. Lepistö and B. Sellergren, *J. Org. Chem.*, 54 (1989) 6010.
14 B. Sellergren and K.J. Shea, in preparation.
15 K.J. Shea and D.Y. Sasaki, *J. Am. Chem. Soc.*, 111 (1989) 3442.
16 G. Wulff and H.-G. Poll, *Macromol. Chem.*, 188 (1987) 741.
17 K.J. Shea and T.K. Dougherty, *J. Am. Chem. Soc.*, 108 (1986) 1091.
18 G. Wulff, B. Heide and G. Helfmeier, *J. Am. Chem. Soc.*, 108 (1986) 1089.
19 O. Norrlöw, M.-O. Månsson and K. Mosbach, *J. Chromatogr.*, 396 (1987) 374.
20 D.J. O'Shannessy, B. Ekberg and K. Mosbach, *Anal. Biochem.*, 177 (1989) 144.
21 B. Sellergren, *Macromol. Chem.*, 190 (1989) 2703.
22 K.J. Shea, G.J. Stoddard, D.M. Shavelle, F. Wakui and R.M. Choate, *Macromolecules*, 23 (1990) 4497.
23 T. Hjertberg, T. Hargitai and P. Reinholdsson, *Macromolecules*, 23 (1990) 3080.
24 S.J. Gregg and K.S.W. Sing, *Adsorption, Surface Area and Porosity*, Academic Press, London, 2nd ed., 1982.
25 G. Wulff, H.-G. Poll and M. Minarik, *J. Liq. Chromatogr.*, 9 (1986) 385.
26 G.S. Weber and P.W. Carr, in P.R. Brown and R.A. Hartwick (Editors), *High Performance Liquid Chromatography*, Wiley, New York, 1989.
27 P. Reinholdsson, T. Hargitai, B. Törnell and R. Isaksson, *Angew. Macromol. Chem.*
28 Y. Kikihira and H. Yamamura, *Macromol. Chem.*, 186 (1985) 423.
29 Micromeritics Corp., personal communication.
30 J. Brandrup and E.H. Immergut, *Polymer Handbook*, Wiley, New York, 3rd ed., 1989, p. VII 519.
31 J.R. Millar, D.G. Smith, W.E. Marr and T.R.E. Kressman, *J. Chem. Soc.*, (1963) 218.
32 A. Guyot, in D.C. Sherrington and P. Hodge (Editors), *Synthesis and Separations Using Functional Polymers*, Wiley-Interscience, New York, 1988; Ch. 1.
33 M. Jelinkova, L.K. Shataeva, G.A. Tischenko and F. Svec, *React. Polym.*, 11 (1989) 253–260.
34 S. Jacobson, S. Golshan-Shirazi and G. Guiochon, *J. Am. Chem. Soc.*, 112 (1990) 6492.
35 M. Kempe and K. Mosbach, *Anal. Lett.*, 24 (1991) 1137.
36 F.H. Dickey, *J. Phys. Chem.*, 59 (1955) 695.
37 G. Wulff, R. Grobe-Einsler and A. Sarhan, *Macromol. Chem.*, 178 (1977) 2817.
38 W.H. Pirkle and C.J. Welch, *J. Chromatogr.*, 589 (1992) 45.

Journal of Chromatography, 635 (1993) 51–60
Elsevier Science Publishers B.V., Amsterdam

CHROM. 24 843

Quantitation of non-ideal behavior in protein size-exclusion chromatography

Paul L. Dubin*, Shun L. Edwards and Mamta S. Mehta☆

Department of Chemistry, Indiana University, Purdue University at Indianapolis, Indianapolis, IN 46205 (USA)

Donald Tomalia

Department of Chemistry and Macromolecular Architecture, the Michigan Molecular Institute, Midland, MI 48640 (USA)

(First received September 11th, 1992; revised manuscript received November 6th, 1992)

ABSTRACT

The size-exclusion chromatographic partition coefficient (K_{SEC}) was measured on a Superose 6 column for three sets of well-characterized spherically symmetrical solutes: the compact, densely branched non-ionic polysaccharide, Ficoll; the flexible chain non-ionic polysaccharide, pullulan; and compact, anionic synthetic polymers, carboxylated starburst dendrimers. All three solutes display a congruent dependence of K_{SEC} on solute radius, R. In accord with a simple geometric model for SEC, all of these data conform to the same linear plot of $K_{SEC}^{1/2}$ *vs.* R. This plot reveals the behavior of non-interacting spheres on this column. Comparison of results for a number of globular proteins at various pH values to this "ideal" curve allows a quantitative measure of protein attraction or repulsion. It is shown that the usual procedure of obtaining a "best-fit" curve for a set of proteins is likely to generate an erroneous calibration curve.

INTRODUCTION

Size-exclusion chromatography (SEC) is an important liquid chromatographic technique for the separation of biopolymers [1,2]. Unlike other chromatographic methods, SEC has the potential of providing information about the molecular weight — or, to be more precise, the molecular size of the solute. It is possible to couple an SEC system to a "molecular weight detector"; then, the liquid chromatograph simply serves as the separation step prior to the analysis of the sample by, for example, light scattering. However, if the column is properly calibrated, the elution volume itself can be correlated with solute size, and hence, molar mass. This calibration is a difficult problem, because (a) the "standards" used in the calibration process must have the same relationship between molar mass and molar volume as the sample being analyzed, and (b) the separation process must be controlled solely by steric or entropic effects for both standards and analytes. The second requirement is particularly difficult in SEC of proteins, because each protein has a unique pattern of surface charge distribution and hydrophobicity. Despite great technological progress is preparing SEC packings that have relatively little hydrophobic character and relatively low surface charge [3,4], it is difficult to ensure that the chromatography of a series of proteins is not affected by the unique electrostatic or hydropho-

* Corresponding author.
☆ Present address: Department of Chemistry, University of Illinois at Urbana-Champaign, Urbana IL 61801, USA.

0021-9673/93/$06.00

bic interactions of the individual proteins with the packing.

The general procedure for calibrating an SEC column for proteins consists of obtaining the dependence of either the retention volume (V_e) or the chromatographic partition coefficient (K_{SEC}) on either molecular weight or the diffusion-related Stokes radius (R_s). K_{SEC} is given by

$$K_{SEC} = (V_e - V_0)/(V_t - V_0) \quad (1)$$

where V_0 is the interstitial volume of the column, obtained as the retention volume of a solute too large to permeate the pores, and V_t is the total liquid volume of the column, obtained from the retention volume of a small solute, such as ^2H_2O, acetone or dextrose. There is some evidence that the diffusional Stokes radius does not unify the data for a variety of solutes as well as the viscosity radius [5]:

$$R_\eta = \{3([\eta]M_r)/10\pi N_A\}^{1/3} \quad (2)$$

(if the units of $[\eta]$ are cm^3/g, then R has units of cm) but for most globular proteins, R_η and R_s are identical, within experimental error [6]. (The frequent use of the term "hydrodynamic radius", which is ambiguous in that the relevant hydrodynamic property may be undefined, has had the unfortunate effect of confusing these two parameters.) However, when either R_s or R_η is plotted against V_e or K_{SEC}, the data typically display some scatter around the best-fit curve. It is usually not clear whether this scatter results from adsorptive or repulsive electrostatic interactions between solutes and stationary phase, arises from excess asymmetry of some of the standards (*i.e.* the set of standards does not represent a geometrically homologous series), or is a consequence of errors in the determination of V_e or R_s, *i.e.* true experimental error. In the absence of this information it is common practice to use the best-fit curve for calibration. This practice leads to a rather large uncertainty in the determination of the molecular mass of protein analytes.

A related problem arises when proteins are used to test SEC theories. In a geometric sense, R_s and R_η are much more clearly defined for proteins than are similar parameters for either flexible chain polymers or rod-like macromolecules. Therefore, data obtained for globular proteins have often been used to determine the validity of relationships between R and K resulting from different models of SEC [7–10]. The effects of adsorptive and repulsive interactions weaken the utility of such evaluations.

In the current work, we compare the retention behavior of proteins on a Superose 6 column to the elution of non-interacting spheres. The solutes that most closely approximate this behavior are fractions of Ficoll, a densely branched, highly compact, non-ionic polysaccharide prepared by polymerization of epichlorohydrin and sucrose [11,12]. Evidence in support of the compact spherical behavior of Ficoll comes from the Mark–Houwink exponent of $a = 0.27$ in the viscosity–MW relationship $[\eta] = KM^a$ [13], and also from measurements of its hindered diffusion through pores [14,15]. In addition to Ficoll, we also report here on the chromatography of carboxylated starburst dendrimers [16]. These solutes are even more impermeable than Ficoll, in view of the value of less than 0.1 [17]. Although these compounds are anionic, an electrolyte content greater than 0.4 M at neutral or acidic pH appears to fully suppress repulsive interactions with the weakly anionic Superose packing. A third solute studied is pullulan, a non-ionic linear polysaccharide [18]. Although the flexible chain structure of this polymer makes its dimensional measurement more ambiguous, a growing body of literature supports the observation that flexible chain molecules co-elute with compact or globular ones that have the same R_η [9,19,20], although there is still some disagreement on this point [21]. The goal of the present study is to determine whether such simple macromolecules can be used to define the "ideal" calibration curve for a given column —*i.e.* the dependence of K_{SEC} on R for non-interacting spheres. If this is the case, then deviations between this curve and the measured values for proteins can be interpreted more clearly than deviations between the best-fit curve for a series of proteins and the results for any apparent "outliers". It is then possible to determine which (if any) proteins exhibit ideal behavior, and to quantitatively determine the

magnitude of solute-packing interaction effects for those that do not.

EXPERIMENTAL

Materials

Table I lists the proteins employed in this study, along with their MW, isoelectric point, and Stokes radius and viscosity radius, where available. Ficoll fractions were a gift of Dr. K. Granath at Pharmacia Biotechnology, Uppsala, Sweden. Their characteristics are listed in Table II. Pullulan fractions were commercial materials obtained from Shodex Corp. (New York, NY, USA), with MW values and polydispersities shown in Table III. Also tabulated are Stokes radii and viscosity radii, measured as discussed below. Carboxylated starburst dendrimers, hereinafter referred to as "dendrimers", were prepared as described in ref. 16, and were characterized by dynamic light scattering and viscometry, as described elsewhere [26]. Values for their viscosity radii and Stokes radii are given in Table IV. All buffers and salts were reagent grade, from Sigma, Mallinckrodt, Fisher or Aldrich.

Methods

Size-exclusion chromatography. SEC was carried out on a prepacked Superose 6 HR 10/30 column, which had a column efficiency of 3800–4600 plates/m throughout most of these studies.

TABLE I

CHARACTERISTICS OF PROTEINS USED IN THIS STUDY

Protein[a]	Source	MW	*pI*	R_s (nm)	R_η (nm)
Ribonuclease (R-5503)	Bovine pancreas	13 700	9.0	1.75 [22]	1.90 [6]
Lysozyme (L-6876)	Egg white	14 000	11.0	1.85 [23]	2.0 [6]
Myoglobin (M-1882)	Horse heart	17 800	7.3	1.9 [22]	2.06 [6]
β-Lactoglobulin (L-2506)	Bovine milk	35 000	5.2	2.7 [24]	2.65 [6]
Albumin (A-7906)	Bovine serum	66 000	4.9	3.5 [22,25]	3.4 [25]
γ-Globulin (G-5009)	Bovine	150 000	7.0	5.6 [24]	–
Catalase (C-40)	Bovine liver	223 000	5.4	5.2 [22]	5.2 [6]
Apoferritin (A-3600)	Horse spleen	443 000	5.0	6.1 [5,24]	6.1 [6]
Thyroglobulin (T-1001)	Bovine	669 000	5.1	8.6 [22]	7.9 [25]

[a] All from Sigma, except γ-globulin also supplied by CalBiochem.

TABLE II

CHARACTERISTICS OF FICOLL FRACTIONS

Fraction	M_w, LS[a]	M_w, SEC[a]	M_n, SEC[a]	M_w/M_n [b]	$[\eta]$[c] (cm^3/g)	R_s [d] (nm)	R_η [e] (nm)
T1800, Fr. 9	714 000	644 000	337 000	1.91	18.5	17	12.4
T1800, Fr. 12	461 000	460 000	257 000	1.79	16.9	13	10.7
T1800, Fr. 15	321 000	332 000	244 000	1.36	15.5	11	9.4
T1800, Fr. 20	132 000	134 000	113 700	1.18	12.1	7.1	6.4
T2580 IV B, Fr. 3	–	66 500	59 000	1.13	10.0	4.7	4.7
T2580 IV B, Fr. 11	–	21 800	20 300	1.07	7.4	3.0	3.0

[a] From supplier.
[b] M_w = Mass-average molecular mass; M_n = number-average molecular mass.
[c] Calculated from $[\eta] = 0.005 \cdot M_w^{0.27}$ [13].
[d] From measured diffusion coefficient.
[e] From columns 3 and 6, via eqn. (2).

TABLE III

CHARACTERISTICS OF PULLULAN STANDARDS

Sample	M_w [a]	M_w/M_n [a]	R_s (nm)[b]	$[\eta]$ (cm^3/g)	R_η (nm)[c]
Pullulan P-800	853 000	1.14	25.8	171	28.5
Pullulan P-400	380 000	1.12	17.6	105	18.5
Pullulan P-200	186 000	1.13	12.8	55	11.8
Pullulan P-100	100 000	1.10	8.8	39.8	8.6
Pullulan P-50	48 000	1.09	6.1	23.4	5.6
Pullulan P-20	23 700	1.07	4.0	15.5	3.9
Pullulan P-10	12 200	1.06	3.0	9.70	2.7
Pullulan P-5	5800	1.07	2.1	6.30	1.8

[a] From manufacturer.
[b] By QELS.
[c] In 0.20 *M* phosphate buffer (pH 7.0).
[d] From columns 2 and 5, via eqn. 2.

The HPLC instrument was a Beckmann System Gold, equipped with a Beckmann Model 156 refractive index detector or a Waters R401 differential refractive index detector, along with the UV detector supplied with the instrument. Solvent was delivered with a Beckmann 110 B pump and an Altex 210A valve with either a 20, 50 or 100 μl loop. A Rheodyne 0.2 μm precolumn filter was placed in-line to protect the column. Flow-rates were measured and found to be constant within ±0.5% by weighing of collected eluant. Sample preparation was accomplished by shaking or tumbling for 1–2 h. The concentration of all polymers and proteins were in the range 2–5 mg/ml, except for concentration effect studies. Samples were filtered through 0.45 μm Gelman filters before injection. K_{SEC} was determined according to eqn. 1 with V_0 determined from the retention of either $2 \cdot 10^6$ MW dextran or $4 \cdot 10^6$ MW PEO as 6.50 ml, and V_t determined from the retention of dextrose as 19.98 ml.

TABLE IV

CHARACTERISTICS OF DENDRIMERS

Generation	MW [a]	R_s (nm)[b]	R_η (nm)[c]
0.5	924	0.95	–
1.5	2173	1.3	–
2.5	4672	1.5	1.5
3.5	9670	2.5	1.9
4.5	19 666	3.1	2.5
5.5	39 657	3.7	3.1
6.5	79 639	4.5	4.0
7.5	159 603	6.0	5.3

[a] Calculated from expected chemical structure.
[b] From diffusion coefficient, by dynamic light scattering.
[c] From ref. 17.

Quasielastic light scattering (QELS). Light scattering measurements were made using one of two systems. With a Brookhaven (Holtsville, NY, USA) system equipped with a 72 channel digital correlator (BI-2030 AT) and using a Jodon 15 mW He-Ne laser (Ann Arbor, MI, USA) QELS measurements were made at scattering angles from 30° to 150°. Samples at concentrations of *ca.* 2 mg/ml were filtered through 0.20 μm Acrodisc filters (Gelman) prior to analysis. Counts were typically collected for one hour. We obtained the homodyne intensity–intensity correlation function $G(q,t)$, with q, the amplitude of the scattering vector, given by $q = (4\pi n/\lambda)\sin(\theta/2)$, where n is the refractive index of the medium, λ is the wavelength of the excitation light in a vacuum, and θ is the scattering angle. $G(q,t)$ is related to the electric field correlation function of concentration fluctuations $g(q,t)$ by:

$$G(q,t) = A[1 + bg(q,t)^2] \quad (3)$$

where A is the experimental baseline and b is the fraction of the scattered intensity arising from concentration fluctuations.

The diffusion coefficients were calculated using

$$D = \frac{\Gamma\lambda^2}{16\pi^2 \sin^2(\theta/2)} \quad (4)$$

where Γ is the reciprocal of the diffusion time constant, which is obtained from the slope of ln $g^2(q,t)$ *vs.* t plots. The diffusion coefficient, D, is directly related to the Stokes radius, R_s, by Stokes' equation

$$D = \frac{kT}{6\pi\eta R_s} \quad (5)$$

where k is Boltzmann's constant, T is the absolute temperature and η is the viscosity of the solvent.

QELS was also carried out with an Oros (Biotage Co. Charlottesville, VA, USA) Model 801 "molecular weight detector" which employs a 30-mW solid-state 780 nm laser, and an avalanche photodiode detector. Samples were introduced into the 7-μl scattering cell (maintained at 26.5 ± 0.4°C) through 0.2 μm Anotec filters. 90° scattering data were analyzed via cumulants. There were no significant differences between the results obtained using the two instruments.

Viscometry. Measurements were made with a Schott AVSN automatic viscometer equipped with a 10-ml capacity glass Type 531 capillary viscometer, at 25.0 ± 0.02°C. Samples were dissolved in the appropriate solvent at concentrations ranging from 6 to 17 mg/ml and filtered through 0.45 μm Gelman filters. Efflux times were obtained with precisions of ±0.05 s. Solute concentrations were adjusted so that the efflux time of the most concentrated solutions exceeded that of the solvent by 10–30%. Intrinsic viscosities were obtained by the usual extrapolation to zero solute concentration.

RESULTS AND DISCUSSION

Fig. 1 shows the dependence of K_{SEC} on solute radius for Ficoll, pullulan and dendrimers. The mobile phase for the first two solutes was 0.20 *M* NaH_2PO_4–Na_2HPO_4, pH 7.0. In order to ensure the suppression of electrostatic repulsive interactions between the dendrimer and the packing, the ionic strength of the mobile phase was increased to 0.30 *M* for that solute. For the first two solutes, we employ the viscosity radius,

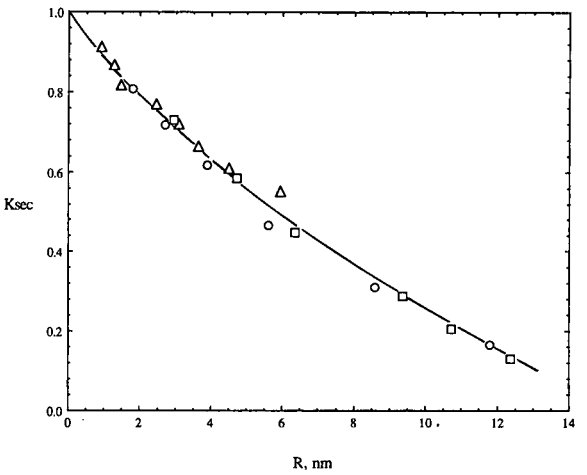

Fig. 1. Dependence of K_{SEC} on solute radius for (□) Ficoll, (○) pullulan, and (△) carboxylated starburst dendrimers, on Superose 6, in pH 7.0 phosphate buffer (0.20 *M* for Ficoll and pullulan, 0.30 *M* for dendrimers). Radii for dendrimers are Stokes radii from dynamic light scattering, all others are viscosity radii (see text for explanation).

obtained from eqn. 2 in conjunction with the intrinsic viscosity measured in the same solvent as the SEC mobile phase. In the case of Ficoll, the Stokes radii are substantially larger than the viscosity radii, particularly for the higher MW samples (see Table II). This result arises from the fact that QELS measures the z-average diffusion coefficient [27] which corresponds to a high moment of the distribution, so that R_s is skewed upward for the high M_w/M_n fractions. R_η corresponds better to the peak-eluting component and is therefore preferable, on these grounds at least. For the dendrimers, viscosity radii and Stokes' radii were measured in the mobile phase 0.38 *M* $NaNO_3$–NaH_2PO_4 (9:1) [17]. For dense spheres such as these dendrimers we should find $R_s = R_\eta$, as one in fact observes for proteins (*viz.* Table I), while for asymmetric solutes, R_η should be larger than R_s [21]. However, as shown in Table IV, we found the viscosity radii to be smaller than the corresponding Stokes' radii. We attribute this unreasonable result to the presence of low MW impurities (detectable by HPLC) which lead to incorrect estimates of the solute concentration and hence negative errors in $[\eta]$ (this hypothesis is also borne out by the scatter of the log$[\eta]$–log M_r plot for the dendri-

mers [17]). These impurities have little effect, however, on the light scattering properties and we therefore employ the measured Stokes radii for the dendrimers.

As seen in Fig. 1, the congruence of the data for the three spherically symmetric solutes is very good. (The only severe deviation is observed for dendrimer G7.5. Since the measured R_s and R_η for this sample are consistent with the lower generation data, we believe these values are reliable, and are inclined to ascribe the result to incomplete carboxylation of this sample, leading to chromatographic adsorption. Such incomplete derivatization for these dendrimers has been noted elsewhere [28].) Furthermore, as previously found [26], the calibration curve so obtained for pullulan and Ficoll on Superose can be very well fitted to a theoretical expression based on the expected permeation of spherical solutes into a collection of somewhat polydisperse cylindrical cavities. It is of interest that the statistical coil nature of pullulan does not perturb its congruence with the more compact spheres. While flexible chains are anisotropic on very short time scales, this "breathing" motion is presumably so fast compared to translation over the length of a pore diameter, that the appropriate time average segment density is spherical. In any event, the good agreement between experiment and theory and the congruence of the data for the three solute sets leads us to identify the calibration curve of Fig. 1 with the behavior of non-interacting spheres.

For spherical solutes in a system of uniform cylindrical pores, K_{SEC} is given by [29,30]

$$K_{SEC} = (1 - R/r_p)^2 \qquad (6)$$

where R and r_p are the dimensions of solute and pore, respectively. (It must be recognized that for any real system, r_p represents a complex average of varying pore sizes and geometries.) A plot of $K_{SEC}^{1/2}$ *vs.* R should be a straight line with a slope of $1/r_p$ and an intercept of unity. Fig. 2 shows the results plotted according to eqn. 6. The data for Ficoll, dendrimers and pullulan conform remarkably well (correlation coefficient 0.993) to a straight line with an intercept of unity. The presence of a pore size distribution should in principle produce curvature in such

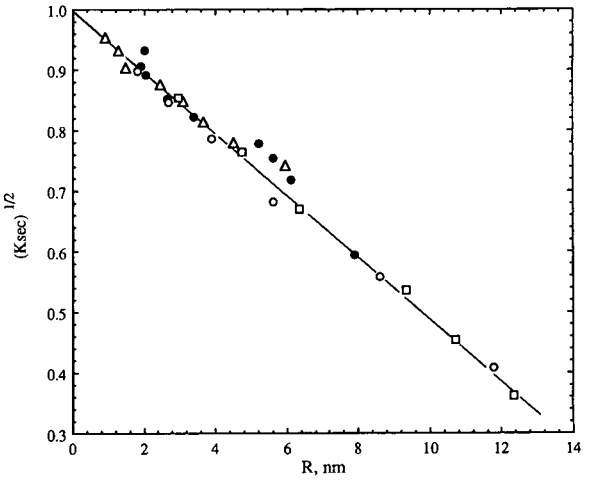

Fig. 2. Data of Fig. 1 plotted according to eqn. 3. Symbols as in Fig. 1, except (●): proteins in 0.50 *M* phosphate buffer (pH 7.0).

plots because the larger solutes sample a different pore size distribution than the smaller ones [26]. While these effects are significant for the present solute set on the lower-pore-size Superose 12 [26], the mean pore size of Superose 6 is much higher [31], *i.e.* twice the size of the biggest solutes studied here. The linearity of Fig. 2 suggests that all solutes sample a similar pore size distribution so that the effective mean pore radius is not solute size-dependent. It is also worth noting here that Waldmann-Meyer [30] did not find an intercept of unity for the elution of dextrans on porous glass and ascribed this

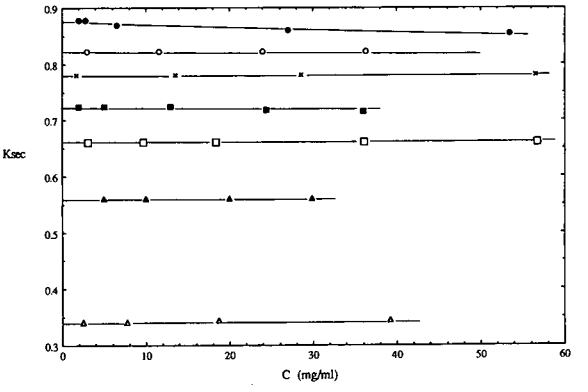

Fig. 3. Concentration dependence of K_{SEC} for proteins in pH 7.0 buffer. ● = Lysozyme; ○ = RNAse; × = myoglobin; ■ = β-lactoglobulin; □ = BSA; ▲ = γ-globulin; △ = thyroglobulin.

effect to permeation of the V_t probe, $2H_2O$, into fissures in the packing material. The linear plot of Fig. 2 facilitates a comparison of the results for proteins to the "ideal" curve.

Fig. 2 also illustrates the deviations from the "ideal" curve for proteins. The values for K_{SEC} for the proteins, shown by the solid symbols in Fig. 2, correspond to the retention volumes measured under conditions of low protein–substrate interaction, *i.e.* 0.50 *M* phosphate buffer (pH 7.0). That the protein results are not influenced by aggregation effects is evident from Fig. 3, which shows that the concentration dependence of K_{SEC} for the proteins studied is negligible, with the possible exception of lysozyme. From Fig. 2 we observe that five of the nine proteins fall on the Ficoll/pullulan/dendrimer curve. Four others, however, elute relatively late. Thus, even neutral pH and a relatively high supporting electrolyte concentration do not ensure the suppression of adsorptive interactions. Given the very low hydrophobicity of Superose [32], it is probable that the adsorptive effects arise from electrostatic interactions with the carboxylic acid groups in the Superose. It is worth pointing out that, in the absence of the data for the synthetic polymers such as was obtained here, the standard procedure for calibration would be to draw the best fit line for the nine proteins. We believe that this would lead to systematic overestimate of the radius of non-adsorbing proteins, and that the error would be large if calibration were in terms of MW as opposed to radius.

At low pH and low ionic strength, the proteins all possess a positive net charge and we would expect the effects of adsorption to be amplified. This is seen in Fig. 4, where protein retentions at pH 4.3 and $I = 0.03$ (filled symbols) are compared to the "ideal" curve, which in this plot is transposed from Fig. 2. This process is justified by our finding that the calibration curve for pullulan is independent of pH or ionic strength, as shown in Fig. 5. It is certainly likely that electrostatic effects could be observed for carboxylated starburst dendrimers; since we conclude from Fig. 1 that, in principle, either Ficoll or pullulan fractions could serve to define the ideal dependence of K_{SEC} on R_η, and since the

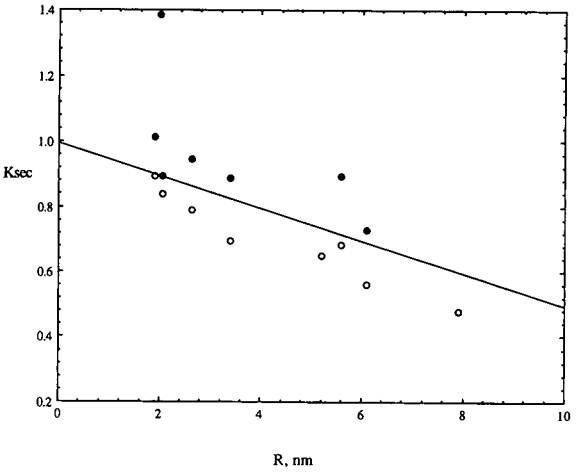

Fig. 4. Comparison of protein chromatography with "ideal" behavior. Solid line is transposed from Fig. 2. ● = Proteins in 0.03 *M* phosphate buffer (pH 4.3); ○ = proteins in 0.03 *M* phosphate buffer (pH 10.0).

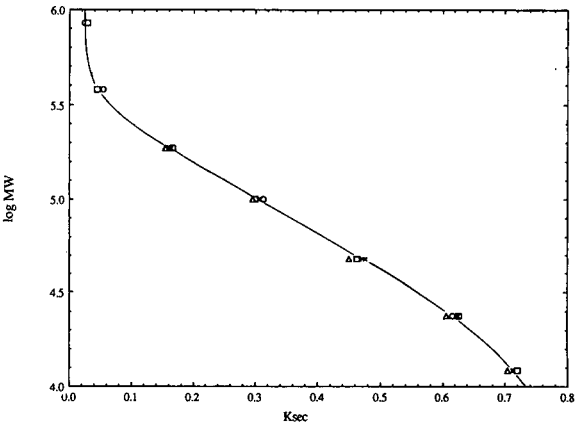

Fig. 5. Effect of ionic strength and pH on elution behavior of pullulan. (○) pH 7.0, $I = 0.1$; (+) pH 10, $I = 0.1$; (□) pH 4.3, $I = 0.1$; (△) pH 10, $I = 0.25$; (×) pH 7.0, $I = 0.25$.

pullulan chromatography is independent of pH and I over a wide range, we believe the transposition of the "ideal curve" from one mobile phase to another is justifiable. At pH 4.3 and $I = 0.03$ *M*, only one of the seven proteins tested falls on the ideal curve, with the other six showing significant positive departures from the expected K_{SEC} values. Conversely, at pH > isoelectric point, both proteins and packing bear a negative charge, and repulsive effects should be strong. The repulsive effect is dominant at high pH, as shown by the open symbols in Fig. 4

measured at $I = 0.03$ M and pH = 10.0. With the exception of RNase, all of the proteins elute before the ideal value of K_{SEC}.

Potschka [33] has noted similar effects for proteins on PW gel. Assuming that the plot of R_η *vs.* K_{SEC} obtained in pH 7.0, 100 mM phosphate buffer corresponded to ideal behavior, Potschka used this calibration curve along with the elution volume measured at higher pH to define an "effective R_η", which he interpreted as a sum of the geometric contribution from the protein and an electrostatic repulsion "length". By using neutral polymers to establish the ideal curve, we are less dependent on the assumption that all protein–packing interactions can be suppressed at some conditions, and the concomitant need to identify these conditions. The horizontal difference between the ideal curve and the measured R_η in Fig. 4 for the proteins at high pH is a similar measure of the contribution of electrostatic repulsion to K_{SEC}, and these values of ΔR are reported in Table V along with the net charge for those proteins where titration data are available. It is possible to interpret positive values of ΔR (in the repulsive regime) as an effective increase in protein size due to electrostatic repulsive forces [33] (although it is no more or less credible to assign the earlier elution to the electrical double layer on the surface of the packing [34]). On the other hand, negative values of ΔR (in the attractive regime) have no physical significance, and are included in Table V only for qualitative consideration.

The data in Table V, listed in order of decreasing protein pI, show the expected qualitative trends in the repulsive regime. At high pH, ΔR becomes more positive with decreasing isoelectric point. At neutral or low pH, the results are more complex. For example, RNase, β-lactoglobulin and BSA, with virtually identical net charges at pH = 4.3, exhibit differing excess retention, as represented by the negative values of ΔR. The magnitude of this quantity varies inversely with molecular mass, suggesting that the mean surface charge density might show better correlation with ΔR. In fact, the correlation coefficient between this last variable and Z/R^2 is found to be 0.99. On the other hand, the retention of lysozyme is clearly outside of this correlation. The data at neutral pH are even less amenable to this analysis, and it is difficult to account for the large retention of γ-globulin and the nearly ideal behavior of BSA on the basis of net charge. These observations are consistent with the findings of Regnier and co-workers [35] who emphasized the role of the "charge patches" in controlling ion-exchange chromatography of proteins, and are analogous to our results for the association of proteins with oppositely charged soluble polyelectrolytes [36], in which the interaction appears to be dominated by some local (as opposed to global) charge density.

The current data base does not allow for a systematic investigation of the correlation of excess retention or repulsion effects with the local and global charge states of the protein. Efforts are currently underway to expand the chromatographic data set, using other proteins and acquiring the necessary pH–titration information. Attempts to correlate protein charge

TABLE V

PROTEIN NET CHARGES AND DISPLACEMENTS FROM IDEAL CURVE IN 0.03 M PHOSPHATE BUFFER

ΔR values are horizontal displacements from "ideal curve" in Fig. 4. Negative values correspond to excess retention, positive values to repulsion.

	pH = 4.3		pH = 7.0		pH = 10.0	
Protein	Z	ΔR	Z	ΔR	Z	ΔR
Lysozyme	+12	(< −30)	+7	(−7)	+3	0
RNase	+9	(−22)	+3	(−1)	−3	(−1)
γ-Globulin	> +30	(−35)	0	(−7)	n.a.	8
β-Lactoglobulin	+8	(−15)	−18	+2	−36	17
BSA	+8	(−12)	−16	(−1)	−39	26

state with retention [37] will employ the computational and graphics capability of finite-element analysis programs, such as UHBD, developed for protein electrostatic modeling [38].

CONCLUSIONS

The dependence of K_{SEC} on the viscosity radius R for three spherically symmetrical synthetic polymers —Ficoll, pullulan and carboxylated dendrimers— conform to a single line which fits the expression $K_{SEC}^{1/2} = 1 - R/r_P$. At moderate ionic strength and neutral pH some globular proteins fall on this curve, which may be viewed as representing the chromatographic behavior of non-interacting spheres. Deviations from this curve may be identified with either significant departure from spherical symmetry, or solute–stationary phase interactions. The positive deviations seen for proteins at pH = 4.3 and $I = 0.03$ M, and the negative deviations for proteins at this ionic strength and at pH 10.0, indicate that these departures from the "ideal" curve arise from repulsive or attractive electrostatic interactions with the packing. By reference to the "ideal" curve these interactions may be measured quantitatively. The magnitude of the repulsive or attractive interactions do not correlate in any simple way with the protein net charge. This finding is consistent with the observation by Haggerty and Lenhoff [39] that the net protein charge does not allow any prediction of the ion-exchange capacity factor, and that the important variable is instead the mean surface potential of the protein.

ACKNOWLEDGEMENTS

Support from the National Science Foundation under Grant CHE-9021484 is gratefully acknowledged. We also thank Dr. K. Granath, of Pharmacia Biotechnology for providing the Ficoll fractions, and Dr. Lars Hagel, Pharmacia Biotechnology for the gift of a Superose column.

REFERENCES

1 K.M. Gooding, *Biochromatography*, 1 (1986) 34.
2 R.C. Montelaro, in P.L. Dubin (Editor), *Aqueous Size Exclusion Chromatography*, Elsevier, Amsterdam 1988, Ch. 10.
3 P.L. Dubin, *Adv. Chromatogr.*, 31 (1992) 122–125.
4 R.W.A. Oliver (Editor), *HPLC of Macromolecules*, IRL Press, Oxford, 1989, p. 5, 79.
5 P.J. Flory, *Principles of Polymer Chemistry*, Cornell University Press, Ithaca, NY, 1953, p. 606.
6 M. Potschka, *J. Chromatogr.*, submitted for publication.
7 T.C. Laurent and J. Killander, *J. Chromatogr.*, 14 (1964) 317.
8 G. Ackers, *J. Biol. Chem.*, 242 (1967) 3237.
9 H. Waldmann-Meyer, *J. Chromatogr.*, 410 (1987) 233.
10 M. le Maire, A. Ghazi, M. Martin and F. Brochard, *J. Biochem.*, 106 (1989) 814.
11 H. Holter and K.M. Møller, *Exp. Cell. Res.*, 15 (1956) 631.
12 T.C. Laurent and K. Granath, *Biochim Biophys. Acta*, 136 (1967) 191.
13 K. Granath, private communication.
14 M.P. Bohrer, G.D. Patterson and P.J. Carroll, *Macromolecules*, 17 (1984) 1170.
15 M.G. Davidson and W.M. Deen, *Macromolecules*, 21 (1988) 3474.
16 D.A. Tomalia, R.M. Naylor and W.A. Goddard, III, *Angew. Chem. Int. Ed. Engl.*, 29 (1990) 138.
17 P.L. Dubin, S.L. Edwards, J.I. Kaplan, M.S. Mehta, D. Tomalia and J. Xia, *Anal. Chem.*, 64 (1992) 2344.
18 T. Kato, T. Okamoto, T. Tokuya and A. Takahashi, *Biopolymers*, 21 (1982) 1623.
19 R.P. Frigon, J.K. Leypoldt, S. Uyeji and L.W. Henderson, *Anal. Chem.*, 55 (1983) 1349.
20 P.L. Dubin, B.A. Smith, J.M. Principi and M.A. Fallon, *J. Colloid Interface Sci.*, 127 (1989) 558.
21 M. le Maire, A. Viel and J. Møller, *Anal. Biochem.*, 177 (1989) 50.
22 M. le Maire, A. Ghazi, J.V. Møller and L.P. Aggerbeck, *Biochem. J.*, 243 (1987) 399.
23 D. Nicoli and G. Benedek, *Biopolymers*, 15 (1976) 2421.
24 R.C. Tarvers and F.C. Church, *Int. J. Pept. Prot. Res.*, 26 (1985) 539.
25 K. Horiike, H. Tojo, T. Yamano and M. Nozaki, *J. Biochem.*, 93 (1983) 99.
26 S. Hussain, M.S. Mehta, J.I. Kaplan and P.L. Dubin, *Anal. Chem.*, 63 (1991) 1132.
27 G.D.J. Phillies, *Anal. Chem.*, 62 (1990) 1049A.
28 P. Russo, in preparation.
29 E.F. Casassa, *J. Phys. Chem.*, 75 (1971) 275.
30 H. Waldmann-Meyer, *J. Chromatogr.*, 350 (1985) 1.
31 L. Hagel, in P.L. Dubin (Editor), *Aqueous Size Exclusion Chromatography*, Elsevier, Amsterdam, 1988, Ch. 5.
32 P.L. Dubin and J.M. Principi, *Anal. Chem.*, 61 (1989) 780.
33 M. Potschka, *J. Chromatogr.*, 441 (1988) 239.
34 P.L. Dubin, R.M. Larter, C.J. Wu and J.I. Kaplan, *J. Phys. Chem.*, 94 (1990) 7244.
35 W. Kopaciewicz, M.A. Rounds, J. Fausnaugh and F.E. Regnier, *J. Chromatogr.*, 266 (1983) 3.

36 J.M. Park, B.B. Muhoberac, P.L. Dubin and J. Xia, *Macromolecules*, 25 (1992) 290.
37 P.L. Dubin, J. Klimkowski, J. Xia and Y. Zhu, in preparation.
38 M.E. Davis, J.D. Madura, B.A. Luty and J.A. McCammon, *Comp. Phys. Comm.*, 62 (1991) 187.
39 L. Haggerty and A.M. Lenhoff, *J. Phys. Chem.*, 95 (1991) 1472.

Journal of Chromatography, 635 (1993) 61–70
Elsevier Science Publishers B.V., Amsterdam

CHROM. 24 800

Retention indices of phenols for internal standards in reversed-phase high-performance liquid chromatography

Application to retention prediction and selectivities of mobile phases and packing materials

Shiro Yamauchi

Analytical Development, Formulation Research Institute, Otsuka Pharmaceutical Co., Ltd., 224-18 Ebisuno, Hiraishi, Kawauchi-cho, Tokushima 771-01 (Japan)

(First received February 17th, 1992; revised manuscript received December 1st, 1992)

ABSTRACT

The retention indices of previously reported phenols were calculated by means of the least-squares method on the basis of *n*-alkyl 4-hydroxybenzoate scales and applied to retention predictions and selectivities of mobile phases and packing materials. A simple method was established which predicts the retention times of phenols as candidates for internal standards in reversed-phase high-performance liquid chromatography. Relationships between log k' and the numbers of carbon atoms in the alkyl chain of *n*-alkyl 4-hydroxybenzoates, which are standard compounds for calculating retention indices, showed excellent linearity under all the tested conditions. The retention time of each phenol was calculated from the retention data for one marker solution consisting of uracil, methyl 4-hydroxybenzoate and ethyl 4-hydroxybenzoate and the retention index of each phenol. The experimentally observed retention times and predicted values agreed to within 10% relative error under several conditions. Using this technique, approximate retention times of phenols can be predicted easily and promptly. In addition, selectivities of the mobile phase and packing materials for phenols are discussed.

INTRODUCTION

Previously, we have reported a group of commercially available phenols and their utility as candidates for internal standards in RP-HPLC [1]. Their most valuable property is that they are eluted in a constant order regardless of the HPLC conditions that are used in pharmaceutical analysis with hydrocarbon chemically bonded silica gel columns. In the process of selecting an internal standard, the retention times of candidate compounds are usually determined and one compound is selected on the basis of the results. In a previous paper [1], we showed only their typical elution pattern in acetonitrile (ACN)–water (20:80 to 60:40) mobile phases with one particular prepacked ODS column (Nucleosil $5C_{18}$, 15 cm × 4.6 mm I.D.). However, the column size, flow-rate and temperature of the column oven and/or particle size of the packing material are not usually identical in each HPLC analysis even though the mobile phase and the kind of packing material are common. Therefore, the retention times of phenols in Fig. 1 in ref. 1 are not always useful.

We considered that a simple method for predicting retention times should be developed for the purpose of selecting a suitable internal standard among candidate phenols. Their elution order was estimated on the basis of the linearity of logarithmic plots of their capacity factors (k') under different conditions. Expressing each

0021-9673/93/$06.00

phenol in terms of a suitable physico-chemical parameter (f), the retention time of each phenol will be able to be predicted by the following equation, based on a linear free energy relationship:

$$\log k' = af + b \quad (1)$$

where k' is the capacity factor of the analyte and a and b are constants.

There have been many investigations relevant to retention time predictions in liquid chromatography, and recently Skelly *et al.* [2] reported "computer-assisted internal standard selection (CAISS) in RP-HPLC". Based on investigations using eqn. 1, Smith and Burr [3–7] have attempted to predict retentions of many kinds of organic compounds by using retention indices based on alkyl aryl ketones and they have been successful in predicting retentions under a wide range of conditions. They used retention indices based on an alkyl aryl ketone scale as f and demonstrated their utility in retention predictions. On the other hand, Hanai and co-workers [8–14] have reported systems for retention predictions of many kinds of compounds by using the logarithms of partition coefficients in 1-octanol–water (log P) according to Rekker's fragment constants [15] as f. In this study, we chose retention index as f because the group of phenols that we selected include *n*-alkyl 4-hydroxybenzoates, which are suitable as standard compounds for calculating retention indices. In this paper, we report the method and some application results for retention prediction and, in addition, selectivities of the mobile phase and packing materials for phenols.

EXPERIMENTAL

n-Octyl 4-hydroxybenzoate was obtained from Lancaster Synthesis. Other chemicals, apparatus and procedures were as described previously [1]. There is no general standard compound or overall method for determining the column void volume, which is necessary for calculating capacity factors, and reviews of this issue have been published [16,17]. We chose uracil to determine the column void volume in this study. All the phenols used are listed in Table I.

TABLE I

PHENOLS USED IN THIS STUDY

The structure and name of each phenol are expressed using abbreviations of substituents: Me = CH_3–; Et = C_2H_5–; iso-Pr = $(CH_3)_2CH$–; *n*-Pr = $CH_3(CH_2)_2$–; *sec.*-Bu = $CH_3CH_2CH(CH_3)$–; *n*-Bu = $CH_3(CH_2)_3$–; iso-Am = $(CH_3)_2CH(CH_2)_2$–; *n*-Am = $CH_3(CH_2)_4$–; *n*-Hex = $CH_3(CH_2)_5$–; *n*-Hep = $CH_3(CH_2)_5$–; Oc = $CH_3(CH_2)_3CH(C_2H_5)CH_2$–; *n*-Oc = $CH_3(CH_2)_7$–; *n*-No = $CH_3(CH_2)_8$–; Ph = C_6H_5–.

No.	Derivative	Substituent
1	4-Hydroxyacetanilide	4-NHCOMe
2	3-Hydroxyacetanilide	3-NHCOMe
3	2-Hydroxyacetanilide	2-NHCOMe
4	4-Hydroxyacetophenone	4-COMe
5	3-Hydroxyacetophenone	3-COMe
6	Methyl 4-hydroxybenzoate	4-COOMe
7	4-Hydroxypropiophenone	4-COEt
8	3-Nitrophenol	3-NO_2
9	Ethyl 4-hydroxybenzoate	4-COOEt
10	4-Chlorophenol	4-Cl
11	4-Bromophenol	4-Br
12	4-Hydroxybenzophenone	4-COPh
13	Isopropyl 4-hydroxybenzoate	4-COOiso-Pr
14	*n*-Propyl 4-hydroxybenzoate	4-COO*n*-Pr
15	4-Hydroxyvalerophenone	4-CO*n*-Bu
16	2,3-Dichlorophenol	2,3-Cl_2
17	2,5-Dichlorophenol	2,5-Cl_2
18	4-Isopropylphenol	4-iso-Pr
19	*sec.*-Butyl 4-hydroxybenzoate	4-COO*sec.*-Bu
20	4-Hydroxybiphenyl	4-Ph
21	*n*-Butyl 4-hydroxybenzoate	4-COO*n*-Bu
22	4-*tert.*-Butyphenol	4-*tert.*-Bu
23	Benzyl 4-hydroxybenzoate	4-$COOCH_2Ph$
24	Thymol	3-Me-6-iso-Pr
25	Isoamyl 4-hydroxybenzoate	4-COOiso-Am
26	*n*-Amyl 4-hydroxybenzoate	4-COO*n*-Am
27	*n*-Hexyl 4-hydroxybenzoate	4-COO*n*-Hex
28	*n*-Heptyl 4-hydroxybenzoate	4-COO*n*-Hep
29	2-Ethyl-hexyl 4-hydroxybenzoate	4-COO-Oc
30	*n*-Octyl 4-hydroxybenzoate	4-COO*n*-Oc
31	*n*-Nonyl 4-hydroxybenzoate	4-COO*n*-No

RESULT AND DISCUSSION

Linear relationship between log k' and the carbon numbers of alkyl chain in alkyl 4-hydroxybenzoates

In RP-HPLC, there is a linear relationship between log k' and carbon numbers of homologues, *e.g.*, 2-ketoalkanes [18], 1-nitroalkanes [19], alkyl aryl ketones [20] and 1-phenylalkanes

[21]. We plotted log k' against the carbon number of the alkyl chain in alkyl 4-hydroxybenzoates. As can be seen in Figs. 1 and 2, the relationship between log k' and carbon number seems to be linear. However, the point for the compound with an alkyl carbon number of 1, *i.e.*, methyl 4-hydroxybenzoate, deviates from each line. These results are similar to what Smith and Burr [5] found with alkylbenzenes and Bogusz and Aderjan [19] with 1-nitroalkanes. In order to determine the extent of the deviation of methyl 4-hydroxybenzoate from the log k' *vs.* number lines, we determined the values of α_n, which is a relative increment of log k' per methylene unit in alkyl 4-hydroxybenzoates, defined by the following equation:

$$\alpha_n = (\log k'_n - \log k'_{n-1})/(\log k'_{n+1} - \log k'_n) \quad (2)$$

where $n+1$, n and $n-1$ are the carbon numbers of the alkyl chain in alkyl 4-hydroxybenzoates. α_n was found to be 0.89 ± 0.01 for $n = 2$ and 0.98 ± 0.02 for $n = 3$–8. We found that the increment of log k' per methylene unit between methyl and ethyl is about 90% of the others. This result indicates that the carbon number of methyl 4-hydroxybenzoate should be estimated as 1.1. This is very significant in the determination of the constants a and b in eqn. 1, as described later. The regression results between log k' and carbon number are shown in Table II, where the carbon number of methyl 4-hydroxybenzoate is 1.1 in accordance with the above result. Excellent linearity was shown under all conditions.

Calculation of retention indices

Based on alkyl 4-hydroxybenzoate scales, the retention index of each phenol was calculated by the least-squares method as reported by Smith and Burr [3,20]. In this process the retention indices of alkyl 4-hydroxybenzoates are equal to 100 times the carbon number of the alkyl chain in alkyl 4-hydroxybenzoates except for methyl 4-hydroxybenzoate, whose retention index is 110. The results of the calculations are given in Tables III–V. None of the values depend on pH (2.0–7.0), ionic strength or counter ion (alkyl sulphonates), as reported previously [1].

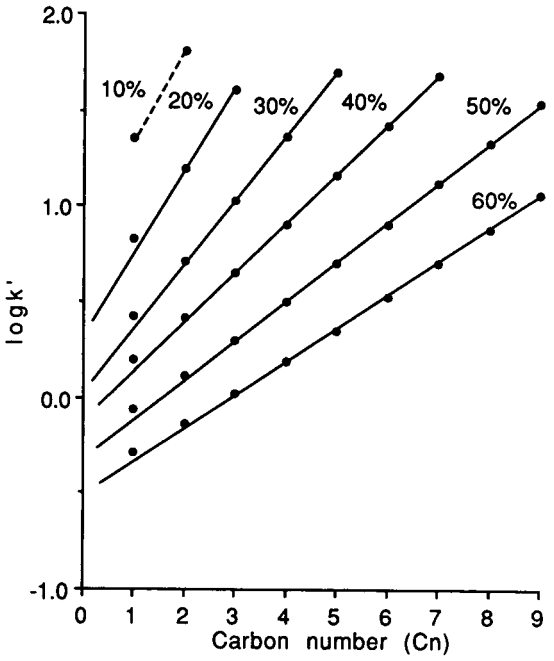

Fig. 1. Relationship between log k' and carbon number in acetonitrile–water mobile phases with Nucleosil $5C_{18}$ column. Percentage values on lines indicate acetonitrile concentration.

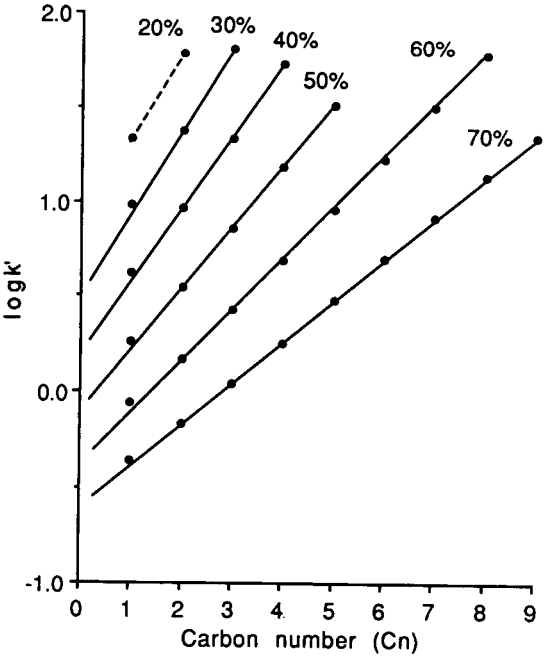

Fig. 2. Relationship between log k' and carbon number in methanol–water mobile phases with Nucleosil $5C_{18}$ column. Percentage values on lines indicate methanol concentrations.

TABLE II

LINEAR RELATIONSHIP BETWEEN LOG k' OF n-ALKYL 4-HYDROXYBENZOATES AND CARBON NUMBER IN RP-HPLC

Log $k' = a \cdot 100C_n + b$. C_n is carbon number of alkyl chain in n-alkyl 4-hydroxybenzoates, except for methyl 4-hydroxybenzoate, C_n for methyl 4-hydroxybenzoate is 1.1.

Column	Mobile phase	a (×1000)	b	r [a]	n [b] (range of alkyl group used in the correlation)
Nucleosil $5C_{18}$	ACN–water (10:90)	5.078	0.793	–	2 (methyl to ethyl)
	ACN–water (20:80)	4.111	0.374	0.99999	3 (methyl to propyl)
	ACN–water (30:70)	3.257	0.060	0.9999	4 (methyl to butyl)
	ACN–water (40:60)	2.521	−0.093	0.9998	7 (methyl to heptyl)
	ACN–water (50:50)	2.030	−0.301	0.9997	9 (methyl to nonyl)
	ACN–water (60:40)	1.704	−0.487	0.9997	9 (methyl to nonyl)
	MeOH–water (20:80)	5.011	0.781	–	2 (methyl to ethyl)
	MeOH–water (30:70)	4.373	0.500	0.99998	3 (methyl to propyl)
	MeOH–water (40:60)	3.776	0.207	0.99995	4 (methyl to butyl)
	MeOH–water (50:50)	3.198	−0.096	0.9999	5 (methyl to amyl)
	MeOH–water (60:40)	2.656	−0.363	0.9998	8 (methyl to octyl)
	MeOH–water (70:30)	2.158	−0.599	0.99997	9 (methyl to nonyl)
Chemcosorb 5-ODS-H	ACN–water (30:70)	3.466	0.019	0.99994	5 (methyl to amyl)
YMC Pack ODS-A, A-302	ACN–water (30:70)	3.521	0.000	0.9999	5 (methyl to amyl)
Nucleosil $5C_{18}$	ACN–water (30:70)	3.257	0.060	0.99993	5 (methyl to amyl)
μBondapak C_{18}	ACN–water (30:70)	2.983	−0.219	0.9998	5 (methyl to amyl)
Zorbax ODS	ACN–water (30:70)	3.357	−0.024	0.9999	5 (methyl to amyl)
Cosmosil 5Ph	ACN–water (30:70)	2.487	−0.004	0.999995	5 (methyl to amyl)
Nucleosil $5C_8$	ACN–water (30:70)	2.763	0.025	0.999994	6 (methyl to hexyl)
Nucleosil $5C_{18}$	ACN–water (30:70)	3.257	0.060	0.99993	5 (methyl to amyl)
	MeOH–water (40:60)	3.776	0.207	0.99995	4 (methyl to butyl
	ACN–THF–water (25:5:70)	3.353	0.140	0.99996	4 (methyl to butyl)
	ACN–MeOH–water (20:20:60)	3.299	−0.005	0.9999	5 (methyl to amyl)
	ACN–MeOH–THF–water (1:1:1:7)	3.501	0.271	0.9998	4 (methyl to butyl)

[a] r = Correlation coefficient.
[b] n = Number of data points.

Long-term reproducibility and universality

Reproducibility and universality of the calculated retention indices of phenols are very important [4]. These were checked over 2 years under various chromatographic conditions. The difference between the maximum and minimum value for each phenol was not more than 10 retention index units. Hence long-term reproducibility and universality were confirmed.

Influence of temperature

All phenols were chromatographed using a Nucleosil $5C_{18}$ prepacked column with ACN–water (40:60) as eluent at 25, 35, 45 and 55°C. The calculated retention indices of each phenol did not change with variation in the temperature of the column oven.

Selectivities of mobile phases and packing materials for phenols

As can be seen from Tables III and IV, the retention indices of phenols having an alkylcarbonate group (of course, n-alkyl carbonate groups are excluded) or an alkylcarbonyl group are independent of the content of organic solvents [ACN or methanol (MeOH)] and the kind of organic solvent in the mobile phase. On the other hand, those of phenols in which the sub-

TABLE III

RETENTION INDICES OF PHENOLS IN ACETONITRILE–WATER AND METHANOL–WATER MOBILE PHASE WITH NUCLEOSIL $5C_{18}$ COLUMN

Values of *n*-alkyl 4-hydroxybenzoates are 100 times the carbon number in the alkyl chain of ester groups except for methyl 4-hydroxybenzoate.

No.	Phenol[a]	Retention index											
		Acetonitrile (%)						Methanol (%)					
		10	20	30	40	50	60	20	30	40	50	60	70
1	4-NHCOMe	−118	−148	−154	–	–	–	−86	−155	–	–	–	–
2	3-NHCOMe	−62	−86	−97	−103	–	–	−74	−95	−103	–	–	–
3	2-NHCOMe	−40	−41	−30	−24	−20	−33	−55	−59	−54	−52	−54	−54
4	4-COMe	29	19	23	20	26	9	34	13	15	6	4	2
5	3-COMe	48	44	49	50	59	53	40	27	30	21	20	17
6	4-COOMe	110	110	110	110	110	110	110	110	110	110	110	110
7	4-COEt	125	119	124	122	131	123	119	110	111	107	110	113
8	3-NO_2	–	141	166	173	184	176	–	–	105	116	134	147
10	4-Cl	–	199	222	231	247	243	–	147	177	187	205	219
11	4-Br	–	230	252	258	272	274	–	179	208	218	238	254
12	4-COPh	–	290	281	269	269	257	–	275	274	259	256	255
13	4-COOiso-Pr	–	284	286	281	284	281	–	276	276	269	268	272
15	4-CO*n*-Bu	–	313	315	309	314	308	–	302	298	302	301	306
16	2,3-Cl_2	–	–	311	319	326	330	–	–	264	282	288	305
17	2,5-Cl_2	–	–	332	343	358	356	–	–	276	302	312	331
18	4-iso-Pr	–	–	335	342	354	359	–	–	286	297	310	323
19	4-COO*sec.*-Bu	–		373	367	371	365	–	–	361	359	352	353
20	4-Ph	–	–	391	387	383	380	–	–	352	360	357	367
22	4-*tert.*-Bu	–	–	398	403	412	416	–	–	352	362	373	387
23	4-$COOCH_2Ph$	–	–	431	412	403	382	–	–	417	409	396	393
24	3-Me-6-iso-Pr	–	–	437	456	468	476	–	–	375	397	406	424
25	4-COOiso-Am	–	–	488	479	477	473	–	–	–	477	476	478
29	4-COO-Oc	–	–	–	–	750	749	–	–	–	–	745	745

[a] Each phenol is expressed using abbreviations of substituents (see Table I).

stituent group is nitro, halogen or alkyl do show a slight dependence. The retention indices increase with increasing the content of organic solvent, indicating that these phenols are more retained than alkylcarbonylphenols and alkyl 4-hydroxybenzoates in a more hydrophobic mobile phase.

The influence of the kind of organic solvent in the mobile phase on selectivity was evaluated from Table IV. The eluotropic strengths of mobile phases I [ACN–water (30:70)] and II (MeOH–water (40:60)] are almost equal in RP-HPLC [22,23]. It seems that phenols in which the substituent group is nitro, halogen or alkyl are more retained in ACN than MeOH by comparison with phenols having carbonyl groups (–NHCOMe, –COR or –COOR, R = alkyl).

Further, in mixtures of organic solvents, additive properties of the selectivity were recognized qualitatively. The selectivity of the packing materials for phenols can be evaluated from Table V. As expected, the three phenols having substituents that include a phenyl group (Nos. 12, 20 and 23) are more retained with a phenyl column (column F in Table V) owing to $\pi-\pi$ interactions. The selectivities of packing materials for other phenols are almost equal with all columns, C_{18}, C_8 and phenyl. As indicated later under

TABLE IV

RETENTION INDICES OF PHENOLS IN VARIOUS MOBILE PHASES WITH NUCLEOSIL $5C_{18}$ COLUMN

Values of *n*-alkyl 4-hydroxybenzoates are 100 times the carbon number in the alkyl chain of ester groups except for methyl 4-hydroxybenzoate.

No.	Phenol[a]	Mobile phase[b]				
		I	II	III	IV	V
1	4-NHCOMe	−154	−169	−179	−164	−183
2	3-NHCOMe	−97	−103	−109	−97	−104
3	2-NHCOMe	-30	−54	−50	−32	−54
4	4-COMe	23	15	11	15	1
5	3-COMe	49	30	37	42	26
6	4-COOMe	110	110	110	110	110
7	4-COEt	124	111	114	120	110
8	3-NO_2	166	105	174	148	187
10	4-Cl	222	177	237	204	253
11	4-Br	252	208	268	236	285
12	4-COPh	281	274	278	276	277
13	4-COOiso-Pr	286	276	286	277	281
15	4-CO*n*-Bu	315	298	312	311	310
16	2,3-Cl_2	311	264	328	294	353
17	2,5-Cl_2	332	276	350	309	372
18	4-iso-Pr	335	286	337	313	335
19	4-COO*sec.*-Bu	373	361	373	364	372
20	4-Ph	391	352	393	369	398
22	4-*tert.*-Bu	398	352	402	378	402
23	4-$COOCH_2Ph$	431	417	431	418	438
24	3-Me-6-iso-Pr	437	375	441	411	442
25	4-COOiso-Am	488	–	490	484	–
29	4-COO-Oc	–	–	–	–	–

[a] Each phenol is expressed using abbreviations of substituents (see Table I).
[b] I = ACN–water (30:70); II = MeOH–water (40:60); III = ACN–THF–water (25:5:70); IV = ACN–MeOH–water (20:20:60); V = ACN–MeOH–THF–water (10:10:10:70).

Application, with the C_4 column the selectivity was also the same as for the others.

A phenolic hydroxy group hardly seems to interact with residual silanol groups, as in Table V the retention indices of phenols, except for *n*-alkyl 4-hydroxybenzoates, with column E, which is not end-capped, are almost identical with those with end-capped ODS columns (columns A–D), and the dissociation constants (pK_a) of phenols listed in Table I are within the range 7.5–10.2. If a phenolic hydroxy group interacts with residual silanol groups under the conditions of this study, the difference in retention indices between non-end-capped and end-capped columns should be recognized in accordance with the pK_a values.

Determination of the coefficients a and b

For calculating the retention times of the phenols from eqn. 1, first the regression coefficients *a* and *b* must be determined. Our method is different from Smith and Burr's [7] or Hanai and Hubert's [8] methods. In our procedure, a marker solution consisting of uracil, methyl 4-hydroxybenzoate (MHB) and ethyl 4-hydroxybenzoate (EHB) is chromatographed under any HPLC conditions. The sample solvent is methanol in each instance because the peak shapes and retention times of three components were independent of the sample solvents [24,25], which were water, methanol–water (50:50), methanol and acetonitrile, under the HPLC conditions used in this study. As MHB and EHB

TABLE V

RETENTION INDICES OF PHENOLS IN ACETONITRILE–WATER (30:70) WITH VARIOUS COMMERCIALLY AVAILABLE COLUMNS

Values of n-alkyl 4-hydroxybenzoates are 100 times the carbon number in the alkyl chain of ester groups except for methyl 4-hydroxybenzoate.

No.	Phenol[a]	Column[b]						
		A	B	C	D	E	F	G
1	4-NHCOMe	−148	−148	−154	−138	−156	−197	−176
2	3-NHCOMe	−92	−92	−97	−87	−102	−123	−114
3	2-NHCOMe	−28	−27	−30	−26	−24	−51	−45
4	4-COMe	22	23	23	24	19	16	15
5	3-COMe	52	54	49	48	46	45	39
6	4-COOMe	110	110	110	110	110	110	110
7	4-COEt	123	123	124	122	121	120	119
8	3-NO_2	167	170	166	161	158	177	165
10	4-Cl	225	229	222	220	227	234	214
11	4-Br	257	259	252	248	254	260	246
12	4-COPh	274	273	281	280	273	307	290
13	4-COOiso-Pr	284	282	286	281	279	287	287
15	4-CO*n*-Bu	314	314	315	309	312	317	309
16	2,3-Cl_2	314	315	311	299	315	328	311
17	2,5-Cl_2	333	333	332	319	333	343	328
18	4-iso-Pr	340	340	335	329	339	341	322
19	4-COO*sec.*-Bu	372	372	373	366	369	376	373
20	4-Ph	390	390	391	377	390	429	396
22	4-*tert.*-Bu	404	403	398	394	402	404	384
23	4-$COOCH_2Ph$	425	423	431	421	423	476	441
24	3-Me-6-iso-Pr	444	445	437	422	443	452	427
25	4-COOiso-Am	486	483	488	485	483	483	483
29	4-COO-Oc	–	–	–	–	–	–	–

[a] Each phenol is expressed using abbreviations of substituents (see Table I).
[b] A = Chemcosorb 5-ODS-H; B = YMC Pack ODS-A, A-302; C = Nucleosil $5C_{18}$; D = μBondapak C_{18}; E = Zorbax ODS; F = Cosmosil 5Ph; G = Nucleosil $5C_8$.

are the first two *n*-alkyl 4-hydroxybenzoate homologues and they are eluted faster than other homologues, the time required to chromatograph the marker solution can be reduced. The excellent linear relationships between log k' and the carbon number of the alkyl chain in alkyl 4-hydroxybenzoates (Table II) make it possible to determine accurately coefficients a and b in eqn. 1 from only the results for one marker solution. As the f values are 110 and 200 for MHB and EHB, respectively, in eqn. 1, a and b can be calculated using the following equations:

$$a = \frac{1}{90}(\log k'_{Et} - \log k'_{Me}) \quad (3)$$

$$b = \frac{1}{9}(20 \log k'_{Me} - 11 \log k'_{Et}) \quad (4)$$

where k'_{Me} and k'_{Et} are the capacity factors of MHB and EHB, respectively. We adopted this procedure for determining a and b because these coefficients change with not only the kind and percentage of organic solvents in the mobile phase and the kind of column but also the manufacturer of columns with nominally the same packing material, *e.g.*, octadecylsilica gels. Hence we think that the best method is determination from experimental data. In this procedure, from experimental retention data for only

one marker solution, we can determine the most important parameters (a and b) in predicting retention data simply, exactly and promptly.

Some retention indices were dependent on the chromatographic conditions. Smith and Burr [3–7] and West [26] reported a quadratic relationship and a linear relationship between retention indices and the percentage of miscible organic solvents in binary mobile phases, respectively, and were successful in predicting the retentions of a large number of organic compounds over a wide range of mobile phases in RP-HPLC. However, our aim is to predict the retention times of the 31 phenols using previously reported HPLC conditions, and the variation of the retention indices is not so large. Accordingly, we decided to use the average values in Tables III to IV to simplify the procedure. The average values are given in Table VI.

The procedure for predicting the retention times of phenols is as follows. In the first step, the marker solution has to be chromatographed. Over the range of previously reported conditions [1], the elution order of three compounds in the marker solutions is always uracil, MHB and EHB. From this result, a and b are calculated through eqns. 3 and 4 experimentally. Next, a, b, the retention indices in Table VI and the retention time (t_0) of uracil are substituted in the following equation and finally the calculated retention times (t) of each phenol can be obtained:

$$t = t_0[1 + 10^{(aI+b)}] \quad (5)$$

In the chromatography of the marker solution, if after the first compound (uracil) has been eluted the second (MHB) is not eluted within a reasonable time in organic solvent-poor mobile phases, the probable candidates are limited to five kinds of phenols (Nos. 1–5 in Table I).

APPLICATION

In order to demonstrate the utility of the proposed method for predicting the retention times of phenols, we applied it under several sets of conditions that we have been using for quantitative analysis by RP-HPLC. The predicted and observed values are shown in Fig. 3, and agree within a 10% relative error. Fig. 3C is a good comparison demonstrating the significance of why the retention index of methyl 4-hydroxybenzoate was defined as 110. If 100 had been used, the relative error between the observed and predicted retention times of Nos. 25–31 would be 14–31%, whereas in Fig. 3C it is less than 4%.

TABLE VI

RETENTION INDICES (I) OF PHENOLS USED FOR CALCULATING RETENTION TIMES IN RP-HPLC

No.[a]	Substituent[a]	I	No.[a]	Substituent[a]	I
1	4-NHCOMe	−148	17	2,5-Cl_2	331
2	3-NHCOMe	−93	18	4-iso-Pr	326
3	2-NHCOMe	−43	19	4-COO*sec.*-Bu	365
4	4-COMe	15	20	4-Ph	376
5	3-COMe	38	21	4-COO*n*-Bu	400
6	4-COOMe	110	22	4-*tert.*-Bu	390
7	4-COEt	117	23	4-$COOCH_2Ph$	412
8	3-NO_2	148	24	3-Me-6-iso-Pr	430
9	4-COOEt	200	25	4-COOiso-Am	480
10	4-Cl	213	26	4-COO*n*-Am	500
11	4-Br	244	27	4-COO*n*-Hex	600
12	4-COPh	270	28	4-COO*n*-Hep	700
13	4-COOiso-Pr	279	29	4-COO-Oc	747
14	4-COO*n*-Pr	300	30	4-COO*n*-Oc	800
15	4-CO*n*-Bu	309	31	4-COO*n*-No	900
16	2,3-Cl_2	309			

[a] See Table I.

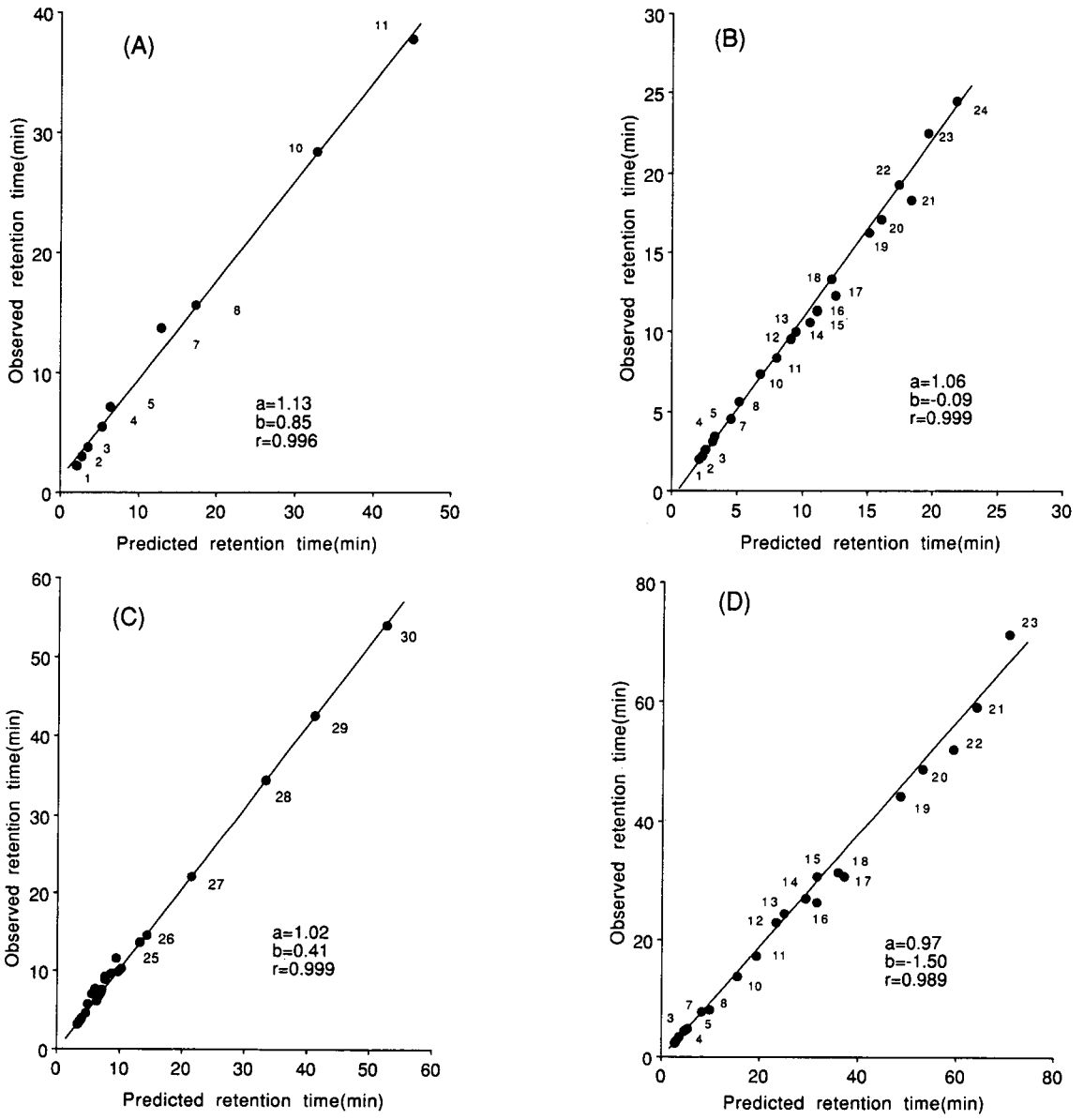

Fig. 3. Plots of predicted retention times using the proposed method and observed retention times under various conditions. a = Slope; b = intercept; r = correlation coefficient. Phenols are expressed using the numbers listed in Table I. Columns and mobile phases: (A) μBondasphere 5 μm C_{18} and ACN–50 mM sodium sulphate–acetic acid (18:82:1); (B) μBondasphere 5 μm C_4 and ACN–water (30:70); (C) YMC Pack ODS-A, A-303 and ACN–MeOH–THF–20 mM sodium sulphate (5:5:5:12); (D) LiChrosorb RP-18 and MeOH–water (45:55).

CONCLUSION

For the purpose of assisting the selection of suitable internal standards among our candidate phenols in RP-HPLC, we established a simple method for predicting the retention times of 31 phenols. Excellent linear relationships between log k' and the carbon number of the alkyl chain in n-alkyl 4-hydroxybenzoates were obtained for a wide range of HPLC conditions and retention indices were calculated on the basis of an n-alkyl 4-hydroxybenzoate scale by the least-squares method. In addition, the selectivities of mobile phases and packing materials were discussed on

the basis of calculated retention index values. Constant retention index values, which are averages, were used in predicting retention times in order to simplify the procedure. The retention time of each phenol could be calculated from the retention data for one marker solution consisting of uracil, methyl 4-hydroxybenzoate and ethyl 4-hydroxybenzoate and the retention index of each phenol. The differences between predicted and observed retention times were not more than 10%. By using this method, we could obtain easily and promptly the approximate predicted retention times of 31 phenols from retention data for only one marker solution, without any trial-and-error experiments.

ACKNOWLEDGEMENTS

The author thanks A.M. Kaneko (Formulation Research Institute, Otsuka Pharmaceutical) for her helpful assistance with data processing, and H. Mori and M. Sugawara (Formulation Research Institute, Otsuka Pharmaceutical) for useful discussions and encouragement.

REFERENCES

1 S. Yamauchi and H. Mori, *J. Chromatogr.*, 515 (1990) 305.
2 N.E. Skelly, S.W. Barr and A.P. Zelinko, *J. Chromatogr.*, 535 (1990) 199.
3 R.M. Smith and C.M. Burr, *J. Chromatogr.*, 475 (1989) 57.
4 R.M. Smith and C.M. Burr, *J. Chromatogr.*, 475 (1989) 75.
5 R.M. Smith and C.M. Burr, *J. Chromatogr.*, 481 (1989) 71.
6 R.M. Smith and C.M. Burr, *J. Chromatogr.*, 481 (1989) 85.
7 R.M. Smith and C.M. Burr, *J. Chromatogr.*, 481 (1989) 325.
8 T. Hanai and J. Hubert, *J. High Resolut. Chromatogr. Chromatogr. Commun.*, 6 (1983) 20.
9 T. Hanai and J. Hubert, *J. Chromatogr.*, 239 (1982) 527.
10 T. Hanai and J. Hubert, *J. Liq. Chromatogr.*, 8 (1985) 2463.
11 T. Hanai, C. Tran and J. Hubert, *J. High Resolut. Chromatogr. Chromatogr. Commun.*, 4 (1981) 454.
12 T. Hanai and J. Hubert, *J. High Resolut. Chromatogr. Chromatogr. Commun.*, 7 (1984) 524.
13 T. Hanai, *J. Chromatogr.*, 324 (1985) 189.
14 T. Hanai, C. Tran and J. Hubert, *J. Chromatogr.*, 239 (1982) 385.
15 R.F. Rekker, *The Hydrophobic Fragment Constants*, Elsevier, Amsterdam, 1977.
16 R.J. Smith, C.S. Neiass and M.S. Wainwright, *J. Liq. Chromatogr.*, 9 (1986) 1387.
17 R.A. Djerki and R.J. Laub, *J. Liq. Chromatogr.*, 10 (1987) 1794.
18 J.K. Baker and C.-Y. Ma, *J. Chromatogr.*, 169 (1979) 107.
19 M. Bogusz and R. Aderjan, *J. Chromatogr.*, 435 (1988) 43.
20 R.M. Smith, *J. Chromatogr.*, 236 (1982) 313.
21 F. Morishita, H. Kakihana and T. Kojima, *Anal. Lett.*, 17 (1984) 2385.
22 P.J. Schoenmakers, H.A.H. Billet and L. de Galan, *J. Chromatogr.*, 185 (1979) 179.
23 P.J. Schoenmakers, H.A.H. Billet and L. de Galan, *J. Chromatogr.*, 218 (1981) 259.
24 N.E. Hoffmann, S. Pan and A.M. Rustum, *J. Chromatogr.*, 465 (1989) 189.
25 D. Vukmainic and M. Chiba, *J. Chromatogr.*, 483 (1989) 189.
26 S.D. West, *J. Chromatogr. Sci.*, 25 (1987) 122.

Journal of Chromatography, 635 (1993) 71–74
Elsevier Science Publishers B.V., Amsterdam

CHROM. 24 835

Chromatographic analysis of the reaction between thiosalicylic acid and selenious acid in methanol

Yoshihiro Saito and Masahiko Chikuma*

Osaka University of Pharmaceutical Sciences, 2-10-65 Kawai, Matsubara 580 (Japan)

(First received October 2nd, 1992; revised manuscript received December 22nd, 1992)

ABSTRACT

A high-performance liquid chromatographic method using a monophenylated reversed-phase column for the determination of thiosalicylic acid, thiosalicylic acid disulphide and thiosalicylic acid selenotrisulphide was developed and applied to studies of the reaction between thiosalicylic acid and selenious acid in methanol. It was confirmed that the molar ratio of selenious acid to thiosalicylic acid is 1:4 at the equivalence point and that equimolar amounts of thiosalicylic acid selenotrisulphide and thiosalicylic acid disulphide are formed in this reaction. These results are consistent with previous information on this kind of reaction in an acidic aqueous solution.

INTRODUCTION

Compounds with mercapto groups are known to react with selenious acid. Busev [1] reported that some compounds reacted with selenious acid in a 4:1 molar ratio and some other compounds in a 2:1 ratio. Thiosalicylic acid is one of these mercapto compounds and has been used as a reagent for the determination of trace elements such as selenium and tellurium [2–4]. The purpose of these previous investigations was to determine selenium by various methods such as gravimetry or spectrophotometry or to study the equilibria of the reaction under acidic conditions by spectrophotometry.

Under highly acidic conditions (4–8 *M* hydrochloric acid), thiosalicylic acid is reported to react with selenious acid in a 4:1 molar ratio [3]. Al-Daher *et al.* [4] also showed that thiosalicylic acid reacts with selenious acid in a 4:1 molar ratio using potentiometric titration. However, Cresser and West [2] reported that the reaction molar ratio of thiosalicylic acid to selenious acid was 3:1 in the pH range 0.5–2.5. These discrepancies in the reaction between thiosalicylic acid and selenious acid need to be investigated further and resolved.

We have already shown that a mixed precipitate of thiosalicylic acid selenotrisulphide and thiosalicylic acid disulphide can be obtained by the reaction of thiosalicylic acid and selenious acid in methanol and succeeded in the purification of the selenotrisulphide [5]. In this study, the reaction of selenotrisulphide formation in methanol was investigated quantitatively by high-performance liquid chromatography (HPLC) and the stoichiometry of the reaction between thiosalicylic acid and selenious acid was determined.

EXPERIMENTAL

Chemicals

Thiosalicylic acid, thiosalicylic acid disulphide and selenious acid were purchased from Nacalai Tesque (Kyoto, Japan). Thiosalicylic acid selenotrisulphide standard was prepared in our lab-

* Corresponding author.

0021-9673/93/$06.00

oratory [5]. Methanol for sample preparation was of analytical-reagent grade and methanol of HPLC grade was used for the preparation of the mobile phase. All other chemicals were of analytical-reagent grade.

Sample preparation

Thiosalicylic acid (100 mg) was suspended in 1 ml of methanol and dissolved by heating on a water-bath (40°C), and various amounts of selenious acid (4.18–41.8 mg) were dissolved in 0.1 ml of methanol. Thiosalicylic acid solution was slowly added to the selenious acid solution while stirring and kept at constant temperature in a water-bath (40°C). Immediately after the addition of thiosalicylic acid, a yellowish white precipitate was formed. A small aliquot of the suspension was taken and diluted with the mobile phase for HPLC analysis as described below. A 5-μl volume of sample was applied to the HPLC column.

High-performance liquid chromatography

A Develosil-ph5 column (250 mm × 4.6 mm I.D.) (Nomura Chemical, Aichi, Japan) was attached to an HPLC system composed of a PU-980 pump, a UV-970 detector and an 807-IT integrator (JASCO, Tokyo, Japan). The composition of the mobile phase was methanol–0.05 *M* phosphate buffer (pH 7.0)–triethylamine (30:70:0.02, v/v/v). The flow-rate was 0.8 ml/min and the detection wavelength was 250 nm. Analysis was performed at room temperature. For the determination of molar absorption coefficients at 250 nm of thiosalicylic acid, thiosalicylic acid disulphide and thiosalicylic acid selenotrisulphide, the compounds were dissolved in the mobile phase at concentrations of 50, 25 and 25 μM, respectively, and the absorption was measured with a spectrophotometer.

RESULTS AND DISCUSSION

Fig. 1 shows representative chromatograms for the reaction mixture of thiosalicylic acid–selenious acid in which the molar ratios were (a) 1:8, (b) 1:4 and (c) 1:2. As shown in Fig. 1a, three peaks corresponding to thiosalicylic acid (peak 1), thiosalicylic acid disulphide (peak 2) and thiosalicylic acid selenotrisulphide (peak 3) could be resolved under the conditions used. The retention times of these compounds were 7.6, 10.1 and 15.8 min, respectively. These peaks were identified by comparison with authentic samples. Furthermore, these compounds were found to be stable during their passage through the column, as each standard sample gave a single, sharp peak.

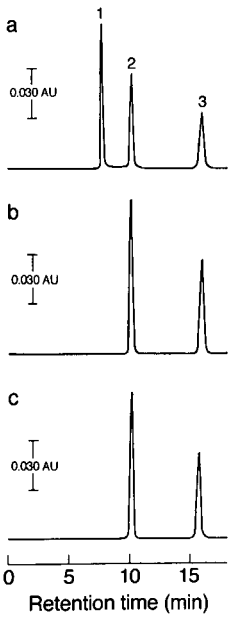

Fig. 1. Chromatograms of the reaction mixtures of thiosalicylic acid and selenious acid. The selenious acid:thiosalicylic acid molar ratios were (a) 1:8, (b) 1:4 and (c) 1:2. Peaks 1, 2 and 3 correspond to thiosalicylic acid (7.6 min), thiosalicylic acid disulphide (10.1 min) and thiosalicylic acid selenotrisulphide (15.8 min), respectively.

When an ODS column was used [5], the retention times of thiosalicylic acid and its disulphide were too close to evaluate them separately under the conditions described. As neutrality was necessary to dissolve these compounds, 0.05 *M* phosphate buffer (pH 7.0) was used. Although the selenotrisulphides are usually unstable in neutral solutions [1,6,7], thiosalicylic acid selenotrisulphide was stable enough during the analysis. Triethylamine in the mobile phase improved the peak shape of thiosalicylic acid, which otherwise showed tailing.

From the peak area data obtained in HPLC

analysis of the reaction mixture, the contents of thiosalicylic acid, thiosalicylic acid disulphide and thiosalicylic acid selenotrisulphide were calculated as described below. The peak areas (%) of these compounds are given in Table I. The thiosalicylic acid:thiosalicylic acid disulphide:thiosalicylic acid selenotrisulphide molar ratio was calculated by dividing each peak area (%) by the molar absorption coefficients, which were 750, 1600 and 1600 m^2/mol, respectively. This molar ratio was corrected using a thiosalicylic acid disulphide or selenotrisulphide structure as a unit, so the values for thiosalicylic acid are represented as half of the usual molar number. The percentage contents of thiosalicylic acid and its products were then calculated so that their sum equalled 100 (Table I). These values were plotted against the reaction molar ratio of selenious acid to thiosalicylic acid (Fig. 2).

The thiosalicylic acid content decreased with increase in the molar ratio and reached zero at a molar ratio of 1:4. This result means that the reaction involving the thiol group is completed

TABLE I

PEAK AREA AND CALCULATED CONTENT OF (A) THIOSALICYLIC ACID, (B) THIOSALICYLIC ACID DISULPHIDE AND (C) THIOSALICYLIC ACID SELENOTRISULPHIDE OBSERVED FOR REACTION MIXTURES IN HPLC ANALYSIS

The content values (%) were calculated as follows: first, the A:B:C molar ratio was calculated by the division of the peak area (%) values by the molar absorption coefficients at the detection wavelength (250 nm), which were 750, 1600 and 1600 m^2/mol for A, B and C, respectively; second, the resulting values were represented as the corrected molar ratio using thiosalicylic acid disulphide or selenotrisulphide structure as a unit; finally, this corrected molar ratio was represented as content (%) after making their sum total 100.

H_2SeO_3:RSH	Peak area (%)			Content (%)		
	A	B	C	A	B	C
0	88	12	0	89	11	0
1:20	67	22	11	68	21	11
1:8	37	35	28	39	34	27
1:4	0	52	48	0	52	48
1:3	0	51	49	0	51	49
1:2	0	53	47	0	53	47

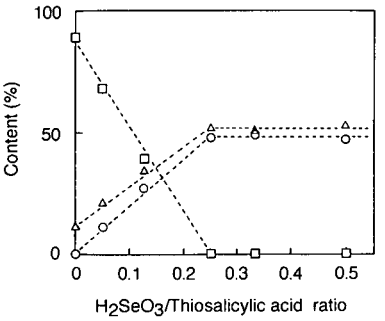

Fig. 2. Contents of thiosalicylic acid, thiosalicylic acid disulphide and thiosalicylic acid selenotrisulphide in the reaction mixture with various selenious acid:thiosalicylic acid molar ratios. The values are given in Table I. □ = Thiosalicylic acid; △ = thiosalicylic acid disulphide; ○ = thiosalicylic acid selenotrisulphide.

when the molar ratio is 1:4. Both the thiosalicylic acid disulphide and selenotrisulphide contents increased almost linearly with increase in the molar ratio and reached the maximum (*ca.* 50%) when the molar ratio was 1:4, and these values remained constant where the molar ratio exceeded 1:4. These results indicate that equimolar amounts of thiosalicylic acid disulphide and selenotrisulphide were formed at least at molar ratios >1:4. Analysis of thiosalicylic acid in the absence of selenious acid showed that *ca.* 10% was present as thiosalicylic acid disulphide, which was probably formed by air oxidation after dissolution and/or during the analysis. Although the content of disulphide was slightly higher than that of selenotrisulphide, this difference decreased with increase in the selenious acid: thiosalicylic acid molar ratio (=0–0.25), which suggests that the amount of thiosalicylic acid disulphide formed by air oxidation is proportional to the residual amount of thiosalicylic acid.

The results described above indicate that the reaction between thiosalicylic acid and selenious acid in methanol proceeds via the following equation:

$$4RSH + H_2SeO_3 \rightarrow RSSeSR + RSSR + 3H_2O$$

That is, thiosalicylic acid reacts with selenious acid at a molar ratio of 4:1 in methanol, and equimolar thiosalicylic acid disulphide and thiosalicylic acid selenotrisulphide are formed by

this reaction. It was further demonstrated that Se(IV) was reduced to Se(II) by the reaction with thiosalicylic acid.

These results differ from those of Al-Daher *et al.* [4] except for the reaction molar ratio. They analysed the composition of the product obtained at the equivalence point in the potentiometric titration and found the molar ratio of selenium and thiosalicylic acid in the product to be 1:4. They did not give any information on the oxidation state of selenium in the reaction. However, as shown in this study, the product should have been an equimolar mixture of thiosalicylic acid disulphide and thiosalicylic acid selenotrisulphide containing Se(II), as the reaction conditions they used seem essentially the same as ours.

Regarding the reaction molar ratio of thiosalicylic acid to selenious acid, our result obtained with a methanol solution is consistent with previous reports in which it was determined in an acidic solution by spectrophotometry [3] or in 95% ethanol and acetate–HCl (pH 2.3) by potentiometric titration [4], although different molar ratios were described by Cresser and West [2].

In this study, the reaction between thiosalicylic acid and selenious acid in methanol was investigated using HPLC. This is the first direct demonstration that thiosalicylic acid reacts with selenious acid at a molar ratio of 4:1 in methanol, that equimolar disulphide and selenotrisulphide are formed and that Se(IV) is reduced to Se(II) in this reaction. These results were in good agreement with those observed in the acidic aqueous solution, and it is considered that the same reaction can occur both in acidic aqueous and in methanol solutions in the case of thiosalicylic acid and selenious acid. This HPLC method will be useful to investigate further the reaction involving thiosalicylic acid selenotrisulphide.

REFERENCES

1 A.I. Busev, *Talanta*, 11 (1964) 485.
2 M.S. Cresser and T.S. West, *Analyst*, 93 (1968) 595.
3 B.W. Budesinsky and J. Svec, *J. Inorg. Nucl. Chem.*, 33 (1971) 3795.
4 I.M. Al-Daher, F.A. Fattah and K.A. Najm, *Analyst*, 115 (1990) 645.
5 Y. Saito and M. Chikuma, *Fresenius' J. Anal. Chem.*, submitted for publication.
6 H.E. Ganther, *Biochemistry*, 7 (1968) 2898.
7 P.D. Whanger, S.C. Vendeland, J.T. Deagen and J.A. Butler, in B. Momčilović (Editor), *Trace Elements in Man and Animals 7*, IMI Institute for Medical Research and Occupational Health, University of Zagreb, Zagreb, 1991, Ch. 17-11.

Journal of Chromatography, 635 (1993) 75–80
Elsevier Science Publishers B.V., Amsterdam

CHROM. 24 815

Salting-out solvent extraction for pre-concentration of benzalkonium chloride prior to high-performance liquid chromatography

J.E. Parkin

School of Pharmacy, Curtin University of Technology, P.O. Box U1981, Perth, Western Australia (Australia)

(First received August 26th, 1992; revised manuscript received December 15th, 1992)

ABSTRACT

Benzalkonium chloride (BAK) can be readily concentrated prior to chromatographic analysis by the addition of appropriate amounts of sodium chloride and acetonitrile to the sample. This affords a two-phase system the upper of which contains the BAK and which can be directly injected onto the chromatographic column. Using this approach analytical methods with and without an internal standard, have been developed and validated that reproducibly afford an approximately ten-fold pre-concentration of the sample to be analysed thereby improving analytical sensitivity.

INTRODUCTION

Benzalkonium chloride (BAK) is an antibacterial preservative widely used in pharmaceutical products. It consists of a variable mixture of the C_8–C_{18} even-numbered alkyl homologues of alkylbenzyldimethylammonium chlorides with the C_{12} and C_{14} homologues predominating [1,2].

A variety of chromatographic procedures have been reported for BAK [3–7]. Because of the relatively low absorbance of the benzyl chromophore at longer wavelengths [6], the necessity to quantitate total BAK by determining the sum of the areas of up to six peaks and as many of the homologues are present in small proportions in the mixture, it is difficult to analyse at concentrations employed as antibacterial preservatives in pharmaceutical products (0.005–0.01%, w/v).

Workers have addressed this problem by monitoring at short wavelength [5–7], by injection of larger volumes (up to 200 μl) [4,5] and by quantitating only the major peaks $C_{12}/C_{14}/C_{16}$ which together make up approximately 95% of most samples of BAK [3–5].

There have been a number of reports of the use of salting-out procedures of solvents such as acetonitrile and acetone with high concentrations of inert electrolytes [8–13]. These procedures have been used to pre-concentrate metal complexes to improve the sensitivity of metal determinations by atomic absorption spectroscopy [8,9] or high-performance liquid chromatography (HPLC) [10,13] and explosive residues from environmental samples by HPLC [11,12].

Studies in these laboratories involving pre-concentration into acetonitrile using sodium chloride as electrolyte of phenylmercuric nitrate in ophthalmic products [13] suggested that this approach may be appropriate for the pre-concentration of BAK into an acetonitrile–water extract suitable for direct injection onto the HPLC column and this paper reports the results of these studies.

0021-9673/93/$06.00

EXPERIMENTAL

Materials

The two samples of BAK which were employed in this study were 50% (w/v) solutions, Vantoc CL (ICI, Melbourne, Australia) (sample A) and from TCI (Tokyo, Japan) (sample B). Authentic C_{12}, C_{14} and C_{16} homologues were also employed (Aldrich, Milwaukee, WI, USA). The dibenzyldimethylammonium chloride (DBDMAC) used as internal standard was prepared by the reaction of benzylbromide (Ajax Chemicals, Sydney, Australia) and N,N-dimethylbenzylamine (Aldrich) [14]. All other chemicals were analytical reagent grade and solvents were HPLC grade.

Chromatographic equipment and conditions

The liquid chromatograph consisted of a Model 501 pump (Waters Assoc., Milford, MA, USA), Rheodyne Model 7125 loop injector (Cotati, CA, USA), Model 484 variable-wavelength absorbance detector (Waters Assoc.) and Model 3396A integrating recorder (Hewlett-Packard, Palo Alto, CA, USA) together with a column of cyanopropyl bonded silica 10 μm particle size, 10 cm × 8 mm I.D. (Waters Assoc., RCM 8 × 10) with a mobile phase of acetonitrile–tetrahydrofuran–0.1 *M* acetic acid/triethylamine buffer (made by adjusting the pH of 0.1 *M* acetic acid to pH 3.8 with triethylamine) (375:20:605) at a flow-rate of 1.5 ml min^{-1}. The injection volume was 20 μl and the monitoring wavelength 262 nm.

Spectra of individual peaks were obtained by use of a Model 991 photodiode array absorbance detector (Waters Assoc.).

Spectrophotometric equipment

UV spectra were obtained using an HP 8450 UV–Vis spectrophotometer (Hewlett-Packard).

Sample preparation for routine analysis

Without internal standard. To a 20-ml glass tube with plastic cap and PTFE wad were added sodium chloride (2.7 g), the sample to be analysed (10 ml) and acetonitrile (3 ml) and the solution was shaken to dissolve the sodium chloride. The layers were allowed to separate and the upper phase was immediately submitted to analysis by HPLC.

With internal standard. To a 20-ml glass tube with plastic cap and PTFE wad were added sodium chloride (2 g), sample to be analysed (10 ml), a $2.5 \cdot 10^{-2}$% (w/v) solution of DBDMAC (1 ml) and acetonitrile (4 ml) and the solution was shaken to dissolve the sodium chloride. The layers were allowed to separate and the upper phase was immediately submitted ot analysis by HPLC.

Validation of analytical methods

Both HPLC methods were applied to BAK solutions containing 0.1, 0.2, 0.4, 0.6, 0.8, 1.0, 1.2 and $1.5 \cdot 10^{-2}$% (w/v) BAK. The relative standard deviations (R.S.D.s) were determined by analysis of 6 replicates at a concentration of $0.5 \cdot 10^{-2}$% (w/v) total BAK.

Composition of BAK samples and identity of homologue peaks

An 0.1% (w/v) solution of both BAK samples was submitted to HPLC analysis by direct injection. Accurate retention times were determined and the void volume determined by injection of a solution of uracil (0.1%, w/v) and capacity factors were calculated for the individual homologues.

Identity of the peaks was confirmed by obtaining UV spectra at peak maxima using the photodiode-array detector and by comparison of the retention times with authentic samples for the C_{12}, C_{14} and C_{16} homologues.

The homologue composition was determined from relative peak-areas of the homologues in the sample.

Effect of quantity of sodium chloride on salting out

The sample preparation method without internal standard was performed substituting sodium chloride 2.25, 2.50, 2.75, 3.00 and 3.25 g and the amount of BAK extracted determined by HPLC. Relative phase-volumes were determined by performing these experiments, scaled up by a factor of 3, in 50-ml measuring cylinders and measuring the two phase-volumes.

Efficiency of extraction by UV spectrophotometry

To a 50-ml glass vial with screw-cap and PTFE wad were added an 0.05% (w/v) solution of BAK (30 ml), water (3 ml), sodium chloride (6 g) and acetonitrile (12 ml). The tube was shaken to dissolve the sodium chloride and the layers allowed to separate. The upper layer (1 ml) was diluted with water (2 ml) and the resulting solution submitted to analysis by UV spectrophotometry at 262 nm using the original solution as the standard. The concentration of BAK in the lower layer was also determined by UV spectrophotometry without dilution.

The efficiency of extraction of the DBDMAC was determined by an identical experiment using a solution of DBDMAC (0.025%, w/v) instead of BAK.

Efficiency of extraction of total BAK and individual homologues by HPLC

Samples of BAK (0.01%, w/v) were submitted to analysis by the sample preparation methods without and with internal standard and the relative peak areas compared with the same BAK samples at a concentration of 0.1% (w/v) by direct injection.

RESULTS AND DISCUSSION

Previously reported HPLC methods for BAK [3,4,6,7] have all used a cyanopropyl-bounded silica column and acetonitrile–buffer systems. The solvent system chosen for this study incorporating a small proportion of tetrahydrofuran afforded improved peak shapes for the higher homologues. The method of Ambrus *et al.* [6], which uses a perchlorate counter-ion in the mobile phase, when used with the work-up procedure outlined here, results in unacceptable peak-broadening of the BAK homologue peaks but the other reported solvent systems have been found to be compatible.

Two samples of BAK solutions were used in this study: sample A which contains all six homologues and sample B which contains only four (C_{10}–C_{16}). Details of the exact composition of each were determined and are given in Table I. Total peak areas for 0.1% (w/v) solutions of both samples of BAK came within 2% of each

TABLE I

STATISTICAL DATA ON PRECISION OF ASSAY WITH AND WITHOUT INTERNAL STANDARD PERFORMED ON $5 \cdot 10^{-3}$% (w/v) BAK

Homologue	Sample A				Sample B			
	Mol fraction of homologue	Concentration of homologue (%, w/v)	R.S.D. (%)		Mol fraction of homologue	Concentration Concentration (%, w/v)	R.S.D. (%)	
			Without internal standard	With internal standard			Without internal standard	With internal standard
C_8	0.0860	$4.30 \cdot 10^{-4}$	±2.00	±1.85	–	–	–	–
C_{10}	0.0943	$4.71 \cdot 10^{-4}$	±1.82	±2.10	0.0053	$0.26 \cdot 10^{-4}$	±11.40	±14.40
C_{12}	0.5056	$25.28 \cdot 10^{-4}$	±1.04	±0.98	0.4619	$23.09 \cdot 10^{-4}$	±0.95	±1.00
C_{14}	0.1695	$8.47 \cdot 10^{-4}$	±1.84	±1.40	0.4602	$23.01 \cdot 10^{-4}$	±1.53	±1.99
C_{16}	0.0835	$4.22 \cdot 10^{-4}$	±2.04	±2.35	0.0762	$3.81 \cdot 10^{-4}$	±3.70	±4.47
C_{18}	0.0603	$3.02 \cdot 10^{-4}$	±3.40	±3.85	–	–	–	–
Total	1.0000	$50.00 \cdot 10^{-4}$	±1.97	±2.10	1.0000	$50.00 \cdot 10^{-4}$	±2.40	±2.37
Calibration lines	With internal standard: peak area ratio = $2.42 \cdot 10^2$ (concn. in %, w/v) $- 3.0 \cdot 10^{-3}$ ($r = 0.9996$, $n = 8$)				With internal standard: peak area ratio = $2.39 \cdot 10^2$ (concn. in %, w/v) $+ 1.5 \cdot 10^{-2}$ ($r = 0.9995$, $n = 8$)			
	Without internal standard: peak area = $5.22 \cdot 10^8$ (concn. in %, w/v) $+ 2.6 \cdot 10^4$ ($r = 0.9995$, $n = 8$)				Without internal standard: peak area = $5.12 \cdot 10^8$ (concn. in %, w/v) $+ 3.5 \cdot 10^4$ ($r = 0.9998$, $n = 8$)			

other and therefore they were considered interchangeable in the study. The identity of the peaks as being due to individual homologues was confirmed by comparison of retention times for the C_{12}, C_{14} and C_{16} homologues with authentic samples, comparison of the UV spectra using photodiode-array detection of all homologues with that of an authentic sample of the C_{12} homologue and by obtaining a linear plot of the logarithm of the capacity factor for the homologues *versus* carbon number as would be expected for such a series in the reversed-phase mode ($r = 0.9967$).

In previous studies of this salting-out phenomena a variety of salts have been investigated [8,9]. Sodium chloride was chosen for this study on the basis of cost and purity.

The phase-volumes produced by salting-out of acetonitrile by sodium chloride is a complex function of volume of acetonitrile and sample and quantity of sodium chloride. By the use of convenient volumes of sample and acetonitrile, 10 ml and 3 ml, respectively, the quantity of sodium chloride to achieve a suitable pre-concentration could be selected (Table II). As the quantity of sodium chloride in the system is reduced the volume of the upper phase becomes smaller leading to greater sampling difficulties but also greater pre-concentration of the BAK.

TABLE II

RELATIONSHIP BETWEEN UPPER-PHASE VOLUME, CONCENTRATION FACTOR AND AMOUNT OF SODIUM CHLORIDE

The concentration factor is defined as the ratio of the concentration of BAK in the original sample to that found in the upper layer.

Mass of sodium chloride (g)	Concentration factor	Phase volumes upper/lower (ml)	Theoretical concentration factor[a]
2.25	18.60	1.5/39.5	20
2.50	14.10	2.0/39.5	15
2.75	11.46	2.5/39.2	12
3.00	10.20	2.7/38.3	11
3.25	9.51	3.0/38.2	10

[a] Determined from the ratio of upper phase volume to volume of sample and assuming complete extraction.

When 2 g of sodium chloride are employed the system becomes homogeneous with no phase-separation and at quantities of sodium chloride greater than 3.25 g the sodium chloride fails to completely dissolve. Therefore the amount of sodium chloride chosen was on the basis of affording an approximately 10-fold concentration factor this being defined as the ratio of the concentration in the sample to that found in the upper-phase. Obviously, quantities of sodium chloride may be chosen such that greater pre-concentration can be achieved should that be considered necessary.

As changes in electrolyte content of the sample may change the volume of the upper phase it was considered desirable to incorporate an internal standard into the analytical method. DMDBAC was found to have appropriate characteristics as it elutes prior to the C_8 homologue and has similar chemical and spectral characteristics to BAK. The addition of the internal standard in water (1 ml) necessitated changes in the acetonitrile (4 ml) and sodium chloride (2.0 g) to maintain relative phase-volumes.

When both samples of BAK were submitted to analysis by both methods linear relationships

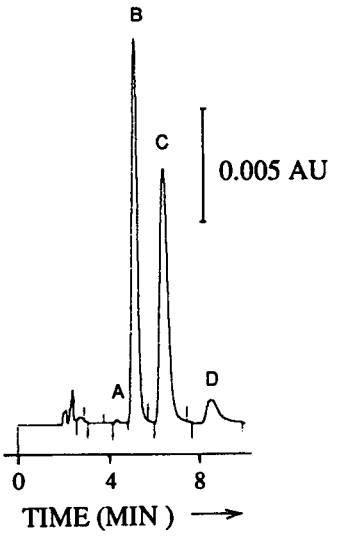

Fig. 1. Chromatogram obtained with BAK sample B (0.01%, w/v) pre-concentrated by salting-out acetonitrile without inclusion of an internal standard. Peaks: A = C_{10}; B = C_{12}; C = C_{14}; D = C_{16} homologue.

between peak-area and concentration of total BAK over the concentration range 0–0.015% (w/v) with satisfactory R.S.D.s at a concentration of $5 \cdot 10^{-3}$% (w/v) (Figs. 1 and 2) (Table I).

An assessment has also been made of the efficiency of extraction of the BAK homologues and total BAK into the upper acetonitrile layer using the quantities prescribed for the assay incorporating an internal standard (see section *Sample preparation for routine analysis*). Measurement of the phase-volumes upper/lower was found to be 3 ml/43.7 ml, which, based on a 30-ml sample should afford an approximately 10-fold increase in concentration of BAK assuming complete extraction into the upper layer. This efficiency of extraction was determined by UV spectrophotometry following partitioning of an 0.05% (w/v) solution of both samples of BAK and an 0.025% (w/v) solution of DMDBAC used as an internal standard and also by HPLC by comparison of peak-area response of the individual homologues against the peak-area response of an 0.1% (w/v) solution of the BAK samples and the DMDBAC internal standard (Table III). Almost quantitative extraction is achieved for BAK and for its individual homologues. The internal standard (DBDMAC) is less efficiently extracted but is satisfactory for its purpose.

This procedure is capable of effectively performing an approximately ten-fold preconcentration in a controlled manner and by adaptation higher concentration factors should be achievable. It provides a quick and convenient procedure for the analysis of BAK at concentrations encountered in pharmaceutical products and

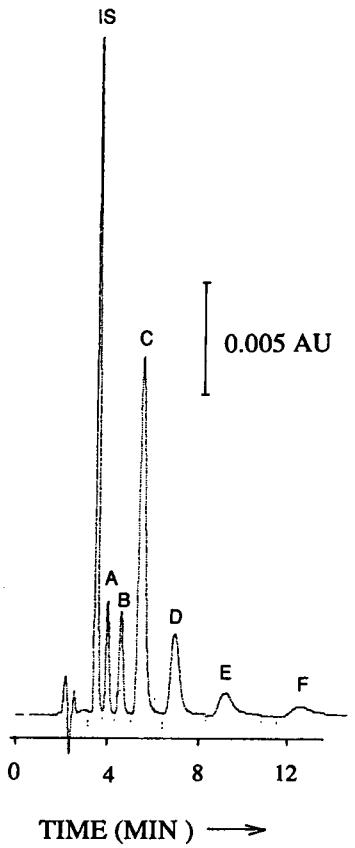

Fig. 2. Chromatogram obtained with BAK sample A (0.01%, w/v) pre-concentrated by salting-out acetonitrile with the inclusion of an internal standard. Peaks: IS = internal standard (dibenzyldimethylammonium chloride); A = C_8; B = C_{10}; C = C_{12}; D = C_{14}; E = C_{16}; F = C_{18} homologue.

TABLE III

PARTITION COEFFICIENTS AND CONCENTRATION FACTORS FOR BAK, HOMOLOGUES AND INTERNAL STANDARD

The concentration factors are defined as the ratio of the concentration of BAK and homologues in the original samples to that found in the upper layer.

Material		Partition coefficient	Concentration factor
BAK sample A	C_8		9.15
	C_{10}		9.57
	C_{12}		9.55
	C_{14}		9.43
	C_{16}		8.82
	C_{18}		8.74
	Total		9.38
		>100[a]	9.15[a]
BAK sample B	C_{10}		9.00
	C_{12}		9.33
	C_{14}		9.56
	C_{16}		8.67
	Total		9.43
		>100[a]	9.27[a]
Internal standard, DBDMAC		14.30[a]	4.93[a]

[a] Determined by ultraviolet spectrophotometry (for the total sample).

should be readily adaptable to other materials where pre-concentration prior to analysis is desirable.

REFERENCES

1 *The British Pharmacopoeia*, Her Majesty's Stationery Office, London, 1988, p. 63.
2 *The United States Pharmacopeia and National Formulary*, US Pharmacopeial Convention, Rockville, MD, 1990, p. 1904.
3 R.C. Meyer, *J. Pharm. Sci.*, 69 (1980) 1148.
4 D.F. Marsh and L.T. Takahashi, *J. Pharm. Sci.*, 72 (1983) 521.
5 P. Leroy, V. Leyendecker, A. Nicolas and C. Garret, *Ann. Falsif. Expert. Chim. Toxicol.*, 79 (1986) 283; *Anal. Abstr.*, 49 (1987) 8E116.
6 G. Ambrus, L.T. Takahashi and P.A. Marty, *J. Pharm. Sci.*, 76 (1987) 174.
7 A. Gomez-Gomar, M.M. Gonzalez-Aubert, G. Garces-Torrents and J. Costa-Segarra, *J. Pharm. Biomed. Anal.*, 8 (1990) 871.
8 C.E. Matkovich and G.D. Christian, *Anal. Chem.*, 45 (1973) 1915.
9 Y. Nagaosa, *Anal. Chim. Acta*, 120 (1980) 279.
10 B.J. Mueller and R.J. Lovett, *Anal. Chem.*, 59 (1987) 1405.
11 D.C. Leggett, T.F. Jenkins and P.H. Miyares, *Anal. Chem.*, 62 (1990) 1355.
12 T.F. Jenkins and P.H. Miyares, *Anal. Chem.*, 63 (1991) 1341.
13 J.E. Parkin, K.L. Button and P.A. Maroudas, *J. Clin. Pharm. Ther.*, 17 (1992) 191.
14 G.P. Schiemenz, *Tetrahedron*, 29 (1973) 741.

Journal of Chromatography, 635 (1993) 81–87
Elsevier Science Publishers B.V., Amsterdam

CHROM. 24 832

High-performance liquid chromatographic determination of PZ-peptidase activity

Toshiyuki Chikuma*, Waka Tanaka, Kanae Yamada, Yoko Ishii and Akira Tanaka

Department of Pharmaceutical Analytical Chemistry, Showa College of Pharmaceutical Sciences, 3-3165 Higashi-tamagawakuen, Machida-shi, Tokyo 194 (Japan)

Takeshi Kato

Laboratory of Molecular Recognition, Graduate School of Integrated Science, Yokohama City University, Yokohama 236 (Japan)

(First received September 4th, 1992; revised manuscript received December 24th, 1992)

ABSTRACT

A rapid and sensitive assay method for the determination of PZ-peptidase activity is reported. This method is based on the monitoring of the absorption at 320 nm of 4-phenylazobenzyloxycarbonyl-L-Pro-L-Leu (PZ-Pro-Leu), enzymatically formed from the substrate 4-phenylazobenzyloxycarbonyl-L-Pro-L-Leu-Gly-L-Pro-D-Arg (PZ-peptide), after separation by high-performance liquid chromatography using a C_{18} reversed-phase column by isocratic elution. This method is sensitive enough to measure PZ-Pro-Leu at levels as low as 10 pmol, yields highly reproducible results and requires less than 5.5 min per sample for separation and determination. The optimum pH for PZ-peptidase activity was 7.5–8.0. The K_m and V_{max} values were 166.7 μM and 5.35 pmol/min · μg protein, respectively, with the use of enzyme extract obtained from mouse whole brain. The approximate molecular mass of this enzyme was estimated to be 64 000 by gel filtration. PZ-peptidase activity was strongly inhibited by Zn^{2+}, Cu^{2+} and *p*-chloromercuriphenylsulphonic acid. By using this method, PZ-peptidase activity could be readily detected in a single mouse pituitary gland. Among the tissues examined in various mouse brain regions, the highest specific activity of the enzyme was found in cerebral cortex. The sensitivity and selectivity of this method will aid in efforts to examine the physiological role of this peptidase.

INTRODUCTION

The collagenase of *Clostridium histolyticum* is commonly assayed with 4-phenylazobenzyloxycarbonyl-L-Pro-L-Leu-Gly-L-Pro-D-Arg (PZ-peptide), a synthetic peptide with an amino acid sequence based on the -Gly-Pro-Xaa- tripeptide repeating pattern of the helical region of collagen [1]. It is not hydrolysed by mammalian collagenase, but is cleaved by another enzyme, PZ-peptidase (EC 3.4.99.31), which is widely distributed in mammalian tissues [2].

The assay method using PZ-peptide as substrate has the advantage that the chromogenic product, 4-phenylazobenzyloxycarbonyl-L-Pro-L-Leu (PZ-Pro-Leu), is not water soluble and can be assayed after extraction with an organic solvent. However, this method also has a few disadvantages. This conventional procedure is obviously non-specific as all PZ-peptides eventually produced by non-enzymatic hydrolysis may be extracted into the organic phase; moreover, the extraction step does not allow the optimum reproducibility to be obtained. A greater disadvantage is the low sensitivity. The direct

* Corresponding author.

0021-9673/93/$06.00

analysis of the reaction mixture by a high resolution technique would alleviate the problems concerning selectivity and reproducibility.

In this paper, we describe an advantageous assay method for PZ-peptidase using high-performance liquid chromatography (HPLC) on a reversed-phase column to achieve a rapid and selective separation of substrate and product. Using this sensitive assay method, PZ-peptidase activity was discovered in mouse pituitary gland for the first time. Moreover, we describe some physico-chemical properties of PZ-peptidase in mouse brain in order to investigate the real physiological roles of this enzyme in the central nervous system (CNS).

EXPERIMENTAL

Materials

PZ-peptide and PZ-Pro-Leu were purchased from Fluka (Buchs, Switzerland). N-2,4-Dinitrophenyl-L-phenylalanine (DNP-Phe), cytochrome *c*, ribonuclease A, myoglobin, α-chymotrypsinogen A, ovalbumin, bovine serum albumin (BSA), BSA dimer, phenylmethylsulphonyl fluoride (PMSF), iodoacetic acid (IAA), N-ethylmaleimide (NEM), *p*-chloromercuriphenylsulphonic acid (PCMS) and pepstatin A were obtained from Sigma (St. Louis, MO, USA). Soybean trypsin inhibitor, bacitracin and 1,10-phenanthroline hydrochloride were obtained from Wako (Osaka, Japan). Sephacryl S-300 HR was purchased from Pharmacia (Uppsala, Sweden). Acetonitrile was of chromatographic grade (Cica–Merck). Other chemicals and solvents were of analytical-reagent grade.

Animals

Male ICR mice weighing 20–25 g were purchased from Charles River and housed on a 12-h light–dark cycle for at least 1 week before the beginning of all experiments. Food and water were available *ad libitum*. All operations were carried out at 0–4°C unless stated otherwise. Mice were killed by decapitation. After washing the whole brain with saline, it was cut into small pieces and homogenized in nine volumes of 0.32 *M* sucrose with a glass–PTFE homogenizer. The homogenate was centrifuged at 100 000 *g* for 80 min and the supernatant obtained was used as an enzyme source.

For the investigation on localization of the enzyme activity, various brain regions, *i.e.*, bulbus olfactorius, pons-medulla, cerebellum, hypothalamus, hippocampus, cerebral cortex, striatum, midbrain and pituitary gland, were dissected on ice. Tissues were homogenized in nineteen volumes of 0.32 *M* sucrose with a glass–PTFE homogenizer. The homogenates were used as an enzyme source.

Assay for PZ-peptidase activity

The principle of the assay method for PZ-peptidase activity is based on the spectrophotometric measurement at 320 nm of PZ-Pro-Leu liberated enzymatically from the substrate, PZ-peptide, after separation by HPLC. The reaction mixture contained 60 m*M* Tris–HCl buffer (pH 8.0), 6 m*M* $CaCl_2$, 240 m*M* NaCl, 0.24 m*M* PZ-peptide and enzyme plus water in a total reaction volume of 250 μl. Incubation was carried out at 37°C and the reaction was terminated by heating at 95°C for 5 min in boiling water. After addition of DNP-Phe as an internal standard, the reaction mixture was centrifuged and the clear supernatant obtained was evaporated *in vacuo* using an AS160 Speed-Vac concentrator (Savant, Farmingdale, MA). The resulting residue was dissolved into acetonitrile–water (55:45, v/v) containing 0.1% of trifluoroacetic acid, and an aliquot of the mixture was subjected to HPLC analysis. For micro-assay, the incubation mixture was reduced to a total volume of 50 μl instead of 250 μl and the volumes of other reagents added were also reduced to one-fifth. The peak height of PZ-Pro-Leu was measured and converted into picomoles from the peak height of DNP-Phe added as an internal standard. One unit of enzyme activity is defined as the amount of enzyme required to convert 1 μmol of the substrate into the corresponding product in 1 min at 37°C.

Chromatographic conditions

Analysis of the product was performed using a Japan Spectroscopic HPLC system consisting of a Model 880-PU pump, 875-UV UV detector

(fixed at 320 nm), 860-CO column oven, 880-50 degasser, 880-02 gradient unit, 802-SC system controller and 807-IT integrator. The system was operated at room temperature at a flow-rate of 1.32 ml/min employing a Finepak SIL C18S (particle size 5 μm) reversed-phase column (150 × 4.6 mm I.D.) (Jasco) fitted with a LiChrosorb RP-18 guard gel (15 × 3.2 mm I.D.; particle size 5 μm) (Cica–Merck). The mobile phase was acetonitrile–water (55:45, v/v) containing 0.1% of trifluoroacetic acid.

Determination of molecular mass

All of the following procedures were carried out at 0–4°C. Mouse whole brain (3.7 g) was homogenized in nine volumes of 0.25 *M* Tris–HCl buffer (pH 8.0) with a glass–PTFE homogenizer. The homogenate was centrifuged at 100 000 *g* for 80 min and the resulting supernatant was concentrated to 5 ml by ultrafiltration (Amicon YM 10 membrane) and subjected to size-exclusion chromatography on a Sephacryl S-300 HR column (96.5 × 2.6 cm I.D.) equilibrated with 0.25 *M* Tris–HCl buffer (pH 8.0), and eluted with same buffer at a flow-rate of 0.5 ml/min. The UV absorbance of the eluate was monitored at 280 nm, and column fractions (2.5 ml per tube) were assayed for enzyme activity. The following proteins were used as molecular mass markers: BSA (dimer 130 000, monomer 67 000), ovalbumin (43 000), α-chymotrypsinogen A (25 000), soybean trypsin inhibitor (20 100), myoglobin (18 800), ribonuclease A (13 700) and cytochrome *c* (12 500).

Effects of various metal ions and inhibitors on enzymatic activity

The active fractions eluted from the Sephacryl S-300 HR column were pooled and used as the source of enzyme for this experiment. Enzyme solution was preincubated in the absence or presence of various chemicals (0.1 and 1 m*M*) in 60 m*M* Tris–HCl buffer (pH 8.0) for 5 min at 37°C. Immediately thereafter, 0.24 m*M* PZ-peptide (final concentration) was added to the reaction mixture and incubated at 37°C for the desired periods. After stopping the reaction, the samples were treated as described above.

Protein determination

Protein concentration was measured by the Lowry method as modified by Hartree [3] using BSA as a standard protein.

RESULTS

This HPLC–spectrophotometric detection system for the measurement of PZ-peptide and PZ-Pro-Leu was found to be very sensitive. The calibration graph for PZ-Pro-Leu injected showed good linearity from 10 to 2000 pmol. The calibration graph for DNP-Phe also showed good linearity from 50 to 2000 pmol. Fig. 1 shows the chromatographic patterns of the reaction mixture after incubation with 24.9 μg of protein prepared from mouse whole brain supernatant for 30 min. The blank incubation (Fig. 1A) contained PZ-

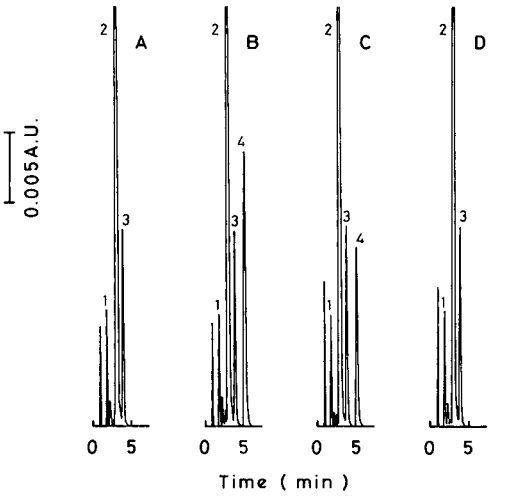

Fig. 1. HPLC elution patterns of PZ-peptidase activity determined using enzyme in mouse whole brain. Conditions as described under Experimental. Peaks: 1 = impurity contained in PZ-peptide; 2 = PZ-peptide; 3 = DNP-Phe; 4 = PZ-Pro-Leu. A 5500-pmol amount of DNP-Phe (internal standard) was added to each sample after incubation. (A) Blank incubation: PZ-peptide was incubated without enzyme at 37°C for 30 min. (B) Standard incubation: 5500 pmol of PZ-Pro-Leu were added to a sample tube before incubation as a standard sample. The two peak heights of DNP-Phe and PZ-Pro-Leu correspond 500 pmol. (C) Experimental incubation: PZ-peptide was incubated with 24.9 μg of protein in mouse whole brain at 37°C for 30 min. (D) Control incubation: a control tube without the enzyme was incubated, the same amount of active enzyme was added and the resulting tube was kept in an ice-bath before heating at 95°C for 5 min.

peptide and DNP-Phe, and the standard incubation (Fig. 1B) contained exogenous PZ-Pro-Leu in addition to PZ-peptide and DNP-Phe. The retention times for PZ-peptide, DNP-Phe and PZ-Pro-Leu were 3.0, 3.9 and 5.1 min, respectively (Fig. 1A and B). As shown in the blank incubation (Fig. 1A), an unknown peak, presumably originating from an impurity in the substrate, was found at 1.8 min near the peak of the solvent. The experimental incubation under the standard assay conditions (Fig. 1C) showed a significant amount of PZ-Pro-Leu at 5.1 min, whereas the control incubation (Fig. 1D) did not show any peak of PZ-Pro-Leu.

The enzyme reaction was found to be linear with time at 37°C for at least *ca.* 60 min (data not shown).

The pH dependence of enzyme activity was investigated in both 60 m*M* sodium phosphate buffer (pH 6.0–8.0) and 60 m*M* Tris–HCl buffer (pH 7.5–9.0). The catalytic activity of the enzyme was greatest at a pH of approximately 7.5–8.0, with very little activity below pH 6.0 and above pH 9.0 (Fig. 2).

PZ-peptidase activity was investigated as a function of the amount of enzyme extract ob-

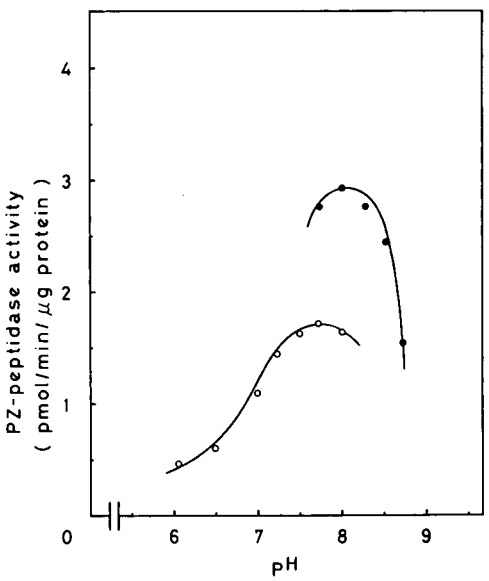

Fig. 2. Effect of pH on PZ-peptidase activity: (○) 60 m*M* sodium phosphate buffer (pH 6.0–8.0) and (●) 60 m*M* Tris–HCl buffer (pH 7.5–9.0) were used. Incubation was carried out at 37°C for 30 min.

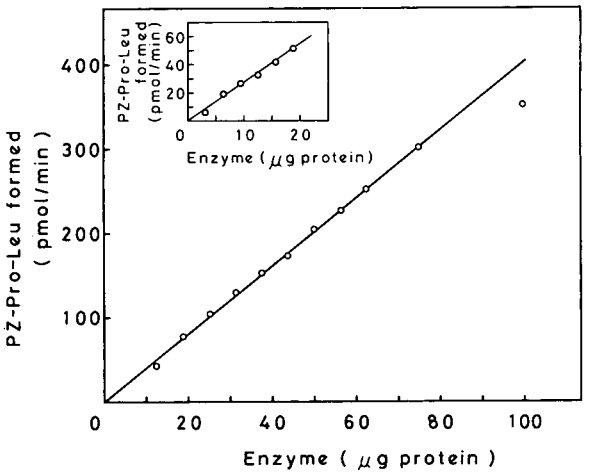

Fig. 3. Velocity of PZ-peptidase reaction determined at various concentrations of enzyme in mouse whole brain. The standard assay conditions were used and incubation was carried out at 37°C for 20 min. Inset: the enzyme activity was measured by means of a micro-assay system.

tained from mouse whole brain. Perfect linearity was observed for plots of the amount of PZ-Pro-Leu, from $7.84 \cdot 10^{-5}$ to $3.02 \cdot 10^{-4}$ units, formed enzymatically from PZ-peptide against those of enzyme (100 000 *g* supernatant fraction). By using the micro-assay system, the enzyme activity was detectable as levels as low as $4.80 \cdot 10^{-6}$ units (Fig. 3).

A Lineweaver–Burk plot was obtained from the effect of the concentration of PZ-peptide on the rate of formation of PZ-Pro-Leu by PZ-

TABLE I

DISTRIBUTION OF PZ-PEPTIDASE ACTIVITY IN MOUSE BRAIN HOMOGENATE

Values are means ±SEM for four experiments.

Brain region	Enzyme activity (pmol/min · mg protein)
Bulbus olfactorius	893 ± 61
Pons-medulla	477 ± 34
Cerebellum	591 ± 32
Hypothalamus	524 ± 33
Hippocampus	756 ± 16
Cerebral cortex	1276 ± 41
Striatum	586 ± 28
Midbrain	779 ± 35
Pituitary gland	1020 ± 46

peptidase. The Michaelis constant (K_m) and the maximum velocity (V_{max}) towards the PZ-peptide were calculated to be 166.7 ± 3.0 μM and 5.35 ± 0.28 pmol/min · μg protein, respectively.

We applied this standard assay method for the detection of PZ-peptidase activity in various mouse brain regions (Table I). It can be seen that the PZ-peptidase activity was distributed unevenly in the mouse CNS. Among the tissues examined, the highest specific activity of the enzyme was found in the cerebral cortex and the lowest in the pons-medulla. A high level of activity was also observed in the pituitary gland. Moderate levels of activity were seen in the bulbus olfactorius, hippocampus and midbrain.

Further, some enzymatic and physico-chemical properties of PZ-peptidase in mouse whole brain were studied by this standard assay method. An estimation of the molecular mass of the enzyme was made by the gel filtration method using a Sephacryl S-300 HR column. The void volume of the column was determined with Blue Dextran 2000. From a plot of log M_r *versus* K_{av} for protein standards, the molecular mass of the enzyme was estimated to be approximately 64 000 (Fig. 4).

The effects of various metal ions and inhibitors on PZ-peptidase activity in mouse whole brain were examined at a final concentration of 1 and 0.1 mM. As shown in Table II, metals such as Zn^{2+} and Cu^{2+} completely inhibited the enzyme activity at 1 mM, whereas Ca^{2+} and Mg^{2+} had no effect. On the other hand, Mn^{2+} enhanced the enzyme activity to 1.6-fold compared with the control level at 1 mM. EDTA, a chelating agent, had no effect on enzyme activity, but 1,10-phenanthroline was found to be inhibitory to the enzyme. PCMS, a typical thiol protease inhibitor, inhibited the enzyme activity completely at a final concentration of 0.1 mM. However, there was no inhibition by other thiol protease inhibitors such as IAA and NEM and PMSF (serine protease inhibitor). Further, the PZ-peptidase activity was not affected by pep-

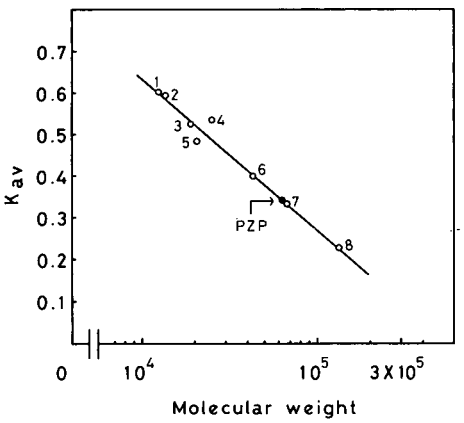

Fig. 4. Estimation of the molecular mass of PZ-peptidase on a Sephacryl S-300 HR column. The protein markers used were (1) cytochrome *c*, 12 500; (2) ribonuclease A, 13 700; (3) myoglobin, 18 800; (4) α-chymotrypsinogen A, 25 000; (5) soybean trypsin inhibitor, 20 100; (6) ovalbumin, 43 000; (7) BSA monomer, 67 000; (8) BSA dimer, 130 000; and PZ-peptidase (PZP), molecular mass estimated to be 64 000. Experimental details as described under Experimental.

TABLE II

EFFECTS OF METAL IONS AND INHIBITORS ON PZ-PEPTIDASE ACTIVITY IN MOUSE WHOLE BRAIN

Reagent	Final concentration (mM)	PZ-peptidase activity (% of control)
None	–	100
$MnCl_2$	1	164.3
	0.1	121.6
$CaCl_2$	1	100.2
	0.1	95.1
$MgCl_2$	1	99.3
	0.1	100.7
$ZnSO_4$	1	0
	0.1	7.5
$CuSO_4$	1	0
	0.1	31.7
EDTA	1	105.1
	0.1	106.5
1,10-Phenanthroline	1	47.0
	0.1	88.6
p-Chloromercuriphenyl sulphonic acid	1	0
	0.1	0
Iodoacetic acid	1	117.3
	0.1	105.5
N-Ethylmaleimide	1	97.4
	0.1	94.7
Phenylmethylsulphonyl fluoride	1	67.3
	0.1	95.6
Pepstatin A	32 μg/ml	95.5
Soybean trypsin inhibitor	32 μg/mol	92.4
Bacitracin	80 μg/ml	89.1

statin A (acid protease inhibitor), soybean trypsin inhibitor and bacitracin.

DISCUSSION

As pointed out in other HPLC enzymatic assays, the direct analysis of the product of enzyme action, separated from the substrate and other interfering substances, offers several advantages over previous spectrophotometric methods.

The proposed sensitive assay method for PZ-peptidase activity using an HPLC–spectrophotometric detection system has a few advantages. First, it is very sensitive. The limit of the sensitivity was about 10 pmol of PZ-Pro-Leu formed enzymatically. On the other hand, the sensitivity of the widely used extraction assay method is only 5 nmol, because the absorbance at 320 nm in controls is very high compared with the present HPLC–spectrophotometric detection system. We especially emphasize that enzyme activity was able to be detected in a single mouse pituitary gland using this sensitive assay method. Typically, 15–20 assays could be performed with the extract from a single mouse pituitary. Second, the substrate and the product are separated completely in less than 5.5 min. The modified assay method for this enzyme activity by HPLC, which we reported previously [4], still had the disadvantage that it is time consuming for the complete separation of several peaks. However, the present assay method overcame this problem. Third, more accurate quantification of the product and better reproducibility were ensured by the use of an internal standard (DNP-Phe) and the elimination of an extraction step.

The physiological role of PZ-peptidase in animals has not been clarified except for the observation that PZ-peptidase plays a part in the late stages of the degradation of collagen in peripheral tissues [5], but there is no direct evidence for this. On the other hand, only one observation has been reported about findings of PZ-peptidase in CNS, in which PZ-peptidase activity continuously decreased with maturation in rat brain [6]. However, the physiological role of this enzyme in CNS is also still unclear. In order to search for it in CNS, some properties of PZ-peptidase in mouse brain were examined and compared with those in peripheral tissues.

The approximate molecular mass of PZ-peptidase from mouse brain is 64 000 on gel filtration, and its optimum pH is *ca.* 7.5–8.0. The effects of various metal ions and inhibitors on the PZ-peptidase are also investigated (Table II). The PZ-peptidase in mouse brain is completely inhibited by metals such as Zn^{2+} and Cu^{2+} and by PCMS, but not by other metals (Ca^{2+} and Mg^{2+}), serine protease inhibitor, acid protease inhibitor and trypsin inhibitor, indicating that this enzyme is a metallo-endopeptidase with thiol dependence. These properties are very similar to those of the enzymes that have been isolated from peripheral tissues and fluids [5–14]. On the other hand, the PZ-peptidase activity in pituitary gland is higher than that in other brain regions (Table I). From these observations, we conclude that some of the enzymes reported as "PZ-peptidases" may function as peptidases hydrolysing collagen-related peptides, but others may be related to the processing of certain hormones. The real physiological role of PZ-peptidase in CNS remains a subject for further investigation. Recently, PZ-peptidase has been shown to be identical with soluble metallo-endopeptidase (EC 3.4.24.15) [15] and endo-oligopeptidase (EC 3.4.22.19) [16]. Because of this, there is considerable interest in the physiological role of PZ-peptidase.

In conclusion, the rapid and accurate assay method described in this paper may be a useful means for investigating the roles of PZ-peptidase *in vivo*.

REFERENCES

1 E. Wünsch and H.G. Heidrich, *Hoppe-Seyler's Z. Physiol. Chem.*, 333 (1963) 149.
2 S. Aswanikumar and A.N. Radhakrishnan, *Biochim. Biophys. Acta*, 304 (1973) 210.
3 E.F. Hartree, *Anal. Biochem.*, 48 (1972) 422.
4 T. Chikuma, Y. Ishii and T. Kato, *J. Chromatogr.*, 348 (1985) 205.
5 T.I. Morales and J.F. Woessner, *J. Biol. Chem.*, 252 (1977) 4855.
6 T. Chikuma, Y. Ishii, T. Miyauchi and T. Kato, *Neurochem. Int.*, 6 (1984) 127.
7 G. Gries, H. Buresch and L. Strauch, *Experientia*, 26 (1970) 31.

8 K.R. Cutroneo and G.C. Fuller, *Biochim. Biophys. Acta*, 198 (1970) 271.
9 S. Aswanikumar and A.N. Radhakrishnan, *Biochim. Biophys. Acta*, 276 (1972) 241.
10 S. Aswanikumar and A.N. Radhakrishnan, *Biochim. Biophys. Acta*, 384 (1975) 194.
11 M. Hino and T. Nagatsu, *Biochim. Biophys. Acta*, 429 (1976) 555.
12 M. Nagelschmidt, T. Unger and H. Struck, *Biochim. Biophys. Acta*, 571 (1979) 105.
13 U. Tisljar and A.J. Barrett, *Arch. Biochem. Biophys.*, 274 (1989) 138.
14 A.J. Barrett and M.A. Brown, *Biochem. J.*, 271 (1990) 701.
15 A.J. Barrett and U. Tisljar, *Biochem. J.*, 261 (1989) 1047.
16 U. Tisljar, A.C.M. Camargo, C.A. Costa and A.J. Barrett, *Biochem. Biophys. Res. Commun.*, 162 (1989) 1460.

Journal of Chromatography, 635 (1993) 89–101
Elsevier Science Publishers B.V., Amsterdam

CHROM. 24 825

Chromatographic investigations of oligomeric α,ω-dihydroxy polyethers by reversed-phase high-performance liquid chromatography and evaporative light scattering and UV detection☆

Klaus Rissler*, Hans-Peter Künzi and Hans-Jörg Grether☆☆

Ciba-Geigy Ltd., Polymer Research, CH-1723 Marly (Switzerland)

(First received July 17th, 1992; revised manuscript received December 17th, 1992)

ABSTRACT

The separation of the three hydroxy-terminated polyethers, polyethylene glycol 1000, polypropylene glycol 1200 and polybutylene glycol 1000, on reversed-phase separation media differing markedly in the length of the alkylsilyl chain is described. Underivatized polyethers were measured by evaporative light scattering detection, whereas the corresponding 3,5-dinitrobenzoyl derivatives were monitored by UV detection at 254 nm. The detection limits were *ca.* 5, 10 and 20 μg for native polyethylene glycol 1000, polypropylene glycol 1200 and polybutylene glycol 1000, respectively, and 0.5, 1 and 2 μg for the corresponding 3,5-dinitrobenzoyl esters. A clear dependence of t_R and R_s values on the polarity of the analyte was observed in the sequence polyethylene glycol 1000 < polypropylene glycol 1200 < polybutylene glycol 1000 for each adsorbent used. Marked attenuation of analyte retention occurred with increasing polarity of the stationary phase in the sequence $C_{18} > C_8 > C_4 > C_{Phenyl} \approx C_1$ and concomitant loss of peak resolution of high-molecular-mass oligomers became increasingly evident. The solvent strength of acetonitrile was not sufficient for complete elution of polybutylene glycol and polypropylene glycol oligomers with higher molecular mass from the strongly hydrophobic C_{18} stationary phase, which however was markedly improved with methanol as organic modifier. Different possible alternatives are discussed in order to give a reasonable explanation of the separation mechanism.

INTRODUCTION

Hydroxy-terminated polyethers find a wide range of application in different fields of chemistry. They are applied as macropolymers for the synthesis of graft polymers [1] and polyurethanes [2]. Further, they have been used as non-ionic detergents [3–11] and as stabilizers and property modifiers in pharmaceutical and biochemical technology [4,12,13]. A new area of polyethylene glycol chemistry was recently opened up by the synthesis of so-called poly-rotaxanes [14,15], consisting of a polyether axis threaded with a multitude of ring systems. For this reason the development and improvement of chromatographic methods in order to obtain more insight into oligomeric distribution and characterization of polyethers is a further expanding area of analytical research.

Polyethers have been investigated by high-performance liquid chromatography (HPLC) in their native structure [16–29] and after derivatization of their hydroxy end-groups with alkyl or aryl functions [3–10,16,21,22,30]. Thin-layer chromatography (TLC) [11,31–33] and super-

* Corresponding author. Present address: Ciba-Geigy Ltd., K-401.2.08, CH-4002 Basle, Switzerland.
☆ Dedicated to Professor Hinrich Cramer on the occasion of his 60th birthday.
☆☆ Present address: Ciba-Geigy Ltd., K-403.3.58, CH-4002 Basle, Switzerland.

0021-9673/93/$06.00

critical fluid chromatography (SFC) have also been used for characterization [21,22,34–36].

The detection of underivatized polyethers is associated with severe problems owing to the poor response at the wavelength range usually applied for UV detection. Significant responses can only be measured below 200 nm, where the high background noise invoked by self-absorption of the solvent system is a strongly limiting factor for routine applications. Nevertheless, detection of oligomeric polyethylene glycol at wavelengths below 200 nm has been described using either isocratic [18,21] or gradient elution [25,37]. Unfortunately, refractometric detection [4,7,17,23,26–29] cannot be used for the gradient HPLC of complex mixtures of multifunctional polyether oligomers. For this reason, evaporative light scattering detection (ELSD) [8,10,22,38–41] represents a powerful tool for the detection of native polyethers. Additionally, UV detection of their 3,5-dinitrobenzoyl esters opens up an efficient alternative method, yielding high sensitivity, reliability and reproducibility of results.

The aim of this study was to optimize the chromatographic conditions for the separation of α,ω-dihydroxy polyethers. For this purpose, a reversed-phase (RP) HPLC system with the gradient elution technique was developed. Polyethylene glycol (polyoxyethylene), polypropylene-1,2-glycol (1,2-polyoxypropylene) and polybutylene-1,4-glycol (1,4-polyoxybutylene or polytetrahydrofuran) were chosen as model compounds:

$HO(CH_2CH_2O)_nH$
polyethylene glycol (PEG)
$HO[CH(CH_3)CH_2O]_nH$
polypropylene-1,2-glycol (PPG)
$HO(CH_2CH_2CH_2CH_2O)_nH$
polybutylene-1,4-glycol (PBG)

The three types of α,ω-hydroxy-terminated polyether differ substantially in their polarities, which decrease markedly in the sequence PEG > PPG > PBG. Therefore, different interactions would be expected between different kinds of polyethers and different stationary and mobile phases. In order to obtain an assessment of these influences, the following parameters were changed stepwise:

stationary phase: C_{18} (octadecylsilyl)-, C_8 (octylsilyl)-, C_4 (butylsilyl)-, C_{Phenyl} (phenylpropylsilyl)- and C_1 (methylsilyl)-silica gel;

mobile phase: acetonitrile–water or methanol–water gradients;

temperature of the stationary phase: ambient temperature (*ca.* 23°C) and 60°C.

For optimum comparison of results, oligomeric mixtures with an approximately identical average molecular mass (1000 for PEG, 1200 for PPG, 1000 for PBG) were used. When this study was made, PPG was not available in the M_r 1000 form.

It is well known that chromatographic behaviour depends additionally on the space-filling properties of analyte molecules and thus can be regarded as a function of the pore size of the stationary phase [42]. However, owing to the choice of polyethers of $M_r < 1500$, interpretation of the results should not be markedly impaired by influences arising from differences in molecular size [19].

EXPERIMENTAL

Separation media

Nucleosil $5C_{18}$ (125 × 4.6 mm I.D., 5 μm particle size), Nucleosil $5C_8$ (125 × 4.6 mm I.D., 5 μm), Nucleosil $5C_4$ (100 × 4.0 mm I.D., 5 μm) and Nucleosil 7Phenyl = C_{Phenyl} (250 × 4.6 mm I.D., 7 μm) adsorbents were purchased from Macherey–Nagel (Oensingen, Switzerland) and Spherisorb $5C_1$ (125 × 4.6 mm I.D., 5 μm) from Metrohm-Bischoff (Wallisellen, Switzerland).

Reagents and solvents

Polyethylene glycol 1000 and polypropylene-1,2-glycol (both of "pract." quality) were obtained from Fluka (Buchs, Switzerland) and polybutylene-1,4-glycol (technical quality) from BASF (Ludwigshafen, Germany). Acetonitrile (HPLC grade) and methanol (HPLC grade) from either J.T. Baker (Deventer, Netherlands) or Merck (Darmstadt, Germany) were used. Water for use in HPLC was purified with a Milli-Q reagent water system from Millipore–Waters (Milford, MA, USA). Pyridine (puriss. p.a. > 99%) and 3,5-dinitrobenzoyl chloride (DNBCl) (purum > 98%) were obtained from Fluka.

Analytical equipment

The HPLC apparatus consisted of a combined SP 8100 system of HPLC pump and autosampler, an SP 8450 UV detector and a Spectra Station data acquisition unit, all obtained from Spectra-Physics (San Jose, CA, USA). For ELSD, a Sedex 45 apparatus from Sedere (Vitry, France) equipped with a 20-W iodine lamp was applied. Separations at elevated temperature were performed with a π type column oven purchased from Portmann Instruments (Therwil, Switzerland).

Derivatization procedure

About 10 mg of polyether and 10 mg of DNBCl (corresponding to an approximately 100% excess of reagent on a molar basis) were dissolved in 100 μl of pyridine and heated at 60°C for about 30 min. After addition of 2 ml of methanol to the slightly brown liquid, excess of reagent was reacted to the corresponding methyl 3,5-dinitrobenzoate for about 30 min at 60°C. An aliquot of 10 μl of the resulting solution was injected on to the HPLC column without further purification.

Chromatographic separation

The time programme of the chromatographic procedure using the solvent gradient technique is depicted in Table I. For the separation of the hydrophilic PEG-1000 in either its native form or as the 3,5-dinitrobenzoyl (DNB) derivative, a gradient starting with 100% of water was chosen (gradient programme I). The significantly more hydrophobic native samples of PPG-1200 and PBG-1000 were eluted with a gradient starting with 80% of water and 20% of organic modifier (gradient programme II). For chromatography of DNB derivatives the terminal isocratic column rinsing with 100% of pure organic solvent was extended from 55 to 75 min in order to achieve extensive elution (gradient programme III). A flow-rate of 1.5 ml/min was chosen. For detection of native polyethers by means of ELSD the nebulization chamber was heated to 40°C and the nitrogen flow-rate was adjusted to 4.5 l/min, corresponding to an inlet pressure of 200 kPa. DNB derivatives were measured at a wavelength of 254 nm.

TABLE I

GRADIENT PROGRAMMES

Gradient programme	Time (min)	Organic solvent (acetonitrile or methanol) (%)	Water (%)
I	0	0	100
	40	100	0
	50	100	0
	51	0	100
	65	0	100
II	0	20	80
	40	100	0
	55	100	0
	56	20	80
	70	20	80
III	0	20	80
	40	100	0
	75	100	0
	76	20	80
	90	20	80

RESULTS

It should be noted that either the length or diameter of the C_4 and C_{Phenyl} columns differ from those of the C_1, C_8 and C_{18} materials. Therefore, substantial deviations from the normally expected k' and R_s values are observed, which were taken into account in the interpretation of the results. Nevertheless, the general chromatographic trend remains unchanged.

The detection limits for native samples of PEG-1000, PPG-1200 and PBG-1000 are *ca.* 5, 10 and 20 μg, respectively, whereas the values for the corresponding DNB derivatives are *ca.* 0.5, 1 and 2 μg.

In the following sections the results obtained from different separation experiments are described.

Gradient of acetonitrile–water

With all the separation media used in the study a dependence of either capacity factor k' or peak resolution R_s on the polarity of the polyethers was observed. Both parameters increase in the sequence PEG-1000 < PPG-1200 < PBG-1000. Further, the chromatograms of PPG-1200 (Fig. 1a–e) and PBG-1000 (Fig. 2a–e) reveal a significant dependence on either the k' or R_s values on

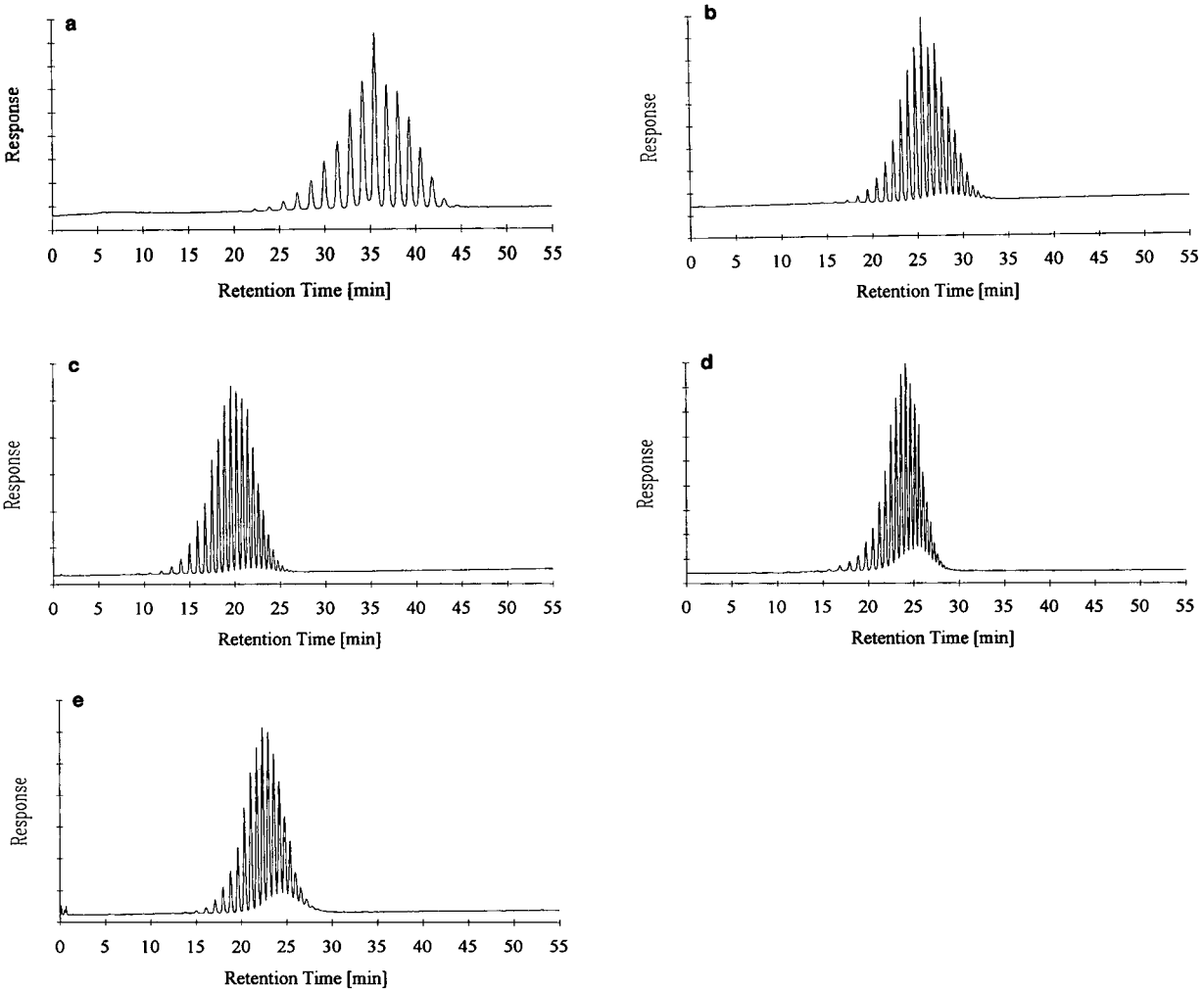

Fig. 1. Chromatograms with PPG-1200 and acetonitrile as organic solvent. (a) C_{18}; (b) C_8; (c) C_4; (d) C_{Phenyl}; (e) C_1.

the polarity of the stationary phase. An increase was observed in the sequence $C_1 \approx C_{Phenyl} < C_4 < C_8 < C_{18}$. It is remarkable that substantial amounts of high-molecular-mass oligomers of PBG-1000 are not completely eluted from a C_{18} stationary phase either at room temperature (RT) or when the column is held at 60°C. However, an elevated temperature markedly improves the elution potency of acetonitrile (Fig. 3a) and complete release of oligomers is achieved at 60°C on a C_8 column (Fig. 3b). In contrast, the significantly less hydrophobic PPG-1200 elutes quantitatively from a C_{18} matrix at 60°C despite its higher average molecular mass (Fig. 4).

Complete elution of PBG-1000 is effected at RT on the more polar C_4, C_{Phenyl} and C_1 materials (Fig. 2c–e). Unlike PPG-1200 and PBG-1000, the PEG-1000 oligomers exhibit incomplete peak resolution on all the separation media tested (Fig. 5a–e). In comparison with PPG-1200 and PBG-1000, the k' and R_s values are substantially decreased, although elution was started with a solvent of lower elution potency (gradient programme I, see Table I) and complete elution of PEG-1000 oligomers is achieved at RT on a C_{18} column. The incompletely resolved peak multiplet of the oligomeric mixture of PEG-1000 becomes larger and more diffuse in the sequence $C_{18} < C_8 < C_4 < C_{Phenyl} \approx C_1$.

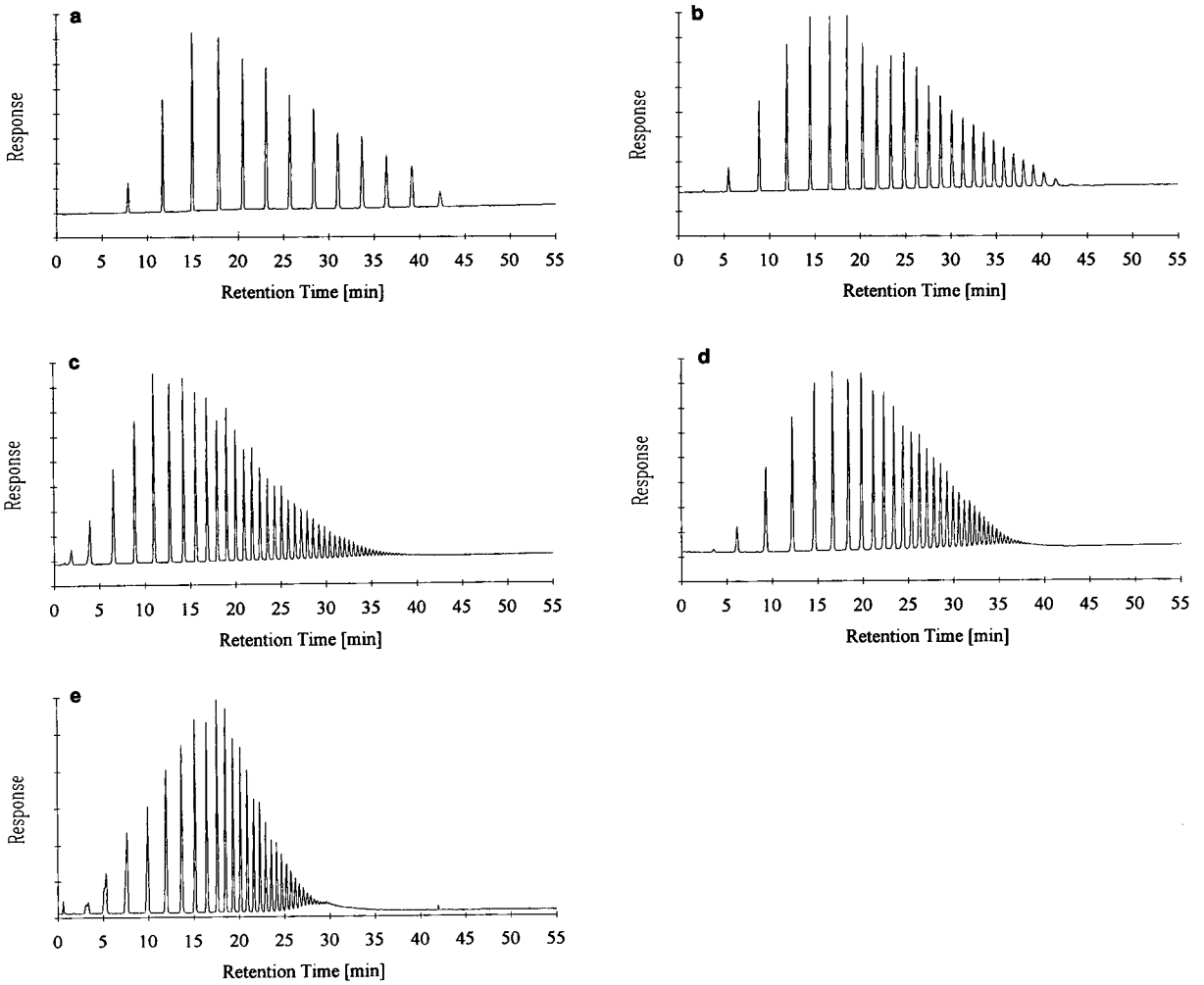

Fig. 2. Chromatograms with PBG-1000 and acetonitrile as organic solvent. (a) C_{18}; (b) C_8; (c) C_4; (d) C_{Phenyl}; (e) C_1.

Derivatization of PPG-1200 and PBG-1000 yielded a similar chromatographic pattern (Figs. 6a–e and 7a–e). As a consequence of the significant increase in hydrophobicity over the native samples, increased k' values are observed. Despite an extension of the isocratic run with pure acetonitrile from 55 to 75 min (gradient programme III), complete elution of DNB-PBG-1000 is only achieved on a C_8 column at 60°C (Fig. 8).

In contrast to these findings, the chromatographic differences between a native polyether and its corresponding DNB derivative are more marked with PEG-1000. The signals of individual oligomers coincide and partial peak resolution, which is observed with the native sample, vanishes completely (results not shown).

Gradient of methanol–water

Whereas acetonitrile as an organic modifier proved to be more efficient in eluting PPG-1200 and PBG-1000 oligomers with low to intermediate molecular masses, methanol is more suitable for elution of high-molecular mass oligomers. With increasing polarity of the stationary phase either the retention or resolution of peaks attributable to high-molecular-mass material decreases dramatically and the signals coincide more and more. These results are shown in Fig. 9a and b for PPG-1200 and Fig. 10a and b for

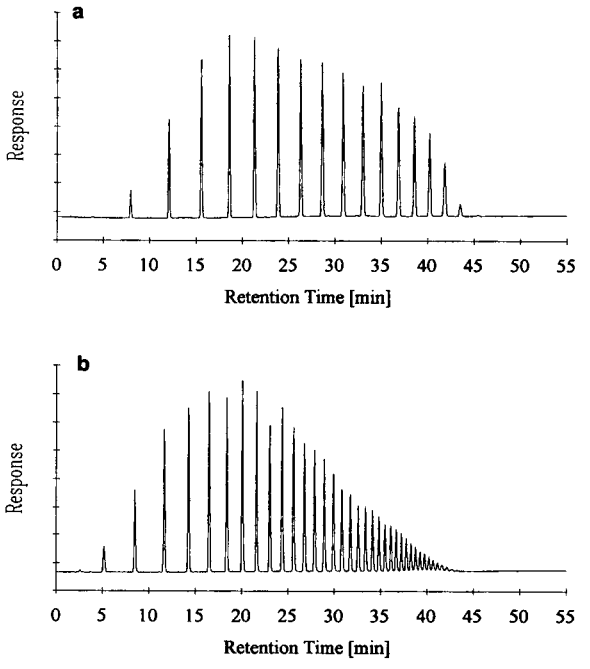

Fig. 3. Chromatograms with PBG-1000 and acetonitrile as organic solvent at a column temperature of 60°C. (a) C_{18}; (b) C_8.

PBG-1000 on C_{18} and C_8 materials, respectively. Complete elution of PPG-1200 oligomers is achieved at RT on a C_{18} column. Under identical conditions, approximately twice the number of PBG-1000 oligomers elute from the column (Fig. 10a) compared with acetonitrile, whereas complete elution of high-molecular-mass material is observed on a less hydrophobic C_8 matrix (Fig. 10b). Elution at a column temperature of 60°C does not influence the elution pattern of either low to intermediate or high-molecular-mass

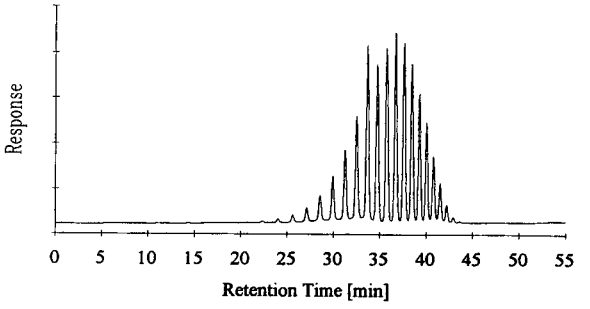

Fig. 4. Chromatogram with PPG-1200 and acetonitrile as organic solvent at a column temperature of 60°C on a C_{18} matrix.

oligomers of PPG-1200 and PBG-1000 (results not shown).

In comparison with acetonitrile, methanol causes a substantially increased retention of PEG-1000 oligomers (Fig. 11a–d). The signals of homologues exhibit a significantly larger and more diffuse peak shape but no improvement in peak resolution over acetonitrile is observed.

Analogous results were obtained with DNB-PPG-1200 (Fig. 12) and DNB-PBG-1000 (Fig. 13) on a C_{18} matrix with respect to the native samples. DNB-PPG-1200 is completely eluted on a C_{18} column at RT, whereas quantitative elution of the more hydrophobic DNB-PBG-1000 is achieved on a C_8 matrix (results not shown). Separation of DNB-PEG-1000 on C_{18}, C_8, C_{Phenyl} and C_4 materials yields an elution pattern similar to that obtained with acetonitrile as modifier (results not shown), whereas a marked improvement in peak resolution is observed on a C_1 column. The differences between acetonitrile and methanol on the C_1 stationary phase are depicted in Figs. 14 and 15.

DISCUSSION

For minimization of influences arising from individual manufacturing processes of stationary phases on the chromatographic properties, separation media from one supplier were used whenever possible. However, the C_1 column required for completion of the study was only available from a different producer. Further, it should be emphasized that the determination of the detection limits of polyethers (see Results) gives rise to some problems owing to the contribution to the total response by a large number of individual values. They must, in the strictest sense, be ascertained individually for each oligomer. Therefore, oligomers only present in low concentrations will be considered insufficiently. For this reason, the given values may be considered as an approximative set of data relating to minimum sample amounts, necessary for an unambiguous identification from the "fingerprint".

The conditions of gradient elution for the chromatography of PBG-1000 and PPG-1200 and their DNB derivatives could not be directly applied to PEG-1000 and its DNB ester owing to

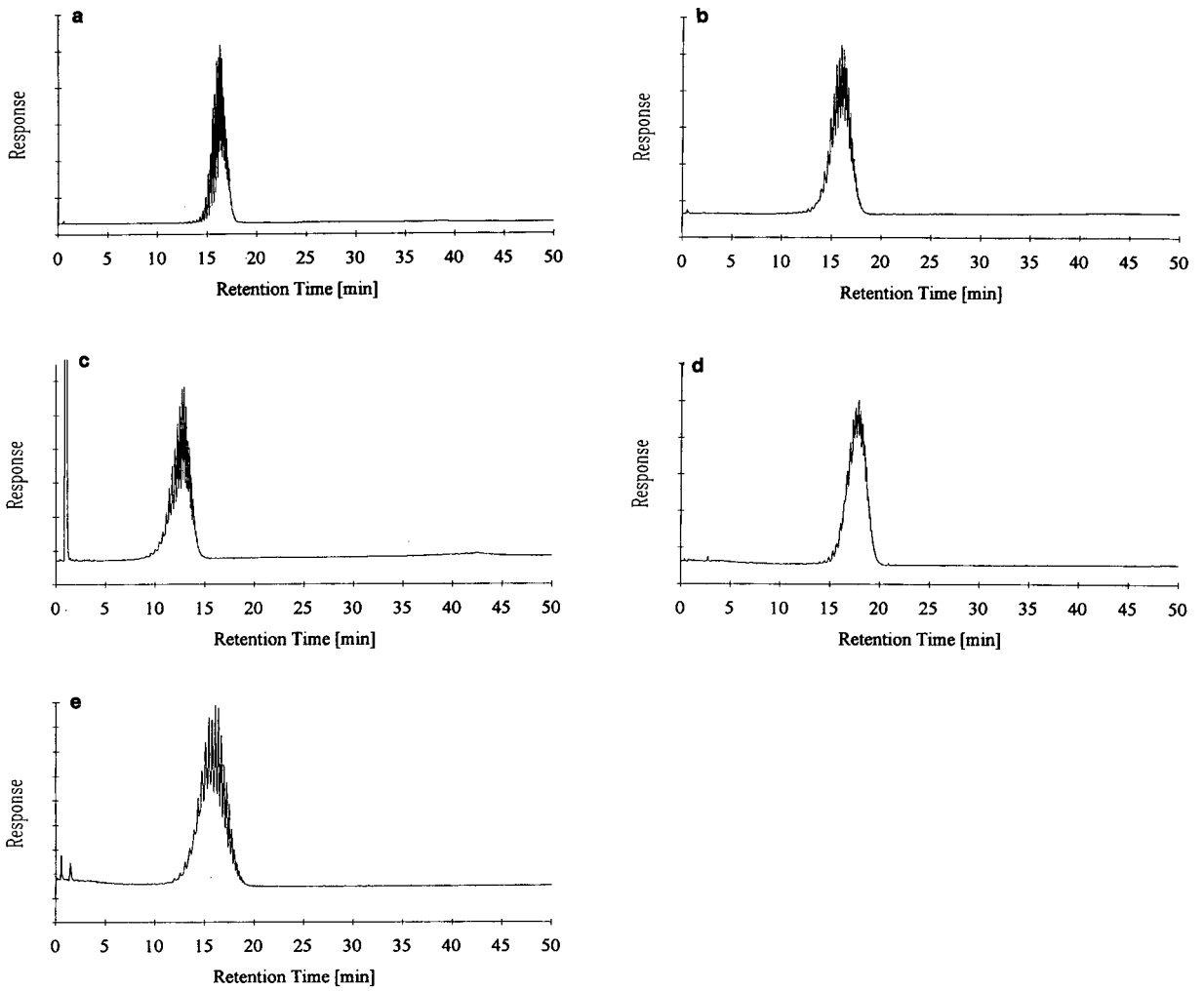

Fig. 5. Chromatograms with PEG-1000 and acetonitrile as organic solvent. (a) C_{18}; (b) C_8; (c) C_4; (d) C_{Phenyl}; (e) C_1.

the very low k' values. For comparison of the results with those from PBG-1000 and PPG-1200, gradient elution was started with a mobile phase of lower solvent strength (see Table I, gradient programme I). The HPLC separation of both native polyethers and DNB derivatives with signal monitoring by means of ELSD and UV detection yielded high sensitivity and no substantial baseline deterioration occurred even at elevated temperature (60°C). The main advantage of ELSD over UV detection is that the detector response is independent of the mobile phase composition and allows the use of solvents that generally cannot be applied in HPLC owing to strong UV absorption, such as acetone or methyl ethyl ketone. Nevertheless, the sensitivity of UV detection after derivatization with DNBCl is about ten times higher and the reaction takes place either rapidly or quantitatively. No significant amounts of interfering by-products are observed and samples can be injected directly without further purification.

Marked hydrophobic interactions between the hydrocarbon backbone of both native and derivatized PPG-1200 and PBG-1000 oligomers and the alkyl chains of the C_{18} matrix favour efficient separation with sharp and well resolved peaks (Figs. 1a, 2a, 6a and 7a), whereas in particular the k' and R_s values of high-molecular-mass oligomers decrease significantly on separation

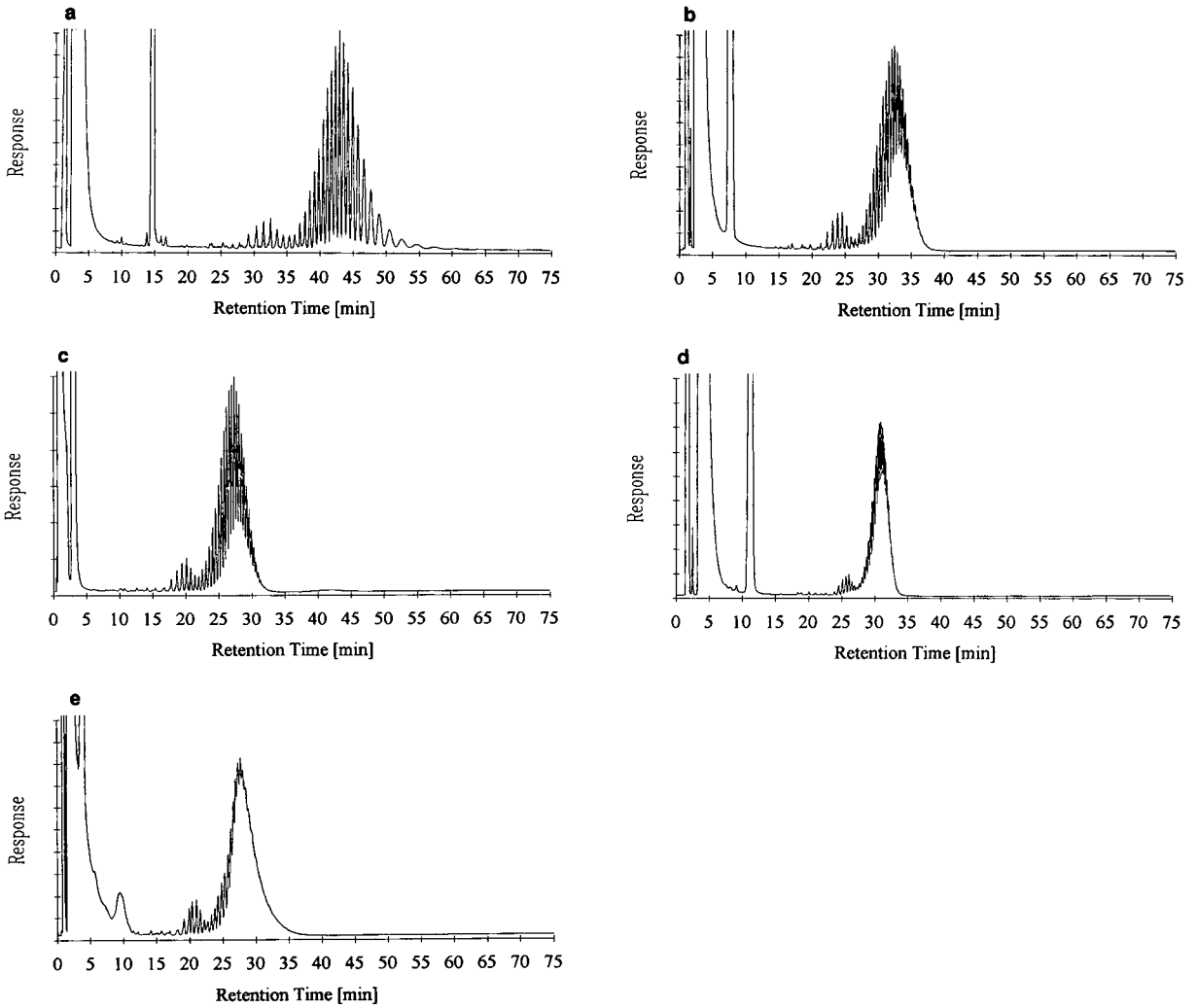

Fig. 6. Chromatograms with PPG-1200 after derivatization with DNBCl and acetonitrile as organic solvent. (a) C_{18}; (b) C_8; (c) C_4; (d) C_{Phenyl}; (e) C_1.

media of intermediate hydrophobicity (*e.g.*, C_8 and C_4) or more polar adsorbents (C_{Phenyl} and C_1) owing to weakened solvophobic interactions (see Figs. 1b–e, 2b–e, 6b–e and 7b–e).

A mechanism of the separation of these polyethers on the basis of their precipitation at the column head and elution of the oligomers in the sequence of their stepwise "redissolution" as a consequence of the gradual increase in the amount of organic solvent [43,44] seems improbable. The solubility of the investigated polyethers in the chosen solvent systems seems to be sufficient. However, precipitation of oligomers with substantially higher molecular mass than those tested may occur. Significant precipitation has been postulated in the normal-phase gradient HPLC of polystyrenes and copolymers of styrene and acrylonitrile [45–48].

Participation of silanophilic interactions [49–52] as described in the HPLC of cyclic polyethers [49] should presumably also be ruled out. This view is supported by the observation that low to intermediate molecular mass oligomers are eluted more rapidly with acetonitrile than with

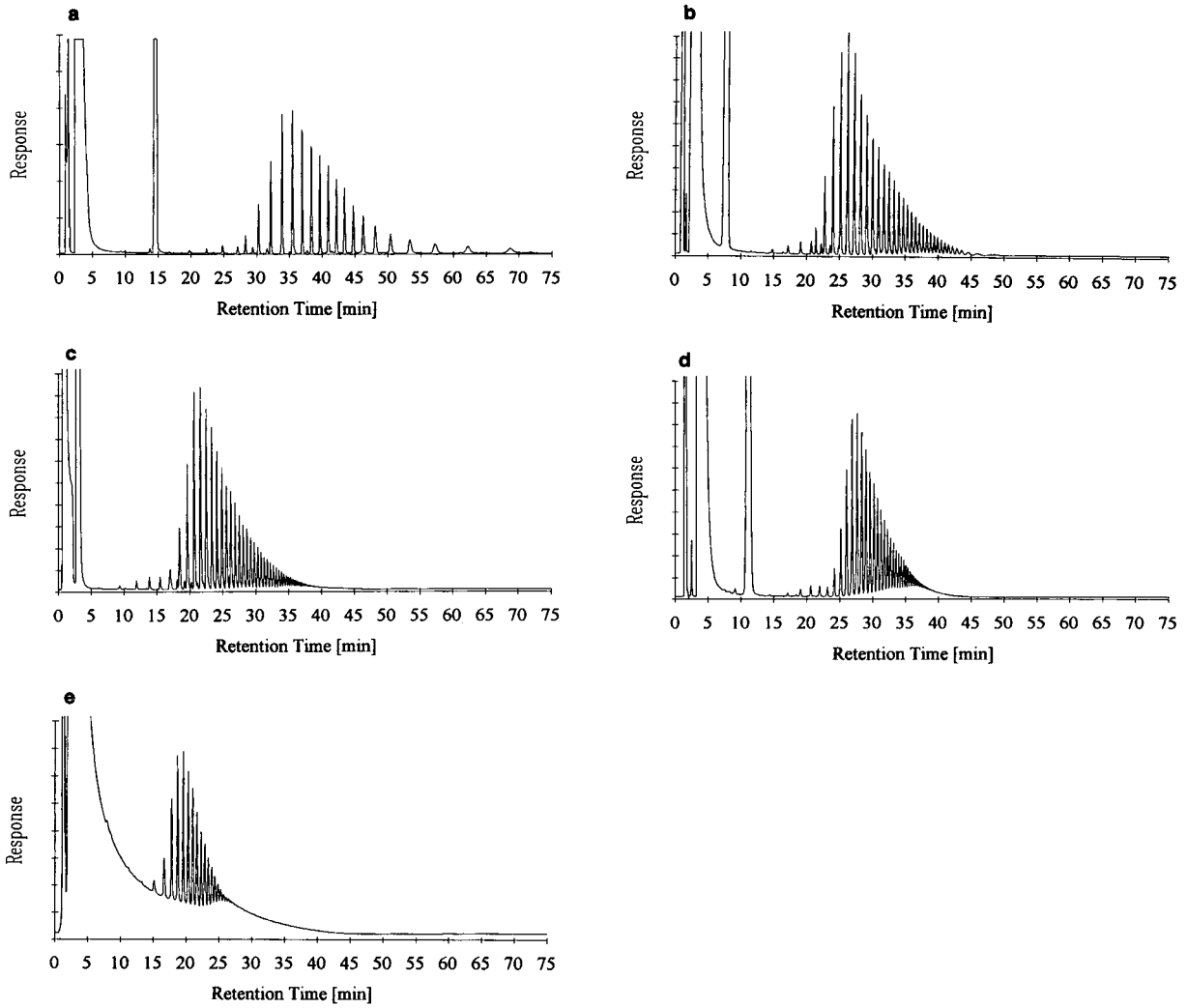

Fig. 7. Chromatograms with PBG-1000 after derivatization with DNBCl and acetonitrile as organic solvent. (a) C_{18}; (b) C_8; (c) C_4; (d) C_{Phenyl}; (e) C_1.

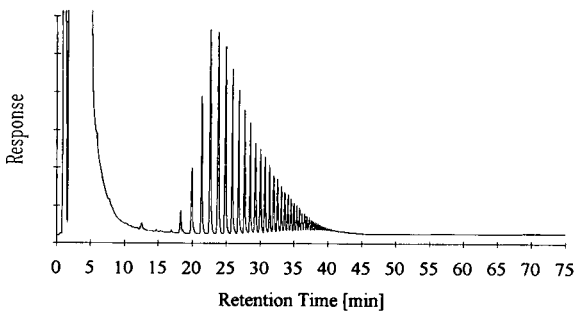

Fig. 8. Chromatogram with PBG-1000 after derivatization with DNBCl and acetonitrile as organic solvent on a C_8 matrix at a column temperature of 60°C.

methanol, although the potency of the protic solvent to cleave hydrogen bonds between ether oxygens and matrix silanols is much higher [49].

Further, it does not seem reasonable that high-molecular-mass sample constituents of PBG-1000 are preferentially able to penetrate the layer of octadecylsilyl chains of the stationary phase in order to reach free silanols. This interpretation is additionally corroborated by the complete elution of high-molecular-mass material from RP materials such as C_4, C_{Phenyl} and C_1, because more facile access to residual silanols should be

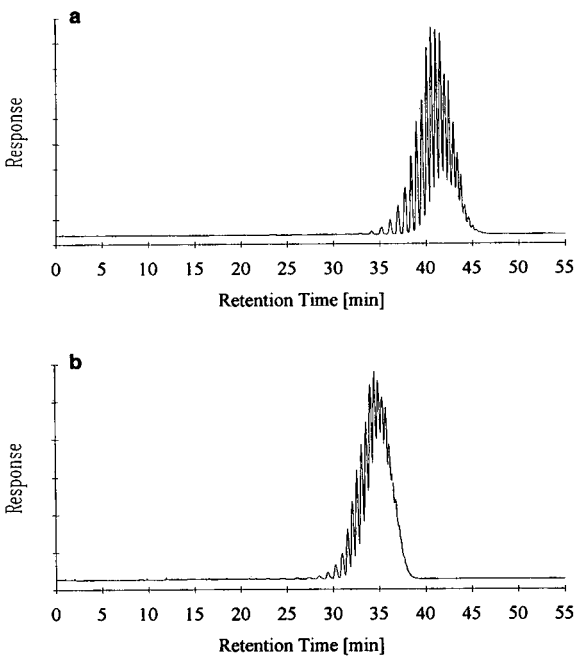

Fig. 9. Chromatograms with PPG-1200 and methanol as organic solvent. (a) C_{18}; (b) C_8.

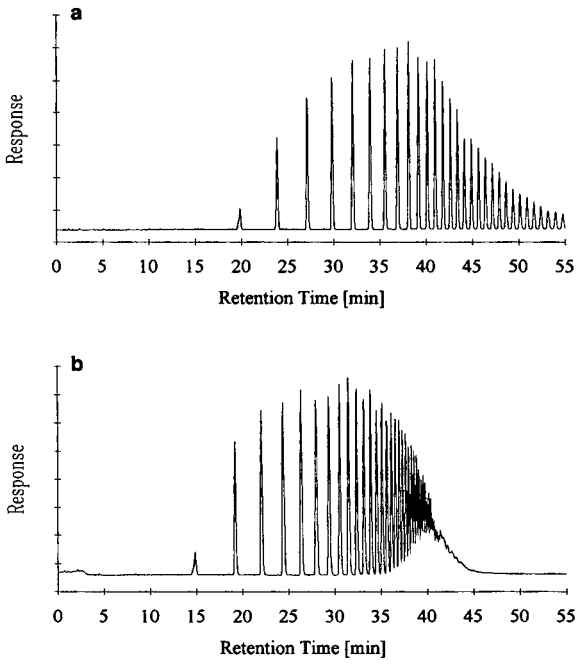

Fig. 10. Chromatograms with PBG-1000 and methanol as organic solvent. (a) C_{18}; (b) C_8.

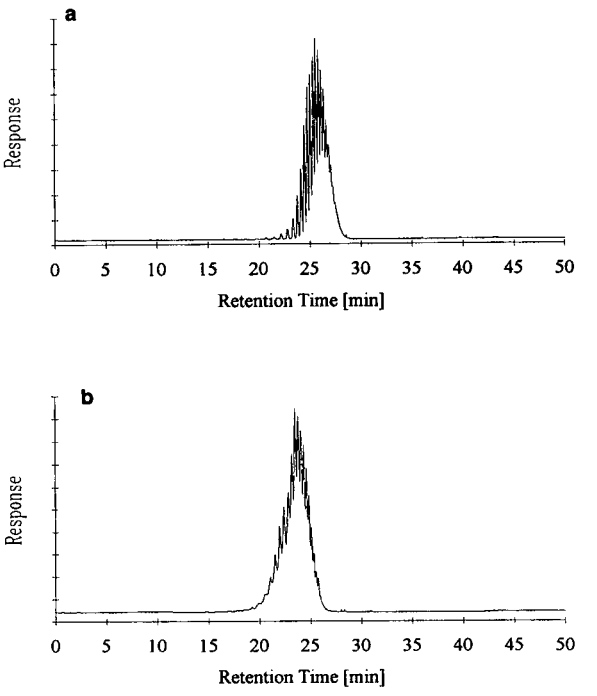

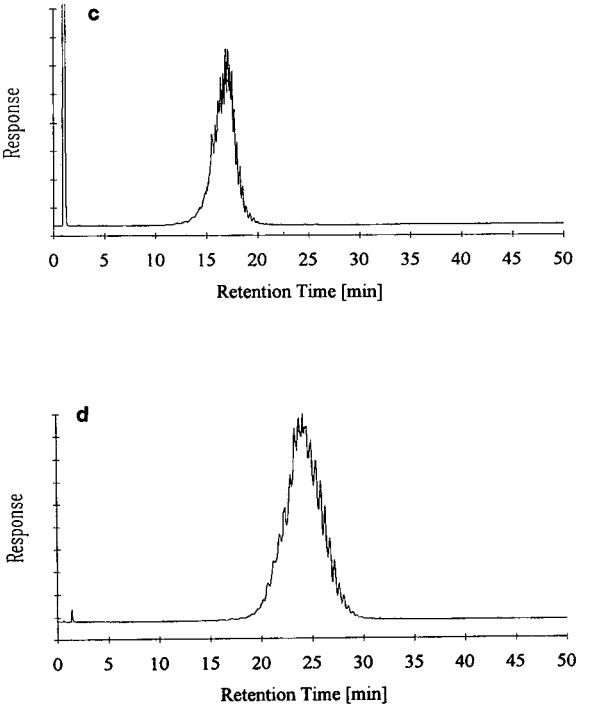

Fig. 11. Chromatograms with PEG-1000 and methanol as organic solvent. (a) C_{18}; (b) C_8; (c) C_4; (d) C_1.

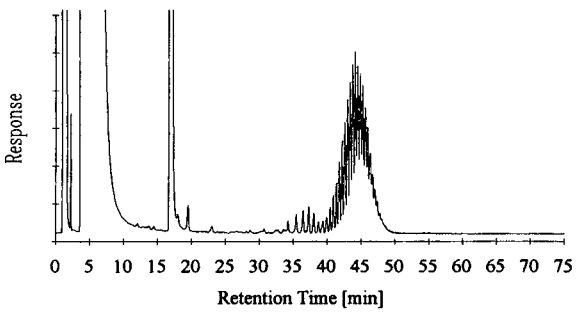

Fig. 12. Chromatogram with PPG-1200 after derivatization with DNBCl and methanol as organic solvent on a C_{18} column.

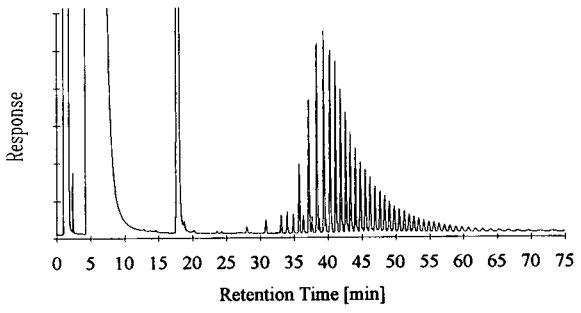

Fig. 13. Chromatogram with PBG-1000 after derivatization with DNBCl and methanol as organic solvent on a C_{18} column.

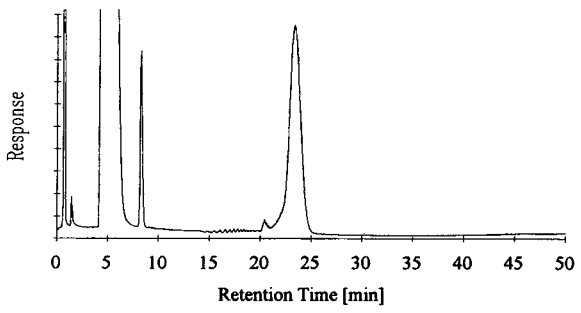

Fig. 14. Chromatogram with PEG-1000 after derivatization with DNBCl with acetonitrile as organic solvent on a C_1 column.

expected in comparison with C_{18} phases (Figs. 2c–e and 7c–e). Therefore, the decrease in retention of polyether oligomers on short-chain alkyl-substituted stationary phases can probably be attributed to either lower hydrophobic solute–matrix interactions or increased repulsive forces between free pairs of electrons on either

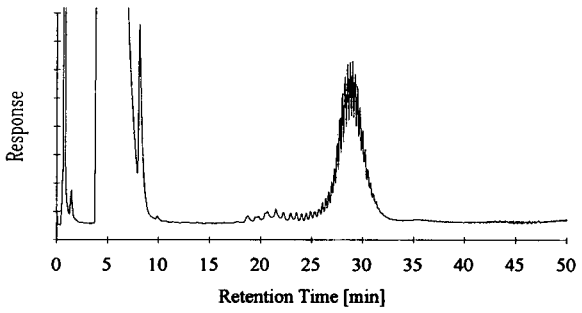

Fig. 15. Chromatogram with PEG-1000 after derivatization with DNBCl with methanol as organic solvent on a C_1 column.

oxygen atoms of the analyte or the polysiloxane backbone of the matrix. Repulsive interactions should be markedly attenuated on C_{18}-modified silica gel by a "shielding effect" of the large alkyl chains.

In addition to a hypothesis like this, a solubility effect seems to be more reasonable, which is further supported by the marked improvement in the elution potency of acetonitrile at elevated temperature. By comparison of the different effects of the two modifiers on the elution behaviour, two mechanisms become evident. On the one hand it can be assumed that the distribution of PBG-1000 between the non-polar stationary phase and the polar but aprotic solvent acetonitrile will be shifted towards an increased concentration of high-molecular-mass oligomers within the layer of C_{18} substituents. Thus decreased retention at elevated temperature can be explained by weakened solvophobic interactions and a concomitant solubility shift towards a higher concentration of analyte in the mobile phase. On the other hand, methanol will exert a solubility increase on the basis of hydrogen bond formation between its hydroxy protons and polyether oxygens. This hypothesis is in accordance with a complete lack of influence of temperature on the k' and R_s values. Similar observations were obtained with PPG-1200 but the differences are much lower owing to its lower hydrophobicity.

The poor peak resolution for PEG-1000 on all the columns tested is indicative of a decrease in hydrophobic solute–matrix interactions due to a significant increase in polarity. Therefore, RP

materials are not suitable stationary phases for separation of polar polyethers. On the other hand, satisfactory separation of alkylphenyl-oligo(ethylene) glycol was reported for "bonded-phase" materials such as 2,3-propanediol- and aminopropyl-substituted silica gel or silica gel alone with normal-phase eluents [22,30]. Further, a dependence of either k' or R_s values on the carbon load of C_{18}-substituted silica gels was established, and the lower the concentration of octadecylsilyl chains the more marked is the peak resolution [30]. Nevertheless, complete loss of peak resolution after derivatization is surprising because, in general, one would expect more marked hydrophobic interactions between the different oligomers and reversed-phase adsorbents at least with a C_{18} column. Conformational changes of analyte molecules may be responsible for this observation, as described for the cyclic polyethers dibenzo-18-crown-6 and dibenzo-24-crown-6, which induced a complete inverse of the usually observed chromatographic behaviour [16,49].

It is assumed that effects such as these will favour a levelling of solute–matrix interactions for the different oligomers. In contrast, the marked separation improvement with methanol on a C_1 column may be attributable to marked interactions between the analyte and methanol on the one hand and methanol and the stationary phase on the other. Either a "coating" effect of silyl ether oxygens by the protic solvent methanol and/or stereochemical factors induced by the special properties of the trimethylsilyl layer may be operating. Obviously the butyl chains of the C_4 column seem to be too large in order to bring about similar interactions (results not shown). In order to give a reasonable explanation of the separation mechanism, investigations on C_3 and C_2 matrices would be useful.

With a phenyl-substituted silica gel stationary phase as used in this study, the possibility of matrix–analyte $\pi-\pi$ interactions [53–56] should be taken into account. Nevertheless, the retention of DNB-polyethers on a C_{Phenyl} column was not markedly affected compared with results with a C_1 stationary phase, which is known to possess a similar matrix polarity. Therefore, an influence of potential $\pi-\pi$ interactions may be considered to be negligible.

CONCLUSIONS

To our knowledge, chromatography of polybutylene-1,4-glycol had not previously been performed. For this reason, this study represents the first report of the RP-HPLC of polybutylene-1,4-glycol. Owing to the characteristic chromatographic "fingerprint", it is possible to identify unambiguously the different types of polyethers. Methanol proved to be the mobile phase of choice especially for the separation of more hydrophobic high-molecular-mass polyether mixtures on a C_{18} stationary phase. This material is superior to the more polar short-chain alkyl-substituted adsorbents owing to its markedly better peak resolution. Overall, liquid chromatography of polyethers offers many advantages over competing methods such as SFC and TLC owing to the multitude of possible experimental approaches and its capability to separate and identify individual kinds of polyethers within complex mixtures with either marked differences in hydrophobicity or molecular masses far above 5000.

ACKNOWLEDGEMENTS

The excellent assistance of Ulf Fuchslueger in the acquisition and reprocessing of analytical data and Dr. Bryan Dobinson for proof-reading of the manuscript is gratefully acknowledged.

REFERENCES

1 W.W. Schulz, J. Kaladas and D.N. Schulz, *J. Polym. Sci.*, 22 (1984) 3795.
2 D. Noël and P. Van Gheluwe, *J. Chromatogr. Sci.*, 25 (1987) 231.
3 M. Kudoh, S. Konami, S. Fudano and S. Yamaguchi, *J. Chromatogr.*, 234 (1982) 209.
4 M. Kudoh, M. Kotsuji, S. Fudano and K. Tsuji, *J. Chromatogr.*, 295 (1984) 187.
5 A. Marcomini, S. Capri and W. Giger, *J. Chromatogr.*, 403 (1987) 243.
6 K.V. Viswanathan and P. Somasundaran, *J. Colloid Interface Sci.*, 126 (1988) 634.
7 I. Zeman, *J. Chromatogr.*, 509 (1990) 201.
8 G.R. Bear, *J. Chromatogr.*, 459 (1988) 91.
9 A. Aserin, N. Garti and M. Frenkel, *J. Liq. Chromatogr.*, 7 (1984) 1545.
10 Y. Mengerink, H.C.J. de Man and Sj. van der Wal, *J. Chromatogr.*, 552 (1991) 593.
11 L.H. Henrich, *J. Planar Chromatogr.*, 5 (1992) 103.

12 B. Weidmann, *Chimia*, 45 (1991) 367.
13 M. Kunitani, G. Dollinger, D. Johnson and L. Kresin, *J. Chromatogr.*, 588 (1991) 125.
14 G. Wenz and B. Keller, *Angew. Chem., Int. Ed. Engl.*, 31 (1992) 197.
15 A. Harada, J. Li and M. Kamachi, *Nature*, 356 (1992) 325.
16 W.R. Melander, A. Nahum and Cs. Horváth, *J. Chromatogr.*, 185 (1979) 129.
17 F. Eisenbeiss and S. Ehlerding, *Kontakte/Merck*, 1 (1978) 22.
18 Sj. van der Wal and L.R. Snyder, *J. Chromatogr.*, 255 (1983) 463.
19 G. Barka and P. Hoffmann, *J. Chromatogr.*, 389 (1987) 273.
20 S.-T. Lai, L. Sangermo and D.C. Locke, *J. High Resolut. Chromatogr. Chromatogr. Commun.*, 7 (1984) 494.
21 R.E.A. Escott, *J. Chromatogr.*, 553 (1991) 423.
22 S. Brossard, M. Lafosse and M. Dreux, *J. Chromatogr.*, 591 (1992) 149.
23 R. Murphy, A.C. Selden, M. Fisher, E.A. Fagan and V.S. Chadwick, *J. Chromatogr.*, 211 (1981) 160.
24 I.M. Kinahan and M.R. Smyth, *J. Chromatogr.*, 565 (1991) 297.
25 M. Bergmann und F.E. Möller, *Labor Praxis*, 1989, 1010.
26 A.V. Gorskov, V.V. Evreinov and S.G. Entelis, *Zh. Fiz. Khim.*, 62 (1988) 490.
27 H. Pasch, H. Much, G. Schulz and A.V. Gorshkov, *LC–GC Int.*, 5 (1992) 38.
28 A.V. Gorshkov, V.V. Jevreinow, B. Jausecker, H. Pasch, H. Becker and G. Wagner, *Acta Polym.*, 37 (1986) 740.
29 A.V. Gorshkov, H. Much, H. Becker, H. Pasch, V.V. Evreinow and S.G. Entelis, *J. Chromatogr.*, 523 (1990) 91.
30 J.N. Alexander, M.E. McNally and L.B. Rogers, *J. Chromatogr.*, 318 (1985) 289.
31 M.T. Belay and C.F. Poole, *J. Planar Chromatogr.*, 4 (1991) 424.
32 B. Krumholz and K. Wenz, *J. Planar Chromatogr.*, 4 (1991) 370.
33 B.G. Belenky, M.D. Valchikhina, I.A. Vakhtina, E.S. Gankina and O.G. Tarakanov, *J. Chromatogr.*, 129 (1976) 115.
34 T.A. Dean and C.F. Poole, *J. Chromatogr.*, 468 (1989) 127.
35 B. Gemmel, B. Lorenschat and F.P. Schmitz, *Chromatographia*, 27 (1989) 605.
36 J.R. Craven, H. Tyrer, S. Pok Lai Li and C. Booth, *J. Chromatogr.*, 387 (1987) 233.
37 V.V. Berry, *J. Chromatogr.*, 236 (1982) 279.
38 J.M. Charlesworth, *Anal. Chem.*, 50 (1978) 1414.
39 T.H. Mourey and L.E. Oppenheimer, *Anal. Chem.*, 56 (1984) 2427.
40 T.H. Mourey, *J. Chromatogr.*, 357 (1986) 101.
41 B.E. Turner, *LC–GC Int.*, 4 (1991) 22.
42 W. Winkle, *Chromatographia*, 29 (1990) 530.
43 D.W. Armstrong and K.H. Bul, *Anal. Chem.*, 54 (1982) 706.
44 D.E. Doster and M. Zentner, *J. Chromatogr.*, 461 (1989) 293.
45 G. Glöckner, J.H.M. van den Berg, N.L.J. Meijerink, T.G. Scholte and R. Koningsveld, *J. Chromatogr.*, 317 (1984) 615.
46 G. Glöckner and J.H.M. van den Berg, *J. Chromatogr.*, 384 (1987) 135.
47 R. Schultz and H. Engelhardt, *Chromatographia*, 29 (1990) 205.
48 R. Schultz and H. Engelhardt, *Chromatographia*, 29 (1990) 325.
49 K.E. Bij, Cs. Horváth, W.R. Melander and A. Nahum, *J. Chromatogr.*, 203 (1981) 65.
50 E.L. Weiser, A.W. Salotto, S.M. Flach and L.R. Snyder, *J. Chromatogr.*, 303 (1984) 1.
51 W.A. Moats and L. Leskinen, *J. Chromatogr.*, 386 (1987) 79.
52 G.C. Fernandez Otero and C.N. Carducci, *J. Liq. Chromatogr.*, 14 (1991) 1561.
53 S.A. Matlin, W.J. Lough and D.G. Bryan, *J. High Resolut. Chromatogr. Chromatogr. Commun.*, 3 (1980) 33.
54 N. Tanaka, Y. Tokuda, K. Iwaguchi and M. Araki, *J. Chromatogr.*, 239 (1982) 761.
55 Y. Saito, M. Mifune, J. Odo, Y. Otsuki, M. Mitsuhashi, Y. Mori, A.E.H. Gassim and J. Haginaka, *Anal. Sci.*, 7 (1991) 805.
56 E. Krause and M. Bienert, *J. Liq. Chromatogr.*, 15 (1992) 1773.

Journal of Chromatography, 635 (1993) 103–111
Elsevier Science Publishers B.V., Amsterdam

CHROM. 24 820

Comparison of different methods for the prediction of retention times in programmed-temperature gas chromatography

G. Castello*, P. Moretti and S. Vezzani

Istituto di Chimica Industriale, Università di Genova, Corso Europa 30, 16132 Genova (Italy)

(First received October 13th, 1992; revised manuscript received December 21st, 1992)

ABSTRACT

Four calculation methods that can be easily applied by simple BASIC programming on personal computers were compared for the prediction of the retention times of various substances during linear temperature programming with and without an initial isothermal period on polar and non-polar capillary columns. The methods are based on curve-fitting techniques or a numeric iterative integration approach (Simpson and trapezoid methods). The comparison with experimental data obtained in various programmed-temperature analyses showed that all the tested methods permit the prediction of the retention times. The computation times and deviations of the results are compared.

INTRODUCTION

The prediction of retention times in programmed-temperature gas chromatography (PTGC) starting from isothermal data has been carried out by different methods [1–12], some of them requiring a complex computational approach or a knowledge of thermodynamic quantities. Other papers were dedicated to the prediction of retention indices under PTGC conditions [1,4,11].

A direct approach that permits the calculation of linear temperature data starting from retention times measured at three isothermal temperatures by means of a curve-fitting technique to replace the inverse retention time function by a function that can be integrated was suggested by Said [13,14] and applied by us previously to the prediction of PTGC retention times of chlorobenzenes [15] with satisfactory approximation. Other integration methods using iterative procedures (Simpson and trapezoid methods) were tested and compared with Said's methods. In order to test the performance of the programs for the prediction of the behaviour of compounds having different polarities and functional groups, a test mixture containing di- and trichlorobenzenes, nitro- and chloronitrobenzenes, chloroaniline and naphthalene was prepared and analysed on polar and non-polar capillary columns.

EXPERIMENTAL

A Model 3600 gas chromatograph (Varian, Palo Alto, CA, USA) equipped with a split–splitless injector and a flame ionization detector, was used for isothermal and PTGC analyses. A methylpolysiloxane DB-1 bonded phase non-polar capillary column, 0.25 μm film thickness (30 m × 0.32 mm I.D.) (J&W Scientific, Folsom, CA, USA), and a polyglycol DB-WAX polar capillary column (same dimensions) were used. The carrier gas was helium with a linear velocity

* Corresponding author.

0021-9673/93/$06.00

ranging between 67 cm s^{-1} (at 45°C) and 57 cm s^{-1} (at 150°C). The isothermal data used for calculation were measured at 60, 80 and 120°C on the non-polar column and at 100, 120 and 140°C on the polar column in order to take into account the longer retention times of polar compounds on the latter column. Table I shows the composition of the test mixture, with the compounds listed in order of increasing retention time on the non-polar column. Molecular masses, boiling points, densities and melting points are also given.

The selected compounds belong to some of the polarity classes suggested by Ewell *et al.* [16]: compounds containing both donor atoms and active hydrogen (chloroanilines); molecules containing donor but no active hydrogen atom (nitro- and chloronitrobenzenes); and molecules with π-electron availability (naphthalene) more or less influenced by the inductive effect of halogens (chlorobenzenes). The mixture used therefore permits a severe test of the calculation methods to be carried out because, mainly on the polar column, co-eluting peaks and inversion of the elution order of some compounds are observed at different temperatures and during various programmed runs.

The retention times were measured with an accuracy of ±0.005 min by using a Varian DS-650 data system. The retention times automatically calculated by the software were verified by using the interactive graphical data system in order to verify that the retention times (t_R) correspond to the maximum height of the peak. The same program also permitted the shape of each peak to be evaluated, in order to take into account the effect of the amount injected on the asymmetry and therefore on the deviation of the actual t_R with respect of the theoretical value at concentrations near zero.

CALCULATION METHODS

The methods that can be used in order to predict the retention of a given compound in a programmed-temperature run have the aim of calculating the retention temperature θ_f, *i.e.*, the column temperature at which the compound elutes from the column. The following equation, used by Said [14] and consistent with that derived by Habgood and Harris [17,18], must therefore be solved:

$$g = \int_{\theta_0}^{\theta_f} \frac{d\theta}{A + a \exp[b/(273 + \theta)]} = \int_{\theta_0}^{\theta_f} y(\theta)\, d\theta \quad (1)$$

where g is the temperature programming rate, θ_0 is the initial temperature, A is the column dead time or gas hold-up time under isothermal conditions, in order to obtain the θ_f value. This integral has no analytical solutions and therefore

TABLE I

COMPOUNDS OF THE TEST MIXTURE LISTED IN ORDER OF ELUTION ON THE NON-POLAR DB-1 COLUMN, THEIR MOLECULAR MASSES M, BOILING POINTS T_b, DENSITIES d, AND MELTING POINTS T_m

No.	Compound	M	T_b (°C)	d	T_m (°C)
1	1,3-Dichlorobenzene	147.01	173	1.2884	−24.7
2	1,4-Dichlorobenzene	147.01	174	1.2475	53.1
3	1,2-Dichlorobenzene	147.01	180.5	1.3048	−17
4	Nitrobenzene	123.11	210.8	1.2037	5.7
5	2-Chloroaniline	127.57	208.84	1.2125	−14
6	1,3,5-Trichlorobenzene	181.45	208	–	63–64
7	1,2,4-Trichlorobenzene	181.45	213.5	1.4542	16.95
8	Naphthalene	128.19	218	1.0253	80.55
9	3-Chloroaniline	127.57	229.92	1.2161	−10.3
10	4-Chloroaniline	127.57	232	1.429	72.5
11	1,2,3-Trichlorobenzene	181.45	218–219	–	53–54
12	1-Chloro-3-nitrobenzene	157.56	235–236	1.343	46
13	1-Chloro-4-nitrobenzene	157.56	242	1.2979	83.6
14	1-Chloro-2-nitrobenzene	157.56	246	1.368	33.5–35

some approximate integration method must be used. Said [13,14] proposed two similar methods in order to obtain an analytical expression for the integral of eqn. 1 and, by using curve-fitting techniques, to replace the $y(\theta)$ with functions that can be integrated.

In the first method suggested by Said, henceforth denoted "Said A", a temperature θ, lower than the temperature θ_i of the inflection point of the function $y(\theta)$, so that $\theta = \theta_i - x$, is considered. In order to obtain an acceptable accuracy, the value of x should be between 50 and 100°C [14]. Empirically, a value of 75°C can be chosen for x and, by comparing the calculated and experimental results, one can see that in this instance the difference is negligible for all the compounds and for all linear programming rates.

In order to ensure that the difference between the predicted and actual programmed retention times of a set of compounds have the minimum value, the best x value should be obtained by the equation

$$x = 50 + 50\left(\frac{\theta_i - 2\theta_0}{2\theta_0}\right) \quad (2)$$

This procedure was applied previously [15] and it was found that, whereas for megabore columns $x = 75$°C gives satisfactory precision, for narrow-bore columns the best correspondence between predicted and true retention times is obtained with x values near zero.

The second method proposed by Said ("Said B") does not employ the empirical x value, but iteratively calculates the intermediate constant values. The other two methods tested in this works in order to solve eqn. 1 are based on numerical integration algorithms, *i.e.*, the trapezoid method and the Simpson method [19–22]. In both instances the integral eqn. 1 is transformed into a sum of terms in order to verify the following:

$$g = \sum_{i=1}^{N} A(i) \quad (3a)$$

where, for the trapezoid method,

$$A(i) = \frac{\Delta\theta}{2}\left[y(\theta_{i-1} + y(\theta_i)\right] \quad (4a)$$

and, for the Simpson method,

$$g = \sum_{i=1}^{M} A(i) \quad (3b)$$

where

$$A(i) = \frac{\Delta\theta}{3}\left[y(\theta_{2i-2}) + y(\theta_{2i-1}) + y(\theta_{2i})\right] \quad (4b)$$

θ being the increment of temperature values used for calculation (0.1°C). In practice, by starting with $i = 1$, the sums of eqns. 3 are calculated by increasing i by 1 at each iterative stop, and this procedure is repeated until eqns. 3 are verified for $i = N$ or M, the final value of θ_f being

$$\theta_f = \theta_0 + N\,\Delta\theta \quad (5a)$$

or

$$\theta_f = \theta_0 + 2M\,\Delta\theta \quad (5b)$$

for the trapezoid and the Simpson method, respectively.

The four methods were applied through BASIC programming on a IBM personal computer (PS2-286) and used to predict the retention times in various programmed runs with and without an initial isothermal period.

RESULTS AND DISCUSSION

The different elution orders on the two columns are shown in Table II, where the gross retention times, t_R, obtained in the various isothermal runs and the retentions relative to nitrobenzene, r, *i.e.*, the ratio between the adjusted retention times, t'_R, are reported, and are graphically illustrated in Fig. 1. Several changes in the elution order and coincidence of the retention times were observed. The Arrhenius plots, *i.e.*, the values of ln t'_R as a function of the reciprocal of the absolute analysis temperature, were linear with a standard deviation of better than 0.99 within the temperature range used on both columns. Only two isothermal runs should therefore be sufficient in order to obtain the input data for the calculation of PTGC retention times, because the third value required by the programs should be linearly interpolated on the Arrhenius plot.

Notwithstanding this, three values of isother-

mal retention times measured experimentally were used in order to evaluate the accuracy of the calculation methods for routine use when the raw data obtained from isothermal runs are directly input without any previous elaboration and control in order to calculate the retention times under PTGC conditions. If the integrating data system can be programmed to extract directly from the analysis reports the retention values of the identified peaks, and the data so obtained are used for further elaboration in the system itself, all the procedure can be made automatic without the need for an external computer and manual transfer of the retention data. The procedures to obtain these results obviously depend on the logic of the integrator used and therefore no further details on the BASIC programming and data transfer of the data system used are given here.

Table III shows some of the PTGC runs carried out in order to verify the performance of the four calculation methods, covering a wide range of possible combinations of initial isothermal temperature and time, programming rate and final temperature, Tables IV and V show the comparison of the values calculated with the four

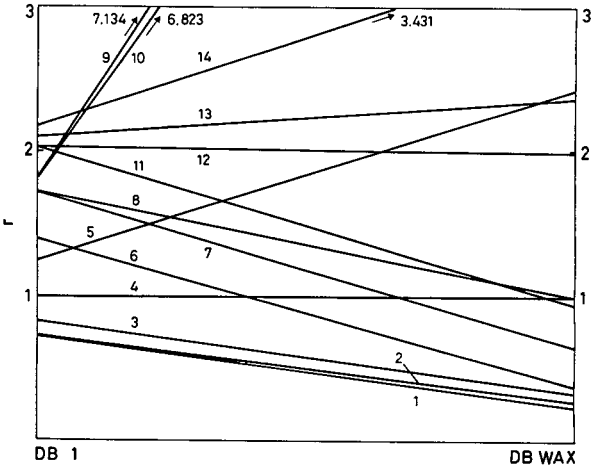

Fig. 1. Retention relative to nitrobenzene, r, at 120°C on non-polar DB-1 and polar DB-WAX capillary columns, showing the change in elution order and of retention times due to polarity. For numbers of compounds, see Table I. r Values at other temperatures are given in Table II.

TABLE II

EXPERIMENTAL GROSS RETENTION TIMES, t_R (min), AND RETENTIONS RELATIVE TO NITROBENZENE, r, IN THREE ISOTHERMAL RUNS ON DB-1 AND DB-WAX COLUMNS

See also Fig. 1 for r values.

Compound[a]	DB-1 column (non polar)						DB-WAX column (polar)					
	60°C		80°C		120°C		100°C		120°C		140°C	
	t_R	r	t_R	r	t_R	r	t_R	r	t_R	r	t_R	r
1	4.254	0.619	2.345	0.653	1.273	0.724	2.687	0.207	1.835	0.236	1.442	0.269
2	4.403	0.645	2.400	0.676	1.273	0.724	2.975	0.239	1.963	0.267	1.522	0.307
3	5.018	0.753	2.655	0.781	1.340	0.829	3.574	0.306	2.226	0.331	1.644	0.366
4	6.424	1	3.188	1	1.450	1	9.804	1	4.976	1	2.971	1
5	8.938	1.441	4.063	1.360	1.607	1.245	26.636	2.875	10.848	2.429	5.380	2.152
6	9.819	1.596	4.464	1.525	1.702	1.393	3.916	0.344	2.399	0.373	1.726	0.405
7	12.874	2.133	5.557	1.975	1.911	1.718	6.530	0.635	3.540	0.651	2.276	0.668
8	13.185	2.187	5.718	2.041	1.911	1.718	9.804	1	4.976	1	2.971	1
9	14.288	2.381	5.841	2.091	1.953	1.783	87.259	9.630	30.188	7:134	12.438	5.525
10	14.512	2.420	5.931	2.129	1.953	1.783	83.048	9.161	28.907	6.823	12.000	5.316
11	15.926	2.668	6.653	2.426	2.111	2.030	9.310	0.945	4.735	0.941	2.847	0.941
12	16.436	2.758	6.744	2.463	2.111	2.030	20.356	2.176	9.051	1.991	4.735	1.843
13	17.404	2.928	7.063	2.595	2.158	2.103	24.545	2.642	10.598	2.368	5.289	2.108
14	18.014	3.035	7.265	2.678	2.191	2.154	42.797	4.676	14.969	3.431	6.610	2.739

[a] See Table I.

TABLE III

PTGC RUNS USED TO EVALUATE THE AVERAGE PERFORMANCE OF THE FOUR CALCULATION METHODS ON DB-1 AND DB-WAX COLUMNS

Initial temperature, θ_0; length of initial isothermal period, t_i, and programming rate, g, are shown.

Column	Programmed run No.	θ_0 (°C)	t_i (min)	g (°C min^{-1})
DB-1	1	45	0	4
	2	45	0	5
	3	50	0	2
	4	50	0	3
	5	60	0	2
	6	70	0	2
	7	45	6	4
	8	50	3	5
	9	50	6	3
	10	60	6	4
	11	70	3	3
DB-WAX	1	45	0	5
	2	60	0	6
	3	45	6	4
	4	50	3	5
	5	70	2	6

methods and of the experimental retention time on non-polar and polar columns for two programmed runs, taken as examples. The parameter showing the performance of each method is the percentage deviation between the experimental, t_R^e, and calculated, t_R^c, values expressed as $E\ (\%) = 100|t_R^e - t_R^c|/t_R^e$. It is not possible to report here the E values for all the compounds of the test mixture obtained with all the programmed runs used and therefore the performance of the four calculation methods is compared by using the E values averaged over the whole set of programmed runs for each compound (Table VI) and over all the fourteen compounds contained in the text mixture for each programmed run listed in Table III (Table VII). The average E values for the DB-1 column are also plotted in Figs. 2 and 3.

The results obtained with the four methods are comparable. The low values show slight negative deviations from the experimental values, whereas high values show smaller but positive deviations. This behaviour, which can be also found in previously published papers [2,7,9,12] in which

TABLE IV

EXAMPLE OF THE VALUES OBTAINED THROUGH DIFFERENT PROGRAMMES COMPARED WITH THE EXPERIMENTAL DATA OBTAINED ON THE DB-1 COLUMN

PTGC parameters: initial temperature, $\theta_0 = 60$°C; initial isothermal period, $t_i = 6$ min; programming rate, $g = 4$°C min^{-1}. Identifying numbers in column 1 refer to Table I.

Compound[a]	Experimental t_R (min)	Said A		Said B		Trapezoid		Simpson	
		t_R (min)	E (%)	t_R (min)	E (%)	t_R (min)	E (%)	t_R (min)	E (%)
1	4.279	4.230	1.15	4.230	1.15	4.230	1.15	4.230	1.15
2	4.430	4.378	1.18	4.378	1.18	4.378	1.18	4.378	1.18
3	5.048	4.988	1.19	4.988	1.19	4.988	1.19	4.988	1.19
4	6.436	6.364	1.11	6.366	1.09	6.362	1.14	6.375	0.95
5	8.344	8.322	0.27	8.331	0.15	8.337	0.08	8.325	0.23
6	8.897	8.889	0.09	8.899	0.02	8.912	0.17	8.925	0.31
7	10.418	10.446	0.26	10.462	0.42	10.462	0.43	10.475	0.55
8	10.571	10.615	0.41	10.629	0.55	10.612	0.39	10.625	0.51
9	10.915	10.934	0.17	10.961	0.42	10.987	0.66	10.975	0.55
10	11.003	11.029	0.23	11.056	0.48	11.062	0.54	11.075	0.65
11	11.598	11.649	0.44	11.673	0.65	11.687	0.77	11.675	0.66
12	11.732	11.782	0.43	11.811	0.67	11.812	0.69	11.825	0.79
13	12.036	12.089	0.44	12.121	0.71	12.112	0.64	12.125	0.74
14	12.220	12.273	0.43	12.308	0.72	12.312	0.76	12.325	0.86

[a] See Table I.

TABLE V

EXAMPLE OF THE VALUES OBTAINED THROUGH DIFFERENT PROGRAMMES COMPARED WITH THE EXPERIMENTAL DATA OBTAINED ON THE DB-WAX COLUMN

PTGC parameters: initial temperature, $\theta_0 = 60°C$; no initial isothermal period; programming rate, $g = 6°C\ min^{-1}$.

Compound[a]	Experimental t_R (min)	Said A		Said B		Trapezoid		Simpson	
		t_R (min)	E (%)	t_R (min)	E (%)	t_R (min)	E (%)	t_R (min)	E (%)
1	5.310	5.207	1.94	5.195	2.17	5.242	1.29	5.250	1.13
2	5.782	5.752	0.52	5.762	0.35	5.792	0.17	5.785	0.02
3	6.475	6.552	1.18	6.593	1.82	6.592	1.80	6.585	1.67
4	10.776	10.755	0.19	10.801	0.23	10.792	0.15	10.785	0.07
5	14.382	14.366	0.11	14.458	0.53	14.458	0.53	14.450	0.47
6	6.954	6.883	1.03	6.923	0.44	6.908	0.66	6.920	0.54
7	9.115	9.077	0.42	9.131	0.18	9.108	0.07	9.120	0.02
8	10.776	10.756	0.19	10.801	0.23	10.792	0.15	10.785	0.07
9	18.312	18.312	0.00	18.296	0.09	18.442	0.71	18.450	0.76
10	18.164	18.161	0.02	18.151	0.07	18.292	0.70	18.285	0.66
11	10.562	10.538	0.23	10.586	0.23	10.592	0.28	10.585	0.20
12	13.609	13.572	0.27	13.640	0.23	13.642	0.24	13.650	0.30
13	14.301	14.223	0.54	14.304	0.02	14.308	0.05	14.320	0.11
14	15.357	15.550	1.28	15.645	1.87	15.675	2.07	15.685	2.12

[a] See Table I.

TABLE VI

VALUES OF E (%) AVERAGED OVER THE PROGRAMMED RUNS LISTED IN TABLE III FOR ALL OF THE COMPOUNDS IN TABLE I, OBTAINED WITH THE FOUR CALCULATION METHODS ON NON-POLAR (DB-1) AND POLAR (DB-WAX) COLUMNS

Compound[a]	Said A		Said B		Trapezoid		Simpson	
	DB-1	DB-WAX	DB-1	DB-WAX	DB-1	DB-WAX	DB-1	DB-WAX
1	0.74	2.87	0.77	2.94	1.08	2.35	1.32	2.31
2	0.79	0.32	0.77	0.32	0.91	0.41	1.00	0.40
3	0.57	1.48	0.68	2.45	0.85	2.23	0.90	2.20
4	0.46	0.32	0.68	0.60	0.84	0.47	0.94	0.46
5	0.24	0.34	0.59	0.80	0.84	0.80	0.86	0.80
6	0.24	1.04	0.65	0.32	0.86	0.53	0.93	0.54
7	0.31	0.40	0.83	0.57	1.02	0.32	1.03	0.29
8	0.44	0.32	0.92	0.60	0.94	0.47	0.91	0.46
9	0.20	0.34	0.85	0.31	0.94	0.87	0.91	0.85
10	0.21	0.35	0.92	0.31	1.00	0.85	0.98	0.85
11	0.39	0.33	0.99	0.62	1.00	0.51	0.99	0.47
12	0.34	0.31	0.99	0.59	1.00	0.58	0.96	0.58
13	0.35	0.41	1.02	0.45	1.03	0.41	1.05	0.46
14	0.36	1.40	1.05	2.32	1.05	2.45	1.17	2.43

[a] See Table I.

different calculation programs were used, therefore do not depend on the computation method but on the choice of the coefficients (A, a and b) of the generally accepted starting eqn. 1. The literature [13,14] suggests that three isothermal runs are sufficient to permit a correct evaluation of these constants. As the same procedure for the calculation of the constants was used as a

TABLE VII

VALUES OF E (%) AVERAGED OVER THE FOURTEEN COMPOUNDS IN TABLE I, OBTAINED WITH THE FOUR CALCULATION METHODS IN THE PROGRAMMED RUNS LISTED IN TABLE III ON NON-POLAR (DB-1) AND POLAR (DB-WAX) COLUMNS

Programmed run No.[a]	Said A		Said B		Trapezoid		Simpson	
	DB-1	DB-WAX	DB-1	DB-WAX	DB-1	DB-WAX	DB-1	DB-WAX
1	0.11	0.81	1.00	1.08	1.17	1.01	1.11	1.02
2	0.47	0.57	1.47	0.60	1.66	0.63	1.67	0.58
3	0.44	1.49	0.83	1.38	0.93	1.18	0.94	1.16
4	0.21	0.56	0.85	1.19	1.07	1.16	1.08	1.14
5	0.37	0.64	0.61	0.71	0.71	0.84	0.89	0.85
6	0.39		0.61		0.72		0.93	
7	0.32		0.79		0.81		0.82	
8	0.61		1.09		1.28		1.28	
9	0.59		0.76		0.76		0.76	
10	0.56		0.67		0.70		0.74	
11	0.36		0.52		0.69		0.73	

[a] See Table III.

starting point for the four calculation methods, in order to avoid introducing a difference in the evaluation of the performance of the four methods, the similar deviations obtained confirm that the problem comes from the basic equation. In fact, a strong reduction in the temperature interval used for each iteration step and therefore an increase in the precision of the approximation do not change substantially the accuracy of the final results. Also, the choice of the three temperatures of the basic isothermal runs influences the values of A and the subsequent calculations, and it was found that the accuracy of the final results increases when the range of the programmed run lies within that of the isothermal runs.

The E values are lower for the non-polar column, but the polar column also shows average

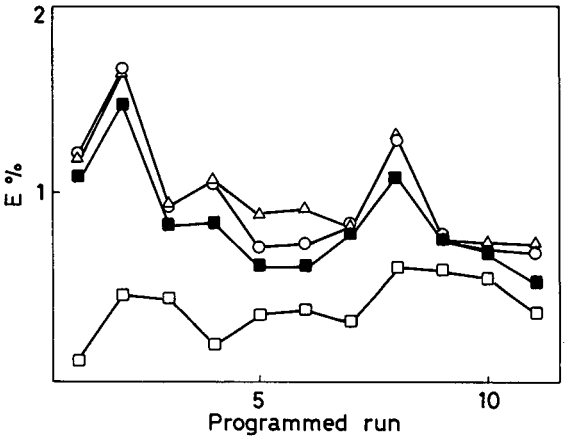

Fig. 2. Values of E averaged over the fourteen compounds in Table I for eleven different programmed runs on the DB-1 column. Methods: □ = Said A; ■ = Said B; ○ = trapezoid; △ = Simpson.

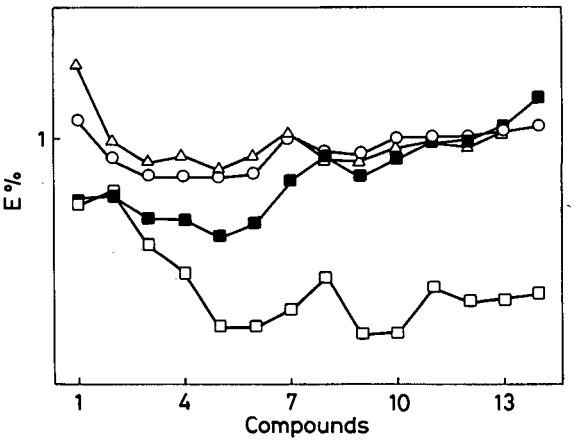

Fig. 3. Values of E averaged over eleven programmed runs on the DB-1 column (see Table III). Methods: □ = Said A; ■ = Said B; ○ = trapezoid; △ = Simpson.

errors smaller than 3%. The scatter of the data does not depend on the type of programmed runs, as no systematic difference connected to the initial temperature, programming rate, etc., is shown by Table VII and Fig. 2. Table VI and Fig. 3, on the other hand, show that early-eluting compounds have a greater influence on the average E values, as affected by a greater uncertainty, probably because the measurement of short t_R comparable to the gas hold-up time is difficult and therefore both the isothermal data used to input the program and the PTGC data measured experimentally are less accurate. This is confirmed by Fig. 4, showing the r^2 values obtained with the equation

$$r^2 = \frac{[\Sigma (t_R^c - \overline{t_R^c})(t_R^e - \overline{t_R^e})]^2}{\Sigma (t_R^c - \overline{t_R^c})^2 \Sigma (t_R^e - \overline{t_R^e})^2}$$

where $\overline{t_R^c}$ and $\overline{t_R^c}$ are the calculated and experimental retention times averaged over the eleven temperature-programmed runs. The value of r^2 is a measure of the best fit between the experimental and calculated values and should be equal to unity for a perfect fit of the values. The results found for the four calculation methods are better than 0.9995 for the compounds eluted after nitrobenzene with gross retention times t_R at the highest isothermal temperature greater than 1.5 and 3 min on the non-polar and polar column, respectively (see Table II). The

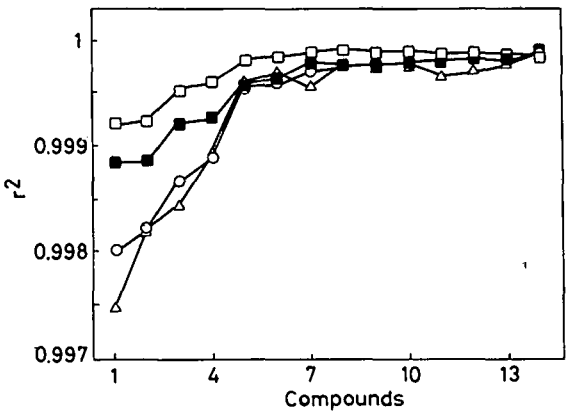

Fig. 4. Values of r^2 as a function of the fourteen compounds in Table I, calculated with the following methods: □ = Said A; ■ = Said B; ○ = trapezoid; △ = Simpson.

results for nitrobenzene and early-eluting peaks show a lower precision, but r^2 values greater than 0.997 indicate a precision high enough for practical purposes.

The computation time necessary to obtain the results with the four programming methods, after the input of the data, was calculated by taking into account the average time required to obtain the calculated retention time of one of the compounds for a given programmed run. This procedure requires $4.6 \cdot 10^{-3}$ s with the Said A, 0.22 s with the Said B, 0.20 s with the trapezoid and 0.13 s with the Simpson method. All these times are so short with respect of the keyboard input time that the use of any of the methods is equivalent from the practical point of view. The complexity and length of the BASIC programs for the four methods are similar.

The Said A method, owing to the simplification due to the choice of a default x value, is more rapid if operated on a personal computer and can also be applied with a simple calculating machine, as it does not require iterative procedures. The iterative methods, moreover, are subject to appreciable fluctuations in the prediction of the early-eluting peaks, as they are more influenced by possible errors in the measurement of short retention times during isothermal runs at high temperature.

The application of the Said B method, *i.e.*, the iterative calculation of the intermediate constants, may fail to give the t_R values in a reasonable computation time if a double precision calculation (with sixteen decimal places) is carried out, because the speed of convergence of the calculation may be too small at this degree of precision. If, by means of a proper adjustment of the program, the convergence was required only to the tenth decimal place, all our experimental data correctly permitted the PTGC t_R to be calculated. This means that, by working with single precision (seven decimal places), convergence of the calculation to the exact values is obtained.

CONCLUSIONS

The prediction of programmed-temperature retention data gives comparable accuracies on

both non-polar and polar capillary columns and for compounds belonging to different homologous series and to many polarity classes.

The comparison of the experimental data with those predicted with the four calculation methods showed that, by using only three isothermal runs as the source of the input data and simple BASIC computer programming, satisfactory accuracy in the prediction of programmed-temperature analyses with various linear speeds and with or without an isothermal period can be obtained. The programming methods are almost equivalent from the point of view of the accuracy and precision of the results, are based on known iterative calculation procedures and can be selected depending on the programming experience of the gas chromatographer, as they do not require sophisticated software.

ACKNOWLEDGEMENT

This work was supported by the Italian Ministry of University and Scientific and Technological Research (MURST).

REFERENCES

1 R.O. Watts and R.G.O. Kekwick, *J. Chromatogr.*, 88 (1974) 165.
2 D.W. Grant and M.G. Hollis, *J. Chromatogr.*, 158 (1978) 3.
3 J. Curvers, J. Rijks, C. Cramers, K. Knauss and P. Larson, *J. High Resolut. Chromatogr. Chromatogr. Commun.*, 8 (1985) 607.
4 E.E. Akporhonor, S. Le Vent and D.R. Taylor, *J. Chromatogr.*, 405 (1987) 67.
5 F. Helaimiam, M. Bourmahraz, H. Sissaoni and M.D. Messadi, *Analusis*, 17 (1989) 596.
6 M. Wernerkenschneider and P. Zinn, *Chromatographia*, 28 (1989) 241.
7 E.E. Akporhonor, S. Le Vent and D.R. Taylor, *J. Chromatogr.*, 463 (1989) 271.
8 J.Y. Zhang, G.M. Wang and R. Qian, *J. Chromatogr.*, 521 (1990) 71.
9 Y. Guan and L. Zhou, *J. Chromatogr.*, 552 (1991) 187.
10 L.H. Wright and J.F. Walling, *J. Chromatogr.*, 540 (1991) 311.
11 Y. Guan, P. Zheng and L. Zhou, *J. High Resolut. Chromatogr.*, 15 (1992) 18.
12 N.H. Snow and H.M. McNair, *J. Chromatogr. Sci.*, 30 (1992) 271.
13 A.S. Said, in P. Sandra (Editor), *Proceedings of the 8th International Symposium on Capillary Chromatography, Riva del Garda, Italy, 1987*, Vol. I, Hüthig, Heidelberg, 1987, p. 85.
14 A.S. Said, in P. Sandra and G. Redant (Editors), *Proceedings of the 10th International Symposium on Capillary Chromatography Riva del Garda, Italy, 1989*, Hüthig, Heidelberg, 1989, p. 163.
15 T.C. Gerbino and C. Castello, in P. Sandra and M.L. Lee (Editors), *Proceedings of the 14th International Symposium on Capillary Chromatography, Baltimore, MD, 1992*, Foundation for the International Symposium on Capillary Chromatography, Miami, FL, 1992, p. 70.
16 R.H. Ewell, J.M. Harrison and L. Berg, *Ind. Eng. Chem.*, 36 (1944) 871.
17 H.W. Habgood and W.E. Harris, *Anal. Chem.*, 32 (1960) 450.
18 W.E. Harris and H.W. Habgood, *Programmed Temperature Gas Chromatography*, Wiley, New York, 1966.
19 F. Ayres, Jr., *Theory and Problems of Differential and Integral Calculus*, Schaum, New York, 1964.
20 C. Caratheodory, *Algebraic Theory of Measure and Integration*, Chelsea Publishing, New York, 1963.
21 E.J. McShane, *Unified Integration*, Academic Press, Orlando, FL, 1983.
22 J.L. Kelley and T.P. Srinmivasan, *Measure and Integral*, Springer, New York, 1988.

Journal of Chromatography, 635 (1993) 113–118
Elsevier Science Publishers B.V., Amsterdam

CHROM. 24 856

Theoretical aspects of chiral separation in capillary electrophoresis

III. Application to β-blockers

Stephen A.C. Wren* and Raymond C. Rowe

Pharmaceutical Department, ICI Pharmaceuticals, Macclesfield SK10 2NA (UK)

(First received August 7th, 1992; revised manuscript received November 6th, 1992)

ABSTRACT

Enantiomers of the β-blockers propranolol, atenolol, metoprolol, and oxprenolol have been separated by the addition of methyl-β-cyclodextrin (MeBCD) to the operating buffer. There is an optimum concentration of MeBCD for separation for each of the β-blockers, the magnitude of which could be ranked by the use of a mathematical model and log *P* data —an indication of the hydrophobicity of the molecule.

INTRODUCTION

Capillary electrophoresis (CE) is a rapidly growing area in the field of separation science. One aspect of current interest is the use of CE to perform chiral separations by the addition of chiral selectors to the buffer. Examples in the literature are: cyclodextrins [1–6], oligosaccharides [7], cyclic ethers [8,9], bile acids [10,11], chiral surfactants [12] and copper complexes using ligand exchange [13]. An alternative approach is to use a cyclodextrin bound in a gel matrix [14] or a capillary which is coated with a cyclodextrin stationary phase [15].

A noteworthy feature of several of the publications is that the degree of separation of the enantiomers is a function of the chiral selector concentration in the buffer. Fanali [2] working with terbutaline and using β-cyclodextrin and di-*o*-methyl-β-cyclodextrin as chiral additives found that while initially resolution increased with increasing cyclodextrin concentration, a point was reached beyond which further increases in concentration actually led to a decrease in resolution. Similarly, Kuhn *et al.* [8] found that the resolution of D- and L-DOPA was dependant upon the concentration of [18]-crown-6 tetracarboxylic acid in the buffer. Initially resolution increased strongly with concentration but then levelled off at a maximum value.

A similar pattern of behaviour was noted by Sepaniak *et al.* [6] who separated dansylated enantiomers of phenylalanine using hydroxy propyl-β-cyclodextrin. In two earlier papers [16,17], these observations were explained by the use of a mathematical model describing the separation process in chiral CE. The model was supported by new work on the separation of the enantiomers of the β-blocker propranolol using β-cyclodextrin and "methyl"-β-cyclodextrin (MeBCD). In this work the mathematical model has been extended further by the application of MeBCD to the separation of the β-blockers

* Corresponding author.

atenolol, metoprolol and oxprenolol and the results compared with those obtained for propranolol.

MODEL

The proposed mathematical model has been fully described in an earlier paper [16]. However it is important, in the context of this study to reiterate the key features.

The model is intended to cover the more simple situations where a freely soluble analyte interacts with a single chiral selector:

$$\begin{array}{ccc} A & \xrightarrow{\mu_1} & B \\ + & & + \\ C & & C \\ \uparrow\downarrow K_1 & & \uparrow\downarrow K_2 \\ AC & \xrightarrow{\mu_2} & BC \end{array}$$

where μ_1 is the electrophoretic mobility of the analyte in free solution, μ_2 is the electrophoretic mobility of the analyte–chiral selector complex and K_1 and K_2 are equilibrium constants. A and B are a pair of enantiomers which have the same electrophoretic mobility in free solution. They interact with a chiral selector C dissolved in the buffer to form the complexes AC and BC, which are assumed to have the same electrophoretic mobility. If the two enantiomers have different affinities for the chiral selector, *i.e.* K_1 and K_2 are different, and the electrophoretic mobilities of the free and complexed enantiomers are different, then chiral resolution is possible. If the exchange of A between the free and bound forms is very rapid then the apparent electrophoretic mobility of A will be a function of the proportion of the time A is free and the proportion it is complexed, *i.e.*,

$$\bar{\mu}_a = \frac{[A]}{([A]+[AC])}\mu_1 + \frac{[AC]}{([A]+[AC])}\mu_2 \qquad (1)$$

Eqn. 1 and a similar expression which describes the apparent electrophoretic mobility of B can be manipulated to produce an equation which describes the difference between the apparent electrophoretic mobilities of A and B, *i.e.*,

$$\Delta\mu_{apparent} = \frac{[C](\mu_1-\mu_2)(K_2-K_1)}{1+[C](K_1+K_2)+K_1K_2[C]^2} \qquad (2)$$

Eqn. 2 is important as it is the difference in apparent electrophoretic mobilities which governs the separation between the two enantiomers.

The optimum concentration (c) of chiral selector is the one which maximises the apparent mobility difference and it can be found from eqn. 2 by the use of differential calculus. It occurs when

$$\frac{d\Delta\mu}{dc} = 0 \qquad (3)$$

It can be shown that in addition to the non useful solutions the condition in eqn. 3 is satisfied when:

$$c = \frac{1}{\sqrt{K_1K_2}} \qquad (4)$$

This is an important result because it predicts that no single chiral selector concentration will be ideal for all separations and that the optimum chiral selector concentration will vary from case to case according to the affinity of the analyte for the chiral selector.

BACKGROUND

The model presented predicts that there will be an optimum concentration of chiral selector and that the concentration will depend inversely upon the affinity of the analyte for the chiral selector. It was decided to check this by using the same chiral selector with a range of chiral analytes. The β-blockers atenolol, oxprenolol and metoprolol (Fig. 1) were selected on the basis of the successful results obtained in earlier work with propranolol which has been included as a comparison. The chiral selector chosen was "methyl"-β-cyclodextrin (MeBCD).

Unfortunately for these systems the values of the equilibrium constants, K_1 and K_2 are not available. Cyclodextrins are believed to act as chiral selectors via inclusion of enantiomers into their hydrophobic cavity. For a series of closely related analytes such as the β-blockers it seems reasonable to assume that the size of the equilibrium constants will be related to the hydrophobicities of the analytes. In this case we would expect the values of the equilibrium constants to correlate with the values of the widely used

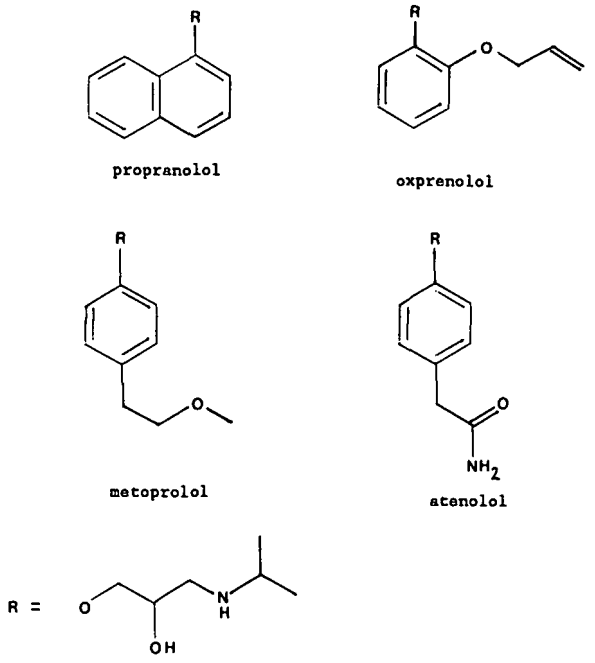

Fig. 1. The β-blockers propranolol, atenolol, metoprolol, and oxprenolol.

hydrophobicity measure, log P (octanol–water partition coefficient).

On the basis of the data in Table I it is to be expected that of the β-blockers, propranolol will have the greatest tendency to include into MeBCD and hence have the largest values of K_1 and K_2. Conversely atenolol should have the least tendency to include and so the smallest values of K_1 and K_2. From this analysis it follows that the optimum concentration of MeBCD will be least for propranolol and greatest for atenolol and will be intermediate for the other two molecules.

TABLE I

HYDROPHOBICITY OF DIFFERENT β-BLOCKERS [18]

β-Blocker	Log P
Atenolol	0.23
Metoprolol	2.15
Oxprenolol	2.18
Propranolol	3.65

EXPERIMENTAL

Work was carried out on a PACE 2100 system (Beckman Instruments, High Wycombe, UK). Using a fused-silica capillary (Beckman) with an internal diameter of 75 μm, a total length of 57 cm and a length of 50 cm from inlet to detector. Samples were loaded by a two-second pressure injection and separated at 25°C using a voltage of 20 kV. Data was recorded at 200 nm using a 2-Hz collection rate. Viscosity was measured using a Bohlin VOR rheometer (Huntingdon, UK). Propranolol and atenolol were manufactured at ICI Pharmaceuticals (Macclesfield, UK) and metoprolol and oxprenolol were obtained from Sigma (Poole, UK). Samples of the β-blockers were dissolved in water at 0.01 mg ml^{-1} except for propranolol which was at 0.05 mg ml^{-1}. MeBCD was a gift from Wacker Chemicals (Halifax, UK) and had the 2,3- and 6-hydroxy groups substituted by methoxy with an average degree of substitution of 1.8. Stock solution of lithium phosphate was prepared by adjusting a 50 mM solution of lithium hydroxide (FSA, Loughborough, UK) to pH 3.0 with orthophosphoric acid (BDH, Poole, UK).

The MeBCD solutions used were all 40 mM in lithium phosphate and were prepared by mixing in the appropriate proportions the following stock solutions: 50 mM lithium phosphate at pH 3.0; 370 mM MeBCD in water; and water. The ten solutions prepared ranged from 0 mM to 74 mM MeBCD and were degassed ultrasonically and filtered through a 0.2 μm filter.

Apparent electrophoretic mobilities were determined by using eqn. 5

$$\mu_{eph} + \mu_{eo} = \frac{lL}{Vt} \quad (5)$$

where l is the length to the detector, L is the total capillary length, V is the operating voltage, t is the migration time and μ_{eph} and μ_{eo} are the electrophoretic and electroosmotic mobilities. The electroosmotic mobility was found to be less than $0.04 \cdot 10^{-4}$ $cm^2/V \cdot s$ and was therefore ignored in the calculations. Duplicate injections of the β-blockers were made at each of the MeBCD concentrations and the average mobility values used. The reproducibility between the duplicates was typically 3% or less.

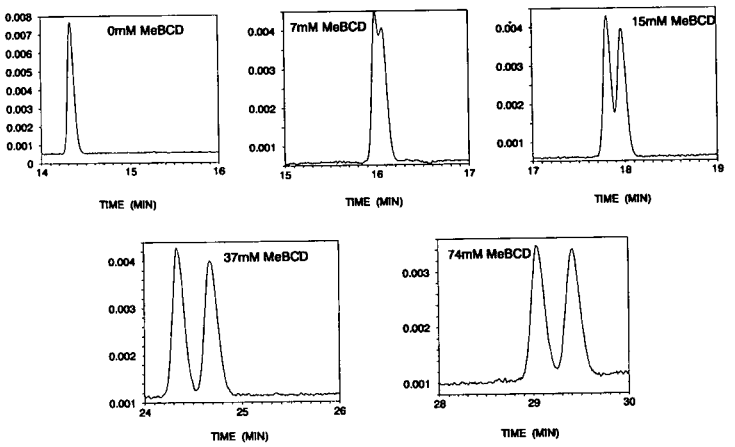

Fig. 2. Separation of atenolol enantiomers at different MeBCD concentrations.

RESULTS AND DISCUSSION

Fig. 2 shows the separation of the enantiomers of atenolol as the concentration of MeBCD is varied. The result is that expected from the theory: separation increases with increasing MeBCD until a maximum at around 37 m*M* MeBCD, with a further increase in MeBCD concentration resulting in a slight decline in separation. The efficiency is unaffected by the concentration of MeBCD with 175 000 theoretical plates being obtained both at 0 m*M* and 37 m*M* MeBCD. This supports the view that the exchange of drug between the free and bound forms is very rapid and does not lead to additional band broadening. In addition this value is between 1 and 2 orders of magnitude greater than that which might be expected from a chiral HPLC separation, indicating great promise for chiral CE.

From Fig. 2 it is clear that the apparent electrophoretic mobility of atenolol decreases with increasing MeBCD concentration. This has two causes: (i) atenolol spends more time as the more slowly moving inclusion complex, and (ii) the buffer viscosity increases with MeBCD concentration. The buffer viscosity affects the electrophoretic mobility of all species and hence the current. Because of this the viscosity affect mentioned in (ii) was compensated for by multiplying the measured apparent electrophoretic mobility, by the ratio of the current at 0 m*M* MeBCD over the current at the MeBCD concentration of interest. The adjustment factor ob-

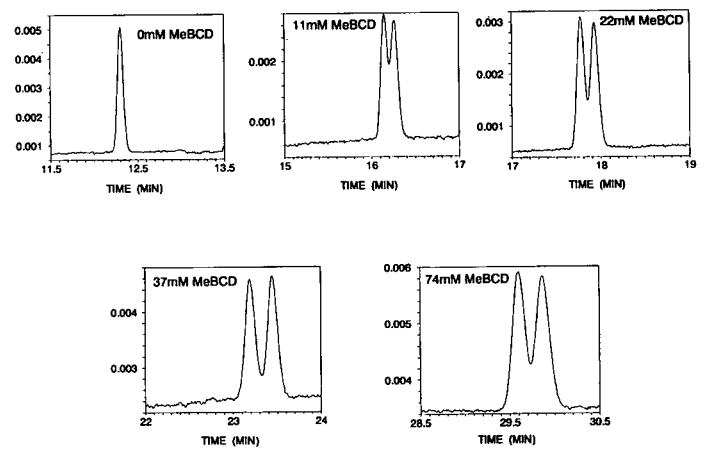

Fig. 3. Separation of oxprenolol enantiomers at different MeBCD concentrations.

tained is in close agreement with the value from the ratio of the absolute viscosities obtained using a rheometer. For example, the buffers containing 75 m*M* MeBCD and 0 m*M* MeBCD had relative viscosities of 1.32 by the current method, in comparison to a value of 1.34 obtained by rheology.

Fig. 3 shows the separations of oxprenolol enantiomers obtained at five of the MeBCD concentrations. The results follow the same pattern as that seen for atenolol and are those expected from the model proposed, with the separation increasing to a maximum at around 37 m*M* MeBCD before declining at higher MeBCD concentrations. The efficiency was again found to be independent of the MeBCD concentration.

The measured apparent electrophoretic mobility differences between the enantiomers as a function of MeBCD concentration are shown for each of the β-blockers in Fig. 4. The figure shows a number of interesting features. The general shape of the curves is the same as that expected from the theory (see ref. 16) and this therefore lends great support to the model proposed. The optimum separation occurs at different MeBCD concentrations for the different β-blockers, with the lowest concentration being required for propranolol and the highest for atenolol. The correlation between the log *P* of the β-blocker and the optimum concentration of MeBCD is that expected from the background discussion with compounds which are most hydrophobic (highest log *P*) requiring the least cyclodextrin. The exception to this general pattern is that of oxprenolol. The affinity of oxprenolol for MeBCD is similar to that of atenolol and is lower than expected. This may well be due to a shape factor with the 2-substituted oxprenolol fitting less well into the MeBCD cavity than the 4-substituted atenolol and metoprolol. Another interesting feature is that the degree of separation of the enantiomers at the optimum MeBCD concentration is different for the different β-blockers. The order of maximum separation is: propranolol > atenolol > oxprenolol > metoprolol with the maximum separation of the propranolol enantiomers being approximately three times greater than the maximum separation of the metoprolol enantiomers. This indicates that the percentage difference between the equilibrium constants K_1 and K_2 is much smaller for metoprolol than for propranolol. This means that for metoprolol the *R* and *S* forms interact with MeBCD to very similar extents, whereas for propranolol the differences are larger. The reason for this is unknown.

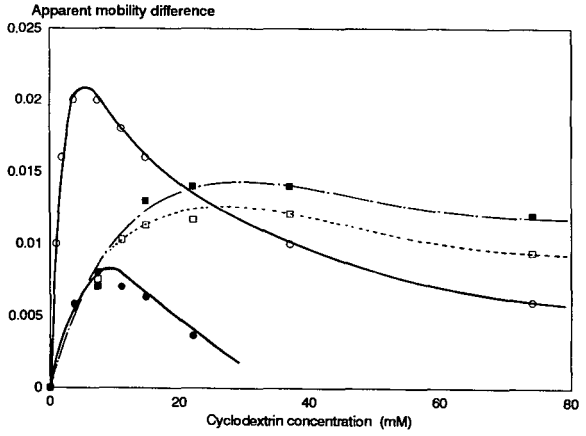

Fig. 4. Experimentally determined apparent mobility difference (10^{-4} $cm^2/V \cdot s$) for the different β-blockers at different MeBCD concentrations. ○ = Propranolol; ■ = atenolol; ● = metoprolol; □ = oxprenolol.

CONCLUSIONS

Chiral separation of the enantiomers of β-blockers using MeBCD has been successfully explained by the use of a mathematical model, which correctly predicts an optimum MeBCD concentration. The size of the optimum MeBCD concentration correlates reasonably well with the log *P* value of the β-blocker although factors such as molecular shape are also very important.

ACKNOWLEDGEMENTS

We wish to thank Allison Clark for typing the document and Doug Bray for making the viscosity measurements.

REFERENCES

1 S. Fanali, *J. Chromatogr.*, 474 (1989) 441.
2 S. Fanali, *J. Chromatogr.*, 545 (1991) 437.
3 G. Persson, S. Palmarsdottir, A. Walhagen and L.E.

Edholm, poster presented at the *15th International Symposium on Column Liquid Chromatography, Basle, June 3–7, 1991.*
4 H. Nishi, T. Fukuyama and S. Terabe, *J. Chromatogr.*, 553 (1991) 503.
5 J. Snopek, H. Soini, M. Novotny, E. Smolkova-Keulmansova and I. Jelinek, *J. Chromatogr.*, 559 (1991) 215.
6 M.J. Sepaniak, R.O. Cole and B. Clarke, *J. Liq. Chromatogr.*, 15 (1992) 1023.
7 A. D'Hulst and N. Verbeke, poster presented at *HPCE 92, 4th International Symposium on High Performance Capillary Electrophoresis, Amsterdam, February 9–13, 1992.*
8 R. Kuhn, F. Stoecklin and F. Erni, *Chromatographia*, 33 (1992) 32.
9 R. Kuhn, T. Bereuter, C. Morin and F. Erni, poster presented at *HPCE 92, 4th International Symposium on High Performance Capillary Electrophoresis, Amsterdam, February 9–13, 1992.*
10 H. Nishi, T. Fukuyama, M. Matsuo and S. Terabe, *J. Microcolumn Sep.*, 1 (1989) 234.
11 R.O. Cole, M. Sepaniak and W.L. Hinze, *J. High Resolut. Chromatogr.*, 13 (1990) 579.
12 K. Otsuka and S. Terabe, *J. Chromatogr.*, 515 (1990) 221.
13 P. Gozel, E. Gassman, H. Michelsen and R.N. Zare, *Anal. Chem.*, 59 (1987) 44.
14 A. Guttman, A. Paulus, A.S. Cohen, N. Grinberg and B.L. Karger, *J. Chromatogr.*, 448 (1988) 41.
15 S. Mayer and V. Schurig, *J. High Resolut. Chromatogr.*, 15 (1992) 129.
16 S.A.C. Wren and R.C. Rowe, *J. Chromatogr.*, 603 (1992) 235.
17 S.A.C. Wren and R.C. Rowe, *J. Chromatogr.*, 609 (1992) 363.
18 J.M. Cruikshank, *Am. Heart J.*, 100 (1980) 160.

Journal of Chromatography, 635 (1993) 119–126
Elsevier Science Publishers B.V., Amsterdam

CHROM. 24 821

Chiral separations by complexation with proteins in capillary zone electrophoresis

Sandra Busch, Johan C. Kraak and Hans Poppe*

Laboratory for Analytical Chemistry, University of Amsterdam, Nieuwe Achtergracht 166, 1018 WV Amsterdam (Netherlands)

(First received November 4th; 1992; revised manuscript received December 22nd, 1992)

ABSTRACT

The direct separation of enantiomeric drugs by capillary zone electrophoresis using proteins as chiral complexing agents in the background electrolyte is described. The influence of protein type and organic modifiers added to the background electrolyte on the resolution of enantiomers was studied. Separations of the enantiomers of tryptophan, benzoin, pindolol, promethazine and warfarin are shown.

INTRODUCTION

Stereochemical effects can be significant for the biological activity of a drug. Racemic drugs exhibit pharmacological activities and/or side-effects different from those of the optically pure drugs [1]. It is therefore important to develop methods for the separation of enantiomers.

A variety of chromatographic approaches, particularly those using high-performance liquid chromatography (HPLC), have been developed [2]. Much work has been reported on the direct resolution of enantiomers by chiral stationary sorbents and a wide variety of these sorbents are now commercially available. These chiral sorbents include the Pirkle type [3], those based on inclusion complex formation with, *e.g.*, cyclodextrin [4] and cellulosic materials [5], ligand exchange [6] and immobilized protein supports [7]. In liquid chromatography, protein-based stationary sorbents have become popular for the direct separation of drug enantiomers because of their broad applicability and the use of aqueous buffered mobile phases that are compatible with many biological samples. The initial immobilized protein HPLC columns for chiral recognition are prepared from bovine serum albumin [8] and α_1-acid glycoprotein (orosomucoid) [9]. Recently, columns based on immobilized human serum albumin [10], conalbumin [11] and some glycoproteins, fungal cellulase [12] and ovomucoid [13], have been used to resolve enantiomers.

Capillary zone electrophoresis (CZE) has been demonstrated to be a highly efficient separation technique suitable for the separation of ionic compounds even with very small differences in migration. However, for stereomers the difference in migration is usually too small to resolve the enantiomers unless specific stereoselective agents are introduced in the running buffer. At present several various chiral complexing agents are available that can be added to the background electrolyte to induce the separation of enantiomers. Enantiomers of drugs could be resolved successfully by the addition of several kinds of cyclodextrins to the buffer system [14–16]. An interesting alternative was demonstrated by Terabe and co-workers [17,18], who separated racemic amino acids using micellar electrokinetic chromatography with chiral surfactants for the formation of micelles. Kuhn *et al.*

* Corresponding author.

0021-9673/93/$06.00

[19] demonstrated the successful separation of racemic compounds using a chiral crown ether as a buffer constituent. Although the above-mentioned enantioselective electromigration methods are suitable for many compounds, we have focused our attention on protein-based separations, primarily because of the general stereoselectivity of enzymes and cell membrane receptors observed *in vivo*. Distinctive features of the various proteins used in this study are shown in Table I. Orosomucoid is an acidic protein with negatively charged groups in the aspartic acid residues and in the terminal serine group, whereas positively charged groups are present in the arginine, lysine and histidine residues. Uncharged, chiral hydrogen bonding sites are present in the peptide chain and in the carbohydrate units that constitute 45% of the molecular mass [23]. The major difference between the ovomucoid and the orosomucoid proteins, apart from the molecular mass, is in their isoelectric points. This is a direct consequence of the higher sialic acid residue content of orosomucoid. Further, the larger number of disulphide bridges contributes to a more rigid structure, which may account for the exceptional stability of the ovomucoid protein [21]. Fungal cellulase is stabilized by twelve disulphide bridges. Fungal cellulase has a low carbohydrate content (6%) in comparison with the other two glycoproteins, ovomucoid (30%) and orosomucoid (45%).

In this paper, we report the preliminary results of an explorative study using the aforementioned types of proteins in the running buffer as chiral selectors for the separation of enantiomers of some test compounds.

EXPERIMENTAL

Instrumentation

Electrophoresis was performed at 25°C in an untreated fused-silica capillary (Polymicro Technologies, Phoenix, AZ, USA) (50.7 cm × 50 μm I.D.). The length from injection to the detection point was 29.8 cm. The UV absorption at different wavelengths was measured with an adapted UV detector (Model 757, Applied Biosystems, Foster City, CA, USA). As a regulated high-voltage power supply, an FUG HCN 35-35000 (FUG Elektronic, Rosenheim, Germany) was used. The total laboratory-built set-up was placed in a Plexiglas box; opening the door automatically shut off the high voltage. The current in the system was measured over a 1-kΩ resistance in the return circuit of the power supply. Samples were injected electrokinetically at constant voltage (10 kV) at the positive side for a fixed period of time (2–5 s). All experiments were carried out with an applied voltage of 10 kV. This voltage was selected to avoid too large a heat production in the capillary with the applied relatively high buffer concentrations. Electropherograms were recorded with a Type BD41 chart recorder (Kipp and Zonen, Delft, Netherlands) at a chart speed of 0.1 mm/s.

Materials

The proteins bovine serum albumin, ovomucoid, orosomucoid fungal cellulase and analytical-reagent grade hydrochloric acid, sodium hydroxide, D,L-tryptophan and warfarin were purchased from Sigma (St. Louis, MO, USA), analytical-reagent grade disodium hydrogenphos-

TABLE I

CHARACTERISTICS OF THE PROTEINS USED AS CHIRAL COMPLEXING AGENTS

Property	Orosomucoid [20]	Ovomucoid [21]	Fungal cellulase [12]	Bovine serum albumin [22]
Molecular mass	41 000	28 800	60 000–70 000	66 000
Isoelectric point	2.7	3.9–4.5	3.9	4.7
Sialic acid residues	14	0.3		
Disulphide bridges	2	8	12	17
Carbohydrate (%)	45	30	6	

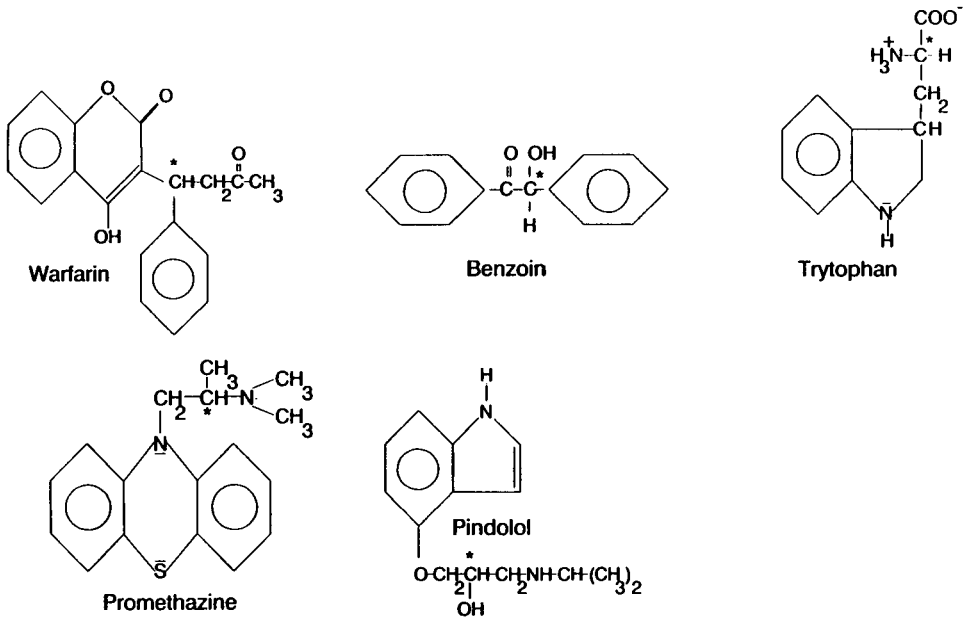

Fig. 1. Structures of the test solutes.

phate, sodium dihydrogenphosphate, ethanol, 1-propanol and benzoin from Merck (Darmstadt, Germany) and N,N-dimethyloctylamine from Aldrich (Milwaukee, WI, USA). The drugs pindolol, promethazine and disopyramide were kindly provided by a local pharmacist. Solute structures are shown in Fig. 1. Distilled water was used to prepare the buffer solutions.

Procedures

The phosphate buffers were 67 mmol/l (pH 7.4), or as given otherwise in the text or figure captions. The buffer was prepared from the two 67 mmol/l solutions in such proportions that the desired pH was obtained. The protein solution was prepared by dissolving the proteins at a given concentration in the phosphate buffer. The two solutions in the two electrode reservoirs were changed after a certain period to avoid changes in pH due to electrolysis of the water. Stock solutions of *ca.* 0.2 mg/ml of all test compounds in phosphate buffer were prepared. Before analysis these stock solutions were diluted in phosphate buffer to give 50 and 100 μmol/l solutions. Tryptophan was available as single enantiomers in this study. Chiral separations were performed using solutions of the racemic amino acid prepared by mixing equal volumes of each enantiomer. The capillary was flushed daily and after a buffer change for 5 min with 1 *M* NaOH and subsequently for 5 min with buffer.

The capacity factor, $\tilde{k}'$, is defined in a similar way to that by Terabe *et al.* [24] for MECC, *i.e.*, using the symbol $\tilde{k}'$ instead of widely accepted k' in order to emphasize the difference in the relationship of the capacity factor to t_R from the well known equation $t_R = t_0(1 + k')$:

$$\tilde{k}' = \frac{t_R - t_0}{t_0\left(1 - \frac{t_R}{t_{Prot}}\right)} \quad (1)$$

For the calculation of the capacity factors the migration time of the drugs in the same buffer without the protein was used as t_0, that of the drug in the buffer system with the protein as t_R and that of the protein in the buffer system without the protein as t_{Prot}. Electroosmotic mobilities in both background electrolytes, with and without the protein, were the same to within 5%. The selectivity factor, α, is equal to $\tilde{k}'_2/\tilde{k}'_1$. The resolution was measured from the electropherograms.

RESULTS AND DISCUSSION

The migration behaviour of the racemic test compounds was investigated with four types of proteins: bovine serum albumin, ovomucoid, orosomucoid and fungal cellulase protein. These four proteins were selected because previous studies, with these proteins immobilized on HPLC sorbents, suggested a broad range of applicability. The separations were performed with electrolyte solutions consisting of only phosphate buffers and organic modifier. The effect of pH, ionic strength and addition of organic modifier (*e.g.*, 1-propanol or dimethyloctylamine) to the running buffer on the resolution of the enantiomers was investigated.

BSA

On the basis of the results of HPLC experiments with native BSA by Sebille and Thaud [25], a 50 μmol/l BSA solution in phosphate buffer was selected. Tryptophan, benzoin and warfarin were taken as test solutes. Under these standard conditions, enantiomeric resolution was observed for tryptophan and benzoin. By addition of a small amount of 1-propanol to the running buffer, resolution of warfarin could also be achieved. The effect of the addition of 1-propanol on $\tilde{k}'$, α, the resolution R_s of the enantiomers and the peak shapes are given in Table II and Fig. 2a–d.

The migration behaviour of tryptophan can be seen in Fig. 2a and Table II. Under standard conditions (1-propanol absent) the enantiomers are well resolved but the L-form shows significant peak tailing. This behaviour might indicate a slow mass transfer between the L-form and the protein or the effect is due to an interaction of the solute with BSA absorbed on the surface of the capillary. However, the latter reason is unlikely in our experiments because the electroosmotic flow with the buffer and buffer + protein is the same. From Fig. 2a it can be seen that the addition of 1-propanol increases significantly the peak shape of the L-enantiomer but the resolution between the two enantiomers decreases. The presence of 1-propanol will decrease the protein binding of the solutes and/or induce a conformational change of the protein.

TABLE II

CAPACITY FACTORS ($\tilde{k}'$), SEPARATION FACTORS (α) AND RESOLUTION (R_s) FOR TRYPTOPHAN, BENZOIN AND WARFARIN

Conditions for tryptophan, benzoin and warfarin as in Fig. 2a, b and c, respectively.

Solute	1-Propanol (%)	$\tilde{k}_1'$ [a]	$\tilde{k}_2'$ [a]	α	R_s
Tryptophan	0	0.03	0.54	14.7	9.1
	3	0.04	0.25	5.7	4.0
	6	0.18	0.28	1.6	3.3
	9	0.29	0.35	1.2	3.1
	12	0.72	0.76	1.1	4.0
Benzoin	0	0.24	0.39	1.6	3.8
	3	0.28	0.54	1.9	4.7
	6	0.18	0.35	2.0	5.6
	9	0.44	0.59	1.3	4.4
	12	0.65	0.73	1.1	3.3
Warfarin	0	7.44	7.44	1.0	0.0
	3	0.32	0.21	1.6	0.7
	6	0.23	0.06	3.5	0.8
	9	0.05	0.05	1.0	0.0
	12	0.02	0.02	1.0	0.0

[a] The $\tilde{k}'$ values given are approximate.

The favourable effect of 1-propanol on the peak shapes is also found with protein-modified packings in HPLC. For tryptophan, 6% 1-propanol seems to be a good choice for resolving the enantiomers.

The results for benzoin are reflected in Fig. 2b and Table II. Under standard conditions the enantiomers of benzoin are completely resolved. With increasing addition of 1-propanol the resolution first increases and then decreases again. The behaviour of the capacity factor with the organic modifier is strange and is not understood. From Fig. 2b it can be seen that 3–6% of 1-propanol is a good composition for resolving the enantiomers of benzoin.

The enantiomers of warfarin could not be resolved under standard conditions. Partial resolution of the enantiomers could be achieved by addition of 3–6% of 1-propanol, as can be seen from Fig. 2c and Table II. At higher modifier concentrations the resolution was lost again. Apart from the organic modifier, the pH and ionic strength of the buffer also might influence the resolution. Lowering of the ionic strength of

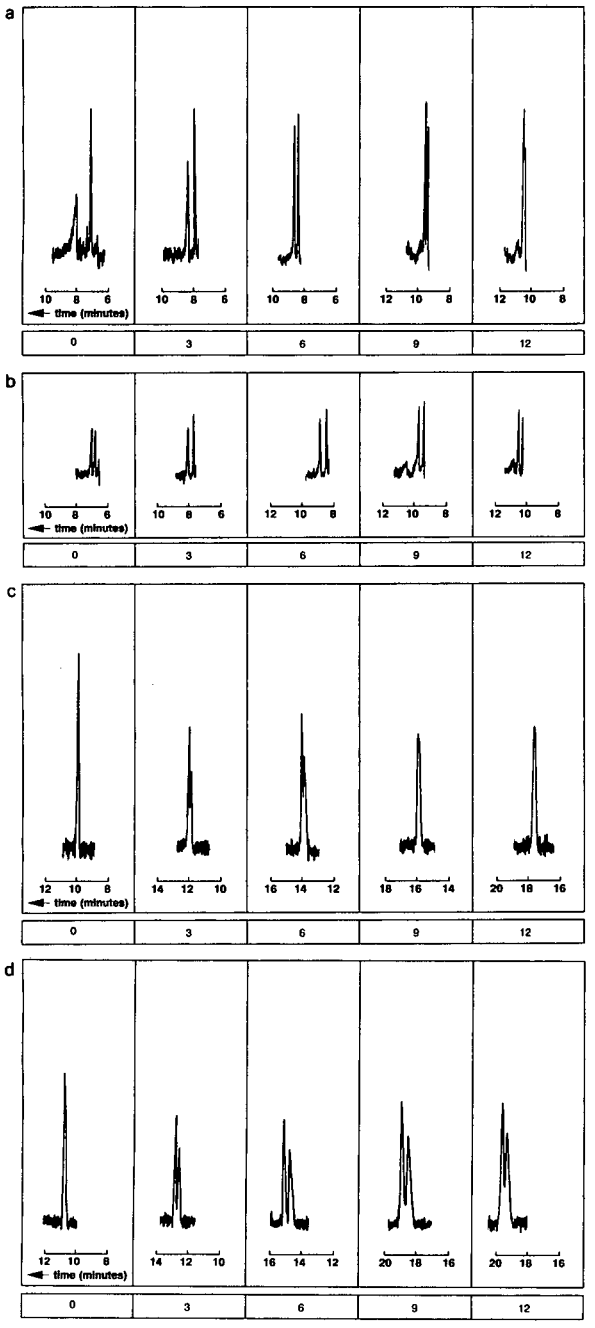

Fig. 2. Electropherograms showing the influence of 1-propanol (% 1-propanol indicated on bottom line of each panel) on chiral separations. (a) D,L-Tryptophan. Conditions: bovine serum albumin solution, 50 μmol/l in phosphate buffer; detection wavelength, 280 nm. (b) (*R,S*)-Benzoin. Detection wavelength, 260 nm. Other conditions as in (a). (c) (*R,S*)-warfarin. Detection wavelength, 315 nm. Other conditions as in (a). (d) (*R,S*)-warfarin. Conditions: bovine serum albumin solution, 50 μmol/l in 50 mmol/l phosphate buffer (pH 6.8); detection wavelength, 315 nm.

the buffer but keeping the pH the same did not improve the resolution. However, a significant improvement in the resolution was gained by lowering the pH of the buffer, as can be seen from Fig. 2c and d. The greatest resolution was again obtained with 6% of 1-propanol.

The separation system with BSA as additive in the running buffer behaves similarly, as expected on the basis of HPLC measurements with immobilized BSA packings. From these studies it became apparent that BSA is suitable for the separation of acidic racemates [21].

Ovomucoid

An interesting protein to be tested was the glycoprotein ovomucoid because we expected from the results obtained with HPLC that the ovomucoid protein might permit the separation of both acidic and basic enantiomers [21]. Several experiments with this protein were carried out by varying the protein concentration in the buffer (5, 15, 50 and 174 μmol/l), the pH (6, 7 and 8) the type and concentration of the modifier (N,N-dimethyloctylamine, methanol, acetonitrile, 1-propanol). However, no separation of the enantiomers of the test components (tryptophan, benzoin, warfarin, propanolol, pindolol and atenolol) could be achieved. A few test solutes showed some interaction with the protein, indicated as a change in migration time and a very broad peak, but changing the pH and modifier did not result in any separation of the enantiomers. In view of the results obtained, the achievements obtained with the ovomucoid protein immobilized on an HPLC sorbent is puzzling. From the results one might conclude that immobilization brings about a change in the (tertiary) structure of the ovomucoid protein that results in an excellent chiral stationary phase for HPLC experiments.

Orosomucoid (AGP)

This glycoprotein is often used for chiral separations in HPLC. This glycoprotein has been shown to be applicable to different types of chiral solutes such as amines, acids and non-proteolytes, which indicates that many different binding groups are present on the protein. It has been demonstrated that the retention and

stereoselectivity on orosomucoid can be varied over a wide range in HPLC by changing the pH of the buffer and the content of charged and uncharged organic compounds [26]. The effects of these changes are highly dependent on the structure of the solute and bear no simple relationship to general properties such as charge or hydrophobicity. In a chiral AGP column, AGP is immobilized on silica particles by a covalent linkage and cross-linking of adjacent protein molecules. Some of the binding groups which are free for interaction in native AGP have been demonstrated to be utilized in the immobilization and cross-linking procedures [23].

The interaction between the solute and the protein was studied by monitoring the effects of 1-propanol and N,N-dimethyloctylamine (DMOA), a cationic additive. The ionic modifiers will influence the coulombic interactions between the protein and the drug. Also, the charged modifier might affect the conformation of the protein and it can compete with the enantiomers for the binding groups on the protein. It has been shown that enantioselectivity can reversibly be induced by organic modifiers [23]. It was suggested that the enantiomers compete with the uncharged modifier for binding to the same site(s) on the protein and that the hydrophobicity and hydrogen-bonding properties are of great importance for the effects on the enantioselectivity. The drugs chosen as test analytes were benzoin, warfarin, pindolol, promethazine and disopyramide. First a 20 μmol/l AGP solution in phosphate buffer was used. Under these standard conditions, resolution was only achieved for promethazine. The electropherogram is shown in Fig. 3. The bad peak shape can be accounted for, at least partly, by the kinetics of the drug–protein interaction. The enantiomers of warfarin are not resolved but elute as a very broad peak. This behaviour indicates that interaction with the protein occurs. In order to improve the separation, different organic modifiers (DMOA and 1-propanol) were added to the running buffer.

Addition of 4.2 mmol/l of DMOA to the running buffer improves the peak shape of promethazine significantly (see Fig. 3) but has no

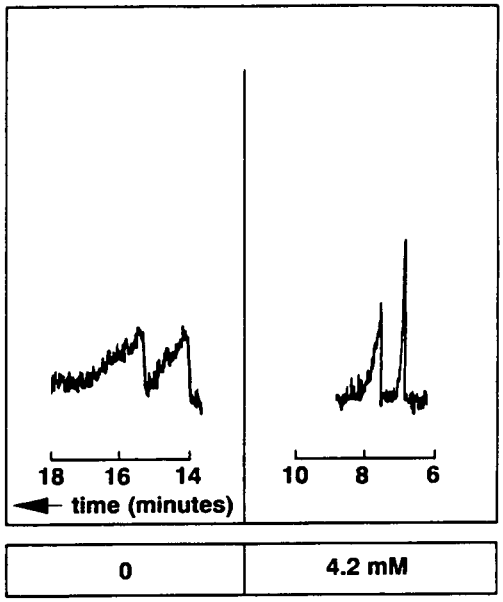

Fig. 3. Electropherograms of (*R*,*S*)-promethazine showing the influence of DMOA (concentration indicated on bottom line) on the chiral separation. Conditions: orosomucoid solution, 21 μmol/l in phosphate buffer; detection wavelength, 260 nm.

effect on the migration behaviour of the other test solutes. This again shows that solutes interact differently with specific sites on the protein.

Addition of 3% of 1-propanol has a negligible effect on the migration behaviour of the test solutes except for warfarin, which elutes as a sharp peak. The improvement of the peak shape of warfarin with 3% of 1-propanol compared with the shape under the standard conditions indicates that the enantiomers can probably be resolved by fine tuning of the organic modifier content or type of modifier. Although the effect of 1-propanol on the resolution of enantiomers with orosomucoid is small, for other types of proteins the effect of 1-propanol can be significant, as is demonstrated for BSA and promethazine in Fig. 4.

Fungal cellulase

Fungal cellulase is a glycoprotein isolated from a culture filtrate of the fungus *Aspergillus niger*. It has been demonstrated that with this (immobilized) protein as a stationary sorbent for chiral HPLC, the enantiomers of acidic and basic

drugs could be resolved [12]. With this glycoprotein as a chiral complexing agent in the running buffer, some explorative experiments were carried out with the same test compounds as used with orosomucoid. Under these standard conditions only the enantiomers of pindolol could be resolved and the separation is shown in Fig. 5.

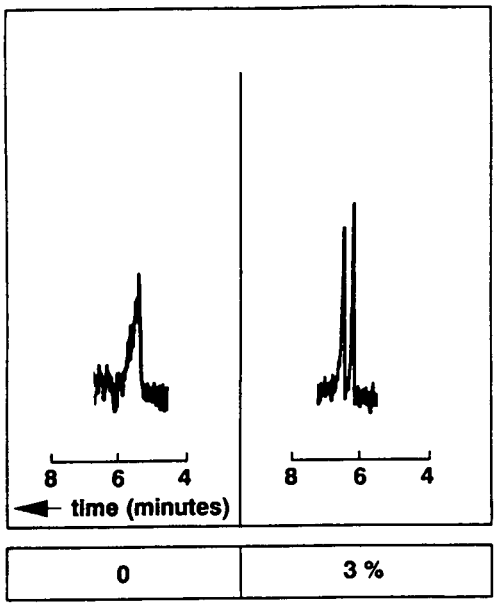

Fig. 4. Electropherograms of (*R,S*)-promethazine showing the influence of 1-propanol (% 1-propanol indicated on bottom line). Conditions: bovine serum albumin solution, 50 μmol/l in phosphate buffer; 3% (v/v) 1-propanol; detection wavelength, 280 nm.

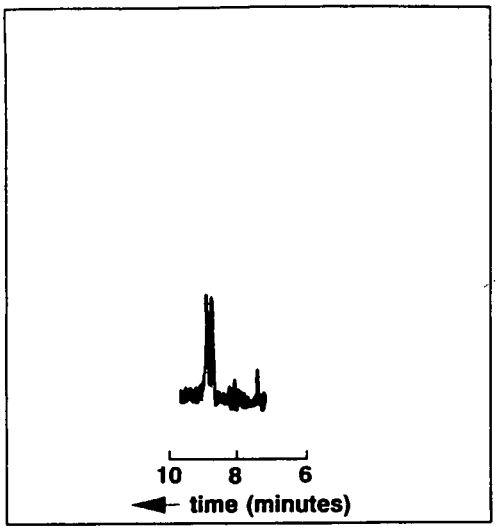

Fig. 5. Electropherograms of (*R,S*)-pindolol. Conditions: fungal cellulase solution, 20 μmol/l in phosphate buffer; detection wavelength, 260 nm.

CONCLUSIONS

From the preliminary experiments it can be concluded that in principle proteins dissolved in the running buffer can be used as chiral complexing agents in capillary zone electrophoresis to induce chiral separations. It is also clear from the above experiments that the enantioselectivity differs with the type of protein, as is known from protein-based packings for HPLC systems. The simplicity of using all types of proteins is a substantial advantage of the CZE technique compared with HPLC, where the immobilization of proteins is laborious. Addition of organic modifiers to the running buffer is sometimes essential to obtain chiral separations. In that respect, addition of compounds that bind specific sites on the protein, *e.g.*, concanavalin A to sugar residues, will provide valuable information about the chiral recognition.

The results also show clearly that CZE is a very useful one-phase separation technique for studying interactions between (bio)molecules. It can also shed light on possible conformational changes induced in proteins by immobilization procedures.

ACKNOWLEDGEMENT

The authors thank Astra Hässle, Sweden, for financial support.

REFERENCES

1 E.J. Ariens, *Schweiz. Med. Wochenschr.*, 120 (1990) 131.
2 W. Lindner, *Chromatographia*, 24 (1987) 97.
3 W. Pirkle and J. Finn, in J.D. Morrison (Editor), *Asymmetric Synthesis, Vol. 1, Analytical Methods*, Academic Press, New York, 1983, p. 87.
4 D.W. Armstrong, *Anal. Chem.*, 59 (1987) 84A.
5 G. Blaschka, *J. Liq. Chromatogr.*, 9 (1986) 341.
6 V. Davankov, *Adv. Chromatogr.*, 18 (1980) 139.
7 G. Schill, I. Wainer and S. Barkan, *J. Chromatogr.*, 365 (1986) 73.
8 S. Allenmark, *J. Biomed. Biophys. Methods*, 9 (1984) 1.

9 J. Hermansson, *J. Chromatogr.*, 269 (1983) 71.
10 T.A. Noctor, G. Felix and I.W. Wainer, *Chromatographia*, 31 (1991) 55.
11 N. Mano, Y. Oda, T. Miwa, N. Asakawa, Y. Yoshida and T. Sato, *J. Chromatogr.*, 603 (1992) 105.
12 I. Marle, P. Erlandsson, L. Hansson, R. Isaksson, C. Petersson and G. Petersson, *J. Chromatogr.*, 586 (1991) 233.
13 T. Miwa, T. Miyakawa and M. Kayano, *J. Chromatogr.*, 408 (1987) 316.
14 S. Terabe, H. Ozaki, K. Otsuku and T. Amdo, *J. Chromatogr.*, 332 (1985) 211.
15 J. Snopek, H. Soini, M. Novotny, E. Smolkova-Keulemansova and I. Jelinek, *J. Chromatogr.*, 559 (1991) 215.
16 S. Fanali, *J. Chromatogr.*, 545 (1991) 437.
17 K. Otsuka and S. Terabe, *J. Chromatogr.*, 515 (1990) 221.
18 K. Otsuku, J. Kawahara, K. Tatekawa and S. Terabe, *J. Chromatogr.*, 559 (1991) 209.
19 R. Kuhn, F. Stoecklin and F. Erni, *Chromatographia*, 33 (1992) 32.
20 J. Hermansson, *Trends Anal. Chem.*, 8 (1989) 251.
21 K.M. Kirkland, K.L. Nielson and D.A. McCombs, *J. Chromatogr.*, 545 (1991) 43.
22 S. Allenmark, *J. Chromatogr.*, 264 (1983) 63.
23 M. Enquist and J. Hermansson, *J. Chromatogr.*, 519 (1990) 285.
24 S. Terabe, K. Otsuka and T.A. Do, *Anal. Chem.*, 57 (1985) 834.
25 B. Sebille and N. Thaud, *J. Liq. Chromatogr.*, 3 (1980) 299.
26 E. Arvidsson, S.O. Jansson and G. Schill, *J. Chromatogr.*, 591 (1992) 55.

Journal of Chromatography, 635 (1993) 127–131
Elsevier Science Publishers B.V., Amsterdam

CHROM. 24 826

Determination of gold(I) and silver(I) cyanide in ores by capillary zone electrophoresis

Manuel Aguilar, Adriana Farran* and Maria Martínez

Department of Chemical Engineering (ETSEIB–UPC), Diagonal 647, 08028 Barcelona (Spain)

(First received September 11th, 1992; revised manuscript received December 22nd, 1992)

ABSTRACT

Capillary zone electrophoresis (CZE) with on-column UV detection at 214 nm was used to detect and determine gold(I) and silver(I) cyanide complexes in alkaline cyanide solution. Under an applied voltage of 25 kV, dicyanoaurate(I) and dicyanoargentate(I) were separated in less than 6 min. Carbonate buffer was used and the separation of both anions was achieved using an anodic injection and cathodic detection scheme. The method was applied to the determination of gold and silver cyanide in ore samples. Quantitative analysis was possible and good agreement between CZE and atomic absorption spectrometric results was obtained.

INTRODUCTION

The recovery of gold and silver from ores is accomplished almost exclusively by cyanidation, which involves leaching of the crushed ore with an alkaline solution of sodium or potassium cyanide. In this process, precious metals and a number of base metals are converted into their soluble cyano complexes.

For many years, the determination of precious metals in ores has been accomplished by a wide variety of analytical methods, *e.g.*, flame and electrothermal atomic absorption spectrometry [1,2], inductively coupled plasma atomic emission spectrometry [3], X-ray fluorescence [4] and neutron activation analysis [5]. The main disadvantages of these methods are their inability to differentiate between oxidation states of the same element, the occurrence of spectral interferences, the complexity of preparation of samples and the insufficient sensitivity.

Chromatographic techniques, however, do not suffer from most of these disadvantages. For this reason some methods, which involve the conversion of precious metals into their anionic chloro or cyano complexes, have been developed either using ion chromatography [6,7] or reversed-phase ion-interaction chromatography [8–10] with conductimetric or spectrophotometric detection.

An important factor in assessing the suitability of a method for monitoring the concentration of precious metals in the leach solution, which typically consists of a mixture of cyanide complexes in excess of cyanide, is the separation between the base metals and the precious metals. This separation is achieved for the gold(I) cyano complex by using the mentioned chromatographic techniques, but some problems arise in the determination of the silver(I) complex [8].

An alternative approach to this problem is to use capillary zone electrophoresis (CZE), in which a narrow band of the sample is introduced into a capillary and subjected to electrokinetic separation. Previous results indicated that CZE is a powerful tool for the separation of many

* Corresponding author.

0021-9673/93/$06.00

compounds, from small ions to biomacromolecules [11].

In this paper, the separation and determination of silver(I) and gold(I) cyano complexes by CZE in solutions containing high concentrations of free cyanide ion is described. The results were applied to the determination of individual metal cyanides in ores.

EXPERIMENTAL

Instrumentation

An ISCO (Lincoln, NE, USA) Model 3850 integrated capillary electrophoresis system equipped with an untreated fused-silica capillary (64 cm × 50 μm I.D.) was used for the separation. Detection was carried out by on-column measurement of UV absorption at 214 nm at a position 34 cm from the cathode. Peak areas were measured by a Spectra-Physics (San Jose, CA, USA) SP-4270 integrator. The sample was introduced into the system by a split-flow manual injector (ISCO) using an HPLC-type syringe.

For the injection conditions adopted in this work, by using a total volume injected from the syringe of 5 μl, the volume of sample loaded into the capillary was 4.6 nl.

A Philips PW 1404 X-ray fluorescence spectrometer was used, with a rhodium X-ray tube operated at 60 kV and 50 mA, an LiF crystal and scintillation detection.

A Perkin-Elmer Model 2380 absorption spectrometer was used to determine the metal content in the aqueous phase by atomic absorption spectrometry (AAS).

Reagents

Stock standard solutions of metal cyano complexes were prepared by dissolution of an accurately weighed amount of the complexes in a 0.01 *M* solution of alkaline sodium cyanide, followed by dilution as required. Analytical-reagent grade potassium dicyanoaurate(I) and potassium dicyanoargentate(I) were obtained from Johnson Matthey Chemicals (Karlsruhe, Germany).

Aqueous cyanide solutions containing gold(I) and silver(I) cyanide complexes were examined qualitatively by UV spectrophotometry over a range of free cyanide concentration between 0 and 0.1 *M*. The UV spectra obtained revealed the presence of only a single gold and silver cyanide complex [$Au(CN)_2^-$ and $Ag(CN)_2^-$] in the aqueous phase, independent of the free cyanide concentration.

Sodium hydrogencarbonate, disodium tetraborate, sodium dihydrogenphosphate, sodium hydroxide from Merck (Darmstadt, Germany), ammonium chloride from Panreac (Barcelona, Spain) and water deionized with a Milli-Q system (Millipore) were used to prepare different buffers. The electrolyte and sample solutions were filtered through a 0.45-μm membrane filter from Lida (Kenosha, WI, USA) and were degassed by ultrasonication.

Procedure for electrophoresis

The capillary tube was filled with a buffer solution by a syringe purge that flushed the entire capillary in a few seconds, and both ends of the tube were dipped into electrode solutions. The sample was introduced into the system by a syringe and a high voltage was applied.

The typical CZE configuration was used, in which the sample is injected at the anode, the detector is placed near the cathode and the electroosmotic flow is from the anode to the cathode [12].

Sample preparation

All experiments were carried out by shaking mechanically in special stoppered glass tubes at 20°C. Two samples of approximately 5 g of each crushed ore were leached with 10 ml of an alkaline solution of 0.01 *M* NaCN for 100 h, which was sufficient to achieve complete recovery from the ores.

After phase separation with a high-speed centrifuge, leach solution was injected directly into the CZE system.

RESULTS AND DISCUSSION

Separation

In a CZE system, the main factors affecting the quality of separation are the buffer composition, the pH and the applied voltage [13,14].

In this work, four different buffers were tested

TABLE I

COMPARISON OF MIGRATION TIMES, NUMBER OF THEORETICAL PLATES AND RESOLUTION AMONG FOUR BUFFER SOLUTIONS AT A CONSTANT CONCENTRATION OF 0.01 *M* AND pH 9.6 AND AN APPLIED VOLTAGE OF 25 kV

Buffer solution	t_m (min)		N	R_s
	$Ag(CN)_2^-$	$Au(CN)_2^-$		
Ammonium	7.3	8.8	34 000	2.2
Phosphate	7.6	8.6	280 000	5.1
Borate	7.2	8.4	210 000	5.4
Carbonate	5.3	5.8	430 000	5.4

for the separation of the Au(I) and Ag(I) cyano complexes. The results obtained are given in Table I, where N was calculated at $16t_m^2w^{-2}$ as in liquid chromatography, where t_m and w are the migration time and the peak width, respectively. The resolution (R_s) was calculated as $2(t_{m_2} - t_{m_1})(w_1 + w_2)^{-1}$, where the subscripts 1 and 2 represent the $Ag(CN)_2^-$ and $Au(CN)_2^-$ peaks, respectively. From these results it can be seen that the best separation, *e.g.*, higher values of the number of theoretical plates (N) and resolution (R_s), in the shortest analysis time (t_m), was obtained by the carbonate buffer. The pH was 9.6 to maintain the free cyanide ion.

From this point, the influence of applied voltage on the separation was studied by using 0.01 *M* carbonate buffer at pH 9.6. As good results (Table II) were obtained for the five voltages tested, an applied voltage of 25 kV, which gave a complete separation of the two cyano complexes in less than 6 min, was chosen. The values of the electroosmotic flow for each voltage are also shown in Table II.

TABLE II

COMPARISON OF MIGRATION TIMES AT DIFFERENT APPLIED VOLTAGES USING 0.01 *M* CARBONATE BUFFER AT pH 9.6

Voltage (kV)	t_m (min)		Electroosmotic flow (10^{-4} cm^2 V^{-1} s^{-1})
	$Ag(CN)_2^-$	$Au(CN)_2^-$	
10	13.8	15.4	4.8
15	9.1	6.7	5.0
20	6.7	7.5	5.7
25	5.3	5.8	7.4
30	4.2	4.7	7.9

Using the selected experimental conditions, the electropherogram in Fig. 1 was obtained, which seems to indicate that $Ag(CN)_2^-$ and $Au(CN)_2^-$ migrate in this order toward the cathode, well separated from each other.

In order to understand the elution order, it has to take into account that the electrophoretic mobility depends on the charge, shape and size of the analyte.

Au(I) and Ag(I) cyano complexes are linear, singly charged anions [$Au(CN)_2^-$, $Ag(CN)_2^-$], so the only difference is in their anionic volume. The elution order can be rationalized by the fact that $Au(CN)_2^-$ seems to be a poorly hydrated anion compared with $Ag(CN)_2^-$ [15]. This difference was ascribed by Nyholm [16] to the large s–p separation energy for gold(I). Hence this lowest hydration will reduce the size of the moving ion. This size reduction may result in greater electrophoretic migration and, accordingly, retardation.

Quantification

Detection limits were calculated as the amount of sample equivalent to a signal due to the analyte equal to three times the standard deviation of a series of ten replicate measurements of

Fig. 1. Electropherogram of a mixture of $Ag(CN)_2^-$ and $Au(CN)_2^-$ standards in excess of cyanide. Capillary fused-silica column (64 cm × 50 μm I.D.); carbonate buffer, 0.01 *M* (pH 9.6); applied voltage, 25 kV; injection volume, 4.6 nl; sample amount, 80 pg Ag and 65 pg Au. Peak assignment: 1 = $Ag(CN)_2^-$; 2 = $Au(CN)_2^-$.

a reagent blank signal [17]. The results obtained were 13 pg for Au and 16 pg for Ag, which correspond to 2.82 and 3.48 pg/nl, respectively.

The relative standard deviation for ten replicate injections of 164 pg of gold and silver, as the dicyanoaurate(I) and the dicyanoargentate(I) complexes, were 6.6% and 4.0% respectively.

The two samples provided good linearity in the concentration range 20–250 pg. The equations of the straight lines obtained by linear regression were $A = -297.6 + 98.1C$ ($r = 0.995$) for Au and $A = -13.5 + 61.8C$ ($r = 0.995$) for Ag, where A is the peak area and C the sample amount in pg.

Application to ore samples

On the basis of the results obtained for the dicyanoaurate(I) and the dicyanoargenatate(I) standards, the application of the CZE method to the determination of gold and silver in ore samples was attempted. Two samples from two different sources, a gold mine of Bolivia and a silver mine of Spain, were analysed.

First, these samples were qualitatively analysed by X-ray fluorescence in order to determine their majority elements. The elements found in the Bolivian sample were Al, Si, P, S, K, Ca, Mn, Fe, Ni, Cu, Zn, As, Sr, Zr, Ba and Pb, the predominant components being Si and Fe. The elements found in the Spanish sample were Al, Si, P, S, K, Ca, Mn, Fe, Ti, Cu, Zn, As, Sb, Zr, Ba and Pb, the predominant components being Si, P, S, K, Fe, As, Ba and Pb.

One interesting observation is that X-ray fluorescence does not have sufficient sensitivity to detect the presence of Au or Ag in the samples. On the other hand, it can be observed that there are some elements capable of forming cyano complexes, *i.e.*, Ag, Au, Cu, Fe, Mn and Zn [8], so after the sample treatment the leach solutions will consist on a mixture of metal cyano complexes in excess of cyanide.

In order to determine gold and silver in the samples, the leach solutions were injected directly into the CZE system and the electropherograms in Fig. 2 were obtained. It can be seen that for the Bolivian sample only one peak, which corresponds to the gold(I) cyano complex, was obtained, and that for the Spanish sample

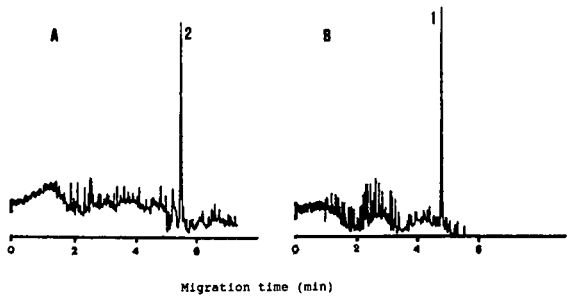

Fig. 2. Electropherograms of leach solutions of (A) Bolivian and (B) Spanish ore. Experimental conditions as in Fig. 1.

the peak obtained corresponds to the silver(I) complex. Further, no other signal corresponding to the base metal cyano complexes was observed.

In order to understand these results, it has to be borne in mind that the different complexes have different negative charges. The Au(I) and Ag(I) cyano complexes have one negative charge, whereas the other cyano complexes have between two and four negative charges. The ionic mobilities of these highly negatively charged metal cyanides would be greater than the electroosmotic flow, so to detect them it would be necessary to inverse the polarity of the power supply [18].

From the electropherograms in Fig. 2, the gold and silver contents in the two samples were determined. The results are given in Table III together with those obtained for the same leach solutions using AAS. Excellent agreement between the two methods was obtained. As AAS gives the total metal concentration for each

TABLE III

COMPARISON BETWEEN THE RESULTS OBTAINED FOR THE SAME LEACH SOLUTIONS USING CZE AND AAS

The results are given as averages for duplicate samples in mg metal/kg ore.

Ore sample	CZE		AAS	
	Au	Ag	Au	Ag
Bolivian	29.90	ND[a]	28.26	ND
Spanish	ND	39.80	ND	41.92

[a] ND = Not determined.

element, this agreement signifies that all the Au and Ag present in the sample are in form of dicyano complexes, and that no other cyano complex of these metals was formed under the experimental conditions used.

CONCLUSIONS

The CZE method developed allows the rapid separation of Au(I) and Ag(I) cyano complexes in leach solutions from ore samples. The leach solutions obtained from the leaching can be introduced directly into the CZE system, without further treatment.

A major advantage of this method over spectrometric methods is its ability to monitor individual precious metal cyanide species. It has the advantage over chromatographic procedures of no interference from the base metals and also the separation of the silver(I) complex.

Further studies are being directed towards the determination and separation of metal cyano complexes, which are commonly present in cyanide leach solutions together with gold and silver complexes, such as zinc, iron and copper complexes, by CZE.

ACKNOWLEDGEMENT

Financial support provided by the CICYT (Project No. NAT-1089), Ministry of Science and Education of Spain, is gratefully acknowledged.

REFERENCES

1 T. Groenewald, *Anal. Chem.*, 40 (1968) 863–866.
2 R.R. Brooks, J. Holzbecher, D.E. Ryan, H.F. Zhang and A.K. Chatterjee, *At. Spectrosc.*, 2 (1981) 151–154.
3 R.B. Wemyss and R.H. Scott, *Anal. Chem.*, 50 (1978) 1694–1697.
4 R.J. Coombes and A. Chow, *Talanta*, 26 (1979) 991–998.
5 E.L. Hoffman, A.J. Naldrett, J.C. Van Loon, R.G.V. Hancock and A. Manson, *Anal. Chim. Acta*, 102 (1978) 157–166.
6 C. Pohlandt, *S. Afr. J. Chem.*, 38 (1985) 110–114.
7 R.D. Rocklin, *Anal. Chem.*, 56 (1984) 1959–1962.
8 D.F. Hilton and P.R. Haddad, *J. Chromatogr.*, 361 (1986) 141–150.
9 B. Grigorova, S.A. Wright and M. Josephson, *J. Chromatogr.*, 410 (1987) 419–426.
10 P.R. Haddad and N.E. Rochester, *Anal. Chem.*, 60 (1988) 536–540.
11 W.G. Kuhr, *Anal. Chem.*, 62 (1990) 403R–414R.
12 J.W. Jorgenson and K.D. Lukacs, *Anal. Chem.*, 53 (1981) 1298–1302.
13 J.W. Jorgenson, in J.W. Jorgenson and M. Phillips (Editors), *New Directions in Electrophoretic Methods* (*ACS Symposium Series*, No. 335), American Chemical Society, Washington, DC, 1987, 182–198.
14 R. Wallingford and A. Ewing, *Adv. Chromatogr.*, 29 (1989) 1–76.
15 H.M.N.H. Irving and A.D. Damodaran, *Anal. Chim. Acta*, 53 (1971) 267–275.
16 R.S. Nyholm, *Proc. Chem. Soc.*, (1961) 273.
17 Analytical Methods Committee, *Analyst*, 112 (1987) 199–204.
18 M. Aguilar, X. Huang and R.N. Zare, *J. Chromatogr.*, 480 (1989) 427–431.

Journal of Chromatography, 635 (1993) 132–136
Elsevier Science Publishers B.V., Amsterdam

CHROM. 24 908

Short Communication

Estimation of inter-detector lag in multi-detection gel permeation chromatography

Ambuj D. Sagar*, Susan J. Sofia and Edward W. Merrill

Department of Chemical Engineering, Massachusetts Institute of Technology, Cambridge, MA 02139 (USA)

(First received October 1st, 1992; revised manuscript received January 13th, 1993)

ABSTRACT

An analytical method for estimating the lag between concentration and molecular-mass-sensitive detectors has been developed. This method is simple in its approach and does not require any knowledge about the molecular mass distribution of the polymer sample used in the analysis. The elution behavior results obtained using the lag value from this method correlate well with those obtained from the traditional gel permeation chromatography peak calibration method.

INTRODUCTION

In recent years, the use of multiple detectors for gel permeation chromatography (GPC) has become more common. Probably the two most common detectors coupled with the traditional differential refractive index (DRI) detector are the differential viscometric (DV) detector and the light scattering (LS) detector. An advantage of coupling either or both of these detectors to the DRI (or some other concentration sensitive) detector is the ability to identify the molecular mass of a polymer in each elution volume increment. However, accurate determination of these absolute molecular masses requires a precise estimation of the inter-detector lag such that the concentration and LS or DV signals corresponding to any elution slice are correlated correctly. Several methods for estimating this lag have been reported in the literature [1–5] that are based on a variety of experimental techniques or analyses. We present here a different method for estimating the detector lag between a concentration detector and a second detector in which the signal is dependent on the molecular mass of a polymer sample. This straightforward method is analytical in its approach and does not require any knowledge about the molecular mass distribution (MWD) of the polymer sample used in the analysis.

THEORY

In GPC, the elution volume of a polymer molecule depends on its hydrodynamic size, not its mass. In most cases, the sample injected in GPC contains molecules of the same class, *e.g.*, linear, star, comb, so that the sizes of molecular species increase as the molecular masses increase. Thus, in general, increasing elution volumes correlate with decreasing molecular masses

* Corresponding author.

0021-9673/93/$06.00

(exceptions being non-homogeneous samples, such as those containing mixtures of both linear and branched polymer molecules). In a multi-detection GPC run, one signal (*e.g.*, DRI) depends only upon the concentration of the solute molecules, while the molecular-mass-dependent signal (LS or DV) is a function of both the concentrations as well as the molecular masses of these eluting molecules. Therefore with increasing elution volumes, the molecular-mass-dependent signal will generally peak before the concentration signal because of the constantly decreasing contribution of the molecular masses of the eluting solute molecules. Consequently, the peaks corresponding to these two signals would be offset even if the two detectors were at the same position in the flow system. In reality, different detectors are at different positions in the flow system which leads to a lag between their signals.

Light scattering detector

If we consider the case of the LS detector, we have the signal measured from any elution slice as being proportional to the excess Rayleigh ratio, R_θ

$$R_\theta = Kc[MP(\theta) - 2A_2cM^2P^2(\theta)] \quad (1)$$

where c is the concentration of the polymer of molecular mass M in that elution slice, and A_2 is the corresponding second virial coefficient. $P(\theta) = 1 - 2\mu^2\langle r_g^2\rangle/3! + \ldots$ is commonly termed as the structure factor (where $\mu = (4\pi/\lambda)\sin(\theta/2)$, λ being the wavelength of the incident light, and r_g the radius of gyration) and K is an optical constant.

In a GPC experiment, realistic upper estimates for the concentration are approximately 10^{-4}–10^{-5} g/ml at the peak of the concentration chromatogram, and generally $A_2 = 10^{-3}$–10^{-4} mol ml/g^2. As a result, the A_2 term in eqn. 1 can usually be neglected for GPC–LS calculations. Therefore, for our purposes, eqn. 1 can be written as:

$$R_\theta = KcMP(\theta) \quad (1a)$$

(although this simplification does not have an effect on the final outcome of our analysis).

For further simplifying the analysis, we would like to set $P(\theta) \approx 1$. If $P(\theta) \neq 1$, then the analysis becomes slightly more complex since $P(\theta)$ is a function of r_g, and r_g, in turn, varies with the elution volume. For a low-angle laser light scattering (LALLS) detector, since θ is small, $P(\theta) \approx 1$ in any case. For a multiple-angle laser light scattering (MALLS) detector, $P(\theta) \neq 1$ for higher-angle detectors unless $r_g \ll \lambda$ (*i.e.*, the scattering molecules are small). However, it is preferable, if possible, to use LS signals from a higher-angle detector (such as 90°, for example) since they are less susceptible to noise due to extraneous scatterers. Therefore, when this analysis is applied to MALLS detectors, the preferred strategy is to use higher-angle LS signals from scatterers small enough such that $P(\theta) \approx 1$.

With the assumption of $P(\theta) \approx 1$, the dependence of the LS signal on the elution volume, v, can be written as:

$$\frac{dR_\theta}{dv} = \frac{\partial R_\theta}{\partial c}\cdot\frac{dc}{dv} + \frac{\partial R_\theta}{\partial M}\cdot\frac{dM}{dv} \quad (2)$$

From eqn. 1a, we obtain

$$\frac{\partial R_\theta}{\partial c} = KM \quad (3a)$$

and

$$\frac{\partial R_\theta}{\partial M} = Kc \quad (3b)$$

The elution dependence of polymer molecules from GPC columns can generally be written as an equation of the general form:

$$\log M = B - Dv \quad (4)$$

Hence,

$$\frac{dM}{dv} = -2.303D\cdot 10^{B-Dv} = -2.303DM \quad (5)$$

The concentration peak occurs at $dc/dv = 0$, while the LS peak occurs at $dR_\theta/dv = 0$.

From eqn. 2, we see that for $dR_\theta/dv = 0$,

$$\frac{\partial R_\theta}{\partial c}\cdot\frac{dc}{dv} = -\frac{\partial R_\theta}{\partial M}\cdot\frac{dM}{dv}$$

$$\Rightarrow KM\frac{dc}{dv} = -Kc\frac{dM}{dv} \quad (6)$$

Using eqn. 5, we rewrite the above condition as:

$$\left[\frac{dc}{dv}\right]_{dR_\theta/dv=0} = 2.303Dc \quad (7)$$

Since all quantities on the right-hand side of eqn. 7 are finite (even though small), we can conclude that under practical GPC conditions, $dc/dv \neq 0$ when $dR_\theta/dv = 0$ (unless the sample is perfectly monodisperse). Thus the peaks of the concentration and the LS chromatograms generally cannot be matched to get the detector lag since they both do not represent the same elution slice.

Given all this, in order to find the inter-detector lag, we need to find the elution slice on the concentration chromatogram that should correspond to a known slice on the LS chromatogram. We choose, as our reference slice, the peak of the LS signal. Referring to eqn. 7, we see that the elution slice corresponding to $dR_\theta/dv = 0$ is the slice on the concentration curve (at elution volume v^*) where

$$\frac{1}{c}\cdot\frac{dc}{dv} = 2.303D \quad (7a)$$

The quantity on the left-hand side is easily evaluated by fitting the peak portion of the concentration chromatogram with a smooth curve, and then calculating the fractional slope as a function of elution volume. The offset between the peaks of the concentration and the LS signals is given by $v_{\text{peak concentration}} - v^*$. The inter-detector lag then is the difference between the $v_{\text{peak LS}}$ and v^* for the data *as it is received by the collection instrument* (since $v_{\text{peak LS}}$ and v^* would coincide if there was no lag).

Once the concentration and LS chromatograms have been obtained for the sample being utilized in the lag estimation procedure, a value for D (the slope of the log molecular mass *vs.* elution volume curve for this polymer–column combination) is required. It is possible to determine the true value of D independently from a traditional GPC calibration procedure, such as the peak calibration method [6]; this true value of D should directly yield, in one step, the correct detector lag using eqn. 7a. However, the availability of the true value of D is not a requirement; some reasonable estimate of D can be used as an initial value in an iterative procedure. The first calculation yields a first estimate of the detector lag. At this point, the GPC–LS calculations should be carried out for the sample with this value of detector lag. These calculations will yield an estimated molecular mass *vs.* elution volume plot for this sample. The slope of this plot should be entered as the next estimate for D in a new iteration of the above procedure to yield another detector lag value and hence another apparent molecular mass *vs.* elution volume plot. These iterations should be carried out until the detector lag converges to a constant value. With this value, the slope of the molecular mass *vs.* elution volume plot is the true D for this polymer–column combination. The final convergence value does not depend on the initial estimate of D. It should be noted here that this iterative procedure is more cumbersome given the necessity of careful evaluations of D from the sample data.

Differential viscometry detector

In a viscometric detector, the signal being measured is the pressure drop of the fluid as it flows through a capillary tube. This pressure drop is proportional to the viscosity, η, of the fluid. For polymer solutions, the intrinsic viscosity, $[\eta]$, is evaluated by the equation:

$$\frac{\ln\left(\frac{\eta_s}{\eta_o}\right)}{c} = [\eta] + k''[\eta]^2 c \quad (8)$$

where the subscript "o" refers to the solvent, and "s" refers to solution containing the polymer at concentration c, k'' is referred to as the Kraemer constant. For low concentrations (typical in GPC experiments), $k''[\eta]^2 c \ll [\eta]$. Therefore, the pressure drop measurement, p, of any elution slice allows the evaluation of the intrinsic viscosity of that slice through the relationship:

$$[\eta] = \frac{1}{c}\ln\frac{p}{p_o} \quad (9)$$

This intrinsic viscosity is dependent upon the polymer molecular mass as $[\eta] = K'M^\alpha$, where K' and α are the Mark–Houwink constants for a polymer. Substituting for $[\eta]$ from the Mark–Houwink equation and rearranging:

$$\ln\frac{p}{p_o} = cK'M^\alpha \quad (10)$$

Differentiating, we get

$$\frac{d\left(\ln \frac{p}{p_o}\right)}{dv} = K'c \frac{d(M^\alpha)}{dv} + K'M^\alpha \frac{dc}{dv} \quad (11)$$

Substituting from eqn. 4 and setting $d(\ln p/p_o)/dv = 0$,

$$K'M^\alpha \frac{dc}{dv} = -K'c \frac{d(10^{\alpha(B-Dv)})}{dv}$$

$$= 2.303D\alpha K'c(10^{\alpha(B-Dv)}) \quad (12)$$

Thus the elution slice on the concentration curve corresponding to $d(\ln p/p_o)/dv = 0$ is given by:

$$\frac{1}{c} \cdot \frac{dc}{dv} = 2.303D\alpha \quad (13)$$

The detector lag can then be evaluated in a method similar to that mentioned in the *Light scattering detector* section. However, in this analysis, the constant α needs to be pre-determined in order to carry out the calculations. One could either use a polymer sample for which α is available in the literature, or use narrow standards of the polymer to determine α from intrinsic viscosity experiments.

EXPERIMENTAL

Experiments were carried out on the DAWN-F (Wyatt Technologies, Santa Barbara, CA, USA) MALLS detector ($\lambda = 6328$ Å) coupled to a 150-C (Waters, Milford, MA, USA) GPC system. The chromatography was carried out using a combination of Waters Ultrahydrogel 500 and 2000 columns, with a guard column, at 25°C. The mobile phase was water (containing 0.02% NaN_3 as a bacteriostat) with a flow-rate of 0.92 ml/min. The analyses were performed using LOTUS 1-2-3 (Lotus, Cambridge, MA, USA) and the ASTRA program provided with the DAWN-F. Curve fitting was carried out with MICROSOFT EXCEL (Microsoft, Redmond, WA, USA). Polymers utilized in the studies were narrow-MWD polyethylene oxide (PEO) standards, molecular masses ranging approximately from 50 000 to 900 000 (Toyo Soda, Japan), and a broad-MWD PEO sample, nominal molecular mass 200 000 (Polysciences, Warrington, PA, USA). The detector lag estimation analyses were carried out on the DRI signals from narrow-MWD PEO samples of molecular mass less than 100 000. The $v_{peak\ LS}$ for each sample was evaluated from the 90° LS detector signal. The resulting mean value of the detector lag was then used in subsequent molecular mass calculations with the GPC–LS data.

RESULTS AND DISCUSSION

The analyses on the low-molecular-mass polymer samples yielded an estimated detector lag of 0.124 ± 0.009 ml. The elution behavior of a number of different PEO samples was then obtained using the mean value of the detector lag in the molecular mass calculations. The elution behavior, thus obtained, for the broad- and narrow-MWD PEO samples overlapped, as they should. Fig. 1 shows the data for the elution dependence of the broad-MWD sample.

As pointed out elsewhere [2], the slope of the elution curve is sensitive to the inter-detector lag. Too high a value of detector lag leads to an artificially flat elution curve, while too low a value leads to too steep a curve. (This is especially noticeable for narrow-MWD samples, since changing the value of the detector lag leads to significant changes in the polymer concentration assigned to any elution slice. Calculations

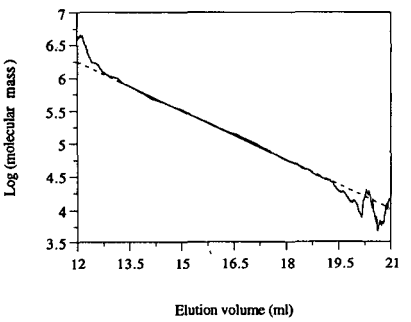

Fig. 1. Data showing elution behavior of broad-MWD PEO sample calculated from GPC–LS data with the detector lag value obtained by this method (rough line) and reference elution curve from traditional peak calibration method using narrow-MWD PEO samples (smooth line). The reference elution curve is extrapolated for clarity (dashed line).

for broad-MWD samples are generally less susceptible to this problem since their concentration chromatograms are spread out.) Therefore, we can use the slope of the elution curve as the parameter to ascertain the accuracy of our method. For this purpose, the absolute reference elution curve was obtained from a traditional GPC peak calibration method using only the DRI detector with narrow-MWD standards (of the same polymer as the samples used for the analysis). Shown in Fig. 1 is the elution dependence (linear over the evaluation range) corresponding to such a GPC peak calibration method using the narrow-MWD PEO standards. Examination of Fig. 1 shows that the elution curve obtained by using the estimated detector lag correlates well with the peak calibration data. Since the detector lag obtained by our analysis yields (from the GPC–LS data) an elution curve for a polymer–column combination that agrees with the reference curve, the value of the lag must be correct.

The methods described by Balke *et al.* [4] and Kuo *et al.* [5] determine the inter-detector lag (for GPC–LS and GPC–DV systems, respectively) by comparison with reference data obtained from calibration with narrow-MWD standards. In a sense, the philosophical underpinnings of our one-step method (*i.e.* utilizing the slope from a reference curve directly for the calculation of the inter-detector lag) are similar to these methods, the major difference being that they obtain the inter-detector lag through an empirical approach, while we use an analytical one. On the other hand, our iterative method, though not as simple, obviates the necessity of the reference data for obtaining the inter-detector lag.

Some points should be noted here: (1) It is easier to carry out the lag estimation with reasonably narrow-MWD samples since they provide high dc/dv values. However, broad-distribution samples are also utilizable, as long as the peak slices can be easily identified. If the iterative procedure is being followed, the intermediate estimates of D (from the sample data) must be evaluated carefully since the data range is small. (2) The calculation for the offset of the two peaks are carried out on the concentration curve. Generally concentration detectors have a less noisy signal than molecular-mass-sensitive detectors since the former are not affected by very small concentrations of large contaminants (mainly dust). Still, the calculations of the fractional slope must be accurate, since the accuracy of the method directly depends on this quantity. (3) If we use the D value from a previous iteration in the next iteration of the analysis, the effects of column dispersion do not bias our values. This is consistent with the fact that one cannot expect the detector lag to be a function of the column efficiency. (4) Since the method described here utilizes GPC columns in-line, both the concentration- and molecular-mass-dependent signals have lower noise by virtue of the columns eliminating most extraneous scatterers in the flow field (particularly important for aqueous systems) as well as suppressing the pressure fluctuations due to the pump. (5) This analysis assumes the elution curve to be linear over the elution volume range under consideration. Generally, this should hold, especially for narrow-MWD samples, but if this linearity condition does not hold, the analysis would need to be modified if it is to be utilized.

ACKNOWLEDGEMENTS

We would like to thank Rohin Mhatre for helpful discussions. The financial assistance of the United States Department of Agriculture is gratefully acknowledged.

REFERENCES

1 D. Lecacheux and J. Lesec, *J. Liq. Chromatogr.*, 5 (1982) 2227.
2 T.H. Mourey and S.M. Miller, *J. Liq. Chromatogr.*, 13 (1990) 693.
3 J. Billiani, I. Amtmann, T. Mayr and K. Lederer, *J. Liq. Chromatogr.*, 13 (1990) 2973.
4 S.T. Balke, P. Cheung, R. Lew and T.H. Mourey, *J. Appl. Polym. Sci. Appl. Polym. Symp.*, 48 (1991) 259.
5 C.-Y. Kuo, T. Provder, M.E. Koehler and A.F. Kah, in T. Provder (Editor), *Detection and Data Analysis in Size Exclusion Chromatography* (*ACS Symposium Series*, No. 352), American Chemical Society, Washington, DC, 1987, p. 130.
6 W.W. Yau, J.J. Kirkland and D.D. Bly, *Modern Size-Exclusion Liquid Chromatography: Practice of Gel Permeation and Gel Filtration Chromatography*, Wiley, New York, 1979.

Journal of Chromatography, 635 (1993) 137–142
Elsevier Science Publishers B.V., Amsterdam

CHROM. 24 872

Short Communication

Multichannel coulometric detection coupled with liquid chromatography for determination of phenolic esters in honey

Elisabeth Joerg and Gerhard Sontag*

Institute for Analytical Chemistry, University of Vienna, Waehringer Strasse 38, A-1090 Vienna (Austria)

(First received October 9th, 1992; revised manuscript received January 12th, 1993)

ABSTRACT

A method for the determination of phenolic esters in different varieties of honey was developed. The substances were separated by RP-HPLC. A coulometric electrode-array system with sixteen electrodes arranged in series and set at increasing potentials (300–900 mV) was used for electrochemical detection of the compounds. Chromatographic peaks for methyl 4-hydroxybenzoate, methyl vanillate, methyl syringate, *trans-p*-methyl coumarate and *trans*-methyl ferulate were identified. The content of the esters varied between 1.3 and 5044 μg per kg of honey with detection limits of 0.1–1.0 μg per kg of honey ($S/N = 3$). The method described is a sensitive assay to differentiate between rape honey and other varieties.

INTRODUCTION

Honey is a well-known and popular foodstuff. Because consumers attach more and more importance to high quality and great variety, reliable methods for its analysis are required. Attention has been focused on investigations to find ingredients that characterize individual types of honey. Among them are phenolic acids [1–11], which occur in trace amounts. Esters of phenolic acids have also been found [5,7,12,13]. Up to now mainly GC and GC–MS methods have been employed for the determination of these compounds in honey.

Since most phenolic compounds are oxidized at easily accessible potentials, electrochemical detection can serve as a highly sensitive tool for their quantification after separation by HPLC. As yet it has only been applied to the determination of the distribution pattern of phenolic acids in different varieties of honey [10,11]. These investigations distinguished between blossom honey, honeydew honey and chestnut honey, but it was not possible to differentiate between rape and robinia honey, two types of blossom honey. The objective of the research described in this paper was the determination of phenolic esters in different varieties of honey using reversed-phase chromatography coupled with a coulometric electrode-array detection system.

EXPERIMENTAL

Apparatus

For single-cell detection a Gynkotek pump

* Corresponding author.

0021-9673/93/$06.00

(Model 300C) was coupled with a Rheodyne injection valve (Model 7125, sample loop: 100 μl), a Bio-Rad RoSiL C_{18} HL (25 cm × 4.6 mm I.D., particle size 5 μm) column and an ESA analytical cell (Model 5011). An ESA coulochem 5100 was used as the controlling and measuring unit. The response of the detection cell was recorded by a Sekonic SS-250-F recorder (Fig. 1). For all the other chromatographic experiments an ESA coulochem electrode-array system was employed, consisting of two HPLC pumps (Model 420) and a multichannel detector with sixteen coulometric electrodes and their electronic control and measuring unit. Chromatographic separation was performed on a Bio-Rad RoSiL C_{18} HL column (25 cm × 4.6 mm I.D., particle size 5 μm). A Rheodyne valve (Model 7125) with a 100-μl sample loop was used for sample injection. Each of the sixteen detector cells consisted of one working electrode made of porous graphite, two platinum counterelectrodes and two reference electrodes of modified palladium. For data processing an Epson Equity 386/25 computer with the appropriate software from ESA was used. The results and the sixteen-channel chromatograms were printed on an Okidata microline 321 printer.

Mobile phase

All chemicals used and not specified were from Merck and of p.a. quality. The mobile phase consisted of 300 ml of methanol, 50 ml of glacial acetic acid and 650 ml of double-distilled water. The pH of the solution was adjusted to 3.0 with an aqueous solution of sodium hydroxide (1 *M*). The mobile phase was filtered through a 0.20-μm membrane.

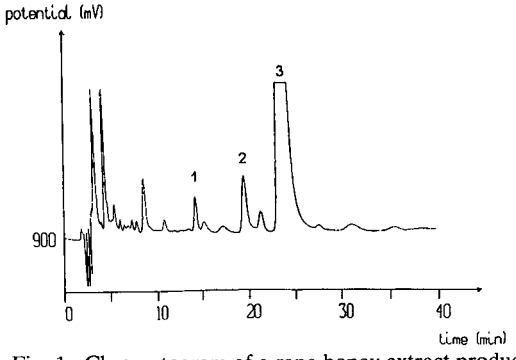

Fig. 1. Chromatogram of a rape honey extract produced by a single detector cell. Full-scale current amounts to 500 nA. Peaks: 1 = methyl 4-hydroxybenzoate; 2 = methyl vanillate; 3 = methyl syringate.

Standards

Stock solutions with a concentration of 25 mg/l methyl 4-hydroxybenzoate, methyl 4-hydroxy-3-methoxybenzoate (methyl vanillate), methyl 4-hydroxy-3,5-dimethoxybenzoate (methyl syringate), *trans*-methyl 4-hydroxycinnamate (*trans-p*-methyl coumarate) and *trans*-methyl 4-hydroxy-3-methoxycinnamate (*trans*-methyl ferulate) were prepared separately in methanol–water (10:90). All chemicals were taken from our own stock. The standard solutions were mixed and further diluted with mobile phase to concentrations between 0.1 μg/l and 1 mg/l. All calibration mixtures were stored in a refrigerator and kept in the dark to prevent light-induced *cis–trans* isomerization.

Chromatographic conditions

The elution of the esters was effected by a flow-rate of 1 ml/min, which resulted in a back-pressure of approximately 180 bar. For single-cell detection a potential of +900 mV was chosen. The sixteen electrodes were set at incrementally (40 mV) increasing potentials, covering a potential range between +300 mV and +900 mV. Temperature in the thermally insulated cell box containing the column, pulse damper, injection loop and coulometric cells was held constant between 31.6 and 31.7°C.

Samples

The types of honey under investigation were commercially available products of chestnut, clover, dandelion, fir, linden blossom, orange blossom, rape, robinia (false acacia) and sunflower honey. All samples were kept in the dark.

Sample preparation

In a beaker 20 g of honey and 18 ml of ethyl acetate (>99%, Fluka) were mixed with a high-speed dispersing apparatus (Ultra-Turrax T-25) and the ethyl acetate phase was decanted. This procedure was repeated three times and all extracts were collected. Then the honey sample

was mixed with diluted hydrochloric acid (4 *M*) until a pH between 1 and 2 was reached. Extraction with 18 ml of ethyl acetate was repeated six times. During the whole procedure the beaker was cooled on ice. The ethyl acetate extracts were combined and concentrated to a volume of about 10 ml using a rotary evaporator and dried over anhydrous sodium sulphate. This procedure was followed by extraction (four times) with 10 ml of sodium hydrogencarbonate solution (5%, w/w) to remove phenolic acids. After drying the ethyl acetate phase over sodium sulphate this solution was evaporated to dryness. The residue was dissolved in 10 ml (in the case of robinia, chestnut, sunflower and orange blossom honey) or in 100 ml of mobile phase (rape, clover, linden blossom, dandelion and fir honey). The solutions were filtered through a 0.2-μm membrane.

Synthetic honey

A mixture of 400 g of D(+)-glucose (Merck) and 400 g of fructose (Apoka) with 200 ml of double-distilled water was prepared. The pH was adjusted to 4.5 with dilute hydrochloric acid (0.01 *M*). Aliquots of 20 g were mixed with 2 ml of the calibration mixture containing all esters in a concentration 0.75 mg/l.

Data analysis

Each substance showing a definite electrochemical behaviour was detected on several adjacent electrodes (channels). Plotting the peak heights (areas) of the substances of interest against the potentials of the channels, peak-shaped hydrodynamic voltammograms were obtained. Chromatographic peaks were identified by retention times as well as the hydrodynamic voltammograms. Peak purity was tested in the following way. The current of the dominant peak (highest response) and the corresponding peaks with the same retention time shown on adjacent channels with lower and higher potentials were measured. The height ratios of the adjacent peaks to the dominant one were calculated. These ratios were compared with the ratios of the standard compounds calculated in the same way. The esters with shorter retention times were quantified by measurement of the recorded chromatographic peak heights. The results of later-eluting esters relied on peak areas. Calibration curves were created each day in a concentration range between 10 and 100 μg/l. The recovery of the overall procedure was determined by analysing three samples of synthetic honey.

RESULTS AND DISCUSSION

Fig. 1 shows a chromatogram of a rape honey extract, which was obtained by single-cell detection at a potential of +900 mV. A preliminary identification of the chromatographic peaks was done by comparing retention times of standard compounds and sample components. However, this detection mode gives only little information about peak purity and allows no reliable peak identification.

Coulometric multielectrode detection and qualitative analysis

The current measured at sixteen electrodes held at different potentials led to several chromatographic peaks for each substance of the honey extracts (Fig. 2). Peak purity could be

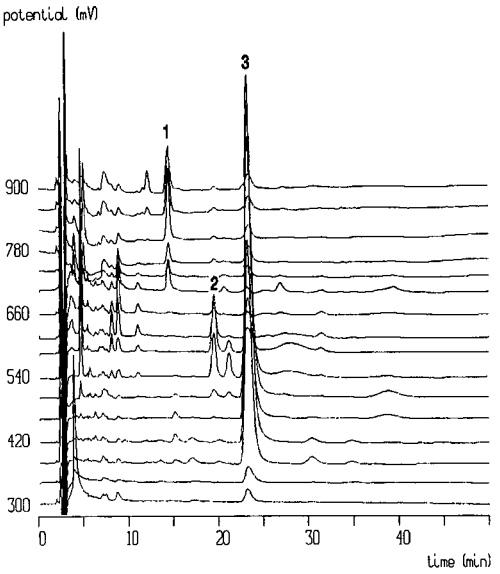

Fig. 2. Chromatograms of a rape honey extract produced by sixteen detector cells. Full-scale current amounts to 500 nA. Peaks: 1 = methyl 4-hydroxybenzoate; 2 = methyl vanillate; 3 = methyl syringate.

TABLE I

CHARACTERISTIC VALUES OF METHYL 4-HYDROXYBENZOATE, METHYL VANILLATE AND METHYL SYRINGATE

	Methyl 4-hydroxybenzoate		Methyl vanillate		Methyl syringate	
	Standard	Honey	Standard	Honey	Standard	Honey
Retention time (min)	14.37	14.38	19.38	19.38	22.28	23.23
Channel of the dominant peak (mV)	+820	+820	+580	+580	+420	+420
Peak-height ratio						
h_{x-1}/h_x	0.305	0.305	0.785	0.772	0.643	0.606
h_{x+1}/h_x	0.803	0.948	0.589	0.602	0.760	0.851

confirmed by calculating the peak-height ratios of the preceding (h_{x-1}) and the following peaks to the dominant peaks (h_x). Table I shows a list of these values. Deviation of the peak-height ratios of sample components from those of standard compounds is due to co-eluted substances. In contrast to single-cell detection, voltammetric characterization of the eluted substances (Fig. 3) could be achieved during one LC–electrochemical detection experiment by plotting the peak heights at definite retention times *versus* the applied potentials of the electrodes (channels). The electrode (channel) potential at which the highest response (dominant peak) is observed corresponds almost exactly to the half-wave potential of the compound. The initial identity assignment by retention times could be confirmed by comparing the channels of the dominant peaks and the shape of the hydrodynamic voltammograms of standard and sample compounds. In this way methyl 4-hydroxybenzoate, methyl vanillate and methyl syringate were identified in rape honey.

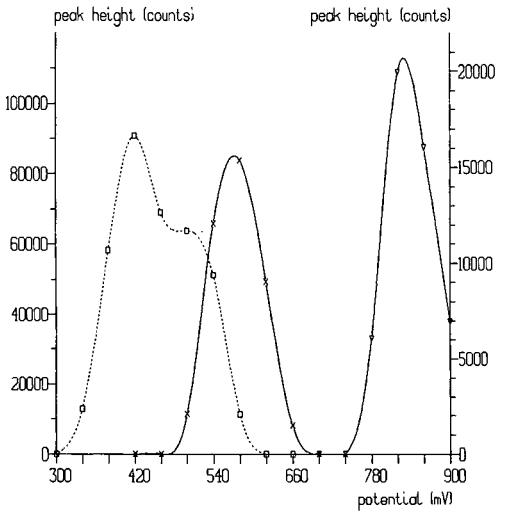

Fig. 3. Hydrodynamic voltammograms of methyl 4-hydroxybenzoate (▽), methyl vanillate (×) and methyl syringate (□) plotted with different sensitivity (left-hand axis: □; right-hand axis: × and ▽).

Quantitative analysis

To three samples of synthetic honey methyl 4-hydroxybenzoate, methyl vanillate, methyl syringate, *trans-p*-methyl coumarate and *trans*-methyl ferulate were added and analysed. The recovery obtained ranged between 65.2 and 79.4% with relative standard deviations between 1.5 and 6.7%.

All these compounds were found in different varieties of honey. In Table II the mean values of three samples of each variety of honey except rape and robinia honey are summarized. The detection limits ranged between 0.1 and 1.0 μg per kg honey (20–200 pg absolute) depending on the retention times of the esters.

Comparing the results of the esters, significant differences between types of honey could be observed. In *robinia honey* only methyl syringate was found, as can be seen in Fig. 4. Methyl 4-hydroxybenzoate and methyl vanillate were near or below the detection limits. *Rape honey* was characterized by its very high concentration of methyl syringate. The amount of this ester in

TABLE II

CONTENT (μg/kg) OF PHENOLIC ESTERS IN HONEY

M4HB = Methyl 4-hydroxybenzoate; MVAN = methyl vanillate; MSYR = methyl syringate; MCOM = *trans-p*-methyl coumarate; MFER = *trans*-methyl ferulate

Variety	M4HB	MVAN	MSYR	MCOM	MFER
Robinia	–	–	281.0	–	–
	–	3.5	93.4	–	–
Rape	177.0	31.3	3865	–	–
	126.2	36.7	4092	–	–
	184.8	237.4	4537	–	–
	167.3	35.2	5044	–	–
Chestnut	18.0	10.9	42.2	–	–
Clover	38.3	11.8	1592	–	–
Linden blossom	7.7	20.2	759.5	–	–
Dandelion	–	11.8	551.5	–	1.3
Sunflower	31.8	8.0	322.7	1.5	2.9
Orange blossom	194.2	18.8	–	–	7.9
Fir	–	14.7	539.5	–	1196

various samples of robinia and rape honey varies naturally, but this did not influence the significant differences. In addition, the content of methyl 4-hydroxybenzoate was higher than in other types except in orange blossom honey. Some small differences were observed between the varieties *chestnut*, *clover*, *dandelion*, *linden blossom*, and *sunflower*, but in this case the results were too few to be significant. The absence of methyl syringate was characteristic of *orange blossom honey*, which also had the highest content of methyl 4-hydroxybenzoate of the varieties analysed. *Fir honey*, the only honeydew honey under investigation, contained a similarly large amount of *trans*-methyl ferulate, whereas this ester was not present or occurred in very low concentration in other types of honey. This made an identification possible.

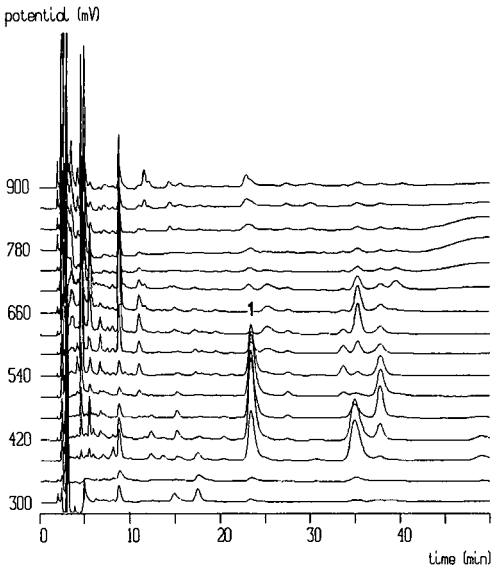

Fig. 4. Chromatograms of a robinia honey extract produced by sixteen detector cells. Full-scale current amounts to 1.5 μA. Peak 1 = methyl syringate.

The results obtained for methyl esters confirm and complement information received from preliminary investigations of phenolic acids in honey [11]. They allowed differentiation between rape honey and robinia honey, which was not possible by analysis of the phenolic acids alone.

CONCLUSION

The coulometric multielectrode detection system provides the trace analyst with another tool for reliable determination of electroactive compounds. This technique can be used to extend the qualitative information without the time-consuming current–potential measurements usually necessary when single-electrode detection is used. A particular advantage is that the optimal detection potential for a compound of

interest is lower than for the detection of the same compound in a single cell. This results in a lower residual current and makes possible very sensitive detection of phenolic esters. In subsequent investigations the selectivity of this detection mode will be evaluated by analysing samples of environmental importance and food.

ACKNOWLEDGEMENTS

We thank the "Fonds zur Förderung der wissenschaftlichen Forschung" (P-8308) and the "Hochschuljubiläumsstiftung der Stadt Wien" for supporting this project.

REFERENCES

1 E. Cremer and M. Riedmann, *Z. Naturforsch. B*, 19 (1964) 76–77.
2 E. Cremer and M. Riedmann, *Z. Anal. Chem.*, 212 (1965) 31–37.
3 E. Cremer and M. Riedmann, *Monatsh. Chem.*, 96 (1984) 364–368.
4 K. Speer and A. Montag, *Dtsch. Lebensm.-Rundsch.*, 80 (1984) 103–105.
5 K. Speer and A. Montag, *Dtsch. Lebensm.-Rundsch.*, 83 (1987) 103–107.
6 E. Steeg and A. Montag, *Z. Lebensm.-Unters.-Forsch.*, 184 (1987) 17–19.
7 E. Steeg and A. Montag, *Dtsch. Lebensm.-Rundsch.*, 84 (1988) 103–108, 147–150.
8 E. Steeg and A. Montag, *Z. Lebensm.-Unters.-Forsch.*, 187 (1987) 115–120.
9 C.E.M. Ferber and H.E. Nursten, *J. Sci. Food Agric.*, 28 (1977) 511–518.
10 E. Joerg, *Thesis*, University of Vienna, Vienna, 1989.
11 E. Joerg and G. Sontag, *Dtsch. Lebensm.-Rundsch.*, 88 (1992) 179–183.
12 M. Wootton, R.A. Edwards, R. Faraji-Haremi and P.J. Williams, *J. Apic. Res.*, 15 (1978) 29.
13 A.D. Graddon, J.D. Morrison and J.F. Smith, *J. Agric. Food Chem.*, 27 (1979) 832–837.

Journal of Chromatography, 635 (1993) 143–150
Elsevier Science Publishers B.V., Amsterdam

CHROM. 24 901

Short Communication

Analysis of phenolic and flavonoid compounds in juice beverages using high-performance liquid chromatography with coulometric array detection

P. Gamache, E. Ryan and I.N. Acworth*

ESA Inc., 45 Wiggins Avenue, Bedford, MA 01730 (USA)

(First received December 7th, 1992; revised manuscript received January 25th, 1993)

ABSTRACT

Analysis of phenolics and flavonoids in juice beverages using reversed-phase HPLC with coulometric array detection is described. Sixteen serial coulometric detectors were used for on-line resolution of co-eluting compounds and generation of voltammetric data. Within each class of compounds, oxidation potential corresponded to specific substitution patterns where: catechol < methoxycatechol < monohydroxyl < methoxyl. Twenty-seven standard compounds were resolved in a 45-min run. The limits of detection were in the low ng/ml range with a linear response range of at least three orders of magnitude. Intra-run retention time variation was <1% (R.S.D.) and adjacent sensor response ratios varied by <5% (R.S.D.). The utility of this technique in generating multivariate data for differentiation of juices and juice mixtures is shown.

INTRODUCTION

Phenolics and flavonoids are common substituents of plant-derived beverages. There is great diversity in the natural occurrence and distribution of these compounds reflecting differences in metabolism and stability. Interest in these metabolites is primarily based on their contribution to such properties as: color (*e.g.* anthocyanins), flavor (*e.g.* flavanone glycosides), fragrance (*e.g.* thymol), nutritional value (*e.g.* antiscorbutic effects), stability (*e.g.* flavanols), therapeutic value (*e.g.* nobiletin), and toxicity (*e.g.* rutin). Changes in these compounds during processing and storage is also important to the quality and safety of commercial food products.

Reversed-phase HPLC with ultraviolet and visible absorbance detection is a common technique for the study of these analytes. Analysis of specific phenolic compounds and profiles of particular classes have been used to examine both source and process-related variability, for example in the detection of fruit juice adulteration [1,2], and in the study of process-related effects on quality [3]. Quantitation and characterization, however, can often be difficult due to sample complexity or if studying these substances at trace levels. HPLC with amperometric electrochemical detection (ED) provides selectivity and sensitivity well suited to the analysis of many of these components in complex matrices [4]. Differences in electroactive substituents on analogous structures can lead to characteristic differences in their voltammetric behavior.

* Corresponding author.

0021-9673/93/$06.00

These properties are thus a basis for selectivity and provide a useful source of qualitative information [5,6].

In our studies we have used a coulometric type flow-through carbon graphite working electrode [7]. This form of highly efficient ED provides mass conversion (oxidation or reduction) of each analyte at its maximum potential. The use of several coulometric sensors in series (coulometric array), maintained at different potentials, provides resolution of co-eluting compounds whose oxidation or reduction potentials differ by as little as 60 mV [8]. This largely extends the resolution capabilities of conventional HPLC–amperometric ED. Also, since the response profile across several electrodes is representative of an analyte's voltammetric properties, useful qualitative information is obtained for several analytes from a single injection. This HPLC coulometric array technique has previously been used for identification and quantitation of phenolic compounds in lemon juice, plant extracts and alcoholic beverages [9] and for the study of process-related changes in reducing substances present in beer [10]. The intent of this paper is to show the applicability of this technique to the study of electroactive substances in fruit juice beverages emphasizing the selective and qualitative characteristics of the array. Analysis of these multi-component HPLC–ED profiles for differentiation of various juice beverages is also addressed.

EXPERIMENTAL

Sample treatment

The samples which were analyzed (*e.g.* apple, orange and grapefruit juice) included: concentrates, fresh squeezed, juice from concentrate, and retail products. Juice from specific varietals and authentic juice samples were generously supplied by the Citrus Research and Education Center, Florida Department of Citrus. Beverage samples were stored at −20°C until preparation on the day of analysis. Concentrates were diluted with deionized water to 11.8° Brix (percentage by mass of apparent solids in a sugar solution determined by the Brix spindle hydrometer). An aliquot (*ca.* 0.5 ml) was centrifuged (10 000 *g*, 4°C, 5 min) and the supernatant was passed through a 0.22-μm filter (Millipore, Bedford, MA, USA) by centrifugation (conditions as above). A 20-μl volume of filtrate was used for analysis by HPLC with coulometric array detection.

Standards

A standard mixture representative of several classes of endogenous electroactive compounds was made using commercially available chemicals. All powders were obtained from Sigma (St. Louis, MO, USA) with the exception of narirutin and tangeritin (Atomergic Chemetals, Farmingdale, NY, USA). Compounds were first dissolved individually at 0.1–1.0 mg/ml in 50% (v/v) aqueous ethanol and stored at −20°C. Aliquots were combined and diluted in 1% (v/v) aqueous methanol to comprise the working standard.

HPLC

Samples were analyzed with a Coulochem Electrode Array System (CEAS, Model 5500; ESA, Bedford, MA, USA) consisting of a Model 460 autoinjector, two Model 420 dual-piston pumps, an M800 high-pressure gradient mixer, and four coulometric array cell modules (each with four working electrodes). A stainless steel 150 mm × 4.6 mm I.D. column, packed with 5-μm M.S. Gel C_{18} (Niko Bioscience, Tokyo, Japan) was used. The column and detector array were housed in a temperature-regulated compartment maintained at 35 ± 0.1°C. System control, data acquisition, and analysis were performed with the CEAS software on an Epson 386 computer. LOTUS 123 (Lotus, Cambridge, MA, USA) and Einsight (Infometrics, Seattle, WA, USA) software were used for data base management and statistical analysis, respectively.

For binary gradient elution, mobile phase A consisted of 0.1 *M* monobasic sodium phosphate containing 10 mg/l sodium dodecyl sulfate (SDS) and adjusted to pH 3.35 with phosphoric acid. Mobile phase B consisted of acetonitrile–0.1 *M* monobasic sodium phosphate containing 50 mg/l SDS–methanol (60:30:10, v/v/v). The pH of this mixture was adjusted to 3.45 with phosphoric

acid. The total flow-rate was maintained at 1.0 ml/min throughout the run. The gradient cycle consisted of an initial 10-min isocratic segment (6% B), a 20-min linear gradient (+1.2% B/min), a 10-min linear gradient (+7% B/min), and a 5-min isocratic segment (100% B) before returning to initial conditions. Samples were injected precisely at 9.0 min after return to initial conditions. The 16 detector array was set from 0 to 900 mV in increments of 60 mV *versus* palladium reference electrodes.

RESULTS AND DISCUSSION

The chromatographic conditions were adapted from HPLC absorbance methods described by Kirksey *et al.* [11] and Rouseff [2] for analysis of a variety of flavonoid compounds (*e.g.* flavanone glycosides, anthocyanins). SDS was included as an ion-pairing reagent for retention of amines. The detectors were configured in an oxidative array to allow voltammetric resolution of compounds based on ease of oxidation across incrementally increasing anodic potentials. Fig. 1 shows a 15-channel chromatogram (channel 16 not shown for clarity) of a 27-component external standard with representative compounds from structural classes including amino acids, coumarins, hydroxybenzoic and cinnamic acids, simple phenolics, purines, in addition to several classes of flavonoids. Analytes were resolved in two dimensions —chromatographic and voltammetric. Each analyte had a specific retention time and a response "signature" across the array. With 60-mV increments between sensors, the majority of response for a single oxidation wave typically occurred across three adjacent sensors. The highest responding sensor was defined as the dominant channel for each analyte while the leading and following channels refer to the adjacent upstream and downstream sensors. Peak comparison by retention time and voltammetric response, measured as ratios between three sensors, was used to increase the confidence in matching sample peaks and external standard peaks.

Table I shows the retention time and dominant oxidation potential for each of these standard compounds. Resolution with the detector array was based on ease of oxidation and may be related to differences in structure where availability of electrons and the capacity for charge stabilization differ (*e.g.* charge delocalization, electron-donating properties). For particular aromatic substituents, a consistent voltammetric relationship was evident both between analyte classes and among analogues. Compounds having catechol groups (caffeic acid, catechin, chlorogenic acid) all responded at lower channels (60

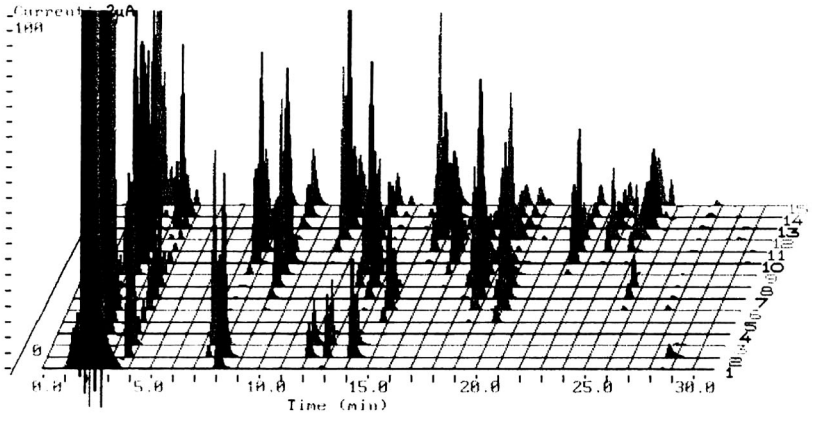

Fig. 1. Fifteen-channel chromatogram of a 27-component standard, 20 μl of a 1 μg/ml solution. Compounds were resolved on the basis of retention time in combination with voltammetric response behavior across the array. Sensor potentials were 0 mV (channel 1) to 840 mV (channel 15) with 60-mV increments (Pd reference). All channels are displayed at 2 μA full scale. See Experimental for further details on analytical conditions and Table I for compound listing, retention times, and dominant oxidation potential.

TABLE I

SUMMARY OF STANDARD MIXTURE

Peak No.	Compound	Retention time (min)	Dominant oxidation potential (mV)	Detection limit (ng/ml)[a]	r^b
1	Ascorbate	1.86	240	200	0.9983
2	Guanine	2.06	540	2	0.9992
3	Tyrosine	2.50	540	1	0.9999
4	Guanosine	3.31	780	2	0.9992
5	Gallic acid	3.65	60	1	0.9992
6	Protocatechuic acid	7.45	120	1	0.9999
7	4-Aminobenzoic acid	7.70	600	2	0.9987
8	Gentisic acid	8.13	60	1	0.9999
9	Tryptophan	9.14	540	2	0.9998
10	4-Hydroxybenzoic acid	11.32	720	1	0.9999
11	Chlorogenic acid	12.12	120	1	0.9939
12	Catechin	12.96	120	1	0.9997
13	4-Hydroxyphenylacetate	130.8	540	1	0.9998
14	Vanillic acid	13.70	420	1	0.9999
15	Caffeic acid	14.12	60	1	0.9967
16	Syringic acid	14.88	300	1	0.9999
17	4-Hydroxycoumarin	15.79	660	3	0.9989
18	Coumaric acid	18.15	540	2	0.9939
19	Syringaldehyde	18.84	360	1	0.9998
20	Umbelliferone	19.09	660	5	0.9995
21	Eugenol	19.70	420	1	0.9992
22	Ferulic acid	20.14	300	1	0.9997
23	Scopoletin	22.53	600	2	0.9998
24	Narirutin	23.90	660	2	0.9996
25	Naringin	24.98	660	3	0.9994
26	7-Methoxycoumarin	25.27	780	25	0.9477
27	Hesperidin	25.83	360	3	0.9993

[a] Signal-to-noise ratio >5, 20 μl injection.

[b] Correlation coefficient obtained from duplicate injections of 1, 2, 10, 20, 50, 100, 250, 500 and 1000 ng/ml standard mixtures.

mV dominant). Differences of greater than 100 mV in dominant oxidation potential were evident among simple phenolics, hydroxycinnamic acids, as well as flavonoids. Within each group, the oxidation potentials followed the order: catechol < methoxycatechol < monohydroxyl < methoxyl. The 60-mV array therefore provided good resolution of analytes on the basis of these substituents. Fig. 2 shows a smaller segment of the standard chromatogram where combined chromatographic and voltammetric resolution are evident for coumaric acid (monohydroxyl), eugenol (methoxycatechol), ferulic acid (methoxycatechol), syringaldehyde (4-hydroxyl, 3,5-dimethoxyl) and umbelliferone (monohydroxyl). Resolution of eugenol and ferulic acid is attributable to resonance delocalization promoting a lower oxidation potential for ferulic acid.

While the flavonoids represent a very diverse class of endogenous plant metabolites, a major aspect of this diversity relates to the pattern of aromatic substituents (*e.g.* alcohol, alkoxyl, carbohydrate) [12]. The flavonoid backbone contains two benzene rings linked by a 3-carbon chain. With several possible oxidizable moieties present (*e.g.* aromatic alcohol and alkoxyl) the voltammetric behavior can be characteristically complex. The voltammetric properties of catechin, hesperidin, and naringin are shown in the hydrodynamic voltammograms (HDV) in Fig. 3.

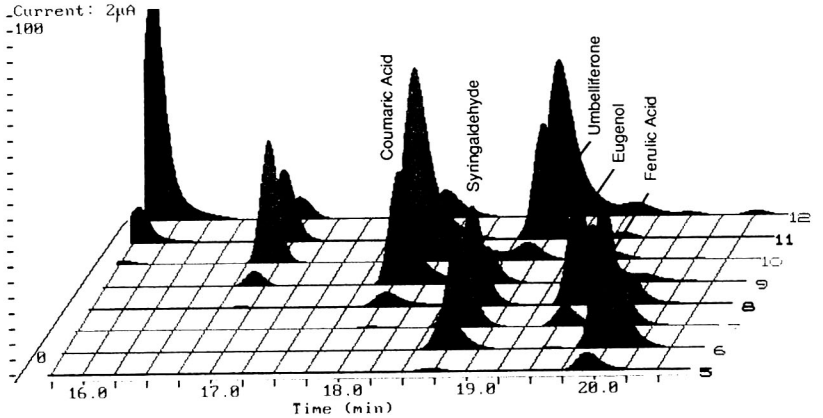

Fig. 2. A smaller time–potential segment of Fig. 1 is shown above. An increasing array of coulometric detectors is used to resolve standard components (20 μl of a 1 μg/ml solution). Detector potentials are 240, 300, 360, 420, 480, 540, 600 and 660 mV (Pd reference). Full scale amplification is 2 μA. See Experimental for further details on analytical conditions.

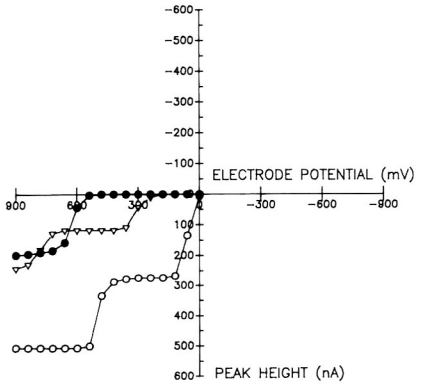

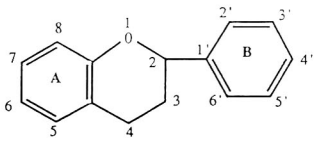

	3	4	5	6	7	3'	4'	5'
Catechin	OH	H	OH	H	OH	OH	OH	H
Naringin	H	=O	OH	H	Rh,Gl	H	OH	H
Hesperidin	H	=O	OH	H	Rh,Gl	OH	OCH_3	H

Rh = Rhamnose, Gl = Glucose

Fig. 3. Summation of peak heights (current) generated across a coulometric array [detector potentials: 0–900 mV, 60-mV increments (Pd reference)] is plotted as a function of electrode potential. Data were obtained under binary gradient conditions as described in Experimental. The characteristic voltammetric behavior of these substituted flavonoids may be used qualitatively (structural identification and peak purity). ○ = Catechin; ● = naringin; ▽ = hesperidin.

The data for these HDVs were generated instantaneously by the array and are represented by plotting the cumulative current across the 16 sensors. The catechol group on the B ring of catechin oxidized at the low potential sensors (0 to 120 mV) with voltammetric response behavior analogous to the simple catechol, caffeic acid. The lower oxidation wave of hesperidin may be attributed to the methoxycatechol group on the B ring similar to the simple methoxycatechol compound, eugenol. The voltammetric response of naringin (single B ring hydroxyl) likewise, resembled *p*-coumaric acid. The second oxidation waves of catechin and hesperidin are likely related to the A ring substituents. Qualitative examination of these "signatures" provided a means of examining peak purity for known compounds as well as an indication of the possible substitution pattern for unknowns.

Juice analysis

A 16-channel chromatogram of an orange juice filtrate is shown in Fig. 4. More than 300 electroactive components were typically resolved in this sample type. Automatic gain ranging with the CEAS allowed measurement of components over a wide range of concentrations (low ng/ml to high μg/ml). The limits of detection using a 20-μl injection volume were typically in the low

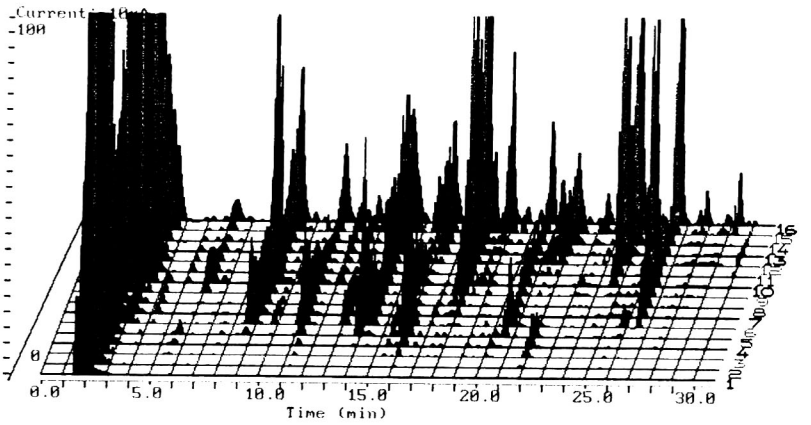

Fig. 4. Sixteen-channel chromatogram of a filtered orange juice from concentrate. Detector potentials were: 0–900 mV, 60-mV increments (Pd reference). Full scale amplification is 10 μA. Single-strength orange juice was passed through a 0.22-μm filter and 20 μl were injected. See Experimental for further details on analytical conditions.

ng/ml range with a linear response range of at least three orders of magnitude (see Table I). Levels of some of the electroactive components found in orange juice are presented in Table II.

In addition to quantitation using available external standards, we have examined the relative concentrations (calculated by peak height) of unidentified components among samples. Relative levels were determined by using a sample pool (*e.g.* authentic orange juice) as an external standard to generate normalized data for a large number of analytes in all samples. An estimation of the intra-assay variability in retention time, response ratios, and resultant quantitative value was made by examination of twenty-five unidentified analytes in ten replicate injections of an orange juice sample. Analytes were chosen to be representative of a wide range of meth-

TABLE II

LEVELS (IN μg/ml) OF SOME ELECTROACTIVE COMPONENTS IN ORANGE JUICE

External standard quantitation.

Compound	Varieties[a]				Mean	S.D.[b]
	Blend	Navel	Hamlin	Valencia		
Ascorbate	276	274	271	270	252	(67.6)
Cysteine	10.0	8.84	13.6	12.3	12.7	(2.53)
Hesperidin	165	219	128	145	76.4	(37.4)
Methionine	11.6	34.3	21.9	17.6	25.2	(29.5)
Narirutin	13.4	54.2	26.3	29.2	32.0	(11.7)
Tryptophan	6.30	3.02	4.26	4.00	5.35	(1.86)
Tyrosine	23.5	9.28	20.3	21.3	29.0	(8.74)
Naringin	0.04	0.17	0.39	0.31	0.79	(2.05)

[a] Navel, Hamlin and Valencia are cultivars of orange (*Citrus sinensis*). "Blend" refers to an adulterated orange juice sample of unspecified composition.

[b] Mean (standard deviation) of 41 commercial samples.

odological parameters: chromatographic (retention time: 3.19–25.4 min), electrochemical (dominant oxidation potential: 60–900 mV), and response (peak height: 0.01–20 μA). The relative standard deviation (R.S.D.) in retention time for each of these 25 analytes ranged from 0.26 to 0.69% (mean = 0.40%) indicating precise gradient control. Variability in peak height at the dominant sensor for each analyte ranged from 0.49 to 4.74% (R.S.D., mean = 1.74%). For 23 analytes, the R.S.D. in response ratio between the dominant and leading sensors ranged from 0.36 to 5.35% (mean = 1.58%). For one analyte, no response ratio was obtained due to insufficient signal at the leading sensor. Another analyte co-eluted with a lower oxidizing compound and high variability (33.5% R.S.D. for the ratio) was evident at the leading sensor. In both cases the variability in response ratios between the dominant and following sensors were low (0.59 and 2.38% R.S.D.). While the response at the following sensor was insufficient to allow ratio determinations in 3 of the 25 analytes good precision was obtained in these cases for the dominant/leading ratios. Variability in response ratios (dominant/following) for the remaining 22 analytes ranged from 0.40 to 7.51% (R.S.D., mean = 2.31%). Based on these performance data, matching criteria of ±2% for retention time and ±10% for response ratios were used. More than 150 components in a juice sample were typically within these criteria. External standard quantitation was performed using either the sum of the peak heights across three sensors when the response ratios were within these criteria, otherwise at the dominant sensor only. The variability in concentration, normalized to an authentic juice sample, for these 25 analytes ranged from 0.53 to 3.04% (R.S.D., mean = 1.11%).

In the investigation for orange juice adulteration we have examined these multivariate data for: endogenous markers of authenticity, peaks introduced by common adulterants (*e.g.* grapefruit, peel, pulpwash), and general dilution of multiple components. We have used this information along with pattern recognition analysis for differentiation of various juice beverages. An example of this approach is shown in Fig. 5. Here the results from principal components

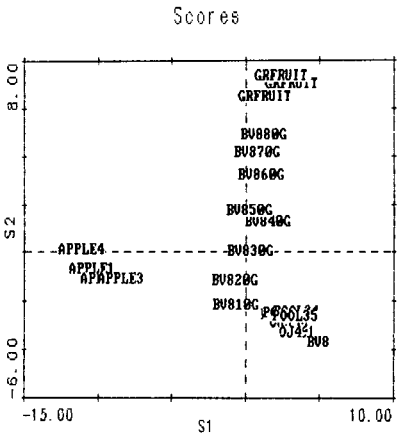

Fig. 5. Plot of vectors 1 (S1) and 2 (S2) from principal components analysis of a 50-variable data base. Grapefruit, orange, and apple juice samples along with various mixtures are differentiated through pattern recognition analysis. Sample key: APPLE 1–4 = different retail brands of apple juice; GRFRUIT = different retail brands of grapefruit juice; BV8 = pure Valencia (*Citrus sinensis* cv *Valencia*) orange juice from Florida; BV810G–80G = 10–80% grapefruit juice content in BV8, respectively. The cluster in the lower right quadrant is solely comprised of 17 orange juice samples as follows: BV8, 4 different retail brands of orange juice, 11 orange juice samples from Mexico and a pool of these 16 orange juice samples. Mexican samples included the following cultivars: Criolla, Hamlin, and Valencia as well as early-mid varieties (made from a mixture of early maturing and mid-season oranges). These varieties were obtained from Puebla, Tabasco, Tamaulipas, Veracruz and Yucatan regions.

analysis (PCA) [2,13] of data from 4 retail brands of apple juice, 17 samples of orange juice, 3 retail brands of grapefruit juice, as well as mixtures of grapefruit and orange juice are graphically represented. These results obtained from a 50 variable database demonstrate the utility of this technique for the differentiation of juice beverages. Clear separation between each fruit juice [orange (lower right quadrant), grapefruit (top right cluster), and apple (left cluster)] is evident. The mixtures (BV810G–BV880G) represent 10–80% grapefruit in orange respectively, and show a consistent progression of points between the respective groups of pure orange and grapefruit. Since several brands, sources, and varieties were included in this group of samples, differentiation in this instance appears to be quite specific to the fruit species.

Future reports will include studies of varietal and source differentiation as well as the detection of adulteration and percent juice analyses.

CONCLUSIONS

Coulometric array detection allows increased resolution for HPLC analysis of phenolic and flavonoid compounds based on differences in their voltammetric properties. Detailed voltammetric data across a wide potential range may be generated on-line from a single injection and with good precision. The basis for differences in ease of oxidation within and among compound classes corresponds to the patterns of aromatic substituents. Comparison of the electrochemical "signature" across the array may be used qualitatively to examine resolution and for some degree of structural characterization. Multivariate data from complex juice matrices can be obtained without extraction and with good precision. Differences in the patterns of endogenous electroactive components can be used to differentiate apple, orange, grapefruit, as well as orange-grapefruit mixtures. This technique may be a useful tool in such areas as adulteration detection, varietal and source classification, the study of process-related variability, and the analysis of percent juice in mixtures.

REFERENCES

1 G.A. Perfetti, F.L. Joe, T. Fazio and S.W. Page, *J. Assoc. Off. Anal. Chem.*, 71 (1988) 469.
2 R.L. Rouseff, in S. Nagy, J.A. Attaway and M.E. Rhodes (Editors), *Adulteration of Fruit Juice Beverages*, Marcel Dekker, New York, 1988, p. 49.
3 G.A. Spanos and R.E. Wrolstad, *J. Agric. Food Chem.*, 38 (1990) 817.
4 P.T. Kissinger, *Anal. Chem.*, 49 (1977) 447a.
5 S.M. Lunte, *J. Chromatogr.*, 384 (1987) 371.
6 O. Friedrich and G. Sontag, *Fresenius' Z. Anal. Chem.*, 334 (1989) 59.
7 R.W. Andrews, C. Shubert and J. Morrison, *Am. Lab.*, Oct. (1982) 140.
8 W.R. Matson, P.J. Langlais, L. Volicer, P.H. Gamache, E. Bird and K.A. Mark, *Clin. Chem.*, 30 (1984) 1477.
9 G. Achilli, G.P. Cellerino, P.H. Gamache and G.M. d'Eril, *J. Chromatogr.*, in press.
10 M. Uchida, Y. Kataoka and M. Ono, presented at the *2nd Brewing Congress of the Americas Meeting, St. Louis, MO, 1992.*
11 S.T. Kirksey, J.O. Schwartz and R.L. Wade, presented at the *2nd Annual Fruit Juice Authenticity Workshop, Herndon, VA, 1989.*
12 T. Robinson, *The Organic Constituents of Higher Plants: Their Chemistry and Interrelationships*, Cordus Press, N. Amherst, MA, 5th ed., 1983, pp. 54–200.
13 J. Arunachalam and S. Gangadharan, *Anal. Chim. Acta*, 157 (1984) 245.

Journal of Chromatography, 635 (1993) 151–154
Elsevier Science Publishers B.V., Amsterdam

CHROM. 24 889

Short Communication

Stability of furosine during ion-exchange chromatography in comparison with reversed-phase high-performance liquid chromatography

J. Hartkopf und H.F. Erbersdobler*

Institut für Humanernährung und Lebensmittelkunde der Christian-Albrechts-Universität zu Kiel, Düsternbrooker Weg 17, 2300 Kiel (Germany)

(First received October 7th, 1992; revised manuscript received January 19th, 1993)

ABSTRACT

Since a furosine standard became available only recently, arginine was used as the external standard in ion-exchange chromatography (IEC) and 2-acetylfuran in a recently proposed HPLC method. Using the pure furosine standard it was subsequently shown that both procedures produced inexact furosine values. With IEC a substantial decrease in the recovery of furosine of up to 30% was found depending on the elution conditions of pH and temperature that were applied. On the other hand, the use of 2-acetylfuran with HPLC led to an overestimation of furosine content of about 20%. However, correct furosine values were obtained using an IEC elution buffer of pH 4.00 at a temperature of 60°C as was shown by comparison with the HPLC method also based on the furosine standard. These results allow correction of the data obtained in earlier studies and more accurate determination of furosine values in future.

INTRODUCTION

For more than 25 years ε-N-(2-furoylmethyl)-L-lysine, named furosine for short, has been used as an indicator of lysine sugar derivatives such as fructoselysine, lactuloselysine and maltuloselysine formed in heated foods in the first steps of the Maillard reaction [1,2]. Furosine analyses are also applied in food science and nutrition, in clinical research and in medical biochemistry (see ref. 2). Furosine is determined by ion-exchange chromatography (IEC) [3,4], HPLC [5–7] and gas chromatography [8,9]. A problem in the determination of furosine was that until recently there was no pure and stable standard available. The furosine peaks were related to peaks of other amino acids such as lysine or arginine.

Recently a reduction in the recovery rate for furosine has been experienced, and therefore the conversion factor used to estimate lysine damage in heated foods was increased [10]. The main change during this time was the use of modern single-column equipment with high-resolving resins running with elution buffer with higher pH values and at higher temperatures. However, the pH value of the buffers known to be important for furosine stability was not increased above pH 6.4. Meanwhile Resmini *et al.* [7] reported that

* Corresponding author.

0021-9673/93/$06.00

considerable amounts of furosine are destroyed during ion-exchange chromatography, although their newly proposed HPLC procedure using low temperatures and a low pH together with 2-acetylfuran as a helpful substitute for the standard should give better results.

In order to determine the real losses of furosine during IEC analysis a set of experiments were carried out utilizing the recently available pure furosine standard as well as heated lysine–glucose models. Subsequently we compared the results of IEC with those of HPLC, first using, also on HPLC, the pure furosine standard.

EXPERIMENTAL

The furosine standard with a purity >99% was obtained from Neosystem, Strasbourg, France. For initial experiments a sample of furosine was provided by Dr. Finot, Nestec, Vevey, Switzerland. An amino acid calibration standard was obtained from Sigma (Deisenhofen, Germany), lysine hydrochloride from Serva (Heidelberg, Germany), 2-acetylfuran from Aldrich (Steinheim, Germany) and other reagents (all analytical-reagent grade) from Merck (Darmstadt, Germany).

An equimolar mixture of lysine hydrochloride and glucose in an 88% (w/v) aqueous solution was used as a model sample, which was heated for 20 h, and then hydrolysed for 20 h with 7.8 *M* hydrochloric acid at 110°C.

Furosine was analysed using a Liquimat III amino acid analyser (BHS-Labotron, Peissenberg, Germany) as previously described [4], using either a long glass column (170 × 4 mm I.D.) or a short column (50 × 4 mm I.D.) filled with the ion-exchange resin MCI Gel CK10F (Mitsubishi, Japan). The amino acids were detected with ninhydrin with a coil temperature of 115°C. Data acquisition and peak integration were evaluated with an integrator CI-10 from LDC (Gelnhausen, Germany). The elution of furosine was performed in a set of experiments using three different sodium citrate buffer solutions —(1) pH 6.40 (0.96 *M* Na^+), (2) pH 4.70 (1.60 *M* Na^+) and (3) pH 4.00 (1.60 *M* Na^+)— while different column temperatures from 45 to 80°C were applied. Furosine was also analysed with the RP-HPLC method [7] using a C_8 column (Spherisorb 5 C_8 column from Promochem, Wesel, Germany), a detection wavelength of 280 nm and either 2-acetylfuran or furosine as external standard. The HPLC system included a Gradientmaster, constaMetric III/IIIG pumps and a SpectroMonitor D UV detector from LDC (Gelnhausen, Germany), an AS-4000A autosampler from Merck-Hitachi (Darmstadt, Germany), and a C-R4A Chromatopac integrator from Shimadzu (Duisburg, Germany).

RESULTS AND DISCUSSION

To evaluate the influence of conditions during IEC on furosine determination, a furosine standard was analysed using elution buffer with different pH values and different column temperatures. The results of these experiments are shown in Fig. 1. Each value represents an average of six determinations. The peak areas of furosine obtained at pH 6.40 clearly decreased

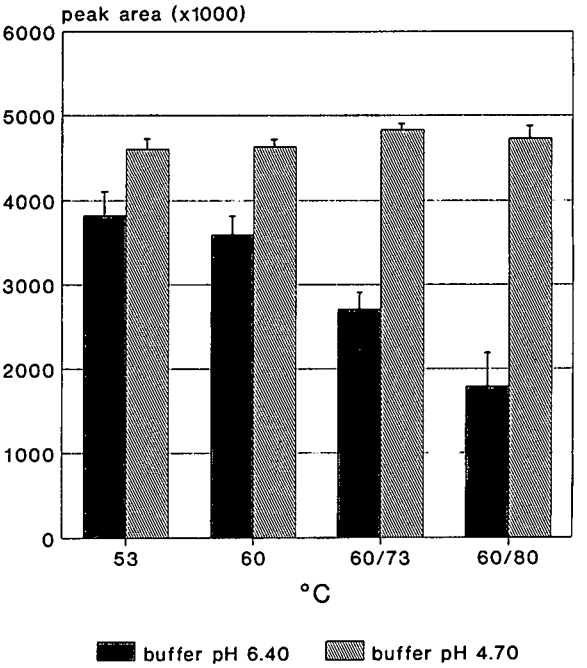

Fig. 1. Comparison of the peak areas of a furosine standard depending on temperature using elution buffers at pH 6.40 and 4.70. 60/73 and 60/80 mean: 30 min at 60°C and 40 min at 73°C or 80°C (pH 6.40) or 20 min at 60°C and 20 min at 73°C or 80°C (pH 4.70).

with increasing column temperature, although the time for elution was shorter at higher temperatures. At 80°C furosine was exposed for 30 min less than at 45°C (elution buffer pH 6.40 in both cases). This indicates destruction of furosine under these conditions. No direct investigation was made for reaction products or fragments of furosine. However, a degradation to lysine was not recognizable, because differences in the lysine peaks could not be detected.

In contrast to the decrease in the furosine peak areas with an elution buffer pH of 6.40, no significant differences depending on temperature were found at pH 4.70 (Fig. 1). Generally, the peak areas at pH 4.70 were higher than at pH 6.40. Also, the lower standard deviations at pH 4.70 indicated a better stability of furosine at this pH.

Fig. 2 compares the IEC method using a long (170 × 4 mm I.D.) and a short column (50 × 4 mm I.D.) and different pH values and column temperatures with the HPLC method. The comparison did not reveal any major differences, the analysed amounts of furosine being quite similar. However, using the long column at 60°C with an elution buffer pH 4.00 resulted in the highest furosine values. Under these conditions clear and well separated furosine peaks were obtained. The quantification was reproducible and correct, as was confirmed by adding a standard to the sample and comparing the furosine levels. The recovery rate was 99%.

The results obtained by IEC are in contrast to the findings of Resmini *et al.* [7], who found higher values with their HPLC method. In fact, our previous investigations using the HPLC procedure of Resmini also resulted in significantly higher values than with IEC using buffer at pH 4.00 and a column temperature of 60°C. On the other hand, the method of Resmini uses 2-acetylfuran as standard and not pure furosine. The results of more recent experiments show a marked difference between the peak values of equimolar concentrations of 2-acetylfuran and furosine. The 2-acetylfuran standard yielded only 80% of the furosine standard, resulting in an overestimation of furosine when 2-acetylfuran is used as external standard. Moreover, the 2-acetylfuran standard was found to be unstable during storage. By using the pure furosine standard instead, the same results as with the improved IEC technique were obtained, as is shown in Fig. 2.

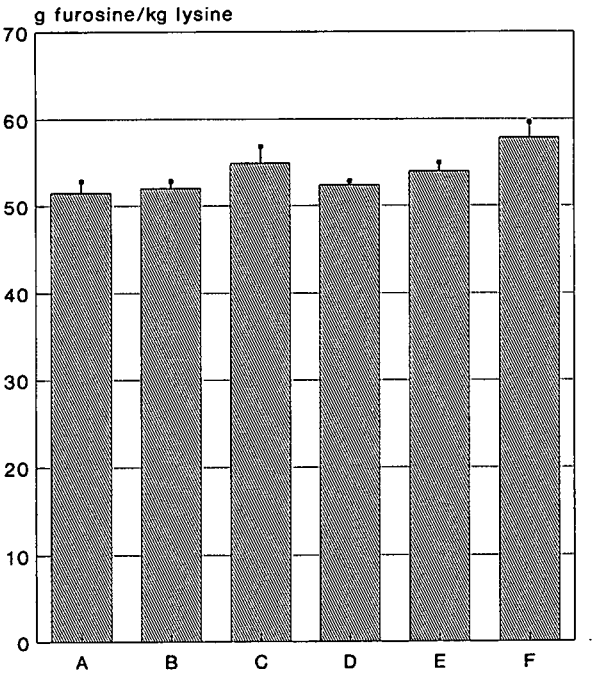

Fig. 2. Comparison of the furosine levels in a heated lysine–glucose model depending on column length, pH of the buffers and temperature. (A) 170 × 4 mm I.D. column, buffer pH 6.40, temperature 45°C. (B) 170 × 4 mm I.D. column, buffer pH 4.70, temperature 60°C. (C) 170 × 4 mm I.D. column, buffer pH 4.00, temperature 60°C. (D) 50 × 4 mm I.D. column, buffer pH 4.70, temperature 50°C. (E) 50 × 4 mm I.D. column, buffer pH 4.00, temperature 40°C. (F) HPLC method according to Resmini *et al.* [7] but using the pure furosine standard.

Since a pure furosine standard is now available, it was possible to re-examine earlier determinations of furosine, when arginine was used as external standard. Arginine standards analysed in the same way as described above showed no recognizable differences when buffer pH and column temperature were changed. Since the arginine–furosine ratio was not constant, one has to consider that the evaluation of furosine by using arginine as external standard led to an underestimation depending on the analytical conditions applied. But the results of these investigations allow correction of data obtained from earlier studies with higher pH and arginine

as external standard. To determine furosine values more accurately in future we recommend using the modified IEC procedure (elution buffer pH 4.00 column temperature 60°C) or the HPLC method using the now available pure furosine standard.

ACKNOWLEDGEMENT

The authors thank Dr. Finot, Nestec Ltd., Vevey, Switzerland, for providing some standard material of furosine.

REFERENCES

1 H. Erbersdobler and H. Zucker, *Milchwissenschaft*, 21 (1966) 564–568.
2 H.F. Erbersdobler, in M. Fujimaki, M. Namiki and H. Kato (Editors), *Amino-Carbonyl Reaction in Food and Biological Systems*, Elsevier, Amsterdam, 1986, pp. 481–491.
3 A. Brandt and H. Erbersdobler, *Landw. Forsch.*, 28/II (Sonderheft) (1972) 115–119.
4 H.F. Erbersdobler, B. Dehn, A. Nangpal and H. Reuter, *J. Dairy Res.*, 54 (1987) 147–151.
5 E. Schleicher and O.H. Wieland, *J. Clin. Chem. Clin. Biochem.*, 19 (1981) 81–87.
6 G.H. Chiang, *J. Agric. Food Chem.*, 31 (1983) 1373–1374.
7 P. Resmini, L. Pellegrino and G. Batelli, *Ital. J. Food Sci.*, 3 (1990) 173–183.
8 W. Büser and H.F. Erbersdobler, *J. Chromatogr.*, 346 (1985) 363–368.
9 J.A. Dunn, J.S. Patrick, S.R. Thorpe and J.W. Baynes, *Biochemistry*, 28 (1989) 9464–9468.
10 H.F. Erbersdobler and A. Hupe, *Z. Ernährungswiss.*, 30 (1991) 46–49.

Journal of Chromatography, 635 (1993) 155–159
Elsevier Science Publishers B.V., Amsterdam

CHROM. 24 803

Short Communication

High-performance liquid chromatographic determination of mexiletine in film-coated tablets using a new polymeric stationary phase

E. Lamparter

Department of Pharmaceutical Development, Boehringer Ingelheim KG, W-6507 Ingelheim am Rhein (Germany)

(First received August 4th, 1992; revised manuscript received December 11th, 1992)

ABSTRACT

The optimum column liquid chromatographic separation of mexiletine and one of its possible impurities is only achievable using alkaline mobile phases. Conventional silica-based reversed phases, however, are subject to considerable stability problems under these alkaline conditions, disqualifying most HPLC columns from routine use. An Asahipak ODP-50 column containing a new polymeric phase with a separation efficiency similar to that of silica-based reversed phases was used to develop an HPLC method for mexiletine that is unaffected by stability problems. The stability of the stationary phase was verified in long-term tests and the suitability of the method for assaying mexiletine in film-coated tablets was demonstrated by determining the selectivity, linearity, accuracy and precision.

INTRODUCTION

Mexiletine [1-(1,6-dimethylphenoxy)-2-aminopropane] is an antiarrhythmic drug used in the treatment of acute and chronic ventricular arrhythmias [1–3]. A variety of gas and column liquid chromatographic techniques for assaying mexiletine, especially in plasma, have been described [4–8]. HPLC methods employ exclusively silica-based reversed stationary phases and mobile phases with added modifiers in order to improve the peak symmetry of the basic substance mexiletine ($pK_a = 9.0$). The problems of analysing basic substances by HPLC on silica-based reversed-phase columns are well documented [9–12]. Low efficiency, tailing peaks, irreversible adsorption and stability problems with the stationary phase are typical symptoms that can be mitigated by mobile phase buffering and/or by the addition of modifiers such as EDTA or triethylamine or by the addition of ion-pair forming agents, *e.g.*, heptanesulphonic acid.

The development and optimization of such HPLC methods are generally difficult and require close monitoring of several parameters such as the influence of additive concentrations on the mobile phase. Furthermore, optimum separation by hydrophobic interactions of the neutral solutes with the stationary phase is only achieved when the pH of the mobile phase is at least 2 units above the pK_a of the basic substance to be analysed. In practice, this means that for basic drug substances with pK_a values around 9, an eluent pH above 11 should be used. This generally gives rise to severe stability problems

0021-9673/93/$06.00

with silica-based stationary phases, as the alkaline mobile phase attacks the silica matrix and gradually destroys the chemical structure of the silica gel.

The recently introduced polymeric phases, in which the polymer is adsorbed on silica gel, aluminium oxide or an organic support material, are much more stable in the alkaline range [13]. However, these phases with polymer coating almost always have the disadvantage of lower efficiency.

In this paper, the suitability of a new polymeric, reversed-phase column developed specially for the chromatography of basic substances is described with specific reference to the assay of mexiletine in film-coated tablets. Asahipak ODP-50 is based on a microparticulate mesoporous poly(vinyl alcohol) which has stearic acid bonded as an ester to the free alcohol groups of the matrix. The polymer is cross-linked with a molecule containing three vinyl groups. The suitability of this material for the determination of mexiletine using a mobile phase adjusted to pH 11 is demonstrated with reference to the test parameters selectivity, linearity, accuracy and precision. The stability of the phase was verified by a long-term test in which a test solution was injected continuously over several weeks and the resolution between mexiletine and the possible impurity 3,9-dimethyl-2,3-dihydrobenzo[*f*][1,4]-oxazepine (**I**) was evaluated in accordance with the system suitability test of the US Pharmacopeia (USP).

EXPERIMENTAL

Chemicals

Mexiletine and **I** were reference substances from Boehringer Ingelheim (Ingelheim, Germany). Acetonitrile and diethylamine were HPLC-grade reagents from Merck (Darmstadt, Germany). The stationary phase for the Asahipak ODP-50HPLC column is manufactured by Asahi Chemical Industry (Kawasaki, Japan) and the columns are filled and marketed by Hewlett-Packard (Waldbronn, Germany).

Equipment

The analyses were carried out using two different chromatographic systems, a Hewlett-Packard Model 1090 liquid chromatograph and a chromatograph consisting of the following components: a Merck–Hitachi L 6000 pump, a Gilson Model 231 autosampler fitted with a Rheodyne Model 7125 injection valve and 20-μl loop and a Merck–Hitachi L 4000 variable-wavelength UV spectrophotometric detector equipped with an 8-μl cell.

The test samples were analysed on an Asahipak ODP-50 (5 μm) column (125 mm × 4.0 mm I.D.). Peak integration and data evaluation were performed on a Hewlett-Packard Model 3357 laboratory data system.

Method

The mobile phase was a 280:720 (v/v) mixture of acetonitrile and purified water adjusted to pH 11.0 with diethylamine with the aid of a pH meter. The flow-rate was 0.9 ml/min and the uncorrected retention times were 8.6 min for mexiletine and 11.8 min for **I**. Detection was performed by UV spectrophotometry at a wavelength of 264 nm.

System suitability test

A solution was prepared containing 80 mg of mexiletine and 8 mg of **I** in 100 ml of mobile phase. The injection volume was 20 μl. The resolution factor had to be greater than 2.5. The tailing factor of mexiletine and **I** was not to be greater than *ca.* 2.5 at 5% of the peak height.

RESULTS AND DISCUSSION

The Asahipak ODP-50 column material was characterized in terms of the most important test criteria. Chromatograms are presented to demonstrate the selectivity of the method, and results for linearity, accuracy and precision are reported. The stability of the column is demonstrated on the basis of a long-term test.

Selectivity of the method

A stability-indicating assay method must be specific, *i.e.*, substance-related impurities, potential decomposition products and interfering excipients must be separated from the active ingredient.

Fig. 1 shows a chromatogram of a sample of mexiletine film-coated tablets with a dosage of

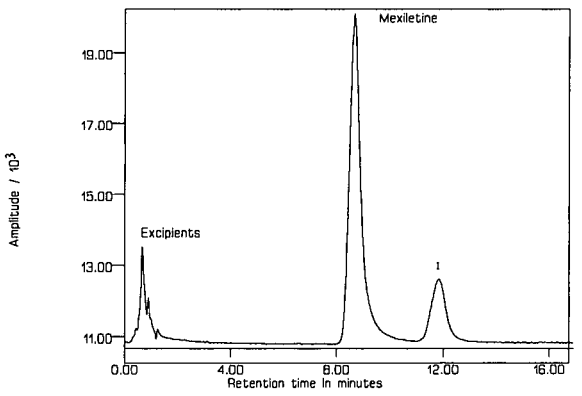

Fig. 1. Chromatogram of mexiletine with tablet matrix spiked with 1% of **I**.

150 mg; 1% of the possible impurity **I** was added to the test solution (for the structures of mexiletine and **I**, see Fig. 2). It is evident from the chromatogram that neither the mexiletine nor the **I** determination is affected by tablet excipients. Most tablet excipients are highly polar and elute with the solvent peak.

Linearity and accuracy

The linearity was determined in the mexiletine concentration range 0.30–0.70 mg/ml. The influence of the excipient matrix was also investigated over the entire range by adding a constant amount of excipient to the calibration solutions. The linearity of the two graphs was characterized by the following equations:

calibration without placebo:

$$y = -13.131.1 + 63.057.3x$$

calibration with placebo:

$$y = -24.083.3 + 63.873.3x$$

where y is the absorbance and x is the mexiletine concentration (mg/ml). The two calibration graphs were compared statistically by means of analysis of variance [14] at a significance level of $p = 95\%$ using a statistics problem from SAS (Cary, NC, USA). The calculation showed that neither the slopes nor the ordinate intercepts of the regression lines differ significantly.

The accuracy of the mexiletine assay was calculated with the same data in the more restricted working range of 80–120%, using five working concentrations. The test solutions were measured against a reference solution of mexiletine adjusted to 100%. The deviation of the measured values from the required standard is stated as the error (Table I). The deviation at the usual working concentration 0.4975 mg/ml (100%) is −0.527%.

Mexiletine

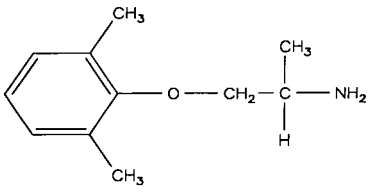

3,9-Dimethyl-2,3-dihydro-benzo[f][1,4]oxazepine (I)

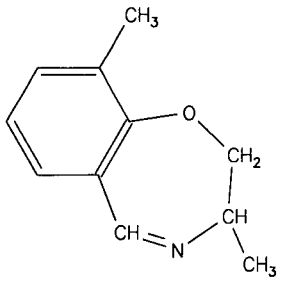

Fig. 2. Structures of mexiletine and 3,9-dimethyl-2,3-dihydrobenzo[*f*][1,4]oxazepine (**I**).

Precision

The precision of the assay of mexiletine film-coated tablets were assessed by analysing the results obtained by two technicians each carrying out three measurements on each of five preparations of the sample. Different HPLC systems and two Asahipak ODP-50 columns were used. The

TABLE I

ACCURACY OF MEXILETINE DETERMINATION IN THE CONCENTRATION RANGE 80–120% IN 150-mg FILM-COATED TABLETS

Theoretical value (mg/ml)	Measured value (mg/ml) (mean, $n = 6$)	Deviation (%)
0.398	0.397	−0.25
0.448	0.447	−0.22
0.498	0.495	−0.50
0.547	0.546	−0.18
0.597	0.604	+1.17

TABLE II

PRECISION OF MEXILETINE DETERMINATION IN 150-mg FILM-COATED TABLETS

Number of technicians, $n = 2$; number of sample preparations, $m = 5$; number of multiple measurements, $l = 3$.

Technician No.	Preparation No.	Measurement (mg)			Mean value (mg)
		1	2	3	
1	1	150.6	151.3	149.9	150.6
	2	149.9	148.3	150.3	149.5
	3	149.0	149.4	150.0	149.5
	4	149.0	149.1	150.6	149.6
	5	148.2	149.3	148.7	148.7
2	1	143.3	143.0	144.1	143.5
	2	144.8	144.2	145.4	144.8
	3	148.0	147.8	148.5	148.1
	4	142.3	142.9	142.3	142.5
	5	145.4	145.4	145.9	145.6
				Total:	147.2

S.D. of ruggedness: 3.6437, R.S.D. 2.47%.
S.D. of method reproducibility: 1.6737, R.S.D. = 1.14%.
S.D. of system reproducibility: 0.6314, R.S.D. = 0.43%.

stationary phases of the columns originated from different batches, and therefore the result for precision also includes the reproducibility of the stationary phase. Table II presents the data for precision with the appropriate evaluation. The data were statistically evaluated by means of hierarchical analysis of variance [14].

The system reproducibility is a measure of the reproducibility of the injection and chromatographic separation, and the method reproducibility additionally includes the sample preparation and ruggedness of the various components of the apparatus and human error of the individual technicians.

Stability of chromatography

The Asahipak ODP-50 column was subjected to a long-term test in which solutions for the system suitability test and test solutions of mexiletine film-coated tablets were injected alternately over several weeks. The chromatographic system was characterised by means of the system suitability test of the USP XXII by determining the resolution factor between mexiletine and **I** and the tailing factor of both substances at 5% of the peak height. Table III gives the minimum and maximum values and the relative standard deviation (R.S.D.) of the system suitability test for both substances.

To determine the influence of the matrix on the reproducibility of the method, the test solution spiked with 10% of **I** was also injected 120 times. The integrator units and retention times of mexiletine and **I** were determined and the R.S.D. was calculated (Table IV).

After about 600 injections the peaks of both substances showed a slight shoulder. This shoulder developed because of shrinkage of the packed column bed in the column which produced a dead volume, and which was rectified by replenishing the stationary phase in the column. A subsequent check on the chromatographic separation revealed that both the tailing factor and resolution data were in conformity with the initial values.

TABLE III

SYSTEM SUITABILITY TEST OF USP XXII

No. of injections: $n = 120$.

Substance	Tailing factor	Resolution	Retention time (min)
Mexiletine	$F_{min} = 2.0$ $F_{max} = 2.3$ R.S.D. = 3.8%	$R_{min} = 3.7$ $R_{max} = 5.0$ R.S.D. = 10.2%	$t_{min} = 8.7$ $t_{max} = 8.8$ R.S.D. = 0.3%
I	$F_{min} = 1.4$ $F_{max} = 1.5$ R.S.D. = 3.1%		$t_{min} = 11.6$ $t_{max} = 12.2$ R.S.D. = 0.4%

TABLE IV

INFLUENCE OF THE MATRIX ON THE REPRODUCIBILITY OF THE METHOD

No. of injections, $n = 120$.

Substance	Integrator units	Retention time (min)
Test solution (mexiletine)	$A_{min} = 639456$ $A_{max} = 716231$ R.S.D. = 1.1%	$t_{min} = 8.6$ $t_{max} = 8.8$ R.S.D. = 1.1%
I	$A_{min} = 891599$ $A_{max} = 921527$ R.S.D. = 0.5%	$t_{min} = 11.7$ $t_{max} = 12.3$ R.S.D. = 1.2%

CONCLUSIONS

The results of long-term testing demonstrate that the Asahipak ODP-50 columns are free from stability problems even when using mobile phases with a pH above 10. Asahipak ODP-50 is therefore superior to conventional silica-based reversed-phase columns when using alkaline mobile phases. Because of its good separation efficiency, Asahipak ODP-50 is suitable for further applications, particularly the determination of substances with basic groups, as the selectivity range in the alkaline environment can be considerably extended for such substances.

ACKNOWLEDGEMENTS

The author thanks Mrs. H. Weitzel for the conscientious performance of the tests and Mrs. H. Voss for the statistical evaluation of the data. Thanks are also due to Hewlett-Packard for donating the Asahipak ODP-50 LC columns.

REFERENCES

1 N.P.S. Campbell, J.G. Kelly, A.A.J. Adgey and R.G. Shanks, *Br. J. Clin. Pharmacol.*, 6 (1978) 103.
2 P. Danilo, *Am. Heart J.*, 79 (1979) 399.
3 C.Y.C. Chew, J. Collett and B.N. Singh, *Drugs*, 17 (1979) 161.
4 F. Susanto, S. Humfeld and H. Reinauer, *J. Chromatogr.*, 21 (1986) 41.
5 B.K. Krämer, K.M. Ress, F. Mayer, V. Knehlkamp, H.M. Liebich, T. Riesler and L. Seipel, *J. Chromatogr.*, 493 (1989) 414.
6 M.C. Contreras de Condado, A. Quinzana de Gainzarain, I. Mendoza Mujica and J.A. Condado Rodriguez, *J. Chromatogr.*, 530 (1990) 164.
7 N. Shibata, M. Akabane, T. Minouchi, T. Ona and H. Shimakawa, *J. Chromatogr.*, 566 (1991) 187.
8 D. Paczkowski, M. Filipek, Z. Mielniczuk, I. Andrzeyczak, W. Poplawaska and D. Sitkiewicz, *J. Chromatogr.*, 573 (1992) 235.
9 M. de Smet and D.L. Massart, *Trends Anal. Chem.*, 8 (1989) 96.
10 W. Jost, K.F. Krebs and H. Winkler, *Kontakte*, 2 (1987) 32.
11 W.D. Hill, *J. Liq. Chromatogr.*, 13 (1990) 3147.
12 R. Hindriks, F. Maris, J. Vink, H. Peeters, M. de Smet, D.L. Massart and L. Buydens, *J. Chromatogr.*, 485 (1989) 255.
13 R.E. Majors, *LC · GC Int.*, 5 (1992) 12.
14 L. Sachs, *Angewandte Statistik*, Springer, Berlin, 6th ed., 1984.

Journal of Chromatography, 635 (1993) 160–164
Elsevier Science Publishers B.V., Amsterdam

CHROM. 24 906

Short Communication

Chemical reduction of FD&C Yellow No. 5 to determine combined benzidine

Valerie M. Davis*

Division of Toxicological Studies, US Food and Drug Administration, Washington, DC 20204 (USA)

John E. Bailey, Jr.

Division of Colors and Cosmetics, US Food and Drug Administration, Washington, DC 20204 (USA)

(First received June 2nd, 1992; revised manuscript received January 7th, 1993)

ABSTRACT

Data are presented suggesting the presence of the aromatic amine benzidine as a combined impurity in the regulated color additive FD&C Yellow No. 5. The benzidine exists as an azo-dye constituent that forms from free benzidine impurities introduced during the manufacture of the color additive. The presence of combined benzidine is ascertained by sodium dithionite reduction of the azo bonds in the commercial color additive. The resulting reduction products are extracted with chloroform, and the liberated benzidine is determined by high-performance liquid chromatography (HPLC). The levels of benzidine determined by HPLC exceed those levels of benzidine accounted for by direct determination of free aromatic amines in the unreduced color.

INTRODUCTION

FD&C Yellow No. 5 is a color additive approved for use in the United States in foods, drugs and cosmetics, and is subject to batch certification by the US Food and Drug Administration [1]. Regulations limiting the levels of chemical impurities allowed in this color additive were revised. The revised specifications restrict the allowed levels for several aromatic amines, including a limit of 1 ppb (w/w) for benzidine as the free amine [2].

Benzidine that occurs as a contaminant in FD&C Yellow No. 5 probably originates as an impurity in the sulfanilic acid intermediate used to manufacture the color additive [3]. Any benzidine present in the sulfanilic acid starting material may also be diazotized and coupled during manufacture, leading to potential contamination of the color additive by combined benzidine in the form of subsidiary dyes (Fig. 1). When azo dyes are ingested, reduction occurs in the intestine, resulting in cleavage of the azo bond and possible liberation of free aromatic amines.

A method [4,5] has been reported for determining residue levels of unsulfonated (free) aromatic amines in color additives, including FD&C Yellow No. 5. In the method, the amines are first extracted from an aqueous, alkaline solution of the color, and then they are diazo-

* Corresponding author.

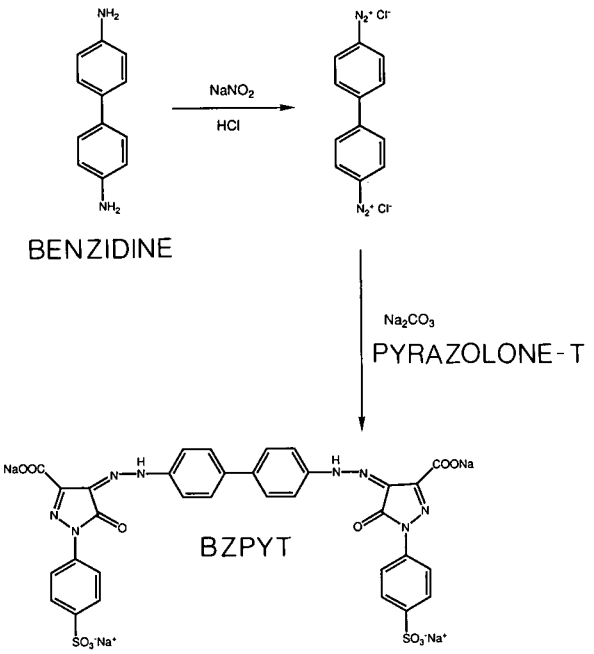

Fig. 1. Diazotization and coupling of benzidine with pyrazolone-T.

tized and coupled. The amines are determined as azo derivatives by high-performance liquid chromatography (HPLC). Although the method determines free amines in the color additive, it does not determine both free and chemically bound amine contaminants.

In this study, the presence of benzidine as a combined impurity in FD&C Yellow No. 5 was investigated. The color additive was chemically reduced at the azo linkage with sodium dithionite. The amines thus liberated were isolated by solvent extraction and determined as previously described [4]. The efficiency of the reduction technique was tested by adding various levels of the combined benzidine impurity to the color additive and measuring the total amount of benzidine released.

EXPERIMENTAL

Materials

Preparation of the diazotization and coupling solutions was described previously [4]. All FD&C Yellow No. 5 dye samples used in this study were from batches of color additive certified during 1985. Extrelut Q.E. disposable columns, Part No. 902050-1, 15 × 4 cm diatomaceous earth, were obtained from EM Science Div., EMS, Inc. (Cherry Hill, NJ, USA). The benzidine–pyrazolone-T coupling product (BZPYT) used as the reference standard (Fig. 1) was synthesized and purified by one of us (J.E.B.) in 1985. The coupling agents, pyrazolone-T and pyrazolone-T acid, were purified by recrystallization twice from hot water; their purity was established by elemental analysis [6]. Water was purified by using the Milli-Q system of Millipore (Bedford, MA, USA). Chloroform and acetonitrile were HPLC grade. Sodium hydrosulfite was purchased from Fisher Scientific, Cat. No. S-309 (Pittsburgh, PA, USA). All other reagents were analytical grade and purchased from commercial sources.

BZPYT standard solutions for calibration

Aqueous stock solutions containing BZPYT reference standard at concentrations of 0.125, 0.25, 0.5, 0.75, 1.0 and 1.25 μg/ml were used to prepare the calibration solutions. For each calibration solution, 1 g of FD&C Yellow No. 5 determined to be free of benzidine when chemically reduced was dissolved in 30 ml of water, and a 1.0-ml aliquot of stock solution was added. The concentrations of BZPYT reference standard in the calibration solutions corresponded to 27, 53, 106, 159, 212 and 265 ppb of free benzidine after liberation of the amine by chemical reduction.

Chemical reduction of FD&C Yellow No. 5

A solution of 1.0 g of FD&C Yellow No. 5 in 30 ml of water was prepared in a round-bottom flask and maintained at 80°C on a hot plate. The pH of the solution was initially adjusted to approximately 8.5 by adding 5 *M* NaOH. Sodium dithionite was slowly added to the solution in small portions until a 10% excess of dithionite over the theoretical amount required for complete reduction had been added (a molar ratio of 2.2 to 1 was employed). This usually required the addition of approximately 0.9 g of dithionite. The sodium dithionite was added in small (mg) quantities until the pH dropped to 7.0. The pH was then readjusted to 8.5 with 5 *M* NaOH.

Nitrogen was bubbled through the solution during the entire reduction procedure to prevent oxidation before the extraction procedure.

Extraction

The extraction step was conducted as described by Richfield-Fratz *et al.* [6] except that the reduced-dye solution (approximately 30 ml) was allowed to cool to room temperature while nitrogen was gently bubbled through the solution. The solution containing the reduced color additive and liberated aromatic amines was carefully poured into the Extrelut cartridge. A few milliliters of water were added to wash the flask, and the liquid was drained into the cartridge. The cartridge was washed with four 25-ml portions of chloroform, and the chloroform eluate was collected in a 250-ml round-bottom flask. A 5-ml portion of 0.05 *M* H_2SO_4 was added to the chloroform extract instead of 5 ml of 0.005 *M* H_2SO_4. Extracts that were not immediately diazotized and coupled were stored in a stoppered round-bottom flask and refrigerated until the following day.

Diazotization and coupling

The diazotization and coupling procedure used was previously reported [5]. A 2-ml portion of 0.1% $NaNO_2$ was added to the flask, the contents were gently swirled to rinse the flask walls and the flask was chilled in an ice bath for 15 min. After 2 ml of the pyrazolone-T coupling solution was added, exactly 13 drops of 0.1 *M* NaOH were added to ensure an alkaline pH during coupling. Each coupled extract was redissolved in 5 ml of water before HPLC determination.

High-performance liquid chromatography

All HPLC determinations were performed within 24 h of extraction, as previously described [5]. A Waters Model 440 dual-channel UV–Vis detector (Waters Chromatography, Division of Millipore, Milford, MA, USA) (2 V output) was set at 436 and at 600 nm to monitor the eluates. A Biosil ODS 5-μm column (25 cm × 4.6 mm I.D.) with a 250-μl injection loop was used at ambient temperature for all separations. A 3-ml aliquot of coupled extract was used to flush the loop before each injection of extract.

RESULTS AND DISCUSSION

The retention times of the products obtained from chemical reduction and analysis of a BZPYT reference solution were determined (Fig. 2A). Although benzidine is usually determined (as the benzidine–pyrazolone-T coupling product) at a detector wavelength of 436 nm, other amine coupling products also absorb at this wavelength and may interfere with the determination. However, at 600 nm one major peak appears at 20.6–20.8 min, the retention time of the benzidine–pyrazolone-T coupling product. Thus, the presence of a chromatograph-

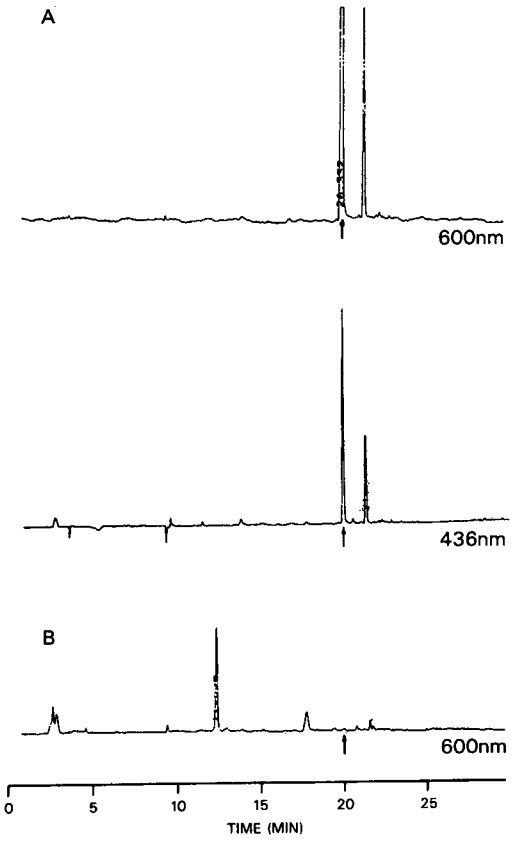

Fig. 2. (A) HPLC chromatograms from analysis of BZPYT reference standard. Detection at 436 and 600 nm. Approximate retention time = 20.7 min. (B) HPLC chromatogram from analysis of FD&C Yellow No. 5 batch containing no chemically bound benzidine or aniline. Detection at 600 nm.

ic peak at both detection wavelengths and calculation of the response ratio (data not shown) provide confirmation of identity during analysis. The small peak appearing just after the major response in the chromatograms in Fig. 2A is probably the monoazo derivative formed when only one benzidine amine group is diazotized.

Fig. 2B shows the HPLC chromatogram obtained from analysis of a previously certified batch of FD&C Yellow No. 5 that was found to be free of both chemically bound benzidine and aniline. (The large amount of aniline that may be produced upon reduction of some commercial batches of FD&C Yellow No. 5 may swamp the HPLC response of the analyte [4,5].) All calibration solutions were chemically reduced and analyzed as described above, and the data were evaluated statistically to measure the linearity of response [7]. The correlation coefficient of 0.97 indicates sufficient linearity over the entire calibration range to allow use of the regression equation to estimate levels of combined benzidine in commercial batches of color, especially at the higher levels.

A total of 14 commercial samples of FD&C Yellow No. 5 were analyzed for total benzidine content by this procedure. The survey included batches submitted for certification during 1985 before restrictions were imposed for aromatic amine residues. The survey also included the batch used in toxicological tests conducted to establish the safety of the color additive. The results of the survey are shown in Table I. The HPLC chromatogram obtained from analysis of the FD&C Yellow No. 5 pharmacology batch (Fig. 3) shows one large peak, at a retention time of approximately 17.5 min, corresponding to aniline, which was liberated during reduction of the color. The chromatogram has only a small peak at the retention time expected for benzidine, suggesting that the test sample does not contain significant levels of combined benzidine.

Fig. 4 shows the HPLC chromatograms obtained for a reduced and for an unreduced commercial batch of FD&C Yellow No. 5 (sample 7 in Table I). Note that the unreduced color produced only a small peak for aniline and no detectable response for benzidine. However, the reduced color produced a large peak for aniline and a small but detectable response at the retention time of the benzidine coupling product. The level of combined benzidine in this batch of color, estimated from the calibration data, is 69 ppb calculated as free benzidine. Similar analysis

TABLE I

HPLC DETERMINATION OF TOTAL BENZIDINE IN COMMERCIAL SAMPLES OF FD&C YELLOW NO. 5.

Sample	Distributor	Retention time (min)	Benzidine found (ppb)[a]
1	A	20.7	245
2	B	20.6	61
3	B	20.7	93
4	C	20.7	40
5	D	20.8	105
6	E	20.7	23
7	F	20.7	69
8	G	20.8	147
9	C	20.7	40
10	H	20.7	19
11	I	20.8	56
12	A	20.6	241
13	F	20.6	38
14	G	20.6	72

[a] Calculated as free benzidine.

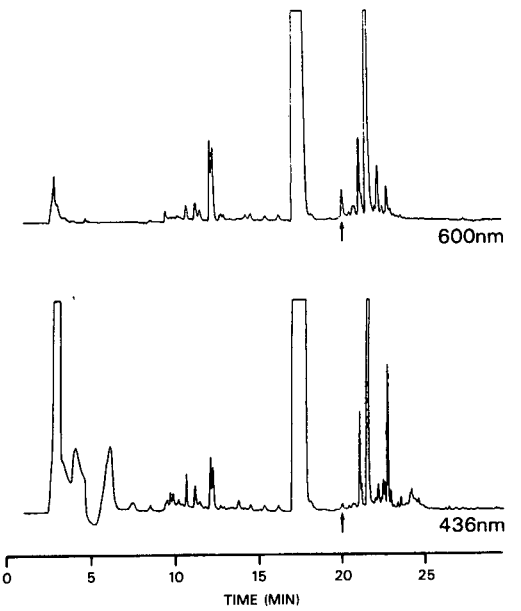

Fig. 3. HPLC chromatogram from analysis of FD&C Yellow No. 5 pharmacology sample. Detection at 436 and 600 nm.

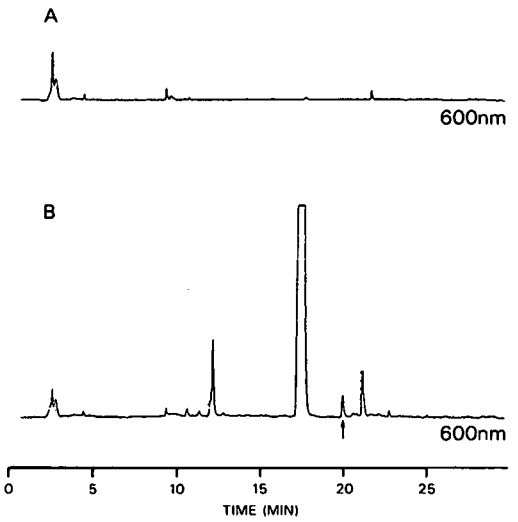

Fig. 4. HPLC chromatograms from analysis of FD&C Yellow No. 5, sample 7: (A) without reduction; (B) with reduction.

of sample 1 in Table I produced the equivalent of 245 ppb of free benzidine, which is the highest level of combined benzidine found in the survey. Analysis of the corresponding unreduced sample found no detectable free benzidine.

The results obtained in this study show that commercial batches of FD&C Yellow No. 5 may contain benzidine as a chemically bound, azo subsidiary color. Although the estimated levels of combined benzidine reported here exceed those observed for free benzidine, the samples surveyed in this study were all manufactured before restrictions were imposed on allowable levels of free aromatic amines. Additional work is under way at the US Food and Drug Administration to refine the analytical methodology used for determining chemically bound benzidine and to develop more complete HPLC characterization of the benzidine analyte. The results presented here will allow an assessment of the effect of restricting the level of free aromatic amine content on the level of total aromatic amine content in the widely used food color.

REFERENCES

1 US Food and Drug Administration, *Fed. Reg.*, 50, Sept. 4 (1985) 35 774.
2 *Code of Federal Regulations*, US Government Printing Office, Washington, DC, 1991, Title 21, Part 74.
3 V. Kratochvil and K. Obruba, *Chem. Prum.*, 29 (1979) 257; *Chem. Abstr.*, 91 (1979) 558.
4 J.E. Bailey, Jr., *Anal. Chem.*, 57 (1985) 189.
5 J.E. Bailey, Jr. and C.J. Bailey, *Talanta*, 32 (1985) 875.
6 N. Richfield-Fratz, J.E. Bailey, Jr. and C.J. Bailey, *J. Chromatogr.*, 331 (1985) 109.
7 C.J. Bailey, E.A. Cox and J.A. Springer, *J. Assoc. Off. Anal. Chem.*, 61 (1978) 1404.

Journal of Chromatography, 635 (1993) 165–170
Elsevier Science Publishers B.V., Amsterdam

CHROM. 24 938

Short Communication

Mapping of derivatised biogenic amines by two-dimensional thin-layer chromatography

A comparative study

Neil P.J. Price* and D. Octavius Gray

School of Biological Sciences, Queen Mary and Westfield College, University of London, Mile End Road, London E1 4NS (UK)

(First received September 3rd, 1992; revised manuscript received January 8th, 1993)

ABSTRACT

The analysis of amines is greatly enhanced by the formation of derivatives with improved chromatographic properties. We have used dansyl chloride, dabsyl chloride, and 7-chloro-4-nitrobenzoxazole to derivatise fourteen structurally diverse amines which occur in biological systems, and have made a comparative study of their thin-layer chromatographic properties. Two-dimensional TLC maps of derivatised amines are presented for the three different procedures, and some factors which influence sensitivity are evaluated. On grounds of sensitivity of detection and chemical stability of the derivatives formed, dansyl chloride is the preferred reagent for chromatographic analysis of complex mixtures of biogenic amines.

INTRODUCTION

Biogenic amines, which include mono-, di-, and polyamines, catecholamines, indoleamines, and imidazoles [1] are difficult to analyse by a single chromatographic technique because of their structural diversity and lack of an easily detectable common chromophore. The usual approach, therefore, has been to derivatise free amines with an easily detected label group (for reviews, see refs. 2 and 3).

An ideal label should be specific for amino groups, forming highly coloured or fluorescent derivatives to allow sensitive detection. Excess reagent and by-products should be colourless, non-fluorescent, or easily eliminated. Non-polar derivatives are desirable to improve chromatographic properties. Chemically stable derivatives suitable for NMR and mass spectroscopic identification are also advantageous.

Three of the more common derivatising agents used are dansyl chloride [4,5], dabsyl chloride [6], and 7-chloro-4-nitrobenzoxazole (NBD chloride) [7]. Unlike fluorescamine [8] or *o*-phthalaldehyde [9] these have the advantage of forming derivatives with both primary and secondary amines, and all three give derivatives

* Corresponding author. Present address: The Complex Carbohydrate Research Center, University of Georgia, 220 Riverbend Road, Athens, GA 30602 (USA).

0021-9673/93/$06.00

stable enough for subsequent spectroscopic analysis [10,11].

Here we describe two-dimensional (2D) TLC systems optimised to separate amines after derivatisation with dansyl chloride, dabsyl chloride, or NBD chloride. Thin-layer chromatography has the advantage of being rapid, simple, and economical. Although much has been published on the TLC separation of dansylated amines [12,13] far less information is available on dabsyl or NBD derivatives, and no comparative study has been previously undertaken.

EXPERIMENTAL

Materials

Chemicals were obtained from Aldrich (Poole, UK). Amine hydrochlorides (100 μg/ml) were prepared as standards. Silica 60 (250 μm) TLC plates (20 × 20 cm) were obtained from Sigma (Poole, UK). Glass distilled water was used throughout.

Derivatisation

For dansylation, aliquots of aqueous amine solutions (=20 μg) were saturated with sodium hydrogen carbonate and reacted for 15 h at room temperature with dansyl chloride in acetone (800 μl, 5 mg/ml), then warmed (60°C, 10 min) to complete the reaction and remove excess acetone. After dilution to 1 ml with water the dansylated amines were extracted with 3 × 2 ml toluene. When necessary the phases were separated by centrifugation. The organic phases were evaporated to dryness under a stream of air and stored in the dark at −20°C.

Derivatisation with dabsyl chloride and NBD chloride were similar to dansylation except that the derivatising agents used were dabsyl chloride in acetone (800 μl, 5 mg/ml), or NBD chloride in ethanol (800 μl, 5 mg/ml). NBD-amines were extracted with ethyl acetate rather than toluene. At all stages exposure to light was kept to a minimum.

Thin-layer chromatography

Derivatised amines were redissolved in ethyl acetate and applied to TLC plates, which were developed in the dark. Fluorescent spots were visualised under 360 nm UV light. Where appropriate plates were sprayed with triethanolamine in *n*-propanol (20%, v/v); glacial acetic acid in *n*-propanol (20%, v/v); or hydrochloric acid in methanol (3%, v/v).

Solvent systems used for TLC were as follows: (1) ethyl acetate–cyclohexane (3:2, v/v); (2) benzene–triethylamine (5:1, v/v); (3) ethanol–15 *M* ammonia (1:1, v/v); (4) ethanol–acetic acid (1:1, v/v); (5) toluene–acetic acid (1:1, v/v); (6) *n*-butyl acetate; (7) toluene; (8) toluene–acetic acid (2:1, v/v); (9) toluene–acetone (4:1, v/v).

TLC plates eluted with aqueous pH buffers were dried at 110°C and cooled before visualising the spots under 360 nm UV light. Buffers were prepared as follows: formic acid–acetic acid–water (4:9:70, v/v/v; pH 2); aqueous potassium hydrogen phthalate (10 g/l; pH 4); phosphate (1.13 g/l Na_2HPO_4; 8 g/l K_2HPO_4; pH 6); and borate (3 g/l boric acid; 1.5 g/l NaOH; pH 10).

pH dependent absorption maximum of dabsyl hexanolamine

Dabsyl hexanolamine (4.88 mg, 10.9 μmol) prepared from dansyl chloride and hexanolamine hydrochloride was purified by two rounds of preparative TLC on silica 60. The purity was verified by proton NMR spectroscopy (data not shown). This was dissolved in aqueous acetonitrile (60%, v/v) and split into five equal aliquots. Aqueous buffers were added (either pH 4, 3, 2.5, 2 or 1; 100 μl), and the concentrations adjusted to 0.73 μmol/ml with acetonitrile. Absorbances were recorded between 390–530 nm on a Pye Unicam SP8100 UV visible spectrophotometer.

RESULTS AND DISCUSSION

The amines chosen for study (listed in Table I) were derivatised with the appropriate reagents as described in the experimental section. Chromatographic separation was initially evaluated by the procedure of Alberts *et al.* [13]. Dansylated and dabsylated derivatives were found to have similar TLC properties and were adequately resolved. NBD-amines, however, were resolved satisfactorally in solvent 1, but not in solvent 2,

TABLE I

MOBILITIES OF NBD-AMINES ON SILICA 60 TLC PLATES

NBD-derivatised amines	Relative mobilities (R_F)[a]				
	1	5	6	8	9
Ammonia	0.26	0.06	0.27	0.45	0.27
Methylamine	0.26	0.17	0.39	0.57	0.37
Ethylamine	0.38	0.24	0.52	0.63	0.45
Ethanolamine	0.07	0.02	0.12	0.30	0.14
n-Butylamine	0.55	0.33	0.69	0.71	0.54
Isobutylamine	0.55	0.32	0.69	0.71	0.54
Putrescine	0.09	0.20	0.38	0.31	0.20
Cadaverine	0.12	0.21	0.39	0.34	0.24
p-Tyramine	0.17	0.08	0.34	0.48	0.34
3-MeO-*p*-tyramine	0.17	0.08	0.34	0.48	0.34
Tryptamine	0.46	n.d.	0.65	0.55	0.36
Spermidine	0.09	n.d.	0.32	0.27	0.17
Spermine	0.09	n.d.	0.34	0.30	0.24
Histamine	0.00	n.d.	n.d.	0.30	0.07

[a] Numbers at the head of each column refer to the solvent system used, as designated in the Experimental section. n.d. = Not determined.

where only five spots moved at all (see Table I). The NBD-amines were initially re-chromatographed in solvent 3 and in solvent 4, to compare the effects of basic and acidic conditions. Little difference was seen between these two systems, with all the spots running too fast. Mobilities in toluene–acetic acid (solvent 5) were assessed to determine the effect of a less polar solvent. Here all the components ran slowly suggesting that polarity rather than pH was the major factor determining elution rate. This is perhaps confirmed by the R_F values obtained subsequently in *n*-butyl acetate (solvent 6) and in toluene (solvent 7). Elution was faster in the relatively polar ester than in the more hydrophobic aromatic solvent.

Solvent 8 [toluene–acetone 2:1 (v/v)] and solvent 9 [toluene-acetone 4:1 (v/v)] were assessed, and although both systems improved resolution some spots eluted too fast in solvent 8. It was concluded that solvent 9 was the most useful solvent mixture devised. R_F values for NBD-amines in the more useful solvent systems tested are listed in Table I.

An optimised 2D-TLC system for NBD-amines was therefore assessed, run in the first direction with solvent 1 and in the second with solvent 9. R_F values were measured and a 2D-TLC map was constructed for this combination (Fig. 1). Comparing the resolving power of this new 2D-TLC system for NBD-amines with that for dansyl-amines (Fig. 2) and dabsyl-amines (Fig. 3) showed that of the fourteen amines chosen for comparison ten were resolved as their dansyl or NBD derivatives, and eight as their dabsyl derivatives. A major problem with the dansyl and dabsyl systems was inadequate separation of the ammonia and polyamine derivatives (especially spermidine, cadaverine and putrescine). NBD-polyamines were better resolved, and completely separated from NBD-ammonia. However, *p*-tyramine and 3-methoxy-*p*-tyramine could not be resolved as their NBD derivatives, but were separated by both the dansyl and dabsyl systems. None of the 2D-TLC systems investigated were able to separate the derivatives of the two butylamine isomers.

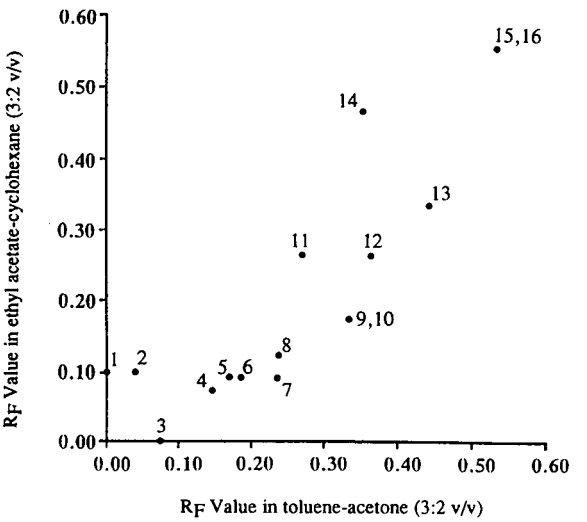

Fig. 1. Two-dimensional TLC map of NBD-amines on silica 60. NBD-derivatives are referred to by number as follows: 1 = NBD-OH; 2 = NBD-Cl; 3 = histamine; 4 = ethanolamine; 5 = spermidine; 6 = putrescine; 7 = spermine; 8 = cadaverine; 9 = *p*-tyramine; 10 = 3-methoxy-*p*-tyramine; 11 = ammonia; 12 = methylamine; 13 = ethylamine; 14 = tryptamine; 15 = *n*-butylamine; 16 = isobutylamine. Derivatisation and chromatographic conditions are described in the text.

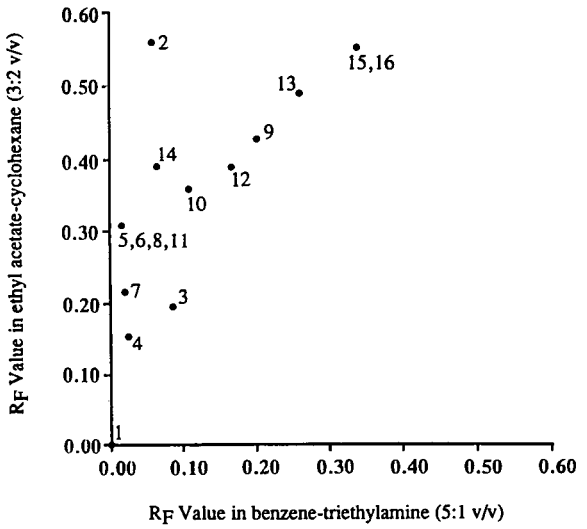

Fig. 2. Two-dimensional TLC map of dansyl-amines on silica 60. Reference numbers are: 1 = dansyl-OH; and 2 = dansyl-Cl. Dansylated amines are numbered as in Fig. 1.

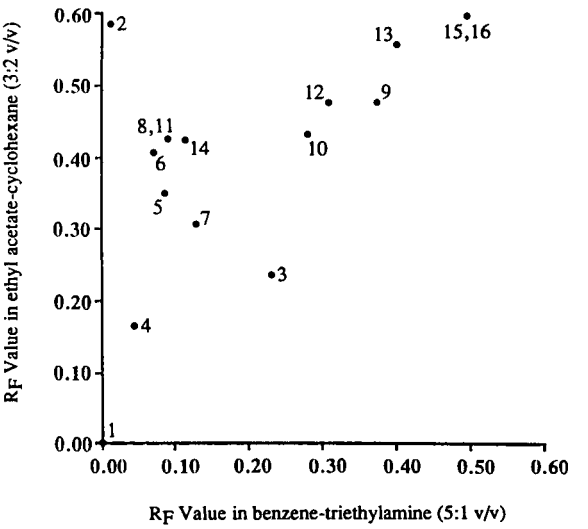

Fig. 3. Two-dimensional TLC map of dabsyl-amines on silica 60. Reference numbers are: 1 = dabsyl-OH; and 2 = dabsyl-Cl. Dabsylated amines are numbered as in Fig. 1.

Separation of NBD-amines with aqueous buffers

When separated in organic solvents NBD-amines tended to distribute across plates as a diagonal. However, their relatively high polarity suggested the possibility of using aqueous pH buffers as the second solvent for 2D-TLC, thereby making the separation dependent on charge rather than polarity. Dansyl and dabsyl derivatives were too non-polar to be separated by aqueous TLC systems.

NBD-amine derivatives were separated on Silica 60 plates using four different buffers (pH 2, 4, 6 or 10). The results are presented in Table II. The reagent blank gave a major non-fluorescent, yellow spot (presumably NBD-OH) that ran with the mobile phase front during chromatography. Most of the NBD-amines gave only one fluorescent spot. However, several proved to be non-fluorescent or had low fluorescent intensity, and consequently were difficult to detect. This, and the generally poor resolution obtained, particularly at high pH, suggested that the procedure was not useful for resolving NBD-amines.

Relative sensitivity of the derivatising reagents

To compare minimum detection levels spots of derivatised ethylamine (0.2–5 ng) were eluted on Silica 60 in solvent 1. Detection was assessed visually either under 360 nm UV light or, in the case of dabsylated ethylamine, under normal

TABLE II

pH-DEPENDENT TLC MOBILITIES OF NBD-AMINES ELUTED WITH AQUEOUS BUFFERS

Chromatographs were run on Silica 60 plates eluted with aqueous pH buffers. Buffers are described in the methods section. Diethanolamine, *tert.*-butylamine and di-N-butylamine gave non-fluorescent derivatives.

Amine derivative	Relative mobilities (R_F)			
	pH 2	pH 4	pH 6	pH 10
Methylamine	0.66	0.28	0.37	streaked
Ethylamine	0.59	0.16	0.38	streaked
n-Propylamine	0.56	0.12	0.38	streaked
Isopropylamine	0.55	0.12	0.36	streaked
n-Butylamine	0.51	0.09	0.35	streaked
Isobutylamine	0.55	0.13	0.37	streaked
sec.-Butylamine	0.52	0.12	0.36	streaked
tert.-Butylamine	–	–	–	–
Isoamyllamine	0.49	0.12	0.36	streaked
n-Octylamine	0.34	0.09	0.03	streaked
Ethanolamine	0.32	0.06	0.02	streaked
Dimethylamine	0.47	0.19	0.35	streaked
Diethylamine	0.43	0.13	0.34	streaked
Di-N-butylamine	–	–	–	–
Diethanolamine	–	–	–	–

daylight. The fluorescence from dansyl-ethylamine and NBD-ethylamine was visible down to 0.5 ng (approximately 27 pmol for either compound). Dabsyl-ethylamine could be detected by its yellow colour down to 3 ng (162 pmol), but this was extended to 1.5 ng (81 pmol) after spraying with 3% (v/v) HCl in methanol. Similar results were obtained for dansyl-*p*-tyramine (lower detection limit 0.25–0.5 ng) and for dabsyl-*p*-tyramine (5–12 ng) indicating that dansyl- and NBD-ethylamine can be detected about 3–5 times more sensitively than dabsyl-ethylamines.

Sensitivity of detection of other amines was assessed by visual comparison with the corresponding ethylamine derivatives, dansyl-amines or dabsyl-amines could all be detected at about the same sensitivity. However, the fluorescent intensities of NBD-amines were far more variable. Bulky amines, such as *tert.*-butylamine, di-*n*-butylamine, and di-ethanolamine gave non-fluorescent NBD derivatives while aromatic amine derivatives gave only low intensity fluorescence. Rather more surprisingly di- and polyamines also gave low intensity fluorescent NBD derivatives. Ghosh and Whitehouse [14] have suggested that the fluorescence of NBD-amines decreases if the amine moiety is out of plane with the NBD ring. Bulky amines or multi-derivatised polyamines are too sterically crowded to allow planarity and therefore only NBD-alkylamines had fluorescent intensities approaching those of the corresponding dansyl-amines.

The fluorescent intensities of dansyl-amines are pH dependent, but can be stabilised by spraying with *n*-propanol–triethanolamine (4:1, v/v) [15]. This reagent had little effect on the colours of dabsyl-amines and NBD-amines, although the fluorescence of the NBD-amines decreased in intensity. The intensity was restored (but not enhanced) by subsequent spraying with either acetic acid–*n*-propanol (20%, v/v), or methanolic HCl (3%, v/v).

Acid-sprayed dabsylated amines all became easier to detect as the orange–yellow spots deepened in colour to red. To investigate this further the absorption spectra of a known concentration of purified dabsyl-hexanolamine (0.73 μg) were measured in five different pH buffers.

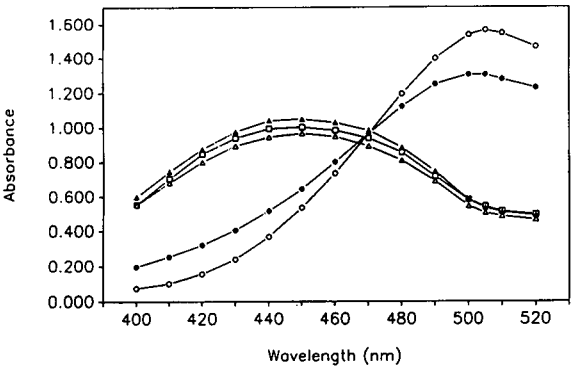

Fig. 4. pH-dependent shift of absorption maximum of dabsyl-hexanolamine. Samples of dabsyl-hexanolamine dissolved in aqueous acetonitrile (60%, v/v) were adjusted to the appropriate pH with the following buffers: (□) pH 4: potassium hydrogen phthalate (10.2 g/l); (●) pH 2: formic acid–acetic acid–water (4:9:70 v/v/v); (○) pH 1: 0.1 *M* HCl. (▲) pH 3 and (△) pH 2.5 buffers were prepared by acidifying pH 4 buffer with HCl. Absorbance measurements were scanned from 390 to 530 nm.

The absorbance maximum changed sharply at pH 2 from 450 nm to 505 nm (a shift from yellow to red) and, at the same pH, the molar extinction coefficient increased by 50%, suggesting a possible doubling of minimum detection limits (Fig. 4). In fact spraying dabsyl-ethylamine on TLC plates with the acidic reagents did lead to an approximate two-fold increase of sensitivity suggesting that the improvement in detection is due to the increased absorptivity of protonated dabsylated amines, rather than red spots simply being an easier to distinguish against a white background.

CONCLUSIONS

Two-dimensional thin-layer chromatography has proved to be a very reliable method for separating amine mixtures as their dansyl derivatives [12,16]. Alberts *et al.* [13] have published an extensive 2D-TLC map showing the positions of 81 dansyl-amines after separation on silica. However, dansyl chloride is not specific to amines but will also derivatise phenols and thiol compounds [15], and also gives rise to fluorescent by-products which can obscure spots of interest. In particular dansyl-ammonia often

elutes at the same rate as dansylated polyamines, and can interfere with their analysis.

Less is known of the side reactions of dabsylation, but dabsyl chloride, its hydrolysis product dabsyl-sulphonic acid (dabsyl-OH), and dabsyl-ammonia are all coloured bright red and therefore potential sources of interference. Dabsyl chloride also reacts with thiol and phenolic compounds.

NBD chloride appears to have many advantages as an analytical derivatising agent. It is selective towards amines because although phenols, anilines, and thiols also react they only give weakly fluorescent derivatives. NBD chloride itself is non-fluorescent, presumably because the electron withdrawing chloro group causes heavy ion quenching.

It was noted that NBD-amines tended to run across 2D-TLC plates in a diagonal regardless of the attempt described to find solvents capable of breaking this pattern. Dansyl and dabsyl derivatives were more randomly distributed when an aliphatic solvent was used in the first direction, and aromatic in the second. The elution rates of the NBD-amines are apparently less sensitive to the aromatic nature of the solvent system used, presumably because the nitrobenzoxazole ring system is less aromatic in character than either the dansyl or dabsyl groups.

Here a comparative investigation of the thin-layer chromatographic properties of various derivatised amines is presented. New 2D-TLC systems for dabsyl- and NBD-amines were developed, and new separating systems for NBD-amines based on pH were investigated. On merit dansyl chloride appears to be the most useful derivatising agent for thin layer chromatographic separation of amines. It fulfils the criteria outlined above, in terms of both sensitivity and, to a lesser extent, resolution. Dabsyl chloride is less suitable because detection was considerably less sensitive, and NBD chloride because of the variable fluorescent intensities, which were dependent upon amine structure.

ACKNOWLEDGEMENTS

We thank J.L. Firmin for helpful discussion and A.R. McDonald for reviewing the manuscript. N.P.J.P. was the recipient of a SERC grant.

REFERENCES

1 T.A. Smith, *Ann. Rev. Plant Physiol.*, 36 (1985) 117.
2 J.F. Lawrence and R.W. Frei, *Chemical Derivatisation in Liquid Chromatography*, Elsevier, Amsterdam, 1976.
3 K. Imai, T. Toyo'oka and H. Miyano, *Analyst*, 109 (1984) 1365.
4 A.R. Hayman, D.O. Gray and S.V. Evans, *J. Chromatogr.*, 325 (1985) 462.
5 N.P.J. Price, J.L. Firmin and D.O. Gray, *J. Chromatogr.*, 598 (1992) 51.
6 J.K. Lin and J.K. Chang, *Anal. Chem.*, 47 (1985) 1634.
7 F. Van Hoof, *Anal. Chem.*, 46 (1978) 286.
8 D.L. Ingles and D. Gullimore, *J. Chromatogr.*, 325 (1985) 346.
9 R.W. Alison, G.S. Mayer and R.E. Shoup, *Anal. Chem.*, 56 (1985) 1089.
10 R.W. Frei, W. Santi and M. Thomas, *J. Chromatogr.*, 116 (1976) 365.
11 A.R. Hayman and D.O. Gray, *Phytochemistry*, 28 (1989) 673.
12 N. Seiler and M. Weichmann, in A. Neiderwieser and G. Pataki (Editors), *Progress in TLC and Related Methods*, Vol. 1, Ann Arbor Sci. Publ., Ann Arbor, 1970, pp. 95–144.
13 L.R.S. Alberts, S.D. Mitchell and D.O. Gray, *J. Chromatogr.*, 312 (1984) 357.
14 P.B. Ghosh and M.W. Whitehouse, *Biochem. J.*, 108 (1968) 155.
15 N. Seiler, in D. Glick (Editor), *Methods of Biochemical Analysis*, Vol. 18, Interscience, New York, 1970, pp. 259–337.
16 N. Seiler and B. Knodgen, *J. Chromatogr.*, 131 (1977) 109.

Journal of Chromatography, 635 (1993) 171–175
Elsevier Science Publishers B.V., Amsterdam

CHROM. 24 842

Short Communication

Electrophoretic determination of stability constants of Zn(II)- and Cd(II)–nitrilotriacetate–penicillamine mixed complexes

S.K. Srivastava, V.K. Gupta, B.B. Tiwari and Imran Ali*

Department of Chemistry, University of Roorkee, Roorkee-247 667 (India)

(First received October 1st, 1992; revised manuscript received December 24th, 1992)

ABSTRACT

A paper electrophoretic method is described for the study of equilibria in mixed ligand [nitrilotriacetate (NTA)–penicillamine] complex systems in solution. The stability constants of Zn(II)–NTA–penicillamine and Cd(II)–NTA–penicillamine complexes were found to be 5.36 and 5.18 (log K values), respectively, at $\mu = 0.1$ and 35°C.

INTRODUCTION

The properties and more important chemical reactions of naturally occurring penicillamine have already been subjected to wide investigations. The main biochemical aspects have been reviewed by Jocelyn [1]. The biological importance is attributed to the capabilities of the mercapto group to undergo various complex formation processes, primarily in non-haem iron proteins [2] and the blue copper proteins [3]. Sorensen [4] has demonstrated the anti-inflammatory activity of the copper–penicillamine complex. The complexes of Zn(II) and Cd(II) with penicillamine and other sulphur-containing amino acids are of great importance because of the interesting biological role of Zn(II) and the toxic nature of Cd(II). The significance of investigations relating to these complexes is further enhanced by the recognition that penicillamine can be advantageously employed for the treatment of metal ion poisoning (Pb, Hg, Cd, Zn, etc.). A search of the literature [4–7] indicated that there is only one report on Zn(II) and Cd(II) binary complexes with penicillamine and no information on ternary (mixed complex) systems.

In view of this, attempts were made to establish the optimum conditions for metal (M)–penicillamine, M–nitrilotriacetate (NTA) and M–NTA–penicillamine complex formation. In addition, this paper describes an electrophoretic method for the determination of the stability constants of these complexes.

EXPERIMENTAL

Apparatus

A Systronic (Naroda, India) Model 604 elec-

* Corresponding author.

0021-9673/93/$06.00

trophoresis system was used. It has a built-in power supply (a.c.–d.c.) that is fed directly to a paper electophoresis tank. In order to maintain the temperature constant, two hollow metallic plates coated with thin plastic paper on the outer surface were used for sandwiching paper strips and thermostated water (35°C) was circulated through these plates. pH measurements were made with an Elico (Hyderabab, India) Model L_{1-10} pH meter using a glass electrode.

Chemicals

Zinc and cadmium perchlorate solutions were prepared as described elsewhere [6]. Metal spots were detected on the paper using dithizone in carbon tetrachloride (BDH, Poole, UK) for Zn(II) and 1-(2-pyridylazo)-2-naphthol (PAN) (Merck, Darmstadt, Germany) for Cd(II). A saturated aqueous solution (0.9 ml) of silver nitrate was diluted with acetone to 20 ml. Glucose, as a black spot, was detected by spraying with this solution and then with 2% ethanolic sodium hydroxide.

Background electrolyte

The background electrolytes used in the study of binary complexes were 0.1 *M* perchloric acid and 0.01 *M* penicillamine. For the study of ternary system the background electrolytes used were 0.1 *M* perchloric acid, 0.01 *M* NTA and various amounts of 0.01 *M* penicillamine. The ternary system was maintained at pH 8.5 by the addition of sodium hydroxide.

Stock solutions of 9.0 *M* perchloric acid, 2.0 *M* sodium hydroxide and 0.5 *M* penicillamine were prepared from analytical-reagent grade chemicals (BDH). A 0.01 *M* NTA solution was prepared from the compound obtained from Merck.

Procedure

The hollow base plate in the instrument was made horizontal with a spirit level. A 150-ml volume of background electrolyte was placed in each tank of the electrophoretic apparatus. Paper strips (Whatman No. 1, 30 × 1 cm) in triplicate were then spotted with metal ion solutions and glucose in the centre with a micropipette and were subsequently placed on the base plate and sandwiched under the upper hollow metallic plate with the ends of strips lying in the two sides of the tank solutions. A 200-V potential difference was then applied between the tank solutions and electrophoresis was carried out for 60 min. Subsequently the strips were removed and the spots were detected. The averages of triplicate strips were noted for calculations and the movement of the glucose spot was used as a correction factor. It was found that the variation in the movement was about 5%. The mobilities were calculated by dividing the distance by the potential gradient and are expressed in $cm^2\ V^{-1}\ min^{-1}$.

RESULTS AND DISCUSSION

M(II)–penicillamine binary system

The plot of the ionophoretic mobility of a metal spot against pH is a curve with a number of plateaux, as shown in Fig. 1. The first corresponds to a region in which metal ions are uncomplexed. The second plateau in each instance with zero mobility indicates the formation of 1:1 neutral complexes. With a further increase in pH the mobility decreases, giving rise to a third plateau lying in negative region, indicating

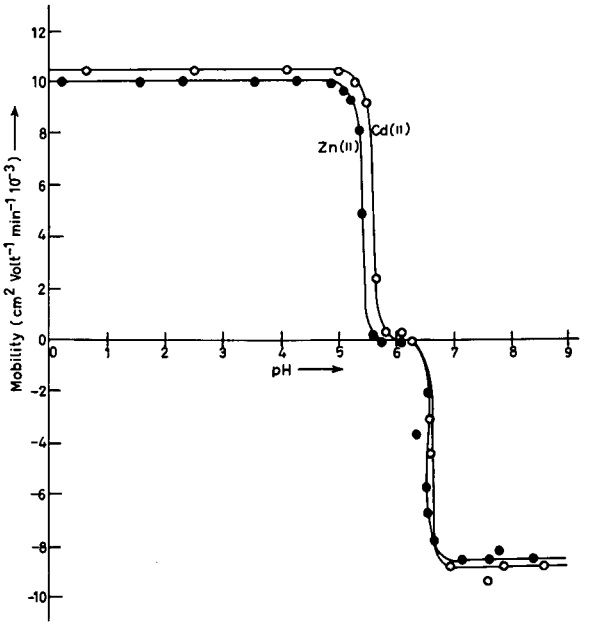

Fig. 1. Mobility curves for the M–penicillamine systems. ● = Zn(II)–penicillamine; ○ = Cd(II)–penicillamine.

an anionic nature of the metal complexes. The predominant liganding properties of unprotonated anionic species of penicillamine have also been reported ruling out any such property of a zwitterion [8]. In view of these observations, the complexation of the metal ions with the penicillamine anion $[L^{2-}]$ can be represented as

$$M^{2+} + L^{2-} \overset{K_1}{\rightleftharpoons} ML \quad (1)$$

$$ML + L^{2-} \overset{K_2}{\rightleftharpoons} ML_2^{2-} \quad (2)$$

The metal spot on the paper is thus a combination of uncomplexed metal ions, a 1:1 complex and a 1:2 complex. The overall mobility of these is given by

$$U = \frac{u_0 + u_1K_1[L^{2-}] + u_2K_1K_2[L^{2-}]^2}{1 + K_1[L^{2-}] + K_1K_2[L^{2-}]^2} \quad (3)$$

where u_0, u_1 and u_2 are the mobilities of the uncomplexed metal ion, the 1:1 metal complex and the 1:2 metal complexes, respectively.

For the calculation of the first stability constant (K_1), the region between the first and second plateaux is pertinent. The overall mobility U will be equal to the arithmetic mean of the mobility of uncomplexed metal ion, u_0, and that of first complex, u_1, at a pH where $K_1 = 1/[L^{2-}]$. With the help of the dissociation constants of penicillamine ($k_1 = 10^{1.90}$, $k_2 = 10^{7.85}$ and $k_3 = 10^{10.55}$), the concentration of the liganding penicillamine, $[L^{2-}]$, is calculated by

$$[L^{2-}] = \frac{[L_T]}{1 + [H]/k_3 + [H]^2/k_2k_3 + [H]^3/k_1k_2k_3} \quad (4)$$

where $[L_T]$ = total concentration.

The stability constant K_2 of the second complex can be calculated by taking into consideration the region between the second and third plateaux of the mobility curve. The calculated values of K_1 and K_2 are given in Table I.

M(II)–NTA binary system

Fig. 2 shows the overall mobilities of the metal spots in the presence of NTA at different pH. The mobility at the last plateau is negative, showing the anionic nature of both the Zn(II) and Cd(II) complexes. The stability constants (K_3) of these complexes were calculated using the same method as described for the M–penicillamine system (the dissociation constants for NTA are $k_1 = 10^{1.66}$, $k_2 = 10^{2.67}$ and $k_3 = 10^{9.49}$) and are presented in Table I. The complexation may be represented as

$$M^{2+} + NTA^{3-} \overset{K_3}{\rightleftharpoons} [M\text{–}NTA]^- \quad (5)$$

M–NTA–penicillamine ternary system

This system was studied at pH 8.5. It is observed from the mobility curves of the

TABLE I

STABILITY CONSTANTS OF BINARY AND TERNARY COMPLEXES OF Zn(II) AND Cd(II)

Ionic strength = 0.1; temperature = 35°C; NTA anion = $N(CH_2COO)_3^{3-}$; penicillamine anion = $(CH_3)_2C(S)CH(NH_2)COO^-$.

Values	Metal ion	Stability constant[a]			
		$\log K_{1\,ML}^{M}$	$\log K_{2\,ML_2}^{M}$	$\log K_{3\,M\text{–}NTA}^{M}$	$\log K_{4\,M\text{–}NTA\text{–}L}^{M\text{–}NTA}$
Calculated (this work)	Zn(II)	9.80	17.11	8.80	5.36
	Cd(II)	9.35	16.70	8.05	5.18
Literature values	Zn(II)	9.40 [9]	19.42 [9]	10.66 [9]	–
		9.42 [10]	19.44 [10]	10.00 [10]	–
		10.00 [11]	18.90 [11]	–	–
		9.51 [11]	18.51 [11]	–	–
	Cd(II)	10.89 [9]	–	9.78 [9]	–
		11.40 [11]	18.50 [11]	9.40 [11]	–

[a] $K_{1\,ML}^{M} = [ML]/[M][L]$; $K_{2\,ML_2}^{M} = [ML_2]/[ML][L]$; $K_{3\,M\text{–}NTA}^{M} = [M\text{–}NTA]/[M][NTA]$; $K_{4\,M\text{–}NTA\text{–}L}^{M\text{–}NTA} = [M\text{–}NTA\text{–}L]/[M\text{–}NTA][L]$; M = metal cation; L = ligand (penicillamine); NTA = nitrilotriacetate.

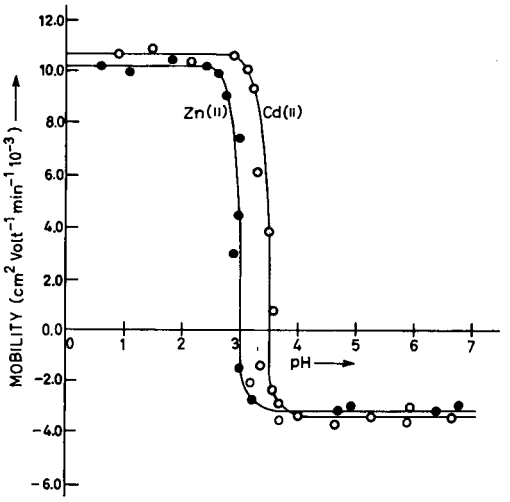

Fig. 2. Mobility curves for the M–NTA systems. ● = Zn(II)–NTA; ○ = Cd(II)–NTA.

M–penicillamine and M–NTA binary systems that binary complexes are formed at pH <8.5. Therefore, it was considered necessary to study the transformation of the $[M–NTA]^-$ binary complex into the $[M–NTA–penicillamine]^{3-}$ mixed complex at pH 8.5 to avoid any side interaction. The plot of mobility against the logarithm of the concentration of added penicillamine gives a curve containing two plateaux (Fig. 3). It is inferred that the moiety in the last plateau is due to coordination of penicillamine anion to the $[M–NTA]^-$ moiety (1:1), resulting in the formation of a 1:1:1 $[M–NTA–penicillamine]^{3-}$ mixed complex:

$$[M–NTA]^- + L^{2-} \overset{K_4}{\rightleftharpoons} [M–NTA–L]^{3-} \quad (6)$$

where L is penicillamine.

In this electrophoretic study, the transformation of a simple complex into a mixed complex takes place, hence the overall mobility (U) of this complex is given by

$$U = u_0 f_{[M–NTA]} + u_1 f_{[M–NTA–L]} \quad (7)$$

where u_0, u_1 and $f_{[M–NTA]}$, $f_{[M–NTA–L]}$ are the mobilities and mole fractions of the $[M–NTA]^-$ and $[M–NTA–L]^{3-}$ complexes, respectively.

On adding values of the mole fractions, the above equation becomes

$$U = (u_0 + u_1 K_4[L^{2-}])/(1 + K_4[L^{2-}]) \quad (8)$$

where u_0 and u_1 are the mobilities in the region of the two plateaux of the curve.

The concentration of penicillamine anion at pH 8.5 was calculated. K_4 is obviously equal to $1/[L^{-2}]$. All these values of K_4 (stability constants of mixed complexes) are given in Table I.

It can be concluded from these studies that penicillamine and NTA can be used to reduce the levels of Zn(II) and Cd(II) in biological systems.

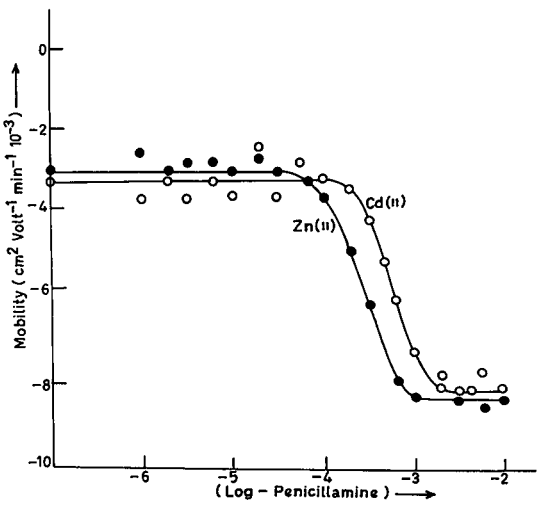

Fig. 3. Mobility curves for the M–NTA–penicillamine systems. ● = Zn(II)–NTA–penicillamine; ○ = Cd(II)–NTA–penicillamine.

ACKNOWLEDGEMENT

I.A. (PO) and B.B.T. (RA) are grateful to CSIR, New Delhi, for providing financial assistance.

REFERENCES

1 C.P. Jocelyn, *Biochemistry of the SH Group*, Academic Press, London, New York, 1972.
2 R.G. Moore and P.J.R. Williams, *Coord. Chem. Rev.*, 18 (1976) 125.
3 A.J. Fee, *Struct. Bonding (Berlin)*, 23 (1975) 11–52.
4 R.J. Sorensen, *J. Med. Chem.*, 19 (1976) 135.
5 B.B. Tiwari, R.K.P. Singh, Kamaluddin and K.L. Yadava, *Trans. Soc. Adv. Electrochem. Sci. Technol.*, 25 (1990) 124.
6 B.B. Tiwari, R.K.P. Singh and K.L. Yadava, *J. Chromatogr.*, 542 (1991) 537.

7 B.B. Tiwari, R.K.P. Singh and K.L. Yadava, *Bull. Soc. Chim. Fr.*, 128 (1991) 141.
8 J.R. Blackburn and M.M. Jones, *J. Inorg. Nucl. Chem.*, 35 (1973) 1605.
9 A.E. Martell and R.M. Smith, *Critical Stability Constants, Amino Acids*, Vol. 1, Plenum Press, New York, London, 1977, p. 48.
10 D.D. Perrin, *Stability Constants of Metal Ion Complexes, Part B, Organic Ligands (IUPAC Chemical Series*, No. 22), Pergamon Press, Oxford, 1979.
11 L.G. Sillen and A.E. Martell, *Stability Constants of Metal Ion Complexes (Special Supplement No. 17)*, Chemical Society, London, 1964.

Journal of Chromatography, 635 (1993) 176
Elsevier Science Publishers B.V., Amsterdam

CHROM. 24 964

Book Review

Thin-layer chromatography; *reagents and detection methods*; *physical and chemical detection methods*: *fundamentals*, *reagents I*, Vol. 1a, by H. Jork, W. Funk, W. Fischer and H. Wimmer, VCH, Weinheim, 1990, 464 pp., ISBN 3-527-27834-6 (VCH, Weinheim) and 0-89573-876-7 (VCH, New York).

This is the English translation by Frank and Jennifer Hampson of the first part of Volume 1 of the German text. Two more parts are in preparation, to be followed by Volume 2 on radiometric detection methods and Volume 3 on biochemical and biological detection methods.

As one would expect from such old hands at thin-layer chromatography (TLC) as, *e.g.*, Jork, who is at the University of Saarbrücken, Stahl's powerhouse of TLC, and Fischer, who is at Merck, the premier manufacturer of TLC supplies, this is an excellent book. Detection methods are not only described in all technical details but also provided with chemical background information and ample references to the literature. What is best is that the procedures have been tested in the authors' laboratories and that their comments, such as helpful hints and precautions, are included.

The first part of the book deals with physical and chemical methods of detection and documentation. Wisely, dipping procedures are given preference over the messy and unsanitary spraying procedures. Eighty individual reagents are dealt with in the second part in the following format: Reagent for..., Preparation of the reagent, Reaction, Method, Procedure tested, and References. A list of name reagents and acronyms and an excellent subject index complete this useful volume.

Physically, this book is very attractive, except for the appearance of the paper, which, however, is acid-free. This is a soft-bound book with durable cover and comes in a handy, small format. It is profusely illustrated with photographs (partly in color), densitometer scans, and chemical structures. It is also remarkably free of technical errors and language problems.

TLC has largely been eclipsed by the (often automated) column methods of chromatography. However, it is still widely used, not only in laboratories that cannot afford the apparatus required for column chromatography, but also in situations where parallel analyses, especially of crude extracts, are routinely performed. All practitioners of TLC will greatly profit from having this reference and handbook at their disposal. The introductory material will also be of value to students of analytical chemistry and beginners in TLC laboratory practice.

Orinda, CA (USA) Erich Heftmann

Experimental Design: A Chemometric Approach

Second, Revised and Expanded Edition

by **S.N. Deming** *and* **S.L. Morgan**

Data Handling in Science and Technology Volume 11

Now available is the second edition of a book which has been described as *"...an exceptionally lucid, easy-to-read presentation... would be an excellent addition to the collection of every analytical chemist. I recommend it with great enthusiasm."* (Analytical Chemistry).

N.R. Draper reviewed the first edition in Publication of the International Statistical Institute *"...discussion is careful, sensible, amicable, and modern and can be recommended for the intended readership."*

The scope of the first edition has been revised, enlarged and expanded. Approximately 30% of the text is new. The book first introduces the reader to the fundamentals of experimental design. Systems theory, response surface concepts, and basic statistics serve as a basis for the further development of matrix least squares and hypothesis testing. The effects of different experimental designs and different models on the variance-covariance matrix and on the analysis of variance (ANOVA) are extensively discussed. Applications and advanced topics (such as confidence bands, rotatability, and confounding) complete the text. Numerous worked examples are presented.

The clear and practical approach adopted by the authors makes the book applicable to a wide audience. It will appeal particularly to those who still need to know efficient ways of carrying out experiments. It will also be an ideal text for advanced undergraduate and graduate students following courses in chemometrics, data acquisition and treatment, and design of experiments.

Contents:

1. System Theory.
2. Response Surfaces.
3. Basic Statistics.
4. One Experiment.
5. Two Experiments.
6. Hypothesis Testing.
7. The Variance-Covariance Matrix.
8. Three Experiments.
9. Analysis of Variance (ANOVA) for Linear Models.
10. An Example of Regression Analysis on Existing Data.
11. A Ten-Experiment Example.
12. Approximating a Region of a Multifactor Response Surface.
13. Confidence Intervals for Full Second-Order Polynomial Models.
14. Factorial-Based Designs.
15. Additional Multifactor Concepts and Experimental Designs.

Appendix A. Matrix Algebra.
Appendix B. Critical Values of t.
Appendix C. Critical Values of F, α=0.05.
Subject Index.

1993 416 pages
Price: US $ 177.25 / Dfl. 310.00
ISBN 0-444-89111-0

ORDER INFORMATION

For USA and Canada
ELSEVIER SCIENCE PUBLISHERS
Judy Weislogel
P.O. Box 945
Madison Square Station,
New York, NY 10160-0757
Tel: (212) 989 5800
Fax: (212) 633 3880

In all other countries
ELSEVIER SCIENCE PUBLISHERS
P.O. Box 211
1000 AE Amsterdam
The Netherlands
Tel: (+31-20) 5803 753
Fax: (+31-20) 5803 705

US$ prices are valid only for the USA & Canada and are subject to exchange rate fluctuations; in all other countries the Dutch guilder price (Dfl.) is definitive. Customers in the European Community should add the appropriate VAT rate applicable in their country to the price(s). Books are sent post-free if prepaid.

ELSEVIER
SCIENCE PUBLISHERS

PUBLICATION SCHEDULE FOR THE 1993 SUBSCRIPTION

Journal of Chromatography and *Journal of Chromatography, Biomedical Applications*

MONTH	O 1992	N 1992	D 1992	J	F	M	A	M	
Journal of Chromatography	623/1 623/2 624/1 + 2	625/1 625/2	626/1 626/2 627/1 + 2	628/1 628/2 629/1 629/2	630/1 + 2 631/1 + 2 632/1 + 2 633/1 + 2	634/1 634/2	635/1 635/2 636/1 636/2	637/1 637/2 638/1 638/2	The publication schedule for further issues will be published later.
Cumulative Indexes, Vols. 601–650									
Bibliography Section						649/1			
Biomedical Applications				612/1	612/2	613/1	613/2 614/1	614/2 615/1	

INFORMATION FOR AUTHORS

(Detailed *Instructions to Authors* were published in Vol. 609, pp. 437–443. A free reprint can be obtained by application to the publisher, Elsevier Science Publishers B.V., P.O. Box 330, 1000 AH Amsterdam, Netherlands.)

Types of Contributions. The following types of papers are published in the *Journal of Chromatography* and the section on *Biomedical Applications:* Regular research papers (Full-length papers), Review articles, Short Communications and Discussions. Short Communications are usually descriptions of short investigations, or they can report minor technical improvements of previously published procedures; they reflect the same quality of research as Full-length papers, but should preferably not exceed five printed pages. Discussions (one or two pages) should explain, amplify, correct or otherwise comment substantively upon an article recently published in the journal. For Review articles, see inside front cover under Submission of Papers.

Submission. Every paper must be accompanied by a letter from the senior author, stating that he/she is submitting the paper for publication in the *Journal of Chromatography.*

Manuscripts. Manuscripts should be typed in **double spacing** on consecutively numbered pages of uniform size. The manuscript should be preceded by a sheet of manuscript paper carrying the title of the paper and the name and full postal address of the person to whom the proofs are to be sent. As a rule, papers should be divided into sections, headed by a caption (*e.g.*, Abstract, Introduction, Experimental, Results, Discussion, etc.) All illustrations, photographs, tables, etc., should be on separate sheets.

Abstract. All articles should have an abstract of 50–100 words which clearly and briefly indicates what is new, different and significant. No references should be given.

Introduction. Every paper must have a concise introduction mentioning what has been done before on the topic described, and stating clearly what is new in the paper now submitted.

Illustrations. The figures should be submitted in a form suitable for reproduction, drawn in Indian ink on drawing or tracing paper. Each illustration should have a legend, all the *legends* being typed (with double spacing) together on a *separate sheet.* If structures are given in the text, the original drawings should be supplied. Coloured illustrations are reproduced at the author's expense, the cost being determined by the number of pages and by the number of colours needed. The written permission of the author and publisher must be obtained for the use of any figure already published. Its source must be indicated in the legend.

References. References should be numbered in the order in which they are cited in the text, and listed in numerical sequence on a separate sheet at the end of the article. Please check a recent issue for the layout of the reference list. Abbreviations for the titles of journals should follow the system used by *Chemical Abstracts.* Articles not yet published should be given as "in press" (journal should be specified), "submitted for publication" (journal should be specified), "in preparation" or "personal communication".

Dispatch. Before sending the manuscript to the Editor please check that the envelope contains four copies of the paper complete with references, legends and figures. One of the sets of figures must be the originals suitable for direct reproduction. Please also ensure that permission to publish has been obtained from your institute.

Proofs. One set of proofs will be sent to the author to be carefully checked for printer's errors. Corrections must be restricted to instances in which the proof is at variance with the manuscript. "Extra corrections" will be inserted at the author's expense.

Reprints. Fifty reprints will be supplied free of charge. Additional reprints can be ordered by the authors. An order form containing price quotations will be sent to the authors together with the proofs of their article.

Reversed Phase CHIRAL HPLC Column

NEW CHIRALCEL® OD-R

Indapamide

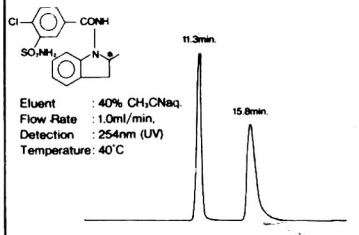

Eluent : 40% CH_3CNaq.
Flow Rate : 1.0ml/min.
Detection : 254nm (UV)
Temperature: 40°C

Verapamil

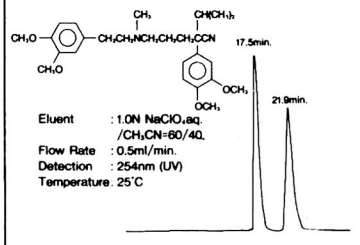

Eluent : 1.0N $NaClO_4$aq. /CH_3CN=60/40.
Flow Rate : 0.5ml/min.
Detection : 254nm (UV)
Temperature: 25°C

Hydroxyzine

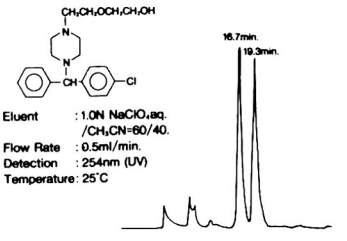

Eluent : 1.0N $NaClO_4$aq. /CH_3CN=60/40.
Flow Rate : 0.5ml/min.
Detection : 254nm (UV)
Temperature: 25°C

Propranolol

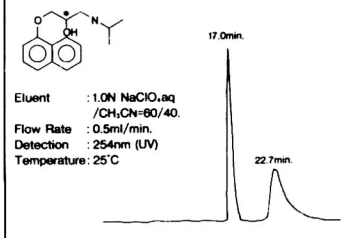

Eluent : 1.0N $NaClO_4$aq /CH_3CN=60/40.
Flow Rate : 0.5ml/min.
Detection : 254nm (UV)
Temperature: 25°C

Pindolol

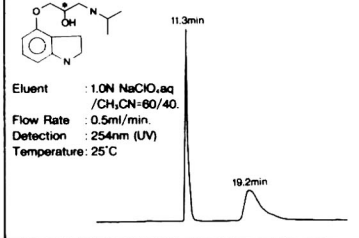

Eluent : 1.0N $NaClO_4$aq /CH_3CN=60/40.
Flow Rate : 0.5ml/min.
Detection : 254nm (UV)
Temperature: 25°C

1-Phenoxy-2-Propanol

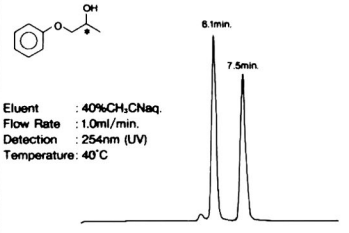

Eluent : 40%CH_3CNaq.
Flow Rate : 1.0ml/min.
Detection : 254nm (UV)
Temperature: 40°C

Alimemazine

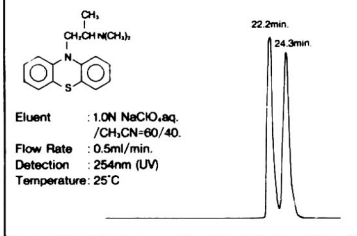

Eluent : 1.0N $NaClO_4$aq. /CH_3CN=60/40.
Flow Rate : 0.5ml/min.
Detection : 254nm (UV)
Temperature: 25°C

Trimepramine

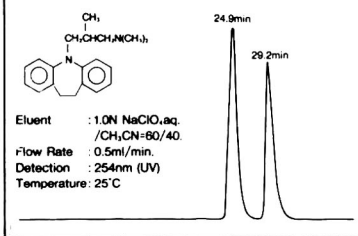

Eluent : 1.0N $NaClO_4$aq. /CH_3CN=60/40.
Flow Rate : 0.5ml/min.
Detection : 254nm (UV)
Temperature: 25°C

4-Pheny-2-butanol

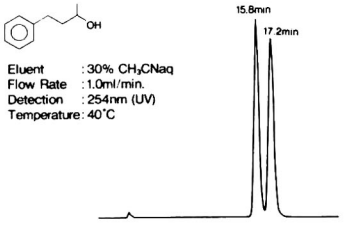

Eluent : 30% CH_3CNaq
Flow Rate : 1.0ml/min.
Detection : 254nm (UV)
Temperature: 40°C

CBZ-Val.

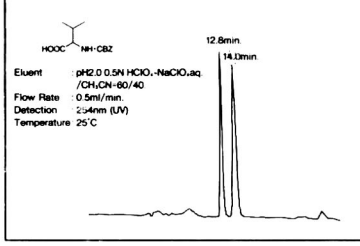

Eluent : pH2.0 0.5N $HClO_4$-$NaClO_4$aq. /CH_3CN=60/40
Flow Rate : 0.5ml/min.
Detection : 254nm (UV)
Temperature: 25°C

3-Phenylbutyric acid

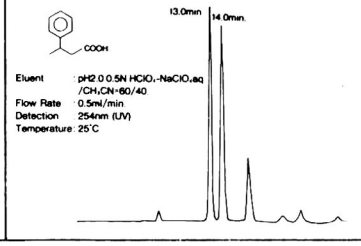

Eluent : pH2.0 0.5N $HClO_4$-$NaClO_4$aq. /CH_3CN=60/40
Flow Rate : 0.5ml/min
Detection : 254nm (UV)
Temperature: 25°C

2-Phenylbutyric acid

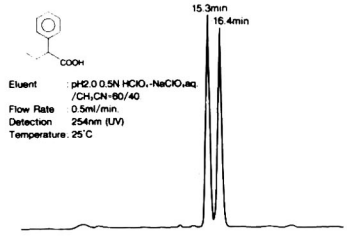

Eluent : pH2.0 0.5N $HClO_4$-$NaClO_4$aq. /CH_3CN=60/40
Flow Rate : 0.5ml/min
Detection : 254nm (UV)
Temperature: 25°C

For more information about CHIRALCEL OD-R column, please give us a call.

DAICEL CHEMICAL INDUSTRIES, LTD.
CHIRAL CHEMICALS DIVISION 8-1, Kasumigaseki 3-chome, Chiyoda-ku, Tokyo 100, JAPAN
Phone: +81-3-3507-3151 Facsimile: +81-3-3507-3193

AMERICA
CHIRAL TECHNOLOGIES, INC.
730 SPRINGDALE DRIVE
DRAWER I EXTON, PA 19341
Phone: 215-594-2100
Facsimile: 215-594-2325

EUROPE
DAICEL (EUROPA) GmbH
Ost Street 22
4000 Düsseldorf 1, Germany
Phone: +49-211-369848
Facsimile: +49-211-364429

ASIA/OCEANIA
DAICEL CHEMICAL (ASIA) PTE. LTD.
65 Chulia Street #40-07
OCBC Centre, Singapore 0104.
Phone: +65-5332511
Facsimile: +65-5326454